

**EEG-BASED IQ AND LEARNING STYLE  
CLASSIFICATION MODEL USING ARTIFICIAL NEURAL  
NETWORK**

**MUHAMMAD MARWAN BIN ANOOR**

**INSTITUTE FOR ADVANCED STUDIES  
UNIVERSITY OF MALAYA  
KUALA LUMPUR**

**2021**

**EEG-BASED IQ AND LEARNING STYLE  
CLASSIFICATION MODEL USING ARTIFICIAL  
NEURAL NETWORK**

**MUHAMMAD MARWAN BIN ANOOR**

**DISSERTATION SUBMITTED IN FULFILMENT OF  
THE REQUIREMENTS FOR THE DEGREE OF MASTER  
OF PHILOSOPHY**

**INSTITUTE FOR ADVANCED STUDIES  
UNIVERSITY OF MALAYA  
KUALA LUMPUR**

**2021**

**UNIVERSITY OF MALAYA**  
**ORIGINAL LITERARY WORK DECLARATION**

Name of Candidate: Muhammad Marwan B. Anoor

Matric No: HMA170022

Name of Degree: Master of Philosophy

Title of Project Paper/Research Report/Dissertation/Thesis (“this Work”):

EEG-Based IQ and Learning Style Classification Model using Artificial  
Neural Network

Field of Study:

Biomedical Signal Processing (Electronics and Automation)

I do solemnly and sincerely declare that:

- (1) I am the sole author/writer of this Work;
- (2) This Work is original;
- (3) Any use of any work in which copyright exists was done by way of fair dealing and for permitted purposes and any excerpt or extract from, or reference to or reproduction of any copyright work has been disclosed expressly and sufficiently and the title of the Work and its authorship have been acknowledged in this Work;
- (4) I do not have any actual knowledge nor do I ought reasonably to know that the making of this work constitutes an infringement of any copyright work;
- (5) I hereby assign all and every rights in the copyright to this Work to the University of Malaya (“UM”), who henceforth shall be owner of the copyright in this Work and that any reproduction or use in any form or by any means whatsoever is prohibited without the written consent of UM having been first had and obtained;
- (6) I am fully aware that if in the course of making this Work I have infringed any copyright whether intentionally or otherwise, I may be subject to legal action or any other action as may be determined by UM.

Candidate’s Signature

Date:

Subscribed and solemnly declared before,

Witness’s Signature

Date:

Name:

Designation:

# **EEG-BASED IQ AND LEARNING STYLE CLASSIFICATION MODEL USING ARTIFICIAL NEURAL NETWORK**

## **ABSTRACT**

Intelligence and learning styles are among most widely studied traits in cognitive psychology. Currently, both aspects of cognition can only be assessed using paper-based psychometric tests. The methods, however, are exposed to inconsistency issues due to the variation of examination format and language barriers. Hence, this study proposes an intelligent system for assessing intelligence quotient (IQ) level and learning style from the resting brainwaves using artificial neural network (ANN). Eighty-five individuals from varying highest educational backgrounds have participated in this study. Resting electroencephalogram (EEG) is recorded from the left prefrontal cortex using NeuroSky. Control groups are established using Kolb's Learning Style Inventory (LSI) and a model developed based on Raven's Progressive Matrices (RPM). Subsequently, theta, alpha and beta power ratio is extracted from the pre-processed EEG. Distribution and pattern of features show a correlation with the Neural Efficiency Hypothesis of intelligence and Alpha Suppression Theory. The power ratio features are then used to train, validate and test the ANN model. The system has demonstrated satisfactory performance for IQ classification with accuracies of 98.3% for training and 94.7% for testing. The proposed model is also able to classify learning style with accuracies of 96.9% for training and 80.0% for testing.

Keywords: EEG, intelligent system, IQ, learning style, neural network

# **MODEL PENGELASAN IQ DAN GAYA PEMBELAJARAN BERASASKAN EEG MENGGUNAKAN RANGKAIAN NEURAL BUATAN**

## **ABSTRAK**

Kecerdasan dan gaya pembelajaran adalah antara ciri-ciri yang paling banyak dipelajari dalam psikologi kognitif. Pada masa ini, kedua-dua aspek kognisi hanya boleh dinilai dengan menggunakan ujian psikometrik berasaskan kertas. Walau bagaimanapun, kaedah-kaedah ini didedahkan kepada isu-isu ketidakcekan disebabkan oleh kepelbagaian format peperiksaan dan halangan bahasa. Oleh itu, kajian ini mencadangkan satu sistem pintar untuk menilai tahap kecerdasan kuantiti (IQ) dan gaya pembelajaran dari gelombang otak berehat menggunakan rangkaian neural buatan (ANN). Lapan puluh lima individu dari pelbagai latar belakang pendidikan tertinggi telah mengambil bahagian dalam kajian ini. Gelombang rehat electroencephalogram (EEG) direkodkan dari korteks prefrontal kiri menggunakan NeuroSky. Kelompok kawalan ditubuhkan menggunakan Inventori Gaya Pembelajaran Kolb (LSI) dan model yang dibangunkan berdasarkan Matriks Progresif Raven (RPM). Seterusnya, nisbah theta, alpha dan beta diekstrak dari EEG yang diproses sebelum ini. Pengagihan dan corak ciri menunjukkan perkaitan dengan Hipotesis Kecekapan Neural kecerdasan dan Teori Pengekod Alpha. Ciri-ciri nisbah kuasa kemudian digunakan untuk melatih, mengesahkan dan menguji model ANN. Sistem ini telah menunjukkan prestasi yang memuaskan untuk klasifikasi IQ dengan ketepatan 98.3% untuk latihan dan 94.7% untuk ujian. Model yang dicadangkan juga dapat mengklasifikasikan gaya pembelajaran dengan ketepatan 96.9% untuk latihan dan 80.0% untuk ujian.

**Keywords:** EEG, system kecerdasan, IQ, gaya pembelajaran, rangkaian saraf.

## ACKNOWLEDGEMENTS

بِسْمِ اللَّهِ , in the name of Allah, the Most Gracious and the Most Merciful. Alhamdulillah, all praises to Allah for His blessing in completing this dissertation. First and foremost, special appreciation to reveal my sincere gratitude to my main supervisor, Dr. Aisyah Hartini Jahidin. Thank you for the continuous support, for the patience, for the immense knowledge, for the time, for the motivation, and for the guidance to help in my research. I'm never imagined that would have the best supervisor for my master study.

My other supervisors, Prof. Dr. Hamzah Bin Arof and Dr Megat Syahirul Amin Megat Ali, I would like to thank both for assisting my research work and encourage me to widen my research from various perspectives. Thank you for working hard together on assisting my research to finish it before deadlines.

This research would not have been accomplished without my family support. Thank you, for the encouragement, enjoyable and understandable in all my pursuits and my dreams although the hair become grey and white.

## TABLE OF CONTENTS

EEG-based IQ and Learning Style Classification Model using Artificial Neural Network	
Abstract .....	iii
Model Pengelasan IQ dan Gaya Pembelajaran Berasaskan EEG Menggunakan Rangkaian	
Neural Buatan Abstrak .....	iv
Acknowledgements .....	v
Table of Contents .....	vi
List of Figures .....	xi
List of Tables.....	xiv
List of Symbols and Abbreviations.....	xv
List of Appendices .....	xvii
<b>INTRODUCTION.....</b>	<b>1</b>
1.1 Overview.....	1
1.2 Problem Statement.....	4
1.3 Research Objectives.....	5
1.4 Scope of Work .....	5
1.5 Significance of Research .....	6
1.6 Thesis organization.....	7
<b>LITERATURE REVIEW.....</b>	<b>9</b>
2.1 Introduction.....	9
2.2 Neuroimaging Modalities .....	9
2.3 Biopotential Measurement Devices .....	12
2.4 Electroencephalogram (EEG).....	15
2.4.1 EEG Dry Electrode Approach.....	20

2.4.2	EEG Signal Processing.....	22
2.4.2.1	EEG Pre-Processing .....	22
2.4.2.2	EEG Feature Extraction .....	25
2.4.3	Synthetic EEG Signals .....	27
2.4.4	EEG Applications.....	28
2.5	Box Plot Analysis as EEG Visual Technique.....	31
2.6	Intelligent Signal Processing (ISP).....	33
2.6.1	Artificial Intelligence (AI).....	34
2.6.2	Modeling Simulation Methods Approaches.....	35
2.6.3	Advantages and Limitations of Several AI Techniques.....	35
2.7	Artificial Neural Network (ANN) .....	38
2.7.1	ANN Algorithm and Structure .....	40
2.7.2	Multilayer Feed Forward Network (MFFN) .....	43
2.7.2.1	MFFN Algorithm .....	45
2.7.2.2	Levenberg-Marquardt (LM) Algorithm .....	50
2.7.2.3	Multiple Input Multiple Output (MIMO) Structure .....	53
2.7.2.4	Early Stopping (ES) .....	54
2.8	Neural Network Performance Evaluation.....	56
2.8.1	Confusion Matrix .....	57
2.8.2	Model Validation (Correlation Function Test).....	60
2.9	Human Brain Cognitive Abilities .....	61
2.9.1	Intelligence Quotient Overview .....	64
2.9.2	Learning Style Overview.....	66
2.9.3	Intelligence Quotient and Learning Style Relationship.....	74
	<b>METHODOLOGY.....</b>	<b>78</b>
3.1	Introduction.....	78



3.2	Sample Selection, Data Acquisition and Cognitive Measures .....	81
3.3	Pre-processing, Filtering and Feature Extraction .....	84
3.4	Statistical Analysis and Validation.....	87
3.5	Synthetic EEG Signals.....	88
3.6	Intelligent IQ-LS Classification Model .....	89
3.6.1	IQ-LS Dataset.....	90
3.6.2	Sample Size Requirement Analysis .....	91
3.6.3	Synthetic EEG Signals and Power Ratio Features Distribution Effects ..	92
3.6.4	Development of IQ-LS Classification Model using MIMO ANN.....	92
3.6.4.1	Parameter optimisation.....	93
3.6.4.2	Performance Measure and Test Fitting .....	94
3.6.4.2.1	IQ Evaluation Performance Setup.....	94
3.6.4.2.2	LS Evaluation Performance Setup .....	96
3.6.4.3	Correlation Function Test.....	97
<b>RESULTS.....</b>		<b>98</b>
4.1	Introduction.....	98
4.2	Samples Distribution of IQ and LS Dataset .....	98
4.3	EEG Signal Processing .....	101
4.4	Observation of PR Features on IQ and LS using Box Plot .....	106
4.4.1	IQ Analysis.....	106
4.4.2	LS Analysis .....	107
4.4.3	IQ-LS Analysis.....	108
4.5	Sample Size Requirement Analysis.....	110
4.6	Synthetic EEG Signals and PR Features Distribution Effects.....	112
4.6.1	Data Enhancement on IQ Analysis .....	113
4.6.2	Data Enhancement on LS Analysis .....	114

4.6.3	Data Enhancement on IQ-LS Analysis .....	115
4.7	EEG-Based IQ-LS Classification Model using MIMO MFNN (ANN).....	117
4.7.1	Parameter of the Network.....	118
4.7.2	Performance Measurement & Test Fitting .....	119
4.7.2.1	IQ Evaluation Performance .....	121
4.7.2.2	LS Evaluation Performance .....	125
4.7.3	Correlation Function Test.....	128
4.7.3.1	IQ Evaluation on Correlation Function Test .....	128
4.7.3.2	LS Evaluation on Correlation Function Test.....	131
4.7.4	Weights and Biases of the Network .....	133
	<b>DISCUSSION.....</b>	<b>135</b>
5.1	Introduction.....	135
5.2	IQ-LS Data Distribution .....	135
5.3	EEG Signal Processing Analysis .....	136
5.4	Evaluation on IQ Level and LS Group Analysis (N=85) .....	138
5.4.1	Intelligence Quotient Analysis .....	138
5.4.2	Learning Style Analysis .....	140
5.4.3	Intelligence Quotient and Learning Style Analysis.....	144
5.5	Evaluation on Synthetic Data Analysis (N=500) .....	147
5.6	IQ-LS Network Model Optimization Analysis .....	150
5.6.1	Parameter .....	151
5.6.2	Performance Measures and Test Fitting.....	153
5.6.2.1	IQ Evaluation Performance .....	153
5.6.2.2	LS Evaluation Performance .....	156
5.6.3	Correlation Function Tests .....	160
5.7	Summary.....	161

<b>CONCLUSION.....</b>	<b>163</b>
6.1 Conclusion.....	163
6.2 Limitations and Future Work .....	165
References .....	166
List of Publications and Papers Presented .....	202
Appendix .....	203

Universiti Malaya

## LIST OF FIGURES

Figure 2.1: The figure shown the International 10-20 Electrode System Placement (Sanei & Chambers, 2013). .....	16
Figure 2.2: EEG Brainwaves Signal from Various Frequency in Relax State with Closed Eyes Condition (Campisi, La Rocca, & Scarano, 2012). .....	19
Figure 2.3: Box plot interpretation.....	32
Figure 2.4: Neural network with multiple input nodes .....	41
Figure 2.5: Neural network layer with (a) single hidden layer and (b) multi hidden layers. ....	42
Figure 2.6: Recurrent neural network with multiple input nodes and multiple output nodes. ....	43
Figure 2.7: Common Multilayer Feedforward Neural Network (MFFN) with single hidden layer.....	45
Figure 2.8: Learning Style groups description (Kolb, 2007). .....	68
Figure 2.9: Mapping scores on learning mode cycle (Kolb, 2007). .....	71
Figure 2.10: Mapping scores on learning style grid (Kolb, 2007). .....	72
Figure 3.1: General concept of research methods.....	78
Figure 3.2: Summarization of the development EEG-Based IQ-LS Classification using MIMO ANN model.....	80
Figure 3.3: Distribution of highest education of all subjects participated in this study..	83
Figure 3.4: Methodology EEG tool experimental setup .....	83
Figure 3.5: Subject with experimental setup.....	84
Figure 3.6: Intelligent IQ-LS classification model network development.....	90
Figure 3.7: Probability density function (PDF) of white Gaussian noise. ....	92
Figure 4.1: Distribution of samples into three distinct IQ levels (85 samples).....	99
Figure 4.2: Distribution of samples in four distinct LS groups (85 samples) .....	100
Figure 4.3: Correlation between IQ level and LS group sample distribution. ....	100

Figure 4.4: EEG signal recorded; (a) Raw EEG signal approximately in three minutes duration, and (b) EEG signal after cut into 2 minutes 30 seconds. ....	101
Figure 4.5: Filtered EEG signal for theta, alpha and beta sub-band. ....	103
Figure 4.6: Power spectrum density (PSD) transformation of each sub-band frequency via EEG signal processes. The red colour indicates theta sub-band, blue colour indicate alpha sub-band and green colour indicates beta sub-band.....	104
Figure 4.7: (a) Energy spectrum density (ESD) transformation via power spectrum density (PSD) of each sub-band frequency and (b) power ratio (PR) feature transformation via energy spectrum density (ESD) of each sub-band frequency.....	105
Figure 4.8: Pattern and distribution of power ratio features for varying IQ levels (N=85). ....	106
Figure 4.9: Pattern and distribution of power ratio features for different learning styles (N=85). ....	107
Figure 4.10: Correlation among distinct LS groups and high IQ level referred (a) theta, (b) alpha and (c) beta sub-band PR. Div, Ass, Con and Acc are refer to Diverger, Assimilator, Converger and Accommodator, respectively. ....	108
Figure 4.11: Correlation among distinct LS groups and medium IQ level referred (a) theta, (b) alpha and (c) beta sub-band PR. Div, Ass, Con and Acc are refer to Diverger, Assimilator, Converger and Accommodator, respectively. ....	109
Figure 4.12: Correlation among distinct LS groups and low IQ level referred (a) theta, (b) alpha and (c) beta sub-band PR. Div and Acc are refer to Diverger and Accommodator, respectively. ....	110
Figure 4.13: Generated Random Array.....	112
Figure 4.14: Original data EEG signal and its Synthetic data EEG Signal with 30 dB SNR White Gaussian Noise, for 1000 Sampling Instances. ....	112
Figure 4.15: Pattern and distribution of power ratio features for varying IQ levels (N=500). ....	113
Figure 4.16: Pattern and distribution of power ratio features for different learning styles (N=500). ....	114
Figure 4.17: Correlation among distinct LS groups and high IQ level referred (a) theta, (b) alpha and (c) beta sub-band PR through synthetic data enchancement. Div, Ass, Con and Acc are refer to Diverger, Assimilator, Converger and Accommodator, respectively. ....	115

Figure 4.18: Correlation among distinct LS groups and medium IQ level referred (a) theta, (b) alpha and (c) beta sub-band PR through synthetic data enhancement. Div, Ass, Con and Acc are refer to Diverger, Assimilator, Converger and Accommodator, respectively. ....	116
Figure 4.19: Correlation among distinct LS groups and low IQ level referred (a) theta, (b) alpha and (c) beta sub-band PR through synthetic data enhancement. Div and Acc are refer to Diverger and Accommodator, respectively. ....	117
Figure 4.20: (a) IQ and LS training accuracy and (b) IQ and LS training MSE through the developed constructive algorithm using 40 repetition times for each cumulative hidden node. ....	119
Figure 4.21: Progression of network convergence. ....	120
Figure 4.22: Predicted and actual IQ (a) before Threshold (b) after Threshold in training dataset; (c) before threshold (d) after threshold in validation dataset; (e) before threshold (f) after threshold in testing dataset. ....	121
Figure 4.23: Predicted and Actual LS (a) Before Threshold (b) After Threshold in training Dataset; (c) Before Threshold (d) After Threshold in Validation Dataset; (f) Before Threshold (g) After Threshold in Testing Dataset. ....	125
Figure 4.24: Correlation function test results for IQ (a) ACF test result of final network model in training, validation, and testing datasets (b) CCF test result of final network model in training, validation, and testing datasets. ....	129
Figure 4.25: IQ Regression Plot for Training, Validation and Testing Datasets. ....	130
Figure 4.26: Correlation function test results for LS (a) ACF test result of final network model in training, validation, and testing datasets (b) CCF test result of final network model in training, validation, and testing datasets. ....	131
Figure 4.27: LS Regression Plot for Training, Validation and Testing Datasets. ....	132
Figure 5.1: Dataset for LS groups, where accommodator union with diverger, while assimilator union with converger in universal set. ....	143

## LIST OF TABLES

Table 2.1: Brainwaves Characteristic Via Certain Sub-Band Frequency. ....	19
Table 2.2: EEG applications and description. ....	29
Table 2.3: Advantages and limitations of several AI techniques.....	36
Table 2.4: Confusion Matrix via Evaluation Performance on First Level. ....	59
Table 2.5: Confusion Matrix via Evaluation Performance on Second Level. ....	59
Table 2.6: Overview group type of Kolb's learning style and combination of learning modes with their characteristics respectively.....	70
Table 2.7: Correlations between learning styles and brainwave pattern through related previous studies.....	73
Table 3.1: IQ Level and IQ Indicator through Threshold Limit for the Prediction .....	95
Table 3.2: LS and LS Indicator through Threshold Limit for the Prediction .....	96
Table 4.1: Particular learning style score assessment through learning style grid.....	99
Table 4.2: Minimum sample size evaluation via theta, alpha and beta power ratios. ....	111
Table 4.3: Final parameters of neural network. ....	118
Table 4.4: Accuracy and MSE of selected final network in training, validation and testing datasets. ....	122
Table 4.5: Precision and sensitivity of overall accuracy for each IQ group samples. ...	122
Table 4.6: Accuracy and MSE of selected final network in training, validation and testing datasets. ....	126
Table 4.7: Precision and sensitivity of overall accuracy for each LS group.....	126
Table 4.8: Neural network weights connecting from input nodes to hidden nodes, and from hidden nodes to output nodes .....	133
Table 4.9: Biases at hidden nodes and output nodes.....	134
Table 5.1: Accuracy and MSE of IQ and LS through training, validation and testing. ....	161
Table 5.2: Precision and sensitivity of overall accuracy for each group samples.....	162

## LIST OF SYMBOLS AND ABBREVIATIONS

ACF	:	Auto Correlation Function
AI	:	Artificial intelligence
ANN	:	Artificial neural network
BCI	:	Brain-computer interfaces
CCF	:	Cross Correlation Function
CT	:	Computerized tomography
ECG	:	Electrocardiograph
EEG	:	Electroencephalogram
ELT	:	Experiential learning theory
EMG	:	Electromyography
EOG	:	Electrooculogram
ES	:	Early stopping
ESD	:	Energy spectral density
FFNN	:	Feed-forward neural networks
FFT	:	Fast Fourier Transform
FIR	:	Finite impulse response
GA	:	Genetic algorithms
IIR	:	Infinite impulse response
IQ	:	Intelligence quotient
ISP	:	Intelligent signal processing
K+	:	Potassium
KLSI	:	Kolb's Learning Style Inventory
LM	:	Levenberg-Marquardt
LS	:	Learning style



LTI	:	Linear time invariant
MFFN	:	Multilayer feedforward neural network
MIMO	:	Multiple input multiple output
MISO	:	Multiple-input single-output
MRI	:	Magnetic resonance imaging
MSE	:	Mean Square Errors
Na <sup>+</sup>	:	Sodium
PDF	:	Probability density function
PET	:	Positron emission tomography
PSD	:	Power spectrum density
RNN	:	Recurrent neural networks
RPM	:	Raven's Progressive Matrices
SFFN	:	single layer feed forward neural network
SIMO	:	Single-input multiple-output
SISO	:	Single-input single-output
SNR	:	Signal noise ratio
SVM	:	Support vector machines
tansig	:	tangent sigmoid

## LIST OF APPENDICES

APPENDIX A: CONSENT FORM .....	203
APPENDIX B: EEG SIGNAL PRE-PROCESSING AND FILTERING .....	206
APPENDIX C: ESD AND PR FEATURE SELECTION AND EXTRACTION .....	208
APPENDIX D: SYNTHETIC DATA GENERATION VIA WHITE GAUSSION NOISE .....	209
APPENDIX E: IQ-LS CLASSIFICATION MODEL USING PR FEATURES .....	210
APPENDIX F: OPTIMUM HIDDEN NEURON NUMBER VIA CONSTRUCTIVE ALGORITHM.....	223
APPENDIX G: MODEL CLASSIFICATION FUNCTION VIA CONSTRUCTIVE ALGORITHM.....	225
APPENDIX H: OPTIMUM PERFORMANCE MODEL SELECTION .....	233
APPENDIX I: EARLY STOPPING PERFORMANCE VALIDATION.....	234
APPENDIX J: PREDICTION ERROR (IQ AND LS).....	235
APPENDIX K: KLSI QUESTIONNAIRE .....	236

## INTRODUCTION

### 1.1 Overview

Human brain is a complex organ and a part of Central Nervous System (CNS), which controls all body functions and interprets information (Jisna, Varghese, Wilson, & Bineesh, 2017). Researches approach in neuroscience through human brain, associated with behavior and mental processes experimented progressively, thus making it possible for researchers to explore widely on psychological study related to brain activity (Bartholow, 2018; Dias et al., 2015; Goodwin et al., 2018). Literatures related to psychology have been published since the 1960s in various fields, ranging from motivation, social psychology, health psychology to cognitive psychology (Silvia, 2015). In this particular research, cognitive psychology introduces an essential new look at intelligence (Holinka, 2015) and learning style (Grey, Williams, & Rebuschat, 2015), in line with cognitive abilities and cognitive processes affecting problem solving and reasoning.

Cognitive ability is defined as characteristic approach of the brain to process information (Neubauer & Fink, 2009a) while cognitive processes are associated with brain activity conversion and functional connectivity (Medaglia, Lynall, & Bassett, 2015). The ability is comprised of diverse range of mental constructs such as intelligence (Duncan et al., 2000) and learning styles (Felder, 1988). Intelligence research approaches learning were analyzed thoroughly comprising of diversity concern problems such as academic achievement, learning disabilities and neurodevelopment disorders (Rashid et al., 2011). Each of these mental constructs has contributed much to the field of psychology and education.

Intelligences and learning styles play crucial role in education learning sector and employment sector. Different individual preferences and intelligences will lead to

development a specific strength style of learning (Tee, Widad, & Yee, 2009). Currently, both intelligence (Crawford, Allan, Stephen, Parker, & Besson, 1989) and learning style (Cassidy, 2004) are assessed using conventional psychometric assessment methods. Among the psychometric tests for intelligence, Raven's Progressive Matrices is most widely used because it is related to fluid intelligence and avoids from some critical issues such as usage of crystallized intelligence, where the intelligence can be improved via knowledge acquired prior learning (Birney, Beckmann, Beckmann, & Double, 2017; Brouwers, Van de Vijver, & Van Hemert, 2009). Meanwhile for learning style, Kolb's Learning style is the best-known style that is widely used by providing a foundation for understanding experiential learning (Duff, 2004; Manolis et al., 2013; Mestre & Mestre, 2012; Poore, Cullen, & Schaar, 2014). In addition, identification of learning style in an individual will enhance a better and more effective learning environment, but it all depends on intelligence suitability of each individual (Grasha, Claxton, & Murrell, 2006; Irving & Williams, 1995; Tee et al., 2009).

Electroencephalogram (EEG) is a non-invasive brain imaging approach that can be categorised as low-cost, economical with convenient measurement technique compared to other modalities in analysing physiological changes related to brain function (Jahidin, 2015). In clinical, EEG is known for tracking how activity in neural circuits creates the different EEG features connected to brain cognition (Cohen, 2017a). Implementation of EEG includes interdisciplinary research that extends to neuroscientific, computation and clinical areas (Cohen, 2017a; Le Van Quyen, 2011; Niedermeyer, 2003; Varela, Lachaux, Rodriguez, & Martinerie, 2001). Presently, EEG signals analysis are incorporated with intelligent signal processing (ISP) approach which takes out greatest information as possible from signal data using smart technique (Gass et al., 1987; Simon Haykin & Kosko, 1998; Jahidin et al., 2015; Papp, Peceli, Bago, & Pataki, 1988). ISP techniques include genetic algorithms (GA), fuzzy rule-based systems, artificial neural network (ANN) and systems of

artificial intelligence (AI) (S. Haykin & Kosko, 1998b; Jahidin et al., 2015). Lately, adaptive ANN has been the most popular and most successful modelling method in biomedical application, specifically in pattern recognition areas (Gajic, Djurovic, Di Gennaro, & Gustafsson, 2014; Göksu, 2018; Jahidin et al., 2015; T. S. Kumar, Kanhangad, & Pachori, 2015; Pachori & Patidar, 2014; Pardo & Sberveglieri, 2002; G. P. Zhang, 2000). The advantage of using ANN as classifiers is its capability to learn and generalize the complex problems solution and provide good performance (I. Y. Khan, Zope, & Suralkar, 2013; Tu, 1996; Verpoort, MacDonald, & Conduit, 2018).

The correlation among EEG, IQ and learning style (LS) exists separately in previous studies (Anokhin & Vogel, 1996; Davidson et al., 1990; Doppelmayr et al., 2002; Doppelmayr et al., 2005; Jaušovec, 1998, 2000; Kounios et al., 2008; Lutzenberger, Birbaumer, Flor, Rockstroh, & Elbert, 1992; Megat Ali, Jahidin, Md Tahir, & Taib, 2014; Megat Ali, Jahidin, Taib, & Md Tahir, 2016; Neubauer & Fink, 2009a; Ono, Mameya, Shimada, & Yamashita, 1982; Rashid et al., 2011; Vernon, 1984). Based on EEG and IQ correlation studies, significant findings were investigated in the tonic state and in the absence of cognitive demanding task (Langer et al., 2012; Lee, Wu, Yu, Wu, & Chen, 2012; Wang, Song, Jiang, Zhang, & Yu, 2011). Meanwhile, based on EEG and learning style (LS) correlation studies, significant findings were observed in resting condition with default of cognitive particular task (Megat Ali, Jahidin, Md Tahir, et al., 2014; Megat Ali, Jahidin, Taib, & Md Tahir, 2016; Rashid et al., 2011). Previously, the studies had also shown that the individuals' intelligent differences can be demonstrated particularly at prefrontal cortex brain areas (Blair, Gamson, Thorne, & Baker, 2005; Fink et al., 2009; Gray, Chabris, & Braver, 2003; Gray & Thompson, 2004; Neubauer & Fink, 2009a; Neubauer, Fink, & Schrausser, 2002; Neubauer, Grabner, Fink, & Neuper, 2005; Staudt & Neubauer, 2006). Furthermore, it is found that the left side of brain hemisphere is more dominant compared to the right side in cognitive task performance (Deary, Penke, & Johnson, 2010). Hence, this shows a great opportunity exists among EEG, IQ and LS as stated above.

Conclusively, knowing human intelligent and learner's learning style impacts economic growth in scope of policies, work life balance, employment, education, health, market efficiency, market development, technology and innovation (Schwab, 2017). Besides that, this research also gives positive effect on social development as matching intelligent and learning style of the individual with social environment. Hence, the human cognitive abilities are important for characterising to allow the individuals to fully utilize their ideal potential at an optimal level.

## **1.2 Problem Statement**

The study has thus far identified three major gaps in the literature and proposes to address those issues. First, while studies have established an alternative technique to assess IQ and learning styles from resting brainwaves, the feature extraction methods are not fully standardized. Second, a unified computational model that assesses both traits of cognition is also yet to be established. Third, a cross-relational analysis between varying IQ levels and learning styles based on brainwave patterns is yet to be confirmed. By solving these issues, the proposed technique is expected to eliminate issues faced by psychologists when using conventional psychometric tests.

In the past, there were already attempts to relate cognitive behavior with EEG (Abdul Rashid, Taib, Lias, & Sulaiman, 2010). The studies however, were based on unconfirmed theories and contradicted the Neural Efficiency Hypothesis in terms of cortical activation behavior (Rashid et al., 2011). Such incongruities would, therefore, require major re-evaluation and should be validated by a stronger body of literature. The study has thus outlined three objectives. First, a standardized feature extraction algorithm for IQ and LS analysis from brainwaves will need to be established. Second, this research needs to develop a unified computational model for assessing both IQ and LS simultaneously with

optimum performance. Finally, the cross-relational analysis verification of brainwave patterns between both traits of cognition will also be required. These present a completely new perspective in which the work attempts to bridge fundamental aspects of brain behavior and the field of psychology via standardized assessment protocols based on EEG and an integrated computational model.

### **1.3 Research Objectives**

The main objective of this research is to develop an intelligent IQ-learning style classification model using brainwave features integrated with artificial neural network.

To achieve main objective, this research has been segregated into several supporting objectives as follows:

1. to develop feature extraction algorithms for IQ and LS analysis from brainwaves,
2. to identify the most optimum computational model in assessing both IQ and LS, and
3. to evaluate and validate the effectiveness of the proposed method in characterising IQ and LS of an individual.

### **1.4 Scope of Work**

The experimental work will revolve around a properly constructed data collection and recording protocols. Apart from that, extensive review will be conducted on scopes of human intelligence, experiential learning, EEG signal pre-processing and feature extraction, statistical analysis, and artificial neural network. The scope of this work is in

respect to experiment protocol approved by the University's Research Ethics Committee and limited as the following:

- i. The participants are limited to Malaysian subjects from different disciplines and professions.
- ii. Age ranges between 17 to 40 years old.
- iii. Healthy and not on prescribed medications.
- iv. EEG signals data are recorded using Neurosky Mobile Wave headset.
- v. EEG signals data are recorded in resting closed-eyes condition for 3 minutes.
- vi. EEG signals are recorded from the left prefrontal cortex.
- vii. IQ control groups are determined by IQ Classification Model that is based on RPM.
- viii. The LS is based on Kolb's Learning Style Inventory (KLSI).
- ix. Data analysis relating to IQ and LS focus on left prefrontal cortex.
- x. Power ratio features will be used as input vectors to develop IQ and learning style classification model.
- xi. Multilayer feedforward network (MFFN) of artificial neural network (ANN) is chosen to develop IQ and learning style classification model.
- xii. Multiple input multiple output (MIMO) model structure is implemented comprising of three inputs (theta, alpha, beta ratio features) and two outputs (IQ levels and LS groups).

## **1.5 Significance of Research**

Based on research area, there are two significant impacts which have contributed in research knowledge. First, sub-band PR features extraction method are contributing to recognize unique patterns among IQ levels and LS groups. Subsequently, EEG-based IQ-LS classification model is developed using intelligent signal processing (ISP) by choosing



suitable type, architecture, and structure of ANN. This approach would remove the limitation of using conventional psychometric test rationally. Thus, the proposed scientific research will allow a crucial part in the neural bases of cognition.

Based on socio-economic area, the implications of this study will resolve the puzzle of human cognitive abilities characterization to allow the individuals to optimize their potential at an optimum level. The study aims at providing a significant impact in the following areas:

- In education sector, new teaching techniques that cater to individuals of difference IQ levels and learning styles are being developed. The proposed classification system is expected to assist instructors to accurately assess individual differences in preferred learning styles. These would allow them to implement suitable teaching approaches to optimize their learning experience.
- For companies in the private sector, this would certainly assist employers seeking suitable employee. Accurate knowledge on individual cognitive traits would allow the management team to select the best candidate for position with specific job descriptions.

## **1.6 Thesis organization**

The study is structured in five chapters as stated below:

Chapter 1 presents general overview of proposed work for IQ and LS classification via EEG sub-band feature using ANN. The problem statement is described as well as to present work which has been done previously and it has been resolved to achieve research objective. Then, this is followed by scope of work, significance of research and thesis organization.

Chapter 2 discusses the literature reviews which are related to the study. The literature concerns on human cognitive abilities, EEG advancements, and intelligent signal processing. An extension focusing on IQ, LS, and artificial neural network (ANN) has also been reviewed. Lastly, this chapter describes the proposed methodology used in this thesis.

Chapter 3 covers research methodology of five major stages which are formulation of experimental framework, data collection, statistical analysis and validation, and development of IQ-LS classification model using ANN.

Chapter 4 provides IQ and LS results of statistical analysis obtained from experimental work. The model results of training, testing and validation ANN system have also been provided.

Chapter 5 deliberates in-depth discussion of the research, comparing it to the previous findings. Correlation between IQ and LS of this study has been elaborated as well as the obtained results. Besides, discussion related to model development with system performance has been defined.

Chapter 6 describes the summarization of overall conclusion about the work done throughout the research in accomplishing the research objectives and recommends implication for future work.

## LITERATURE REVIEW

### 2.1 Introduction

This chapter elaborates the literature review on three major divisions which are neuroimaging modalities, intelligence signal processing and cognitive abilities of human brain. These three main areas are converging into specific area overview related to this research.

Based on neuroimaging modalities, EEG is selected as one of convenient, affordable, and non-invasive diagnostic tool to detect brain behaviors. Application of EEG and their signal processing are described in this chapter. Based on intelligence signal processing, we will explain in detail about artificial intelligence, artificial neural network structure, architecture, and its limitation. With reference to human brain cognitive abilities, the IQ and LS are also included in the cognitive abilities of human brain which are related to this research work. Each cognitive ability has unique characteristic, and they are correlated to each other in similarities or optimum way.

### 2.2 Neuroimaging Modalities

Neuroimaging is the utilization of different methods to either directly or indirectly representing the image structure or function of the nervous system, specifically of the brain (Buxton, 2002). Neuroimaging is segregated into two categories, which are structural imaging and functional imaging. Structural imaging utilizes the images of the anatomical brain structure, while functional imaging utilizes the images of the brain function by completing the task given. However, benefit of using functional imaging is to allow processing of the information by brain center to be envisioned directly (Genovese, Lazar, & Nichols, 2002). Throughout brain processing, the metabolism changing different localization of the brain are involved.

Nowadays, there are lots of methods to assist an investigation of correlation between neuroscience and human behaviors. Common modalities utilized with neuroimaging are magnetic resonance imaging (MRI), computerized tomography (CT) scan, positron emission tomography (PET), and electroencephalogram (EEG) (Waldman, Balthazard, & Peterson, 2011). There are advantages and disadvantages to various neuroimaging modalities through quantifying or qualifying views of the brain's physiology, anatomy, and activity.

MRI is a popular medical tool that uses a forceful magnetic field and radio waves to generate detailed brain images. In order to utilize this tool, circular arc of electromagnet is placed around human's head and MRI produces variant frequencies relying on specific atom location through interrupting atoms' nucleus in the brain (Rausch et al., 2017). MRI allows to utilize frequency information to produce a visual representation of human brain. Clinically, MRIs have been greatly applied to analyze blood clots, tissue degeneration, and tumors (Hara et al., 2018). Currently, there is an updated version of standard MRIs, known as the functional MRI scan (fMRI). The fMRI technique is a measure of brain activity by relying on changing cerebral blood flow or blood oxygen level dependence (BOLD) through neuronal activation (Huber et al., 2018). As a tool for IQ and LS, MRI is relatively limited due to efficiently focusing on brain anatomy rather than concern on psychology correlation, while fMRI is an indirect measure of neural activity, which relies on the cerebral blood flow itself and common procedure costly.

CT scan is particular X-ray analyzers that produce cross-sectional images by moving in a small circular arc penetrate through a patient's head using X-rays with assist of the computer (Messaris et al., 2018). The various X-ray intensities are utilized in order to analyze the density, location, and others to identifying the features. Clinically, CT scan was used in investigating clots, bleeding or blockages inside the brain such as distinct

density than common tissues are visualized via computer composite (Ambrose, 1973; Hounsfield, 1973). As a tool for IQ and LS, such MRI, CT scans are a limited form of neuroimaging because focus is on brain anatomy rather than concern on psychology behaviors.

PET is a medical tool that is used to detect metabolic or biochemical process in human body by nuclear medicine functional imaging technique (Ferda et al., 2017). PET detects emission of radiation by PET detector through injection of radioactive chemicals into the bloodstream metabolism (Lazor, Schmitt, Loevner, & Nabavizadeh, 2018). Based on emission positron via injection of radioactive solution, there are short monitoring causes of radioactivity decay rapidly (Gundlich, Musmann, Weber, Nix, & Semmler, 2006). Furthermore, screening procedure repetitions are impractical due to hazardous impact of radioactive solution consumption (Smith-Bindman et al., 2009). Emission data via chemical distribution can create 2-dimensional or 3-dimensional images by computer-processing (Gundlich et al., 2006). Previous studies showed that PET has been used to investigate attention and perception of the brain function (Pourtois, Schettino, & Vuilleumier, 2013). However, the radioactive represents an unnecessary or unwarranted risk for non-clinical research, specifically in psychology.

EEG is one of biopotential measurement devices, where this medical tool records and examines human electrophysiological through fluctuation of electrical activity because of ionic current within the neurons of the brain (Cohen, 2017b). EEG can analyse changes in brain activity and helpful to detecting, diagnose or treat brain disorder. Basically, the brainwaves need to be segregated into several sub-band frequencies for analysis depend on selection of feature. There are numerous methods to analyse the brainwaves, especially towards amplitude and frequency. The advantage of using this medical tool is convenient, affordable, and non-invasive diagnostic tool to detect brain behaviours.

Among these neuroimaging modalities, there are pros and cons in analyzing brain behaviours. CT, PET, and fMRI/MRI are commonly measuring the brain activity through blood flow dynamics with assist of EEG in neuronal activity. During metabolism activity, the instant synaptic activity or electrical impulses are taking place before resultant of blood flow changes. Thus, EEG has better real-time system and is more robust for data analysis. EEG is also highly portable, mobilized, and inexpensive in comparison to MRI, CT scan, PET, and fMRI, which need unnatural setup. Although CT, PET and MRI/fMRI have higher spatial resolution than EEG, EEG provides higher temporal resolution compared to others. Furthermore, EEG is relatively non-invasive medical tool and does not cause any dangerous effects on human health. As a conclusion, EEG applications are emerging in this study as this tool allows comfortable and safe assessment for research participants.

### **2.3 Biopotential Measurement Devices**

Biopotential is defined as an electric potential that is produced by a combination of various cells with accompanies of biochemical process (Yazıcıoğlu, Van Hoof, & Puers, 2009). Biologically, the action potential of cells is activated when the cells are stimulated from resting membrane state and this allows each cell to interchange molecules ions passing via the membrane. Resting potential is membrane potential of the cell in passive condition. During this condition, the concentration of potassium ( $K^+$ ) in the interior cell is higher compared to exterior and allows the cell to be more permeable to potassium ions ( $K^+$ ) than sodium ions ( $Na^+$ ). Through this chemical gradient, the interior of cell membrane builds up electrical field more negative than exterior. Diffusion gradient of potassium ions are stabilized by electrical field and the polarization voltage of cell polarized at around  $-70mV$ . During electrical potential being activated via central nervous

system, the cell membrane increases its permeability to sodium ions. The sodium ions diffuse into interior cell which effect the potential to increase. When depolarization voltage achieves +40mV, potassium ions start increasing again while sodium ions decrease in cell membrane interior causing the membrane potential back to rest state known as repolarization. This cycle of electrical impulse of cell is known as action potential. These electrical impulses can be captured by using biopotential measurement devices such electrocardiogram (ECG), electromyography (EMG) and electroencephalography (EEG) (Caldwell, 2010).

Electrocardiograph (ECG) is a biopotential measurement device that records the electrical impulse through the heart over a period of duration. ECG electrodes identify the electrical impulse through the skin that arise by electrophysiologic cardiac cells. This is done from the depolarizing and repolarizing potential. Commonly, the electrical activity is involved temporally with mechanical activity for heart rhythm. Depolarization electrical potential causes cardiac muscles to contract, meanwhile repolarization electrical potential caused cardiac muscles to relax. Sinoatrial node and atrioventricular node play crucial role in electrical impulses for mechanical cardiac activity. Based on electropsychological waves, it is convenient to diagnose any cardiac problems.

Electromyograph (EMG) is a biopotential measurement device that records the electrical impulse through skeletal muscle or motor neurons. To record it, the EMG electrodes are placed near to interest and particular neuromuscular location. Electrical potential depolarization of motor neurons causes muscle contraction, whereas electrical potential repolarization of motor neurons causes muscle relaxation. The implementation of EMG is widely used in clinical and biomedical application. Generally, EMG is used for diagnostic tool and research tool related to kinesiology and neuromuscular field. EMG signals are benefited to diagnose muscle abnormalities or nerve dysfunction and are

currently utilized for application involved in electrical impulse measurement through gastrointestinal peristaltic movements. Nowadays, EMG is integrated with prosthetic devices such prosthetic limb by adapting with control signal to help disability patient.

Electroencephalograph (EEG) is a biopotential measurement device that records the electrical impulse through brain scalp. To record it, the highly sensitive electrode sensor is placed through the scalp surface to obtain brainwaves data. In addition, the brainwaves data are recorded numerous times per second and make EEG highly temporally precise (Babusiak, Borik, & Balogova, 2018). The brainwaves signal was gained by addition of dendrite synaptic currents activated on billions of neurons which are located under a few centimeters of the scalp surface (K. Kim et al., 2014). Normal functioning human brainwaves are divided into five sub-band frequencies which are, delta (1 - 4 Hz), theta (4 - 8 Hz), alpha (8 - 12 Hz), beta (12 - 30 Hz), and gamma (30 - 100 Hz) band waves (S.-K. Kim & Kang, 2018). Throughout these brainwaves, there are a lot of methods to analyze the brainwaves, especially toward amplitude and frequency, and are currently generated into graphical image of electrophysiological activity.

Obviously, the crucial things in electrical signal through ECG, EMG and EEG recording are frequency and amplitude characterizations. To extract the features of raw biopotential signal, the raw electrical signal needs to pre-process before obtaining the real signal information. This topic will explain this further in more detail throughout the literature review. Cognitive abilities such intelligence and learning style are in respect to brain and neglect other human body. Integration of EEG with the brain studies, cognitive studies or psychology studies give impact to research knowledges related to undiscovered complexity of human brain.



## 2.4 Electroencephalogram (EEG)

The beginning of electroencephalogram (EEG), was to investigate the electrical activity through rabbits and monkeys brain by Richard Caton (Niedermeyer & Schomer, 2011; Piccolino, 1997; Swartz & Goldensohn, 1998). Subsequently, German neuropsychiatrist, Hans Berger (Barwick, 1971) had investigated the electrical activity through human brain or cerebral cortex and the approach begin by attaching electrodes to the scalp and a galvanometer (La Vaque, 1999; Leiser, Dunlop, Bowlby, & Devilbiss, 2011; Millett, 2001). However, this application is not a well-known practice in healthcare fields. In 1934, Adrian and Matthews replicated the Beiger's research work until it became acceptable in healthcare field to diagnose brain condition (Adrian & Matthews, 1934; Adrian & Yamagiwa, 1935; Panteliadis, Vassilyadi, Fehlert, & Hagel, 2017). Nowadays, EEG has been adopted in various field such marketing, psychology (Martins & Szrek, 2019), neuroscience, clinical, psychiatric (Michel et al., 2004) and brain computer interfaces (Jeunet, Glize, McGonigal, Batail, & Micoulaud-Franchi, 2018).

EEG is essentially a non-invasive electrical recording of brain activities. Despite its poor spatial resolution (Srinivasan, 1999), EEG is still considered an efficient method for measuring brainwaves. Its' advantages include non-invasiveness (J. Webster, 2009), minimal risk exposure, very high temporal resolution, versatile (Bunge & Kahn, 2010) and a low-cost alternative (DellaBadia, Bell, Keyes, Mathews, & Glazier, 2002). Miniaturization of electronic components has resulted in the development of wearable devices increasing its efficiency (Casson, Yates, Smith, Duncan, & Rodriguez-Villegas, 2010). Furthermore, the International 10-20 System for electrode placement has allowed efficient localization of brain activity on the scalp (Ives-Deliperi & Butler, 2018). The figure below shows the International 10-20 System for electrode placement by placement for each channel to analyze the interest brain functions.

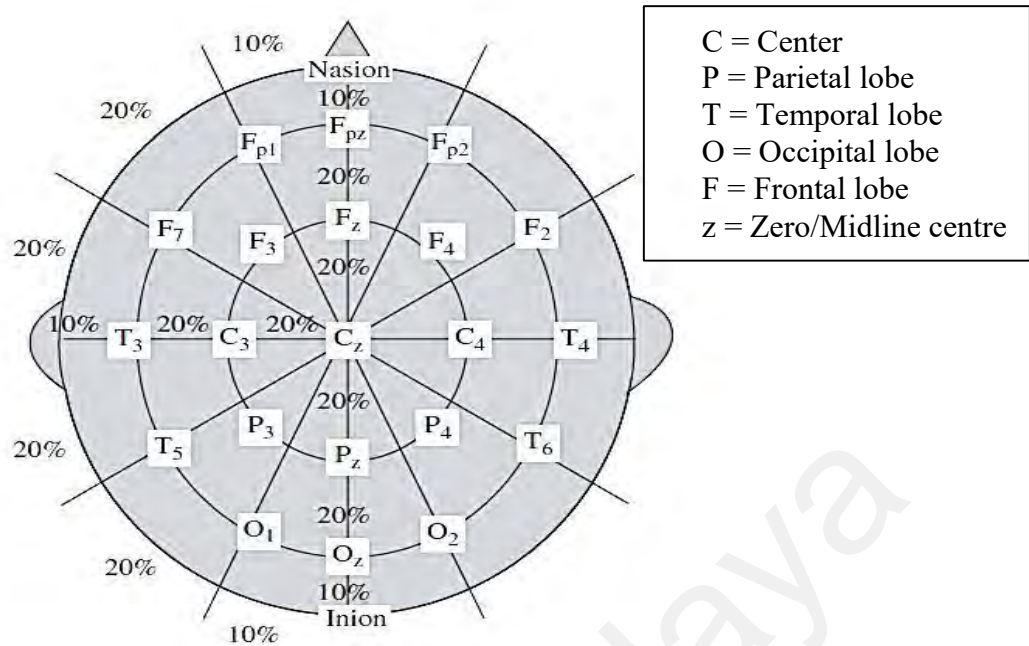


**Figure 2.1: The figure shown the International 10-20 Electrode System Placement (Sanei & Chambers, 2013).**

International 10-20 Electrode System Placement is internationally acknowledged technique utilized to illustrate the exact and standard electrode location. This system is commonly more limited in its capacity to record and not to respect anatomical function consideration such Brodmann areas concept. Based on measurement, the straight line, circular line and “10-20” number as in the figure 2.1, represents length percentages of 10 percent or 20 percent between two midlines. The brain center can be measured through nasion to inion in vertically and left preauricular to right preauricular horizontally. Nasion was located in between forehead and nose, meanwhile inion was located at end skull of back brain. As human has various range head size and anatomy, the percentage localization basing is efficient and maintains well the relationship between brain region and skull anatomy rather than having fixed distances localization basing.

Based on the letters around the brain illustration shown in the figure above, C letter known for brain center, P letter known for parietal lobe, T letter known for temporal lobe, O letter known for occipital lobe, and F letter is known for frontal lobe. Meanwhile, Fp letter is known for front-polar or prefrontal which integrated with F letter. However, C letter is known for front-polar or prefrontal which integrated with F letter. However, C letter approximately doesn't have center lobe and in between frontal and parietal lobe. Basically, C letter label is used to determine brain center through skull purposes only and z letter known as zero refers to midline center. Based on numbers around the brain illustration as figure above, the left side of the brain contain with odd numbers begin from 1, 3, 5 and 7, meanwhile the right side of the brain contain with even numbers start from 2, 4, 6 and 8.

Electrode impedance in research practices was stated to maintain below than 5 k $\Omega$  to acceptable minimum mismatch impedance between references and common electrode during EEG recording (Ferree, Luu, Russell, & Tucker, 2001). Commonly, 0.5 to 100 Hz was pre-amplified to remove direct current (DC) offset, meanwhile notch filter was used to remove power line interference whether 50Hz or 60 Hz notch (Kappel, Rank, Toft, Andersen, & Kidmose, 2019). Sampling rate of EEG signal was captured whether 128, 256 or 512 Hz based on EEG instrument itself.

Currently, EEG implementation outspread is utilized along with human knowledge and modern technology progression. Throughout modern centuries, EEG was adopted successfully with neuroimaging to record neuronal electrical activities. The concentration of neuronal activation effected various brainwave frequencies. Every single frequency has its unique characterization, thus advantageous to diagnose normal and abnormal human state (Casson et al., 2010). In addition, an uneven brainwave is commonly produced between 0.5 Hz until 100 Hz of frequency range. Generally, it can be divided into delta (0.5 Hz – 4 Hz), theta (4 Hz – 8 Hz), alpha (8 Hz – 13 Hz), beta (13 Hz – 30

Hz) and gamma (30 Hz to 45 Hz) waves (Cohen, 2017c). It is also found that each of the frequency bands contain exclusive information related to the mental processes (Hanslmayr, Sauseng, Doppelmayr, Schabus, & Klimesch, 2005; Harmony et al., 1996; Klimesch, 1999; Posthuma, Neale, Boomsma, & De Geus, 2001; Schmid, Tirsch, & Scherb, 2002; Thatcher, North, & Biver, 2005; Vakili, Tehranchian, Tajziehchi, Mohammad Rezazadeh, & Wang, 2012; Wróbel, 2000). Delta waves are dominant in deep sleep while theta waves are evident in light sleep (J. G. Webster, 2009). Meanwhile, alpha waves are visible during wakeful but resting condition (J. G. Webster, 2009). Conversely, beta waves become dominant when the brain is engaged in intense mental activity (J. G. Webster, 2009). Last but not least, gamma waves are less utilized in cognitive studies and commonly involved in active sensory processing (Cohen, 2017c). As this study will investigate in closed-eyes resting state, theta wave, alpha wave and beta wave are involved.

Table 2.1 shows the summarization of brainwaves through sub-band frequency for theta, alpha and beta wave. The uneven waves can be obtained among these waves as the frequencies will be activated via different brain condition. Meanwhile, Figure 2.2 shows the EEG rhythms or waves through sub-band frequency.

**Table 2.1: Brainwaves Characteristic Via Certain Sub-Band Frequency.**

Brainwaves	Brief Characteristic and Applications
Theta wave (4 - 8 Hz)	This wave is related to unconscious, creative and deep meditation state. Greater intensity of theta wave obtained during conscious state showed abnormal by cause of different pathological issues. Lowest intensity of theta waves obtained during awake or in light sleep condition showed drowsiness approach. Furthermore, mental and attention processes have also been investigated via this wave (Anokhin, Lutzenberger, & Birbaumer, 1999; Sanei & Chambers, 2013).
Alpha wave (8 - 13 Hz)	This wave is related to conscious, relax and alert state. Greater intensity of alpha wave obtained during relax state such being relax and closed eyes condition. Meanwhile, lower intensity of alpha wave is obtained during alertness mental activity activation such opened eyes, mental concentration and attention (Pivik et al., 1993; Sanei & Chambers, 2013).
Beta wave (13 - 30 Hz)	This wave is related to conscious, focus, active thinking, and active attention. Greater intensity of beta wave is obtained during human panic condition. Furthermore, higher beta waves are associated with intense mental and can activate in higher frequency (Sanei & Chambers, 2013; J. Webster, 2009).

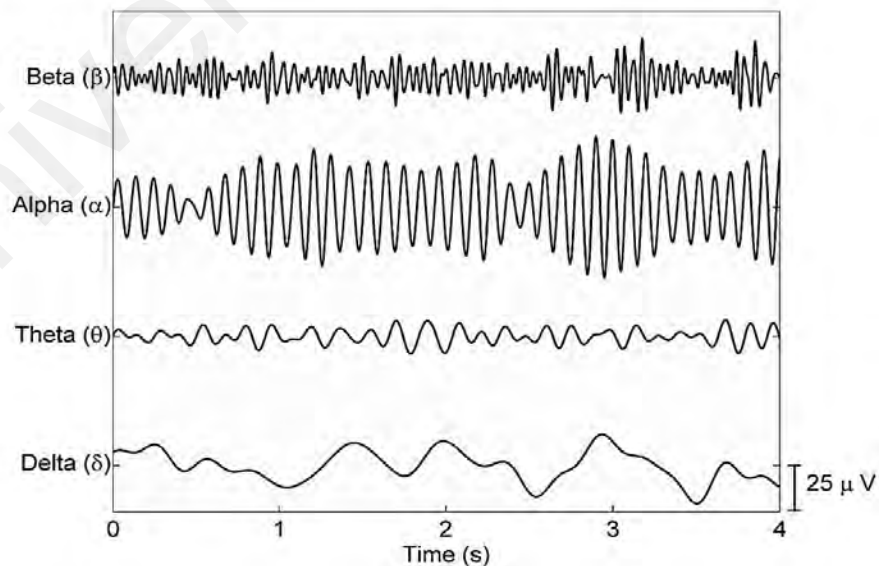


**Figure 2.2: EEG Brainwaves Signal from Various Frequency in Relax State with Closed Eyes Condition (Campisi, La Rocca, & Scarano, 2012).**

### 2.4.1 EEG Dry Electrode Approach

EEG electrode models are divided into two types, which are wet electrode (gel-based electrode) and dry electrode (gel-free electrode). Clinically, wet electrode is well-known EEG recording and has become “gold standard” practice due to high reliability and ideal signal to noise ratio. Nevertheless, EEG setup and preparation for wet electrode is time-consuming and requires EEG specialist staff (Teplan, 2008). Furthermore, the gel based electrode caused discomfort via dirty conductive gel and hair damage for the users (Liao et al., 2012; Searle & Kirkup, 2000). Regardless of reliable signals in clinical field, the uncomfortable and inconvenience problems of wet electrode limit the prominent application of EEG in other fields.

To solve wet electrode issues, previous researchers take an approach to create dry electrodes. Dry electrode commonly made by silver/silver chloride (Ag/AgCl) which is electronic conductor and does not require conductive gel. Confidently, using dry electrode give benefit through fast setup, clean setup, convenience with user and self-application through rejection of conductive gels. However, there are several issues related to dry electrode such as electrode-skin impedance and scalp abrasion, but now such effects have now been minimized. Along current technology, EEG instrumentation has been upgrading to achieved high-quality EEG recordings and to obtain actual signal.

First issue of dry electrode is related to electrode-skin impedance. As dry electrode do not use conductive gel or electrolyte, commonly dry electrode has high electrode-skin impedance. As wet electrode has a few kilo Ohms, an electric current flows through an impedance, there is low and acceptable potential drop in comparison to dry electrode which has several hundreds of kilo Ohms or even greater (Li, Wang, & Duan, 2017). Cristian et al. reported that the minimum dry electrode impedance without skin preparation is around 80 k $\Omega$  (Grozea, Voinescu, & Fazli, 2011; Kitoko, Nguyen, Nguyen,

Tran, & Nguyen, 2011). Furthermore, dry electrode is rigid, which cannot fix on skin surface, thus making it an unstable interface position and sensitive through motion noise (Yao & Zhu, 2016). Consequently, the EEG signals produce weak signal quality (Chi, Jung, & Cauwenberghs, 2010; Fatoorechi et al., 2015; Kappenman & Luck, 2010; Mota et al., 2013; Tautan et al., 2014).

In order to solve this issue, the utilization of preamplification inside the electrode (active electrode) was required to improve signal quality (Fonseca et al., 2007; Guger, Krausz, Allison, & Edlinger, 2012; Mullen et al., 2015; Ribeiro, Fu, Carlós, & Cunha, 2011; Sellers et al., 2009; Tsai, Hu, Kuo, & Shyu, 2009). Active electrode makes the pre-amplified signal minimize as much the effect of environmental noise (Mota et al., 2013). Safety protection is also confidently guaranteed due to having high impedance, thus high the isolation barrier. In this case, electrocution can be avoided compared to using the passive electrode. Nowadays, 'isolated common' electrode is implemented in modern amplifiers to isolate the electrical from ground of power supply. Thus, the potential difference just measured between reference electrode and common electrode through pre-amplified. However, active electrodes utilization is large and expensive (Mota et al., 2013).

Second issue of certain dry electrode is scalp abrasion requirement to reduced impedance. During scalp abrasion, skin wound can occur and sharing non-sterile electrode caused infection due to blood product contact (Ferree et al., 2001). Based on Center for Disease Control and Prevention guidelines, sterilized electrodes are required for contact of broken skin. Clinically, to use it for new patient, sterile processing is required for usable electrode or use the new sterile electrode. Thus, this technique consumes money to ensure the material is sterile. Other fields are avoided from skin abrasion to avoid infection risk and commonly choose wet electrode to investigate.

Modernly, Chaudhari & Patil present that without scalp abrasion, high quality EEG signal can be gained through having input impedances much greater than the scalp-electrode impedances (Chaudhari & Patil, 2015).

Nowadays, developed EEG instrumentation is applied for these advancements to have high-quality EEG recordings and actual signal. Previous study suggests around  $40\text{k}\Omega$  until  $200\text{k}\Omega$  of scalp-electrode impedance for accurate signal ( $\approx 0.1\%$  error) through high input impedances (Ferree et al., 2001). Furthermore, by avoiding skin abrasion which has infection risk, modern EEG instrumentation has underpinned with new dry electrode advances without skin abrasion. Based on psychology scope, the modern EEG instrumentation are benefitting to ensure human safety, comfortable and convenience.

## **2.4.2 EEG Signal Processing**

In biomedical engineering, EEG signal processing analysis and method are crucial to understand. The significance of EEG signal processing in this study are artifact removal, artifact filtering, feature selection, feature extraction, classification, and modelling. There are separation parts that review in detail and are related to sub-scope of EEG signal processing.

### **2.4.2.1 EEG Pre-Processing**

To obtain good performance of model classification, an appropriate EEG signal processing is important. EEG pre-processing refers to preliminary processing data by rejecting noise to obtain actual neural signal. There are some purposes for conducting EEG data pre-process. Firstly, EEG signal is commonly electrical sensitive and there are a lot of artifacts or noise influences. Secondly, relevant neural signal separation



requirement is needed to split the random neural activity. Finally, as EEG recordings are worst in spatial resolution, the whole brainwave signals are not much accurate and need pre-processing.

In signal processing, artifacts known as noises or errors that occur by undesirable signal, influence the actual neurological signal. EEG artifacts can be divided into two parts which are environmental and biological part. Rejection of artefact needs to be handled carefully as it's crucial to have original neurological signal (Anderer et al., 1999). Previous studies represent that the artifact produces amplitude exceeding from the ranges of  $\pm 50 \mu\text{V}$  to  $\pm 100 \mu\text{V}$  (Croft & Barry, 2000; Schlögl et al., 2007). These artifacts produced by different sources, such as main power line, electrical noise, muscle movement, eye movements or heartbeat, affected the EEG signal (Fatourehchi, Bashashati, Ward, & Birch, 2007; Schlögl et al., 2007). Commonly electrooculogram (EOG) and electromyogram (EMG) affect EEG signal. EOG refers to a biopotential measurement that records the electrical impulse through cornea and ocular fundus meanwhile EMG refers to biopotential measurement that records the electrical impulse through skeletal muscle or motor neurons. EOG affected EEG through eye blink or eye movements contamination (Fatourehchi et al., 2007; Schlögl et al., 2007), where alpha wave was certainly sensitive to eye blink (Croft & Barry, 2000). Besides, EMG affected EEG through body, head, face, tongue movement, swallowing and includes heartbeat (Anderer et al., 1999; Fatourehchi et al., 2007). In order to manage the artifacts, the implementation of automatic rejection, manual rejection, principal component analysis (PCA) and independent component analysis (ICA) helped to gain actual signal which was free from artifacts (Anderer et al., 1999; Çiçek & Naçac, 2001; Debener et al., 2000; M. Doppelmayr et al., 2002; Fatourehchi et al., 2007; Howells, Ives-Deliperi, Horn, & Stein, 2012; L. Li, 2010; Thatcher, North, & Biver, 2008). In spite of other methods, automatic

rejection approach through instrumentation itself is enough to reject artifact without require EOG and EMG during EEG recording (Fatourechhi et al., 2007).

Furthermore, implementation of band pass filters are used to enhance signal noise ratio (SNR) performance and minimize noise (Abdulkader, Atia, & Mostafa, 2015). Increasing the SNR by increasing the signal and decreasing the noise is one way to have better spatial and temporal resolution. There are some methods of spatial filtering which, these methods have integrated by the instrumentation itself (McFarland, McCane, David, & Wolpaw, 1997). Furthermore, distinct instrumentation and distinct authors have their own distinct range of band pass filter and spatial filter methods (J. Khan et al., 2001).

Band pass filter is classified via linear time invariant (LTI) which can be divided into two types, which are infinite impulse response (IIR) filters and finite impulse response (FIR) filters (Callegari & Bizzarri, 2015; Ibarra & Jimenez-Lizarraga, 2014). Infinite impulse response is the response of circuit to the infinite short duration and infinite power signal (Barnichon & Matthes, 2018; Chaparro & Akan, 2019; Piskorowski, 2013). IIR filter confront with nonlinear-phase response and are dependent upon nonlinear phase characteristics, whereas FIR filter confront with linear-phase response over the interest frequency range and are dependent upon linear phase characteristics (Luo & Johnston, 2010). Some of these techniques are associated with IIR filter such Butterworth, Chebyshev Types I and II, direct design, elliptic, parametric modeling and Bessel. Meanwhile, FIR filter techniques are windowing filter, equiripple filter, arbitrary response filter, constrained least squares filter and raised cosine filter. Complicated design required for IIR filter to ensure stability design compared to FIR filter (Okoniewski & Piskorowski, 2015). There are some advantages of FIR in terms of stability, exact linear phase, efficiency in hardware, linear designation technique, and filter startup transients with finite duration (Ghani et al., 2018). However, FIR filter's important con is that it

needs a greater filter order than IIR filters to gain performance level. Therefore, robust, and stable designs are needed for FIR filter due to model classification implementation.

#### **2.4.2.2 EEG Feature Extraction**

Based on definition, feature extraction refers to transformation process of input data into features set which well represent an input data. In pattern recognition and machine learning, the first step to recognize the pattern is through feature extraction where it creates derived values (features). To extract EEG features, spectrum analysis is used for analyzing statistically EEG signal. The most significant contribution comes from the amplitude measurement, wavelength, speed, and duration itself. The amplitude measurement is implemented to analyze human brain condition (Thatcher et al., 2005). Power (amplitude) spectrum or known as power spectral density refers to signal power distribution over the frequency in every single brain location.

Feature extraction are required to be handled carefully to keep signal originality and to analyze the brain conditions correctly. Before proceeding into feature extraction part, signal pre-processing is required due to noises, artifacts, and interferences removal. To extract the feature, feature selection is needed to choose suitable subset of feature set input. Proper feature selection gives large impact on accomplishment of pattern recognition system. In addition, the aim of feature extraction is not just to decrease the dimensionality but to get the most useful information which is unrevealed in the signals through despising unwanted or redundant information.

Based on literature finding, there are some EEG feature extractions which had been done in previous work (Boonyakitanont, Lek-uthai, Chomtho, & Songsiri, 2020; Javidi, Mandic, Cheong Took, & Cichocki, 2011; Lu et al., 2020; Sharma, Kolekar, Jha, &

Kumar, 2019). The examples include, minimum or maximum amplitude, standard deviation or variance, PSD, ESD or FFT values, mean or RMS value of signals, entropy, kurtosis, wavelet or STFT domain features, signal derivatives, higher order statistics, NEO (Non-linear Energy Operator) and others. The selection of feature extraction through related study is important due to analysis of statistical data. Afterwards, classification technique takes place after obtaining appropriate feature extraction. Classifier performance relies on the proper signal pre-processing and proper feature extraction.

While features that rely on statistical descriptors are not sufficient to generalize the pattern of observed phenomena, the more powerful method such as wavelets are exposed to shift invariance property and lack of directional selectivity. Meanwhile, the drawback of using NEO is the restrictions for handling signal with relatively low amplitude. In the past, energy spectral density has been widely established for quantifying brainwaves (Neubauer & Fink, 2009b). However, derivative features known as power ratio have also been adopted in many EEG studies (Kerson et al., 2019; Priya, Mahalakshmi, Naidu, & Srinivas, 2020; Vishwanath et al., 2020). Previously, the analysis related to intelligence and learning style have implemented energy spectral density, spectral centroid, and power ratio (Rashid et al., 2013, Jahidin et al., 2014, Megat Ali, Jahidin, Md Tahir, et al., 2014, Jahidin, Megat Ali, Taib, Md Tahir, & Yassin, 2015, Megat Ali, Jahidin, Taib, Tahir, & Yassin, 2016). While the first two feature extraction method is based on power spectral density, power ratio is the direct derivative of energy spectral density. Comparatively, power ratio feature is much efficient as it considers the relationship of brainwaves in the respective EEG bands. Meanwhile, the use of spectral centroid will be computationally costly. The information provided by this feature is twice more than that of power ratio. Therefore, power ratio has proven efficient in ensuring good model performance. These have been shown in past studies that focus on IQ (A. H. Jahidin et al., 2012) and learning

styles (Megat Ali, Jahidin, Md Tahir, et al., 2014). The features are not only used to statistically analyze the results, but also used for classification (A. H. Jahidin et al., 2013) and modelling purposes (A. H. Jahidin et al., 2014).

### 2.4.3 Synthetic EEG Signals

Basically, synthetic data are generated based on original data set to overcome imbalance sample size (Alharbi, 2018). Throughout the adaptive synthetic data to the model, it will enhance and improve the classifier performance model (Yang, Ma, Zhang, Guan, & Jiang, 2018). The method to overcome imbalance sample size distribution condition is increasing the number of synthetic data by using minimum sample size analysis and also through common research practice by extending factor of 10 in minimum sample size (Alwosheel, van Cranenburgh, & Chorus, 2018; Haykin, 2009). In order to improve synthetic data for EEG signal, a technique using random white Gaussian noise is integrated via simulation on real data (Ur Rehman & Mandic, 2011). However, the signal-to-noise ratio (SNR) requires to be handled cautiously to gain desirable synthetic data that is identical to the original data. If SNR is inadequate, the noise content creates and modifies the real data, which is not identical to original data (Roberts, 2004). As a result, the ANN model classifier will contribute to misclassification performance (Azami, Mohammadi, & Bozorgtabar, 2012).

To gain EEG synthetic data,  $V_{synt}$ , is attained by implementing the generated noise,  $V_{noise}$ , into original EEG,  $V_{EEG}$ . Basically, generated noise,  $V_{noise}$ , or known as noise array, is generated through multiplication of random white Gaussian noise,  $W_{noise}$ , and the noise voltage,  $V_{attn}$ , where  $V_{attn}$  is the attenuated voltage and derived voltage through SNRdB input (Sevgi, 2007). The derivations or expressions are shown in the equations below:

$$V_{synt} = V_{EEG} \times V_{noise} \quad (2.1)$$

$$V_{noise} = W_{noise} \times V_{attn} \quad (2.2)$$

#### 2.4.4 EEG Applications

As stated before, Hans Berger method to record the brain activity or EEG signal started to be well-known in analyzing brain activity (Barwick, 1971; La Vaque, 1999; Leiser et al., 2011; Millett, 2001; Sanei & Chambers, 2013). This work investigated the electrical activity through human brain or cerebral cortex and the approach begin by attaching electrodes to the scalp and a galvanometer. However, this application is not well-known practice in healthcare fields. Then, Adrian and Matthews replicated the Beiger's research work until it became acceptable in healthcare field to diagnose brain condition (Adrian & Matthews, 1934; Adrian & Yamagiwa, 1935; Panteliadis et al., 2017). Nowadays, there are distinct EEG applications adopted in different fields, such as cognitive science, neuroscience, psychology, physiology, medicine, clinical and other life science fields. Even though EEG can be used for various applications, but there are several common applications of EEG.

**Table 2.2: EEG applications and description.**

EEG applications	Descriptions
Neuromarketing field	Human reaction depends on brain processing or brain activation during product or service selection through buyer decision
Human factors field	Scientific principles related with recognizing human interaction with other elements
Social interaction	Investigation of cognitive process respect to self-evaluation, social behavior, and social perception
Neuroscience and psychology	Mind or brain processing that controls behavior
Medical, clinical and psychiatric	Investigate symptoms, cognitive state and lesion location of the patients
Brain-computer interfaces	Direct interchange pathway between brain processing and external devices through the connection such electrical wires

First, EEG has been adopted in neuromarketing field. As a buyer in context of marketing, human reaction depends on brain processing or brain activation during product or service selection through buyer decision. Furthermore, mental state of the buyer during exploring virtual or physical store is one factor reflected in marketing. Thus, economist start to investigate cognitive processing through accurate and scientific way via EEG application. Nowadays, the neuromarketing research has begun to conduct the research into shopping behaviors and decision making in real-world situation (Bastiaansen et al., 2018; Golnar-Nik, Farashi, & Safari, 2019; Koc & Boz, 2018).

Secondly, EEG has been adopted in human factors field. Human factors or ergonomics are the scientific principles related with recognizing human interaction with other elements. Commonly, human factors purposes are to increase productivity, decrease human error, increase the safety and comfort through the interaction between tool and human as well as social interaction. Thus, EEG research begin by investigating brain process in respect to psychology, especially to personality traits. Furthermore, EEG also has been adopted in interaction between human and machine via cognitive processing of

human brain nowadays (Acı, Kaya, & Mishchenko, 2019; Cha & Lee, 2019; Jebelli, Hwang, & Lee, 2018; Shan, Yang, Zhou, & Chang, 2019).

Thirdly, EEG has been adopted in social interaction. Human lives are interacted with each other over time. Based on social interaction, investigation of cognitive process is in respect to self-evaluation, social behavior, and social perception. Crucially, communication and social interaction are not a form of brain processing approach stimuli. As human communicate with each other or human solve the problems together, they need to “synchronize” their interaction with each other. Throughout human synchronization, the brain processes are required. EEG research through social interactions give benefits for human life style (Blume et al., 2015; Knyazev, Merkulova, Savostyanov, Bocharov, & Saprigyn, 2019; Nicolardi, 2018; Noreika, Georgieva, Wass, & Leong, 2020).

Fourthly, EEG has been adopted in neuroscience and psychology. The main contrariety between neuroscience and psychology is that neuroscience is concerning nervous system while psychology concerns on human behavior. The overlapping between both, refers to the mind or brain processing that controls behavior. Psychologists and neurologists aggressively began the studies using EEG to understanding brain process that controls behavior such learning, attention, and memory. EEG can characterize the surprise state, processing face, words and meaning or memory recall through event-related potential (ERP) in certain timescale. The primary advantage investigating neuroscience and psychology is to understand the human mind, human behavior and human nervous system interactively (Benedek & Fink, 2019; Karakas & Yildiz, 2020; Lou, Feng, Li, Zheng, & Tan, 2020; Papousek et al., 2019).

Next, EEG is adopted in medical, clinical, and psychiatric. Human mental disorder can be diagnosed, prevented, and cured through extension of EEG. Previous study shows that brain damage or impair can be observed through their cognitive processing, behavioral,



meditation and attention state. In medical, clinical, and psychiatric terms, the utilization of EEG is to investigate symptoms, cognitive state, and lesion location of the patients. Furthermore, neurosurgeons also utilized this application to avoid patient paralyses. In psychiatric areas, brain treatment is utilized via virtual reality technology and recording EEG signal to analyze patients' brains performance improving over time (Amato et al., 2013; Debener et al., 2000; Sanei & Chambers, 2013; Shirwaikar et al., 2019; Smailovic et al., 2018).

Finally, EEG has also been adopted in brain-computer interfaces or known as BCI. BCI refers to direct interchange pathway between brain processing and external devices through the connection such as electrical wires. Currently, BCI concerns to neuroprosthetic application to assist human healthcare such as movement, hearing, and sight. This makes EEG instrumentation to be well known, as BCI is primarily integrated with EEG tool. Furthermore, military also start to look over human machine control through BCI and EEG. In future, there are still a lot of opportunities in various fields can be integrated with EEG tool (Alazrai, Alwanni, & Daoud, 2019; Minguillon, Lopez-Gordo, & Pelayo, 2017; Qin & Li, 2018; Tariq, Trivailo, & Simic, 2018).

## **2.5 Box Plot Analysis as EEG Visual Technique**

Box plot analysis can be used to interpret EEG data and to handling outliers. There are several reasons that outlier happen due to noisy data from tail of noise distribution or erroneous measurement. Requirement of handling the outliers sample data before network training is needed. If the outliers are present in data set, the developed model may attempt to adapt those improper data, which causes learning systems to be corrupted (Chuang, Su, & Hsiao, 2000) and also produces huge inaccuracy of the model (Liano, 1996). Therefore,

handling outlier's requirement plays crucial role to develop acceptable network in IQ-LS classification model.

Statistical methods can assist in investigating patterns through data collection and experimentation. Box plot plotting analysis are benefitting due to investigating pattern and also handling of abnormal data (outlier) (Williamson, Parker, & Kendrick, 1989). Box plot has been broadly integrated for analysis due to utilization of visual comprehension to relate groups of the data. Therefore, the data interpretation in complex table can be enhanced in reasoning term related to quantitative information (Williamson et al., 1989).

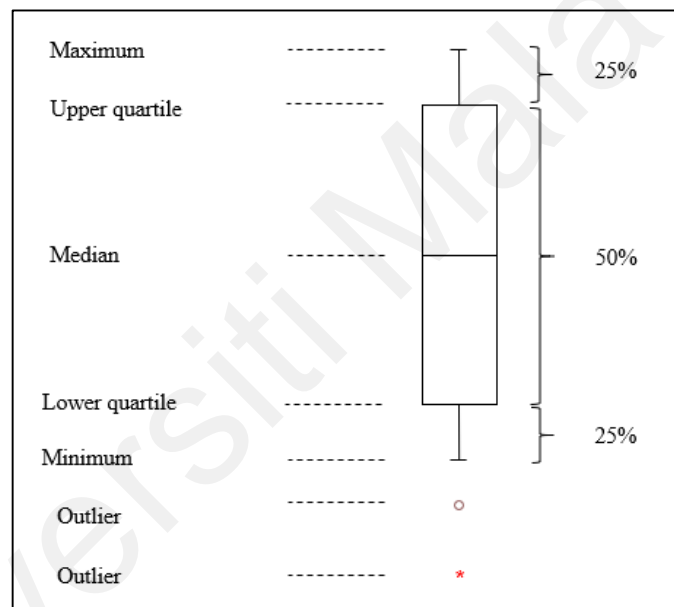


**Figure 2.3: Box plot interpretation**

A box plot presents five number summarization of data set, which are maximum, upper quartile, median, lower quartile and minimum, applied to express the level, spread, and symmetry of data distribution. The lower quartile and upper quartile are fifty percent in between the median value, meanwhile the minimum and maximum data set are twenty five percent at the end of lower quartile and upper quartile, respectively. Therefore, 25<sup>th</sup> and 75<sup>th</sup> percentiles of top and bottom from median, can be illustrated as Figure 2.3.

The interquartile range is referred to the interval between lower quartile and upper quartile. Furthermore, additional whisker line is used to expanding above and below from the end of lower quartile and upper quartile, respectively, the furthest observations within the whisker length. Outlier data is produced through whisker line, where the outlier data generated away from more than 1.5 times of interquartile range at the end of minimum and maximum value. There are two types of outlier, which are usual outlier and extreme outlier, denoted as 'o' and red '\*' symbol. Furthermore, definition of outlier can be regulated with additional input arguments (Williamson et al., 1989).

Based on median sample data, it represents the second quartile and is known as middle line of boxplot. Corresponding to this information, the box plot also shows the sample distribution skewness. The significance level is due to normal distribution assumption, however the medians differences also are practically robust for other distributions (Potter, Kristin and Hagen, Hans and Kerren, Andreas and Dannenmann, 2006). Therefore, the box plot differentiation approach are commonly used similar as hypothesis test, analogous to the t-test used for means (Mathworks, 2017).

## **2.6 Intelligent Signal Processing (ISP)**

Based on classification or pattern recognition, intelligent signal processing (ISP) approaches are proficient techniques in investigating specific and complex data purpose. Intelligent signal processing (ISP) is described as complex signal processing system that is modelled by applying "model-free" or "intelligent" approaches which lead to real-world signal systems, instead of classical signal processing which has mostly worked with mathematical models that are stationary, local, linear, and Gaussian (Haykin & Kosko, 2001). ISP field has been enhanced by latest advances in artificial intelligence (AI)

leading to new tools for classification, signal estimation, prediction, and manipulation (Salehi & Burgueño, 2018).

### **2.6.1 Artificial Intelligence (AI)**

Intelligence is demonstrated by a machine through hard computing and soft computing techniques. Hard computing is in respect to numerical system, binary logic, crisp systems, precisely stated analytical model and higher computation time meanwhile, soft computing is with respect to probabilistic reasoning, fuzzy logic, neural nets, where it has approximation and dispositional characteristic by evolving their own programs (Pedrycz, 1990). Furthermore, hard computing is deterministic and needs precise input data, however the advantages of using soft computing are it's incorporates stochasticity, and it can handle with unknown and noisy data. Thus, soft computing is beneficial to EEG signal or brainwave signals as the EEG data stochastic and nonlinear deterministic (Cestari & Rosa, 2017).

Artificial Intelligence (AI) is a part of soft computing technique, which can handle and incorporate stochasticity of data. AI is referred as an advancement from intelligent signal processing and refers to machine capability to mimic human intelligent behavior. As mimic to human intelligent behavior, AI can solve approximate conventionally defiant problems through human-inspired algorithm. Currently, there has been a raising scientific interest in AI based techniques, for example fuzzy logic, genetic algorithms (GA), support vector machines (SVM) and artificial neural networks (ANN). These several AI technique's advantages, and limitation will elaborate in section 2.6.3. Other than that, AI applications are actively in automated planning, knowledge representation, reasoning, perception, learning, robotics, natural language processing and general intelligence (Fogel, 1995; Luger, 2005; Nilsson, 1998; te Velde, 2000).

### **2.6.2 Modeling Simulation Methods Approaches**

Nowadays, the models or systems development are derived from previous information about system and empirical data obtained from observation. Based on aim of modeling process, modeling simulation methods approaches are segregated into three parts which are white-box, grey-box and black-box (Wang & Srinivasan, 2017). White-box modeling refers to hard computing constructed from prior information and physical insight during model identification. Furthermore, white-box still uses empirical data for validation process only and is commonly utilized in expert system method. Next, black-box modeling refers to soft computing with absence of prior information and without knowing internal relationship to create the model. This model benefits through flexibility parameterized function to fit the sample data and commonly referred to AI-based method. Finally, grey-box modeling refers to hybrid method which integrate both techniques; white-box and black-box methods to avoid the limitations of both techniques. Grey-box modeling is soft computing constructed through prior information and development model through data driven technique (Fogel, 1995; Mamlook, Badran, & Abdulhadi, 2009; Wang & Srinivasan, 2017).

### **2.6.3 Advantages and Limitations of Several AI Techniques**

Currently, there has been a raising scientific interest in AI based techniques, such as fuzzy logic (Ahmadi, Gholamzadeh, Shahmoradi, Nilashi, & Rashvand, 2018), genetic algorithms (GA) (Tamerabet, Adjadj, & Bentrucia, 2018), support vector machines (SVM) (Zhang, Jiao, Bai, Wang, & Hou, 2018) and artificial neural networks (ANN) (Najafi, Nowruzzi, & Ghassemi, 2018). These four techniques are frequently being developed and applied in distinct of applications for the reasons of their explanation capabilities, symbolic reasoning and flexibility (Agwu, Akpabio, Alabi, & Dosunmu, 2018). Agwu

(2018) was provided the criterion on six criteria of weaknesses and strengths of these four techniques which the researchers have done before. The criteria are robustness to counter noise, rate of convergence, sensitivity to overfitting, data volume necessary, ability to self-organize and generalization ability (Agwu et al., 2018).

**Table 2.3: Advantages and limitations of several AI techniques**

Criterion	Fuzzy	GA	SVM	ANN
Robustness	High	High	High	High
Convergence rate	Fast	Slow	-	Slow
Generalization Capability	-	-	Yes	Yes
Data necessary	-	-	Small	Small
Overfitting control	-	-	No	Yes
Self-organization	-	No	-	Yes
Pattern classification	Yes	Yes	Yes	Yes
Prediction	Yes	Yes	Yes	Yes (Often)
Control and optimization	Yes	Yes	Yes	Yes

(Agwu et al., 2018; Gordan, Razak, Ismail, & Ghaedi, 2017; Iplikci, 2010; Mahela, Shaik, & Gupta, 2015; Refoufi & Benmahammed, 2018)

According to Luchian et al. (2015), in order to decide which techniques should be preferred, there is more advantage in aiming on problem-solving instead of fiddle around to discover the best technique (Bautu & Breaban, 2015). Although Luchian et al. (2015) neglected the technique selection, this research still considers deciding the technique with respect to robustness, generalization capability, data necessary, overfitting control, self-organization, pattern classification, prediction, control and optimization. The highest advantages of AI technique based on Table 1 is ANN. ANN are good performances at tasks such as pattern matching, classification, optimization, data clustering and function approximation (Ajil et al., 2010; Gordan et al., 2017). Even though ANN has weakness on convergence rate, it has overfitting control ability, where overfitting controls are important to avoid overtraining model, which means the model "memorizes" training data instead of "learning" to generalize the classification.

The additional consideration of technique selection is with respect to biomedical application and related research model attempts. Based on biomedical application, ANN technique has been implemented in broader biomedical field application such as data analysis, modelling and diagnostic classification (Ahmad et al., 2014). ANN is also in line with new scientific accomplishments in order to discover the potential and accessibility of ANN. Recently, ANN was implemented in prediction of chronic kidney disease (Almansour et al., 2019), neonatal apnea prediction (Shirwaikar et al., 2019), walking gait event detection based on electromyography signals (Nazmi, Rahman, Yamamoto, & Ahmad, 2019), computed tomography perfusion deficits detection (Vargas, Spiotta, & Chatterjee, 2019), cancer diagnosis and prognosis (Huang, Yang, Fong, & Zhao, 2020), load prediction in a long bone (Mouloodi, Rahmanpanah, Burvill, & Davies, 2020), degradation rate of genipin cross-linked gelatin scaffolds prediction (Entekhabi, Nazarpak, Sedighi, & Kazemzadeh, 2020), epileptic seizure occurrences prediction and dysfunctional urinary bladder filling (Rong, Mendez, Assi, Zhao, & Sawan, 2020). This shows that ANN is an important recent technology in solving biomedical problems.

Based on related research model attempt, previously the separate classification model of IQ and LS via brainwaves signal has been attempted through ANN technique with convincing result, although the methodologies were different (Jahidin, 2015; Jahidin, Megat Ali, Taib, Md Tahir, & Yassin, 2015; Jahidin, Taib, et al., 2015; Megat Ali, Jahidin, Md Tahir, et al., 2014; Megat Ali, Jahidin, Tahir, & Taib, 2014; Megat Ali et al., 2016). Since, our research is first attempt to classify both IQ-LS simultaneously, the selection should be in consideration with previous approaches, which using ANN technique. Therefore, this specific technique was decided carefully to ensure IQ and learning style classification model perform well.

## 2.7 Artificial Neural Network (ANN)

An artificial neural network (ANN) is mathematical models set operation via the behaviour of the biological neural networks (Dande & Samant, 2018). In other words, ANN generally mimics the biological behavior of interconnecting neurons when learning new information. In various fields, the application of artificial neural network can be used as a powerful tool for solving most complex problems (Mamlook et al., 2009). Most ANN applications comprise of three categories which are prediction and data analysis, control and optimization and pattern classification (Kamaruddin & Shogar, 2011). In order to classify IQ and learning style, pattern classification of ANN been preferred.

Based on general topology, learning algorithm and structure are being considered. According to learning algorithm, there are two major categories which are unsupervised learning and supervised learning (Demuth, Beale, & MathWorks, 1998). Unsupervised learning requires input data only while supervised learning requires input-output data. Supervised machine learning method is being preferred as this research involves input-output data. This learning method iteratively adjusts the weights between the nodes using back-propagation algorithms and stops when the error is minimal (Negnevitsky, 2005) to ensure good generalization performance, early stopping criterion is implemented (Pérez, Wohlberg, Lovell, Shoemaker, & Bevilacqua, 2014).

Generally, neural networks are typically structured in layers, which are input layer, hidden layer and output layer. According to the input-output structures, the structures consists of multiple-input multiple-output (MIMO), single-input single-output (SISO) (Ruano et al., 2014), single-input multiple-output (SIMO) (Piri, Delen, & Liu, 2018), and multiple-input single-output (MISO) (Arabasadi et al., 2013). Based on this research, the multiple input with multiple output are considered in order to develop the model. Thus,



MIMO system is suitable as the technique is also compatible with parameters representing the input features.

Based on hidden layer, the number of hidden layers is crucial to ensure overall neural network architecture performance. However, single layer is sufficient as it has been proven and performed similarly to complex deep nets (Ba & Caruana, 2014). Hidden layer consists of selected activation function or transfer function. Basically, the most used transfer functions for multilayer network are hyperbolic tangent sigmoid (tansig), log-sigmoid (logsig) and linear (purelin) transfer function. Throughout input values consists of negative to positive infinity, hyperbolic tangent sigmoid transfer function generates the output values between -1 to 1, while log-sigmoid transfer function generates the output values from 0 to 1. The linear transfer function generates the output values outward to the range -1 to +1. These output values provide the limited and small range to construct convenience value. In developing the model, the activation function encompassing hyperbolic tangent sigmoid transfer function was selected for the hidden layer and pure linear activation functions for the output layer (Negnevitsky, 2005) which would allow direct mapping to the IQ and learning style indexes.

To verify the model, system validity is needed to examine the acceptability of the models. Requirement of system validity is to solve design flaws, since neural network may be exposed to insufficient training, inappropriate network, input selection and overfitting (Ghritlahre & Prasad, 2018). It's really crucial to investigate whether the neural network complies adequately well with the observations (Zhang, Zhu, & Longden, 2009). Statistical methods, which evaluate error and accuracy are needed for the purpose of validation, comparison and determining the optimal performance of ANN model, such as Mean Square Errors (MSE) and correlation coefficient (R) (Najafi et al., 2018). ANN model replicative is validated whenever the data has been matched between recent model

evaluated from real systems and observation in before ANN modelling development (Gass, 1983; Power, 1993).

### 2.7.1 ANN Algorithm and Structure

Artificial neural network involves interconnection among artificial neuron that use a computational model for processing through connectionist approach. Practically, ANN model composed of non-linear and linear structure between input and output in order to solve the model pattern. During learning phase, the ANN adjust the model structure through input or output information to achieve the performance. In simple words, during learning process, knowledge of the system is obtained by neural network (Alarabi & Mishra, 2010).

Basically, ANN consists of neurons or processor units which has local memory in there. The unidirectional connection channel carries numeric data to communicate. Based on Figure 2.4, there are a set of inputs labeled with P (P1, P2, P3, ..., Pz) known as input neuron. This inputs set will multiplies with set of weights labeled with W (W1, W2, W3, ..., Wr). Additional bias (b) function provided to form the input n, and the total function can be presented in transfer function (f) as Equation 2.3.

$$a = f(n) = f (WP + b) \quad (2.3)$$

Where  $a$  is activation function,  $f$  is transfer function,  $W$  is the weight matrix,  $P$  is the input vectors, and  $b$  is bias.

The available scalar parameters network can be adjusted through weight ( $W$ ) and bias ( $b$ ) in order to obtain desired behavior performance of the network (Demuth et al., 1998). Activation signal that undergoes activation function or transfer function will produce

neuron output. Transfer functions are crucial for ANN to convert signal input of node to an output signal, then that output signal will transfer to next node. Basically, the most used transfer functions for multilayer network are hyperbolic tangent sigmoid (tansig), log-sigmoid (logsig) and linear (purelin) transfer function. Throughout input values consist of negative to positive infinity, hyperbolic tangent sigmoid transfer function generates the output values between -1 to 1, while log-sigmoid transfer function generates the output values from 0 to 1. The linear transfer function generates the output values outward to the range -1 to +1. These output values provide the limited and small range to construct convenience value.

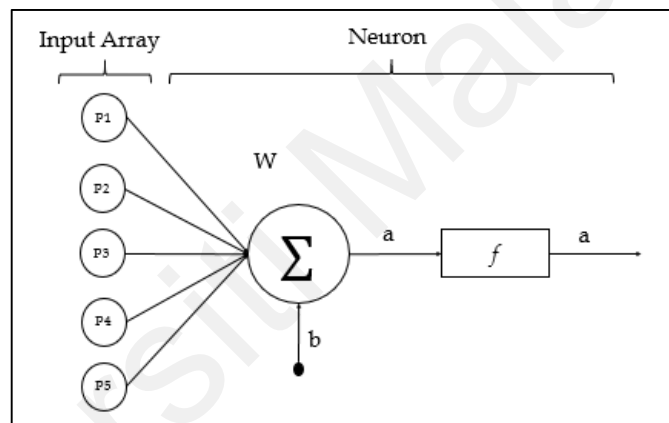


**Figure 2.4: Neural network with multiple input nodes**

Generally, neural networks are typically arranged in layers, which are input layer, hidden layer, and output layer. Input layer consists of input neurons that transmit data to hidden layer. Then, hidden layer consists of hidden neurons transmitting data to output layer. Basically, neuron consists of synapses (weighted inputs), activation function (hidden neuron) and one output (Buscema et al., 2018). This shown that neural network was reflected in human neuron. To conduct neural network training, the parameters need to be adjusted or tuned to ensure the model will perform well.

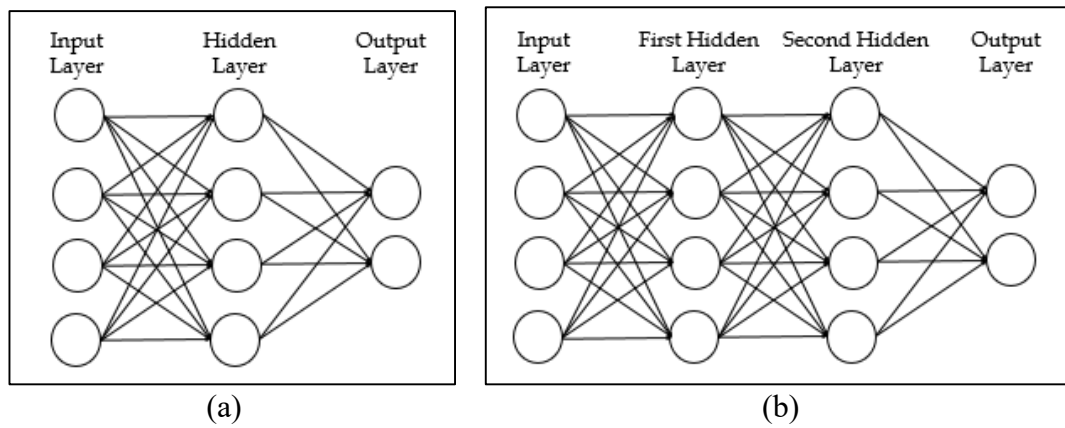


**Figure 2.5: Neural network layer with (a) single hidden layer and (b) multi hidden layers.**

Based on Figure 2.5, the neural network layer shows input, hidden and output layer. Based on hidden layer, the number of hidden layers is crucial to ensure overall neural network architecture performance. However, single layer is sufficient as it has been proved that it performs similarly to complex deep nets (Ba & Caruana, 2014). In addition, the variety of activation function encompassing hyperbolic tangent sigmoid transfer function was chosen for the hidden layer and pure linear activation functions for the output layer (Negnevitsky, 2005) that would allow direct mapping to the IQ and learning style indexes.

Basically, there are three model architectures for ANNs, feed-forward neural networks (FFNN), recurrent neural networks (RNN) and hybrid (Ghritlahre & Prasad, 2018). FFNN refers to forward processing information flows in one-way direction from input to output layer. FFNN is simplest ANN architecture, where the network does not have feedback or loop. The most common ANN architecture in FFNN is Multilayer Feed Forward Network (MFFN) (Maier, Jain, Dandy, & Sudheer, 2010). On the other hand, RNN refers to loop processing information flows moving both direction between input and output layer, where RNN consists of feedback connections. RNN is a complex neural network architectural structure, where the feedback connection is dynamic and continuously changes. Thus, the processing will be complicated in order to pass activation function. As

examples of RNN are Kohonen self-organizing map, Elman neural network, and Hopfield network. Finally, hybrid refers to combinations of several model of FFNN and RNN, which resulted to the improvement of performance model (Pradeepkumar & Ravi, 2018).

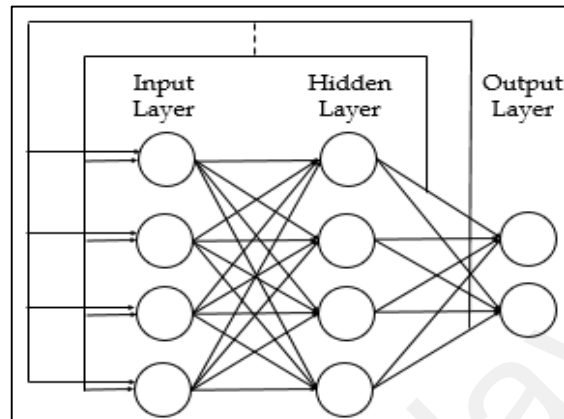


**Figure 2.6: Recurrent neural network with multiple input nodes and multiple output nodes.**

To have convincing ANN model, the neural network is required to be trained with satisfying performance result. Neural network training concerns with learning process knowledge by adjusting the parameters to have best possible input-output mapping and improve model performance. This learning method iteratively adjusts the weights between the nodes using back-propagation algorithms and stops when the error is minimal (Negnevitsky, 2005). To ensure good generalization performance, early stopping technique is implemented (Pérez et al., 2014).

### 2.7.2 Multilayer Feed Forward Network (MFFN)

Feed forward neural network (FFNN) is the neural network link between each node, in which information flow in one direction and not forms a cycle (Yang & Ma, 2018). In FFNN network flow the information from input nodes through hidden nodes and finally to the output nodes. There are two types of FFNN which are single layer feed forward neural network (SFFN) and multi-layer feed forward neural network (MFFN). The

difference between SFFN and MFFN is that the neural network in SFFN contained input layer and output layer, meanwhile the neural network in MFFN contained input layer, hidden layer and output layer (MacLennan, 2017; Meyer-Baese & Schmid, 2014).

There are various applications of pattern recognition using MFFN (Amaral, Lopes, Jansen, Faria, & Melo, 2015; Içer, Kara, & Güven, 2006). Commonly, MFFN involves applications of prediction, function approximation, optimization, modelling, or pattern classification purposes (Chen & Jain, 1994; Chen, Jakeman, & Norton, 2008; Faisal, Ibrahim, & Taib, 2010; Kalogirou, 2000; Masters, 1993). This technique has been widely used in various ranges of biomedical application (Azar, 2013; Ebrahimzadeh & Khazaei, 2010; Faisal et al., 2010; F Ibrahim, Faisal, Salim, & Taib, 2010; Salchenberger, Ventat, & Venta, 1997; Zadeh, Khazaei, & Ranaee, 2010). MFFN has been utilized in cancer detection and classification (Khan et al., 2001; Kuruvilla & Gunavathi, 2014), modelling of heart disease recognition (Zadeh et al., 2010), diagnosis of coronary artery disease (Alizadehsani et al., 2013), disease recognition (Faisal et al., 2010), prognosis of dengue fever (Faisal et al., 2010; Fatimah Ibrahim, Taib, Abas, Guan, & Sulaiman, 2005), physiological analysis and modelling (Duta, Alford, Wilson, & Tarassenko, 2004), and other related studies (Amaral, Lopes, Faria, & Melo, 2015; Fernandez de Canete, Gonzalez-Perez, & Ramos-Diaz, 2012; Kara, Güven, & Öner, 2006; Kupusinac, Stokić, & Doroslovački, 2014; Lisboa, 2002; Poletti, Grisan, & Ruggeri, 2012; Talu, Gül, Alpaslan, & Yiğitcan, 2013; Zecchin, Facchinetti, Sparacino, & Cobelli, 2014). Thus, MFFN architecture technique can be implemented in psychological traits and brainwaves, even the complex problem issues can be utilized.

### 2.7.2.1 MFFN Algorithm

MFFN structure comprises of one input layer, one or more hidden layers and one output layer. The quantity of input and output nodes are depending on the model and application itself (Faisal et al., 2010), whereas for the hidden nodes, it will be based on experimental investigation. The minimum hidden nodes are required for better classification and performance. Smaller number of hidden nodes will lead to the incapability of the model to formulate precise algorithm between input and output, while larger hidden nodes will cause overfitting issues which affected generalization ability. With regards to the number of hidden layers, more than one layer can be implemented in any applications. However, studies have shown that a single hidden layer is sufficient to perform classification with acceptable accuracy and arbitrary function (Chen & Billings, 1992; Cybenko, 1989). The structure of MFFN can be shown as Figure 2.7.

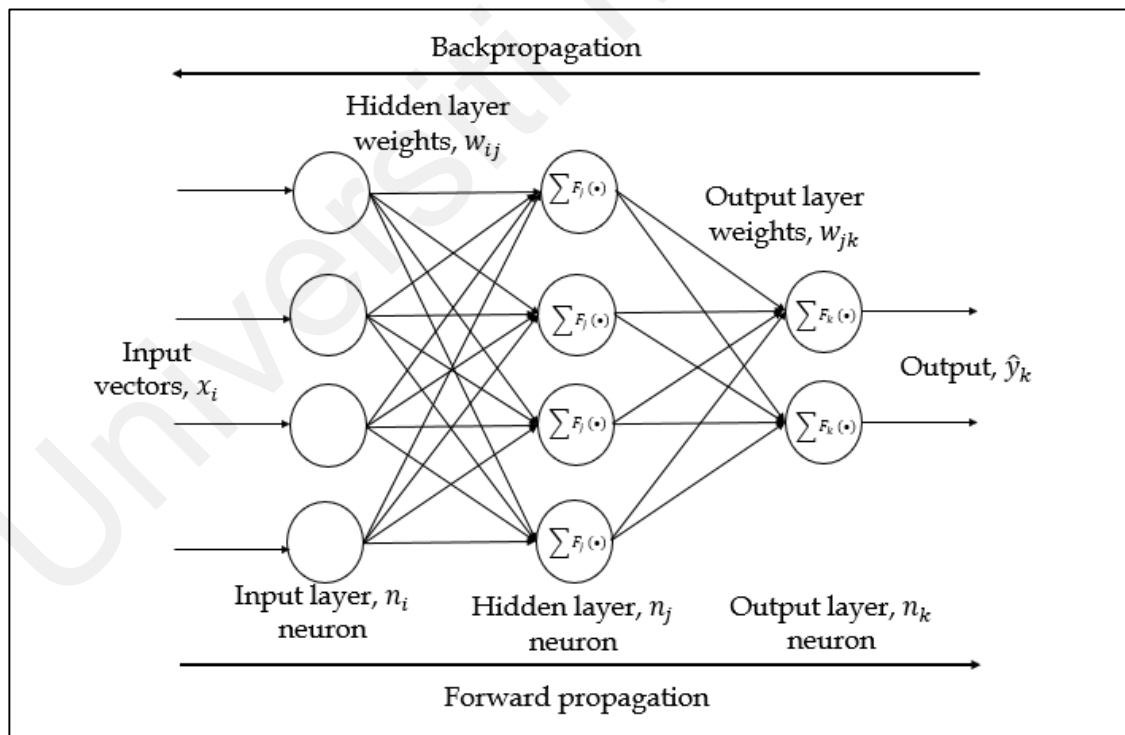


**Figure 2.7: Common Multilayer Feedforward Neural Network (MFFN) with single hidden layer.**

As in Figure 2.7, input nodes in input layer are represented as  $n_i$  neurons, hidden nodes in hidden layer represents as  $n_j$ , and output nodes in output layer are represented

as  $n_k$ . Input vectors and output vectors are known as  $x_i$  and  $y_k$  respectively. In addition, the weight of neurons is represented as  $w_{ij}$  while summation of activation function is represented as  $\sum F_j (\bullet)$ .

During forward propagation, the output network is activated with respect to function of its inputs. The input vectors ( $x_i$ ) to hidden nodes are summarized product of weights and activation function, and it needs to pass through activation function before sending out from node. The forward propagation equation between input and hidden layer is as below:

$$y_j = F_j \left( \sum_{i=1}^M w_{ij} x_i \right) \quad (2.4)$$

Where  $y_j$  is into a vector of intermediate variables,  $F_j$  is activation function,  $M$  is input variable numbers,  $w_{ij}$  is connection weight between input neurons ( $i$ th) to hidden neurons ( $j$ th), and  $x_i$  is input vectors. Based on activation function, hyperbolic tangent sigmoid (tansig) is always utilized and selected in hidden layer (Taib, Andres, & Narayanaswamy, 1996). Hyperbolic tangent sigmoid (tansig) can be represented mathematically as below:

$$F_{\text{tansig}}(x) = \left( \frac{2}{1 + \exp(-2x)} \right) - 1 \quad (2.5)$$

Subsequently, the integration hyperbolic tangent sigmoid activation function in forward propagation equation is represented as equation below:

$$y_j = F_j \left( \sum_{i=1}^M w_{ij} x_i \right) = \left( \frac{2}{1 + \exp(-2 \sum_{i=1}^M w_{ij} x_i)} \right) - 1 \quad (2.6)$$

As output network which activated with respect to function of its inputs, the product from hidden nodes  $n_j$  will pass through output node. The similar process occurs



as forward propagation equation through input and hidden layer. The forward propagation equation between hidden and output layer is as below:

$$\hat{y}_k = F_k \left( \sum_{j=1}^N w_{jk} y_j \right) \quad (2.7)$$

Where  $\hat{y}_k$  is the predicted output,  $F_k$  is activation function,  $N$  is intermediate input variable numbers,  $w_{jk}$  is connection weight between hidden neurons ( $j$ th) to output neurons ( $k$ th), and  $y_j$  is output neuron. Similar equation as represented in Equation 2.7 is implemented to output node, however it limits the dynamic range output which is smaller than one (Taib et al., 1996). Therefore, a pure linear (purelin) activation function approach is another way to allow larger dynamic range of output (Billings, Jamaluddin, & Chen, 1992; Taib et al., 1996). Pure linear (purelin) activation function can be represented mathematically as below:

$$F_{purelin}(x) = x \quad (2.8)$$

Subsequently, the integration pure linear activation function in forward propagation equation is represented as equation below:

$$\hat{y}_k = F_k \left( \sum_{j=1}^N w_{jk} y_j \right) = \sum_{j=1}^N w_{jk} y_j \quad (2.9)$$

Throughout model training, MFFN learn and gain the knowledge through relationship between input vectors ( $x_i$ ) and actual outputs ( $y_k$ ) by changing the weights of network connection using backpropagation algorithm (Billings et al., 1992). To explain details on network training, there is an introduction of additional variable known as  $t$ , where  $t$  is introduced to differentiate between updated and its preceding weights or known as training iteration. Beginning by  $t = 1$  (first training iteration), the initial input set computes in network through forward propagation process, then further yields the output prediction,  $\hat{y}_k(t)$ . Based on this computation, the error,  $\varepsilon_k(t)$ , can be calculated

via difference between predicted output and actual output. This error equation is represented mathematically as below:

$$\varepsilon_k(t) = \hat{y}_k(t) - y_k(t) \quad (2.10)$$

This error parameter is essential which effects learning rate in backpropagation algorithm. Correlation between network error and network performance will be discussed later.

With respect to the network weight, the correction of weight conducted in backward direction and back propagates compute from output nodes to hidden nodes and from hidden nodes to the input nodes. Then, the initial phase of weight update between hidden node and output node can be shown mathematically as below:

$$w_{jk}(t+1) = w_{jk}(t) + \beta \times \Delta w_{jk}(t) \quad (2.11)$$

where,  $w_{jk}(t+1)$  is updated weights between output node ( $k$ th) and hidden node ( $j$ th),  $w_{jk}(t)$  is preceding weights between output node ( $k$ th) and hidden node ( $j$ th),  $\beta$  is the momentum constant and  $\Delta w_{jk}(t)$  is the correction weight term for output-hidden node. Extensively, the correction term can be expressed in mathematically as below:

$$\Delta w_{jk}(t) = \alpha \times \hat{y}_k(t) \times \delta_k(t) \quad (2.12)$$

where  $\Delta w_{jk}(t)$  is the correction weight term for output-hidden node,  $\alpha$  is step size,  $\hat{y}_k(t)$  is output prediction and  $\delta_k(t)$  is learning rate. Extensively, learning rate can be expressed mathematically as below:

$$\delta_k(t) = \hat{y}_k(t) \times [1 - \hat{y}_k(t)] \times \varepsilon_k(t) \quad (2.13)$$

where  $\delta_k(t)$  is learning rate of output-hidden node,  $\hat{y}_k(t)$  is output prediction and,  $\varepsilon_k(t)$  is error of  $k$ th.

Then, the phase of weight update between input node and hidden node can be shown in similar mathematically as the initial phase of weight update between hidden node and output node:

$$w_{ij}(t+1) = w_{ij}(t) + \beta \times \Delta w_{ij}(t) \quad (2.14)$$

where,  $w_{ij}(t+1)$  is updated weights between hidden node ( $j$ th) and input node ( $i$ th),  $w_{ij}(t)$  is preceding weights between hidden node ( $j$ th) and input node ( $i$ th),  $\beta$  is the momentum constant and  $\Delta w_{ij}(t)$  is the correction weight term for hidden-input node. Extensively, the correction term can be expressed in mathematically as below:

$$\Delta w_{ij}(t) = \alpha \times x_i(t) \times \delta_j(t) \quad (2.15)$$

where  $\Delta w_{ij}(t)$  is the correction weight term for hidden-input node,  $\alpha$  is step size,  $x_i(t)$  is input vector and  $\delta_j(t)$  is learning rate. Extensively, learning rate can be expressed mathematically as below:

$$\delta_j(t) = y_j(t) \times [1 - y_j(t)] \times \sum_{k=1}^N \delta_k(t) \times w_{jk}(t) \quad (2.16)$$

where  $\delta_j(t)$  is learning rate of hidden-output node,  $y_j$  is actual output vector,  $\delta_k(t)$  is learning rate of output-hidden node and  $w_{jk}(t)$  is preceding weights between output node ( $k$ th) and hidden node ( $j$ th).

The training repetition process occurs with new set of information and weights consistently updated until stopping criteria is attained. The early stopping criteria will be reviewed further. Last but not least, mean squared error (MSE) has been observed in order

to control error convergence for the model network. Hereafter, the whole section will be presented further.

### 2.7.2.2 Levenberg-Marquardt (LM) Algorithm

ANN and brainwaves statistical analysis are frequently used techniques for frequency series prediction. Practical results have revealed that ANN work well in linear regression through complex, nonlinear and dynamic data (Mammadli, 2017; Shachmurove & Witkowska, 2001). ANN are homologous to nonparametric and nonlinear regression, where assumption from common statistical analysis is used. As modelling nonlinear and dynamic signals, the requirements of backpropagation neural network (BPNN) are needed (Demuth & Raelle, 2009; Hagan, Demuth, & Beale, 2014). Standard BPNN applied first order steepest descent methods respect to evaluation of the gradient of the MSE error for each layer:

$$E(n) = \frac{1}{2} \sum_{k=1}^m e_k^2(n); e_k(n) = d_k(n) - y_k(n) \quad (2.17)$$

where  $n$  is a training epoch,  $d$  is desired or target output,  $y$  is ANN actual output, and  $m$  is number of outputs.

Based on weight update, mathematical expression of weight update with a training rate ( $\eta$ ) is revealed as below:

$$W(n+1) = W(n) + \Delta W(n) \quad (2.18)$$

$$\Delta W(n) = -\eta \frac{\partial E(n)}{\partial W(n)} = -\eta \nabla E(n) \quad (2.19)$$

Practically, MSE ( $E(n)$ ) surface has saddle interval, flat sections, local minimum and others (Demuth & Raelle, 2009; Hagan et al., 2014; Mammadli, 2017). A basic

steepest descent minimization algorithm via first order minimization is delay cause of serial error computation on layer-by-layer basis. In other words, this network needs numerous training repetition to gain minimum error. To accelerate training speed and keep off oscillation around a local minimum, the weight update is implemented using merge methods such as momentum rate ( $\alpha$ ) and learning rate ( $\eta$ ). Therefore, the integration expression shows as below:

$$\Delta W(n) = -(\eta \times \nabla E(n)) + \alpha \Delta W(n-1) \quad (2.20)$$

Through measuring gradient mean locally, the momentum technique attempts to obtain some curvature information with respect to error surface. Later update of the steepest descent methods is obtained utilizing distinct algorithms, such as smoothing a zig-zag way on error surface implementing conjugate gradient algorithm and effective initialization of ANN using Nguen-Widrow algorithm.

Afterwards, there are second order derivatives of cost function  $J(w)$  or performance index through optimization methods to reduce error  $E(n)$  minimization (Demuth & Ruele, 2009; Hagan et al., 2014; Mammadli, 2017). Cost function  $J(w)$  expansion through Taylor series express mathematically as below:

$$J(w_{n+1}) = J(w) + \Delta w \nabla J(w) + \frac{1}{2} \Delta w \nabla^2 J(w) + \dots \quad (2.21)$$

where,

$$\nabla J(w) = \frac{\partial E(n)}{\partial (w(n))} = g \quad (2.22)$$

The  $g$  defines performance index gradient. Meanwhile Hessian matrix,  $H$  gain through second order of cost function as in equation below:

$$\nabla^2 J(w) = \frac{\partial^2 E(n)}{\partial^2(w(n))} = H \quad (2.23)$$

As a mean to have second-order training speed, the designation of Levenberg-Marquardt (LM) algorithm had been developed by absent of Hessian matrix computation (Hagan & Menhaj, 1994). Once the performance function has the construct of a sum of squares (commonly in training FFN networks), Hessian matrix can be determined as

$$H(n) = J^T(n) J(n) \quad (2.24)$$

Meanwhile, the gradient can be assessed as:

$$g(n) = J^T(n) E(n) \quad (2.25)$$

Where  $H(n)$  is Hessian matrix,  $g(n)$  is gradient matrix, and  $J$  is Jacobian matrix. The Jacobian matrix comprised of first derivatives of the network error through biases and weights. Furthermore, it also can be computed easily over a standard backpropagation method compared rather than complexity of Hessian matrix computation. LM algorithm utilizes this approximation to Hessian matrix pursuing Newton-like weight update equation (Hagan & Menhaj, 1994; Mammadli, 2017; Ranganathan, 2004; Roweis, 1996).

$$W(n+1) = W(n) - [J(n)^T J(n) + \mu I]^{-1} J^T(n) E(n) \quad (2.26)$$

Where  $I$  is an identity matrix, and  $\mu$  is a nonnegative scalar, that handles both direction and magnitude. Newton's technique is whenever scalar  $\mu$  is zero, meanwhile higher scalar  $\mu$  causes gradient descent with a low step size. Though shifting Newton's technique approaches, this technique ensures high accuracy and faster computation in obtaining an error minimum (Demuth & Raele, 2009). Therefore, scalar  $\mu$  is reduced once every successful step in performance function reduction and increased once tentative step would increase the performance function. The performance function will always be decreased at

every iteration of network. LM algorithm original description is provided in (Hagan & Menhaj, 1994; Roweis, 1996). This popular backpropagation algorithm is the fastest technique, which is best training medium-sized sample in FFN network. Furthermore, LM is very effective through MATLAB implementation, by cause of matrix equation solution built-in function in MATLAB setting (Demuth & Raelle, 2009).

### **2.7.2.3 Multiple Input Multiple Output (MIMO) Structure**

Generally, neural networks are typically structured in layers, which are input layer, hidden layer, and output layer. The quantity number of input and output are important in model classification and their performance. According to the input-output structures, the structures consist of multiple-input multiple-output (MIMO), single-input single-output (SISO) (Ruano et al., 2014), single-input multiple-output (SIMO) (Piri et al., 2018), and multiple-input single-output (MISO) (Arabasadi et al., 2013). MIMO and MISO architectures are two frequent structures that have been reported in literature, meanwhile SISO and SIMO are difficult to achieve the accuracy through single output.

The primary difference between MIMO and another structure is, MIMO neural network uses multiple inputs to predict or classify multiple outputs. MIMO is composed of three layers network which are input layer, hidden layer, and output layer. Input layer consists of multiple input neuron nodes, meanwhile output layer consists of multiple output neuron nodes. Hidden layer can be single or multiple hidden layer and the hidden nodes will be adjusted through the experiment (Güven, Günal, & Günal, 2017). Although the structure is complex in network structure, MIMO is best and better choice to achieve performance compared to MISO (Pandey, Das, Pan, Leahy, & Kwapinski, 2016).

To classify more than one category of neural network, commonly researchers focus on MIMO categories than other structures. Previously, neural network in MIMO structure has been utilized for pattern recognition of various scientific and engineering fields such as flood forecasting (Chang, Chiang, & Chang, 2007), meteorological parameters prediction (Raza & Jothiprakash, 2014), energy related analysis (An, Zhao, Wang, Shang, & Zhao, 2013; Gareta, Romeo, & Gil, 2006; R. Kumar, Aggarwal, & Sharma, 2013), air pollutant emissions (Antanasijević, Pocajt, Perić-Grujić, & Ristić, 2018), physical and chemical properties prediction (Ghaedi, 2015) and others. The benefit of MIMO is having desired accuracy with the minimum input as possible (Antanasijević et al., 2018).

MIMO system is suitable as the technique is also compatible with parameters representing the input features. In this study, ANN is considered suitable as it can function as multiple-input multiple-output (MIMO) systems and the technique is also compatible with parameters representing the input features. The variety of activation function encompassing hyperbolic tangent and pure linear activation functions (Negnevitsky, 2005) would allow direct mapping to the IQ and learning style indexes.

#### **2.7.2.4 Early Stopping (ES)**

The main advantage of ANN is their ability to generalize or generalization. The word of “generalization” means that a trained network can classify the data from equivalent class once using new or unknown learning data. Meanwhile, over-generalization (or known as overfitting) causes to lose the ability to generalize and predicts the output network lean to data memorization (Schittenkopf, Deco, & Brauer, 1997). The common problem that MFFN has always faced is overfitting issue. Although MSE error showed minimum or ideal error during sufficient network performance training, overfitting



caused the network performance decline leading to failure of dealing with future untested data (or known as new or unknown input data). As an example of overfitting issue, assuming the network has been trained very well on training dataset, however when inserting new or unknown input data to trained network, the result shows inaccurate prediction which caused useless network model. Therefore, this issue caused the neural network performance is ineffective to adapt and generalize unknown data set.

In order to overcome this issue and to gain best generalization, early stopping (ES) approach will be implemented (Gençay & Qi, 2001; Pérez et al., 2014) where the available data are divided randomly into three section, which are training set, validation set and testing set (Bishop, 1996; Pérez et al., 2014). The training network involved training set and validation set, meanwhile testing set was used after complete network trained to verify network accuracy. Beginning with training set, training set is used to compute the gradient and adjust the weights on the neural network during training iterations. On the other hand, validation set used to assist training network by minimizing overfitting issues and not used in adjusting the weights. Validation set minimizes overfitting through investigating the error and accuracy of both, training data set and validation data set. Provided that accuracy through the training data set increases and at the same time the accuracy through the validation data set still stays the same or decreases, the neural network begins to overfit, optimistically biased and required to stop training network. Therefore, to stop the train network, the finalization of weights are decided at location where minimum validation error through ES approach (Prechelt, 1998). Last but not least, testing data set is used to verify actual prediction network performance and determine the generalization error of the completed trained network using unbiased or unknown data set (Bishop, 1996; Gardner & Dorling, 1998; Polat & Güneş, 2007; Prechelt, 1998).

## 2.8 Neural Network Performance Evaluation

In reliance on assessing the model performance and validity, there are several techniques that can be used. Evaluation of model network performance is commonly evaluated through the residuals obtained. The residual will show how accurate and validated the model is, once it exhibits white noise characteristics. The model prediction capability qualified the generated model behavior which can be resolved by evaluating the residual between actual and predicted output data (Awadz et al., 2010; S. Haykin, 2005; Nelles, 2001; Rahiman, Taib, & Salleh, 2009). Thus, this work model evaluates the performance through prediction error, mean squared error (MSE), and confusion matrix. Meanwhile, the correlation function test is decided to assess validation of the model.

### *i Prediction Error*

Based on prediction error, or known as  $\varepsilon$ , refers to residual differentiation between the actual output and the predicted output of the network. This can be shown through Equation 2.27. The great model performance through prediction error evaluation is once the residual between actual and the predicted output is randomly distributed around zero (Zhang et al., 2009). This prediction error will be utilized into MSE section and also in correlation function test section to evaluate the performance.

$$\varepsilon_i = y_i - \hat{y}_i \text{ and } i = 1, 2, 3, \dots, N \quad (2.27)$$

Where  $\varepsilon$  is prediction error,  $y$  is actual output,  $\hat{y}$  is predicted output,  $i$  is instances number.

### *ii Mean Squared Error (MSE) - Model Fitting*

Mean squared error or known as MSE is standard technique for evaluating the magnitude errors toward the regression and model fitting issues. MSE can indicate

dissimilarity error between the predicted observation values and the actual observation values of the model. Commonly, MSE is used to estimate the prediction capability of intended models and the minimum values of MSE closer to zero means good model fitting (Pardo & Sberveglieri, 2002; Prechelt, 1998). MSE parameters can be expressed mathematically based on Equation 2.28.

$$\bar{\varepsilon} = \frac{\sum_{i=1}^n (y_i - \hat{y}_i)^2}{N} \quad (2.28)$$

Where  $\bar{\varepsilon}$  is MSE,  $y$  is actual output,  $\hat{y}$  is predicted output,  $i$  is instances number, and  $N$  is instances length. Thus,  $\bar{\varepsilon} \approx 0$  is appropriate and acceptable as the zero is the ideal case.

### 2.8.1 Confusion Matrix

In machine learning field, especially in the statistical classification of the model, error matrix should be known. This error matrix is allowed contingency table layout to show algorithm performance. Supervised technique used confusion matrix, where actual output and predicted output were required (Deng, Liu, Deng, & Mahadevan, 2016; Ruuska et al., 2018), meanwhile unsupervised technique used matching matrix, which required predicted output only (Hoadley & Hopkins, 2013; Tsuchiyama, Katsuhara, & Nakajima, 2017). However, both matrices allow visualization of the performance that analyze the model itself. Hereafter, this research model algorithm utilized supervised technique, wherever the concern on confusion matrix.

Previously, confusion matrix has been broadly implemented in distinct fields such as science, medicine, engineering and business (Akobeng, 2007; Matei, Pop, & Vălean, 2013; Subasi & Erçelebi, 2005; Zadeh et al., 2010). In the model classification, confusion

matrix comprises of the revealed data information through the actual classification and predicted classification which are being tested by classification model. Based on contingency table categorical of confusion matrix, there are True Positive (TP), True Negative (TN), False Positive (FP) and False Negative (FN) categories. True and False refers to outcome correctness, meanwhile Positive and Negative refers to model outcome of classifier itself.

Based on four category types, TP, TN, FP, and FN are different in their information. TP refers to model outcome correctly classified into positive class (class members predicted as class members), meanwhile TN refers to model outcome correctly classified into negative class (class members predicted as class members). However, FP refers to model outcome incorrectly classified into positive class (class non-members predicted as class members), meanwhile, FN refers to model outcome incorrectly classified into negative class (class members predicted as class non-members). These fundamental concept parameters of confusion matrix need to recognize and understand deeply, before undergoing in to complex cases, which are more than two classes. Throughout straightforward concept, the two conditions or 2x2 matrix was presented and manipulated. This concept shows the exact information via TP, TN, FP, and FN. The ideal model classification shows all prediction classified into TP and TN cells only, and also there are none prediction classified into FP and FN cells (Chris M. Bishop, 1994).

Basically, the predicted output, which resulted by classification network, will evaluate through actual output, which is real and target data of classification. Therefore, this evaluation provides the assessments investigation via accuracy (Acc), sensitivity (Se) and precision (Pp). Accuracy refers to rate of correct classification via sensitivity and precision of the classification model. The parameter of accuracy, sensitivity and precision are expressed mathematically as in Equation 2.29, 2.30 and 2.31, respectively.

**Table 2.4: Confusion Matrix via Evaluation Performance on First Level.**

	Levels	Actual		Performance (Precision)
		1	2	
Predicted	1	TP	FP	Pp <sub>1</sub>
	2	FN	TN	
Performance (Sensitivity)		Se <sub>1</sub>		Acc

**Table 2.5: Confusion Matrix via Evaluation Performance on Second Level.**

	Levels	Actual		Performance (Precision)
		1	2	
Predicted	1	TN	FN	
	2	FP	TP	Pp <sub>2</sub>
Performance (Sensitivity)			Se <sub>2</sub>	Acc

where Se<sub>1</sub> and Se<sub>2</sub> are sensitivity on each level, Pp<sub>1</sub> and Pp<sub>2</sub> are precisions on each level, and Acc is the total network prediction.

$$Acc = \left( \frac{TP+TN}{TP+TN+FP+FN} \right) \times 100\% \quad (2.29)$$

$$Se = \left( \frac{TP}{TP+FN} \right) \times 100\% \quad (2.30)$$

$$Pp = \left( \frac{TP}{TP+FP} \right) \times 100\% \quad (2.31)$$

Commonly, the evaluation of model performance always refers to its accuracy. However, sensitivity and precision also need to evaluate the performance. Sensitivity refers to completeness measurement, where the classification and evaluation are categorized correctly, meanwhile precision refers to exactness measurement, where the classification and evaluation are categorized correctly. These two-parameter comprised inverse relationship with the error, but both are not sensitive to data distribution compared to accuracy.

### 2.8.2 Model Validation (Correlation Function Test)

Model validation is needed to verify the acceptancy of discovered fitted model. Basically, Correlation Function Test was used to investigate residual test. This test will be benefitting to detect neural network model design flaws which led to improper network issues, such inadequate input data, network training and network overfitting. Therefore, validation of the developed model is required and crucial to ensure the neural network sufficient enough via observation (actual output data) (Zhang et al., 2009). Correlation tests are efficient techniques of validating developed neural network through investigating the whiteness of its residuals by estimating the similarity among the datasets. In the absence of these tests, the performance of neural network model cannot be guaranteed (Zhang et al., 2009).

There are two type of correlation tests which are auto-correlation function, known as ACF and cross-correlation function known as CCF (Awadz et al., 2010; Rahiman et al., 2009; L. F. Zhang et al., 2009). ACF refers to similarity evaluation between the residual and itself, meanwhile CCF refers to similarity evaluation between the residual and actual output. It is standard to carry out the ACF AND CCF between lag  $\pm 20$  (Norgaard, Ravn, Poulsen, & Hansen, 2000). Both tests were performed by changing the signals at distinct lags and estimating the correlation coefficients between each lag.

Unmodeled dynamic that have not been supposed by MFFN, once there is high correlation recognition. Thus, based on this case, this model of MFFN would be unsuitable and unacceptable. However, if the correlation test fits with all essential requirement, the models of MFFN are accepted. Mathematically, the equation of ACF and CCF can be expressed via Equation (2.32) and Equation (2.33), respectively.

$$\theta_{\varepsilon\varepsilon}(\tau) = E[\varepsilon(t - \tau)\varepsilon(t)] = \delta(\tau) \quad (2.32)$$

$$\theta_{y\varepsilon}(\tau) = E[y(t - \tau)\varepsilon(t)] = 0, \forall \tau \quad (2.33)$$

where,  $\theta_{\varepsilon\varepsilon}(\tau)$  is ACF equation,  $\theta_{y\varepsilon}(\tau)$  is CCF equation,  $\delta(\tau)$  is Kronecker delta,  $E(\bullet)$  is the correlation function in mathematical expectation,  $y(t)$  is actual output,  $\varepsilon(t)$  is prediction error based on residual, and  $\tau$  is lag space,

The correlation tests are supposed to achieve the outcome as Kronecker delta equation with specific tolerance level. Based on Kronecker delta equation,  $\delta(\tau)$ , it is defined as:

$$\delta(\tau) \begin{cases} 1, & \tau = 0 \\ 0, & \tau \neq 0 \end{cases} \quad (2.34)$$

In order to have acceptable model, the correlation coefficient in each lag should remain inward of 95 percent interval limits, where data points number is in specific set except at lag 0 for ACF test (Awadz et al., 2010; Rahiman et al., 2009; L. F. Zhang et al., 2009). The MFFN model is accepted once these essential requirements are fulfilled.

## 2.9 Human Brain Cognitive Abilities

As this study approaches between artificial neural network and human neuroscience, the general concept should be elaborated in literature as well. Beginning with human potential, human potential is a direct reflection of the anatomy and physiology of the nervous system. The nervous system is one of human body systems that controls complex nerves network by transmitting signals to various areas of the body. Biologically, the nervous system splits into two part which are the central nervous system (CNS) and the peripheral nervous system (PNS). CNS is a crucial part or main part of nervous system and consists of the brain and spinal cord, meanwhile PNS is a support part or subpart of

nervous system and consists mainly of nerves which provide the signal from CNS to various part of human body (Clark, Boutros, & Mendez, 2010).

With respect to cognitive function, human brain part of CNS is involved. Human brain weighs around 1400g and occupies the majority intracranial compartment where the structure comprises of cerebrum, brainstem and cerebellum (Matta, Menon, & Smith, 2011). Each parts has its own function; cerebrum function controls voluntary actions (Hikosaka, 1998), brainstem function controls involuntary actions (Smith & DeMyer, 2003), while cerebellum controls muscular movement, posture and balance (Morton & Bastian, 2004). The major portion of the brain structure is cerebrum, which high brain volume compared to cerebellum and brainstem. The cerebrum is essentially a paired structure, with left and right hemispheres (Clark et al., 2010). Each of the hemispheres is associated with somatosensory receptors and motor control on the other side of the body (A. Li, Yetkin, Cox, & Haughton, 1996). The specific brain hemispheres have their own certain functions which can be related with cognitive abilities (Van Der Knaap & Van Der Ham, 2011).

Basically, the cerebrum is divided into frontal, parietal, occipital and temporal lobes. Initially, the frontal lobe position is located at most anterior of cerebrum and its function controls intellectual activities, behavior, personality and emotional control (Duncan, Emslie, Williams, Johnson, & Freer, 1996; Hogeveen, Salvi, & Grafman, 2016; Lhermitte, Pillon, & Serdaru, 1986). Subsequently, the parietal lobe located behind frontal lobe and its function regulates the ability to read, write, and understand spatial relationships. Meanwhile, the occipital lobe is located at most posterior of cerebrum and its function controls sight. Last but not least, the temporal lobe is located in inferior of frontal lobe and its function is to control memory, speech and comprehension (Lisman, 2015).



Principally, the cognitive abilities related to cognitive processes are located in the frontal region; specifically the prefrontal cortex, where this region enables human to think, plan, solve problems and make decisions (Marieb & Hoehn, 2015). Cognitive abilities are defined as characteristic approach of the brain to process information (Neubauer & Fink, 2009a) while cognitive processes are associated with brain activity conversion and functional connectivity (Medaglia et al., 2015). Usually, brain activity encompasses cognitive activity or cognitive process in human brain. Consequence without the cognitive activity leads to deep coma while without brain activity it leads to brain death (Rosenberg, 2009).

Biologically, cognitive processes occurred when the chemical process in the brain transmits signals through the neurons. These are the cells called neuroglia existing between the neurons in nervous system and the ratio of neuroglia is around 3 to 1 more numerous than nerve cells in the brain (Purves et al., 2001). Current research indicates the neuroglia specifically astrocyte cells, interact with the neurons and hormones chemically in the production of thought or cognitive function by expressing the excitable molecules such as the neurotransmitter receptors, the intracellular signaling chains and the voltage-gated ion channels (Verkhratsky, Parpura, & Rodríguez, 2011). Furthermore, these astrocyte cells are capable of progressing propagation signals either via the gap junctions or via gliotransmitters release. Conceptually, these glial cells can perform all physiological processes such as identifying information (informational input), generate propagating signals, and secrete the transmitters (informational output), though the neuroglia executing these physiological processes in a specific way. (Illes & Verkhratsky, 2016; Verkhratsky et al., 2011)

With respect to the research, cognitive abilities are characteristic approach of the cognitive processes, such as perception, attention, intelligence, learning, memory,

language, executive functions and others (Cabeza, Nyberg, & Park, 2016; Duckworth & Yeager, 2015; Redick et al., 2016). Advantages of investigation among cognitive abilities gives a high impact to individual's, social, economy and environment. Generally, as human know their expertise on specific cognitive ability, they will know their potential in their career, thus providing work performance efficiency as well as work life balance. Therefore, based on this research, cognitive psychology introduces an essential new look at intelligence (Holinka, 2015) and learning style (Grey et al., 2015), in order to improve individual potential.

### **2.9.1 Intelligence Quotient Overview**

Since a long time ago, the research began to explore the human intelligence nature in mental abilities and continues to be debatable. Intelligence is defined as the ability to comprehend complex ideas, to efficiently adapt to the surroundings, to be engaged in various forms of reasoning, taking thought to overcome obstacles and learning from experience (Haler, Siegel, Tang, Abel, & Buchsbaum, 1992). The beginning of intelligence theory started from 1904. General intelligence or known as g factor was introduced by Charles Spearman to evaluate overall intelligence performance on mental ability tests. The rejection of unitary g factor by Raymond Cattell caused g factor separate into two parts, which are fluid intelligence known as Gf factor and crystallized intelligence known as Gc factor. Throughout Cattell's and Hon's publications, this separation factor into fluid and crystallized intelligence has turned as established in intelligence field (Horn, 1982).

General intelligence is highly associated with fluid intelligence (Deary, 2001) and working memory (Kane & Engle, 2002). Fluid intelligence is defined as pure or abstract problem solving capability and established in psychological basis, meanwhile crystallized

intelligence is defined as intelligence gain involved with acculturate knowledge (Horn, 1982; Schroeders, Schipolowski, & Wilhelm, 2015). Furthermore, fluid intelligence strongly predicts pure intelligence compared to crystallize intelligence due to fluid intelligence involved in short-term memory through abstract problem solving, while crystallize intelligence involves long-term memory through knowledge gain. The relationship between Gf and Gc is the greater Gf capacity attending to receive more Gc knowledge at faster rates (Dehn, 2017).

Individual differences in intelligence are quantified as intelligence quotient (IQ). Previous study revealed that in between forty percent and eighty percent of IQ variability is obtained through genetics, where IQ differences among individuals play crucial role in human life (Plomin & Spinath, 2004). The trait can be measured using various forms of fluid intelligence psychometric tests such as Cattell's Culture Fair (Duncan, Chylinski, Mitchell, & Bhandari, 2017), Weschler Intelligence Scale (D. Wechsler, 2008) and Raven's Progressive Matrices (RPM) (Duncan et al., 2017; Raven, Raven, & Court, 1998). Among the assessment techniques, RPM is considered as the most optimum domain-independent measure of general intelligence (Gray & Thompson, 2004). Thus, an approach of fluid intelligence is often utilized as closest to the true measure of intelligence.

Studies have also established through the Neural Efficiency Hypothesis that the brain of intelligent individual exhibits efficient use of cortical areas compared to the less gifted ones (Neubauer & Fink, 2009a). These are attributed to the well-functioning excitatory and inhibitory neurotransmitters that effectively reduce cortical noise and cerebral arousability (Fidelman, 1999). Hence, the oscillation of brainwave at rest is more synchronized and is reflected in higher alpha power (Doppelmayr et al., 2002). The energy expenditure is also lower in intelligent individuals (Haier et al., 1988).

Furthermore, the dominant alpha power maintains sustained attention by inhibiting task-irrelevant cortical activities (Dockree, Kelly, Foxe, Reilly, & Robertson, 2007). Hence, intelligent individuals also demonstrate shorter reaction time than the less gifted ones (Jensen, 1993).

Currently, the AI modeling approach to the cognitive abilities are limited to certain mental construct. Based on intelligence abilities, the AI model integrated with ANN technique has been implemented using single output only (Anoor, Anwar, Ali, & Jahidin, 2018; Jahidin et al., 2014; Jahidin, Taib, et al., 2015). Throughout the previous work, the study between AI modeling, specifically ANN, with the IQ level classification has been assessed, where this established EEG-Based IQ classification model has been utilized forward in this research to classify subject IQ level only (Anoor et al., 2018; Jahidin et al., 2014). The result of IQ level can be re-evaluated via the brainwaves feature pattern, which reflects Neural Efficiency Hypothesis theory. The performance of ANN was obtained with 100% accuracy in training, 100% accuracy in validation, and 88.9% accuracy in testing, meanwhile in MSE error had been obtained with 0.01 in training, 0.02 in validation and 0.05 in testing (Jahidin et al., 2014). However, the limitation of this model contained robustness issue using Hamming filter and the ANN structure architecture algorithm have single output (intelligence abilities). Hence, the model improvement is needed to upgraded using equiripple filter to robust the model and utilizing MIMO structure to identify more than one cognitive ability.

## **2.9.2 Learning Style Overview**

Style is defined as the manner or way of processing information or, detailly is defined as behavioral self-consistencies in processing information that form in congenial ways around underlying personality trends' (Messick, 1984). Meanwhile, learning styles refer

to variety of contested and competed theories that are purposed to assess the differences of individuals' learning (Eddy & Glass, 1981). The whole related theories suggest that everyone can be classified respecting their 'style' of learning, even though every theory has its own perspective views on how the style should be interpreted and categorized (Rayner, 2015). An identical concept found is that everyone is different in how they learn (Willingham, Hughes, & Dobolyi, 2015). Previous research found that there are 71 different models of various learning style theories (Coffield, Moseley, Hall, & Ecclestone, 2004). Currently, there are certain learning style models that have been integrated with experiential learning theory (ELT), which are most broadly implemented and established.

Experiential learning theory (ELT) is an important element in constructivist philosophy in education. The philosophy proposes knowledge as being created through a process of interaction between ideas and experience. The concept has been widely accepted due to its success in fostering effective teaching. Through such approach, instructors will function as facilitators with the goal of providing the most optimum learning experience to students (Cassidy, 2004). Several learning style models have been developed with Kolb's Experiential Learning Theory (Kolb's ELT) being the most widely implemented in education and management research (Kolb & Kolb, 2009).

Kolb's ELT defines learning to be the process whereby knowledge is created through the transformation of experience. The ELT portrays two dialectically related modes of Absorption and Comprehension dimensions also known as grasping and transforming experience, respectively. Absorption dimension refers to the process of taking in information, while Comprehension dimension is how individuals interpret and act on that information (Magfirah, 2017). The Absorption dimension comprises of Concrete Experience (CE) and Abstract Conceptualization (AC) learning modes, while the

comprehension dimension is comprising of Reflective Observation (RO) and Active Experimentation (AE) learning modes (Kolb & Kolb, 2005). Combination of dominant modes in both dimensions result in preferred learning style; Converging, Diverging, Accommodating and Assimilating styles. Each of styles influences how individuals learn (Kolb, 2007).

Each one of learning style has its own basic strength and unique characteristics. Particularly a dominant learning style might perform well in certain learning situation, but still the other minor learning style should be considered as the dominant style cannot be put superior to another (Larkin-Hein & Budny, 2003). Nevertheless, a learner is effectual to obtain great understanding and gain the excellent learning outcomes by attaching through whole four components of learning cycle (Chan, 2012). The individual that has balanced ability interprets that the individual is using differ learning styles (Kolb & Kolb, 2005)

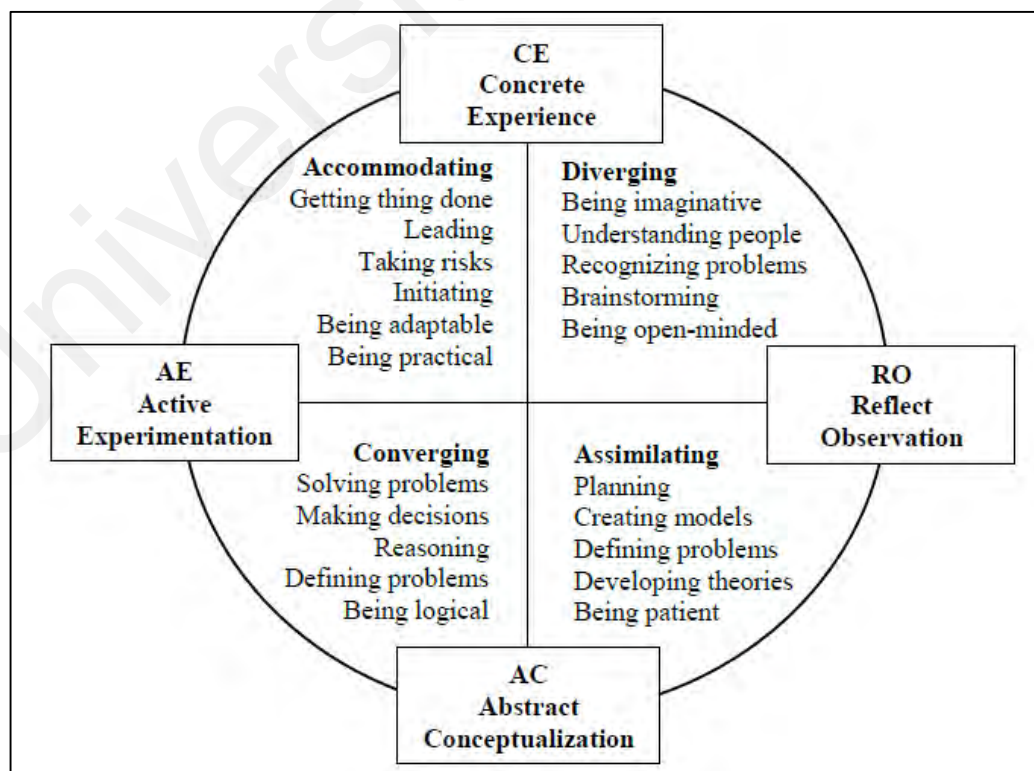


Figure 2.8: Learning Style groups description (Kolb, 2007).

The distribution of learning style and combination of learning modes are shown as below. Based on concrete experience (CE) mode, CE refers to a new or existing experience confrontation compared rather than to think (Larkin-Hein & Budny, 2003; Richmond & Cummings, 2005). Furthermore, this group type of person tend to be intuitive decision-makers (Larkin-Hein & Budny, 2003). Based on reflective observation (RO) mode, RO refers to reflecting on experience or understand the meaning ideas (Larkin-Hein & Budny, 2003; Richmond & Cummings, 2005). In addition, this group type of person prefer to reflect and observe rather than act and also prefer abstract understanding over practical applications (Larkin-Hein & Budny, 2003; Richmond & Cummings, 2005). Based on abstract conceptualization (AC), AC refers to reflection gain rise to new idea, which influencing the ideas and concepts investigation (Richmond & Cummings, 2005) and think over rather than how the person feels (Larkin-Hein & Budny, 2003). Furthermore, this group type of person tends to have a scientific manner through problem solving (Larkin-Hein & Budny, 2003) and is characterized by precedence on cognitive skills (Richmond & Cummings, 2005). Based on active experimentation (AE), AE refers to practical manner prominence solution compared to reflective problem understanding. Besides, this group type of person tend to be pragmatist, concerned on doing compared rather than observing, efficient during hands-on, and satisfied when completed job (Richmond & Cummings, 2005).

**Table 2.6: Overview group type of Kolb's learning style and combination of learning modes with their characteristics, respectively.**

<b>Kolb's Learning Style</b>	<b>Learning Mode Combination</b>	<b>Characteristics of Learning Style</b>
Diverger	CE and RO	Preferred imaginative ability in assign task and sensibility of value and meaning (Cagiltay, 2008; Richmond & Cummings, 2005). Able to recognize various perspectives and simply generate ideas (Healey & Jenkins, 2000; Richmond & Cummings, 2005) Preferred to be very creative (Richmond & Cummings, 2005).
Assimilator	RO and AC	Preferred to reason wisely (Cagiltay, 2008; Richmond & Cummings, 2005) Possess abstract and logical thinking instead of practical aspects of theories (Richmond & Cummings, 2005).
Converger	AC and AE	Preferred at hypothetical-deductive reasoning and efficiently in problem solving (Cagiltay, 2008; Healey & Jenkins, 2000; Richmond & Cummings, 2005). The problem solving by applying practical ideas (Richmond & Cummings, 2005). Adaptation in emotions controlling (Richmond & Cummings, 2005)
Accommodator	CE and AE	Preferred in informative manner than technical analysis via problem solving (Cagiltay, 2008; Richmond & Cummings, 2005). Systematically at carry out tasks via following directions, precisely planning, and problem solving based on intuitive trial-and-error approach (Richmond & Cummings, 2005)

An assessment tool to investigate Kolb's learning style is known as Kolb's Learning Style Inventory (KLSI), which was constructed with ELT (Kolb, 2006). Based on this study, KLSI is implemented and investigated due to comprehensive theory of learning, personality and development in education field rather than other tests (Kolb & Kolb, 2005). Besides, KLSI was constructed to achieve two aims which are, to assist in educational tool and research tool (Kolb & Kolb, 2005). In educational tool, the purpose



is to improve individuals' understanding of learning process from experience and individual's characteristic approach through learning styles. In research tool, the purpose is to analyzing ELT and individual's characteristic of learning styles. In general, previous researches had been investigating the individuals' characteristic of learning styles, that give impact on achievement and improvement through fostering their unique learning habits (Moran, 1991).

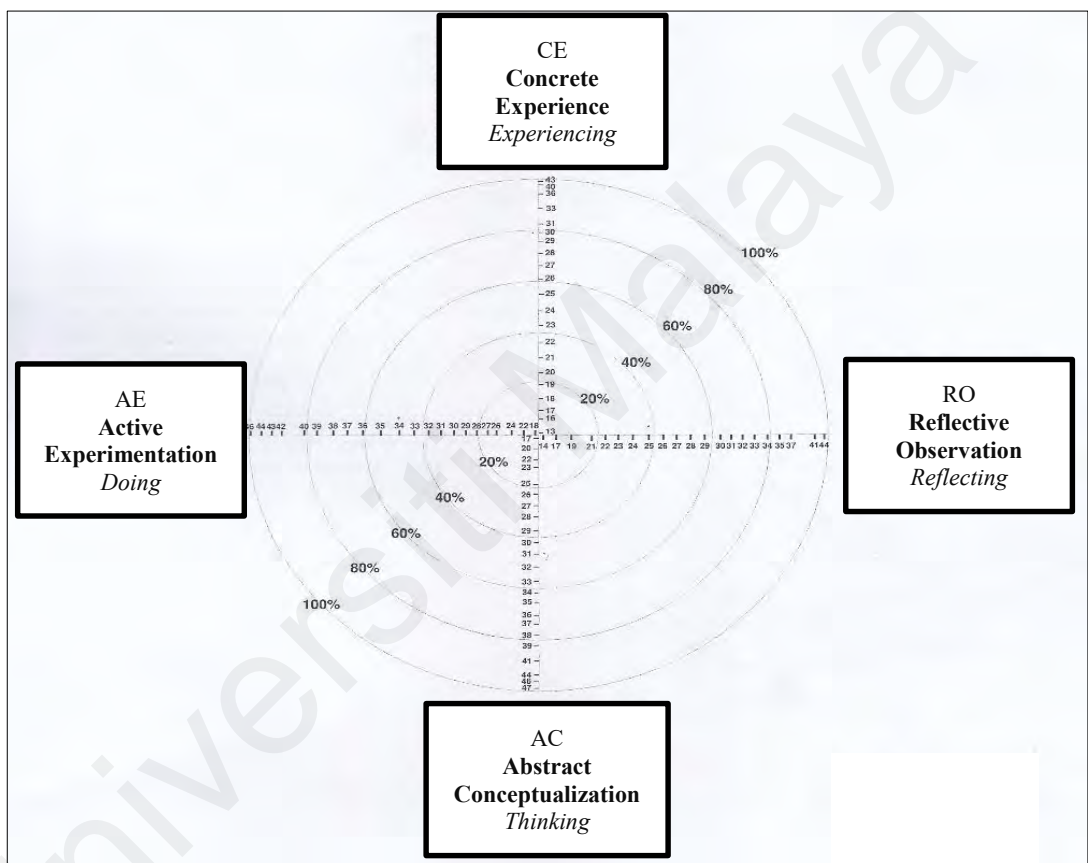
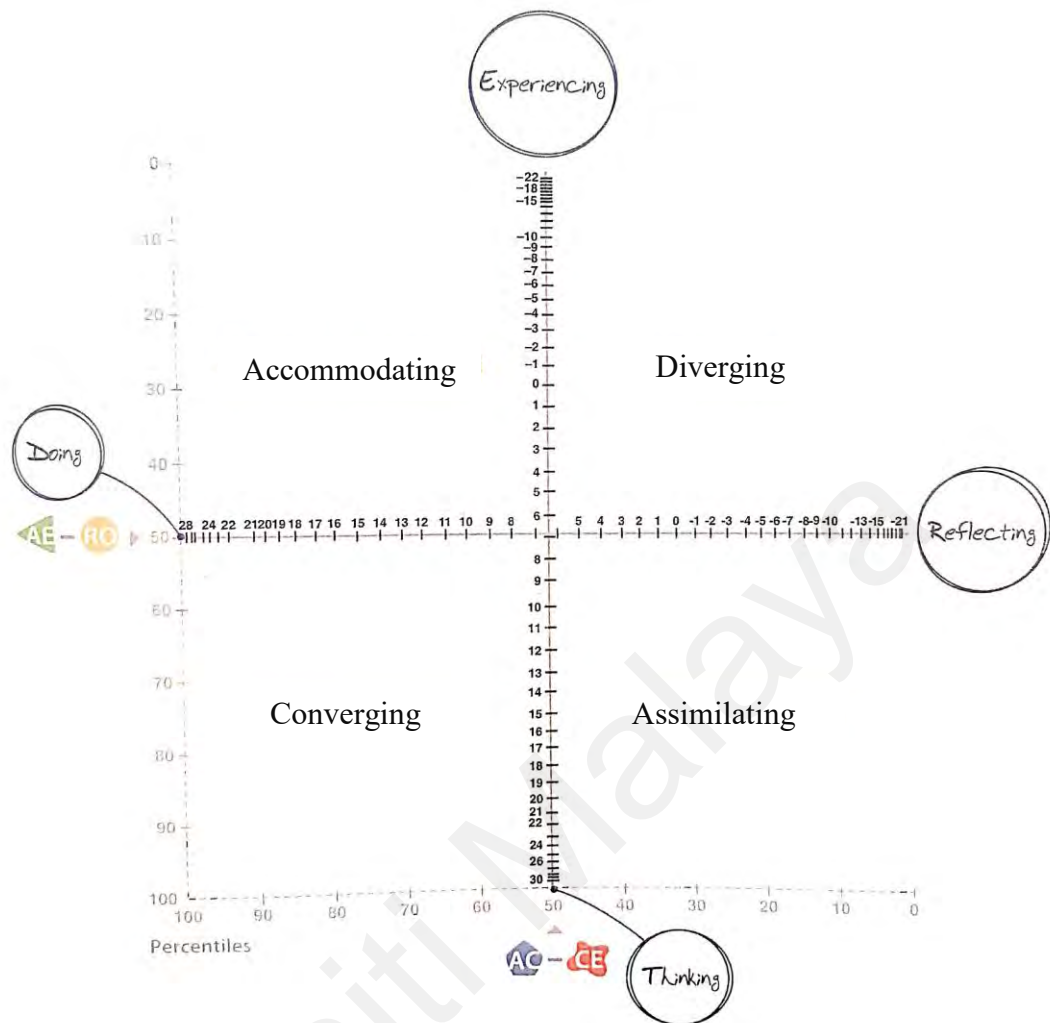


Figure 2.9: Mapping scores on learning mode cycle (Kolb, 2007).



**Figure 2.10: Mapping scores on learning style grid (Kolb, 2007).**

By completing KLSI questionnaire, scores need to be evaluated and mapped on four different learning modes (CE, RO, AC and AE) in Figure 2.9. The closer the dots to 100% circle, the higher is the individual's learning to use that learning manner. To determine learning style, four learning mode scores need to subtract to obtain two combination scores, which two combination scores reflect to how individual takes in experience (AC - CE) and how individual deals with experience (AE - RO). The individual data point scores will map on learning style grid as Figure 2.10 and the specific learning style will indicate. Both mapping through learning mode cycle and learning style grid express the strength and weaknesses of inherent learning style.

In research or scientific manner, learning style which is related to cognitive processing can be investigated through EEG. There is assorted brainwave feature extracted through brainwave localization. However, left frontal brain location in resting state are commonly selected due to cognitive processing such as intelligence (Jahidin, Megat Ali, Taib, Md Tahir, & Yassin, 2015) and learning style (Megat Ali, Jahidin, Taib, Tahir, & Yassin, 2016). Findings have also found that there are correlations between learning styles and brainwave pattern (Megat Ali, Jahidin, Md Tahir, et al., 2014; Rashid et al., 2011, 2013). Based on alpha sub-band, Rashid et al. (2011) showed the lowest alpha ESD feature belongs to diverger, followed by converger, assimilator and accommodator (Rashid et al., 2011) meanwhile Megat Ali et al. (2014) showed that the lowest alpha SC feature belongs to accommodator, followed by diverger, assimilator and converger (Megat Ali, Jahidin, Md Tahir, et al., 2014). Based on beta sub-band, the others finding show the lowest beta PSD feature belongs to converger, followed by diverger, assimilator and accommodator (Rashid et al., 2013). Based on theta sub-band, finding show the lowest theta SC feature median belongs to assimilator, followed by converger, diverger and accommodator (Megat Ali, Jahidin, Md Tahir, et al., 2014).

**Table 2.7: Correlations between learning styles and increasing brainwave pattern through related previous studies**

Feature selection/ Sub-band brainwaves	Energy spectrum density (ESD) Rashid et al. (2011), Rashid et al. (2013)	Spectral centroid (SC) Megat Ali et al. (2014)
Alpha	Diverger, Converger, Assimilator and Accommodator	Accommodator, Diverger, Assimilator and Converger
Beta	Converger, Diverger, Assimilator and Accommodator	Assimilator, Converger, Diverger and Accommodator

Presently, the AI modeling approach to the cognitive abilities are restricted to specific mental construct. Based on Kolb's learning style abilities, the AI model integrated with ANN technique has been implemented using single output only (Megat Ali, Jahidin, Taib, Tahir, & Yassin, 2016; Megat Ali, Jahidin, Taib, & Md Tahir, 2016; Megat Ali, Jahidin, Md Tahir, et al., 2014; Megat Ali, Jahidin, Tahir, & Taib, 2014). Throughout the previous work, this model performance discovered 85.1% accuracy in training dataset and 91.3% accuracy in testing dataset, meanwhile, in MSE error was 0.0995 in training dataset and 0.0901 in testing dataset (Megat Ali, Jahidin, Taib, Tahir, et al., 2016). However, this model has minimum accuracy compared to established IQ classification model, which is 100% accuracy in training and validation. Thus, in this research the conventional psychometric test method (KLSI) is required to achieve accurate classification.

In the end, the prior benefits through Kolb's learning style are concerning the transaction between personal and social knowledge, and also between internal and external characteristics. Furthermore, Kolb's learning style presents experiential learning cycle description which involved overall learner understanding in real- world situation. Consequently, as learning style are integrated through intelligence and brainwaves signal, it is assisted each individual to obtain achievement with their maximum capability in real-world environment.

### **2.9.3 Intelligence Quotient and Learning Style Relationship**

Hypothetically, the primitive difference between intelligence theories and learning style theories is intelligence's role as a core on the learning contents and products process, meanwhile learning style role is as a side core and focused on differences in learning process (Snyder, 1999). Currently, they are absent of researchers' approach exploring intelligence and learning style utilizing Kolb's ELT and IQ. Despite that, based on

McKenna theory demonstrates there are several differences between intelligence and learning style (Diseth, 2002; McKenna, 1984). First, intelligence ability is more related with achievement level, while learning style concerns on the way of achievement. Secondly, intelligence ability is unipolar which means this ability dimension is valued and the other is not, whereas learning style is bipolar which means ability dimension has neither end nor been considered better overall. Finally, intelligence ability has a limited range of application compare to learning style, which has diverse range of application.

Generally, Cattell (1963) asserts that the fluid intelligence refers to intentional mental operations to solve novel problems and abstract thinking (Cattell, 1963), which is related to abstract conceptualization based on Kolb's ELT (Kolb, 2007). Abstract conceptualization was concerned with most of the critical thinking dispositions: analyticity, self-confidence, truth-seeking, systematicity and maturity (Colucciello, 1999). According Patterson (1994) work, supported the view that accommodators scored lowest in critical thinking (Patterson, 1995), meanwhile Gyeong and Myung's (2008) found the divergers correlated with the lowest and convergers with the highest critical thinking (Gyeong & Myung, 2008). Despite that, others finding also present that assimilator and converger encompass thinking in their learning process related to the critical thinking dispositions (Andreou, Papastavrou, & Merkouris, 2014).

Generally, intelligence and learning style relationship approach can lead the individual to ensure effective performance in the learning process by their suitable intelligence and adaptive learning style (Hamada & Hassan, 2017). In other words, it means suitable intelligence levels enable learners to obtain the most suitable learning preferences that might be matched with their learning styles. Thus, integration of intelligence and learning style with brainwaves signal into ANN approach is beneficial as well as allows the relationship between psychological traits.

The correlation among EEG, IQ and learning style (LS) exists in previous and current studies (Anokhin & Vogel, 1996; Davidson et al., 1990; Doppelmayr et al., 2002; Doppelmayr et al., 2005; Jaušovec, 1998, 2000; Kounios et al., 2008; Lutzenberger et al., 1992; Megat Ali, Jahidin, Md Tahir, et al., 2014; Megat Ali, Jahidin, Taib, & Md Tahir, 2016; Neubauer & Fink, 2009a; Ono et al., 1982; Rashid et al., 2011; P. E. Vernon, 1984). Based on EEG and IQ correlation studies, significant findings were investigated in the tonic state and apart from cognitive demanding task (Langer et al., 2012; Lee et al., 2012; Wang et al., 2011). Meanwhile, based on EEG and LS correlation studies, significant findings were observed in resting condition with absence of cognitive demanding task (Megat Ali, Jahidin, Md Tahir, et al., 2014; Megat Ali, Jahidin, Taib, & Md Tahir, 2016; Rashid et al., 2011). Previous studies also showed the individuals' intelligent differences are demonstrated particularly at prefrontal cortex brain areas (Blair et al., 2005; Fink et al., 2009; Gray et al., 2003; Gray & Thompson, 2004; Neubauer & Fink, 2009a; Neubauer et al., 2002, 2005; Staudt & Neubauer, 2006). Furthermore, right and left sides of brains hemispheres are considered in cognitive studies (Corballis, 2003; Martindale, Hines, Mitchell, & Covello, 1984; Rashid et al., 2011). However, left side of brains hemisphere is more dominant compared to right side in cognitive task performance (Deary et al., 2010). Hence, this shows a great opportunity existed among EEG, IQ and LS as stated above.

Based on McKenna theoretical, there are some differences involved between intelligence and learning style (Diseth, 2002; McKenna, 1984). First concept is intelligence ability is involved with achievement level, meanwhile learning style is involved with achievement manner. Second concept is intelligence ability is unidirectional, meanwhile learning style is bidirectional. Third concept is intelligence ability has measurements joined to one end of dimension ability that is valued and the otherwise is not valued, meanwhile learning style has dimension where neither end is

supposed to be better overall. Final concept is intelligence ability has narrower and tighter application areas compared to learning style (Diseth, 2002). Throughout this concept, it can be assisted to enhance variants or proper learning approaches via appropriate intelligence approaches.

Integration of learning style and intelligence into learning systems can be matched with adaptive learning system that can adapt the content for the purpose of ensuring the better performance in the learning process (Hamada & Hassan, 2017). That means suitable intelligence levels enable learners to acquire the most suitable learning objects that might be compatible with their learning styles. In addition, previous investigation between intelligence ability and learning style, found that learning style has significant positive influence via intelligence ability (Busato, Prins, Elshout, & Hamaker, 2000). Thus, the cognitive individualities will impact effectively on the capability, improvement, development, and effectiveness of education approach.

## METHODOLOGY

### 3.1 Introduction

This section explains the method employed throughout the whole study. The study is comprised of six major stages; formulation of experimental framework, data collection, statistical analysis and validation, development of IQ-learning style classification model using ANN, as well as documentation and thesis writing. The methods proposed for this study is outlined in Figure 3.1.

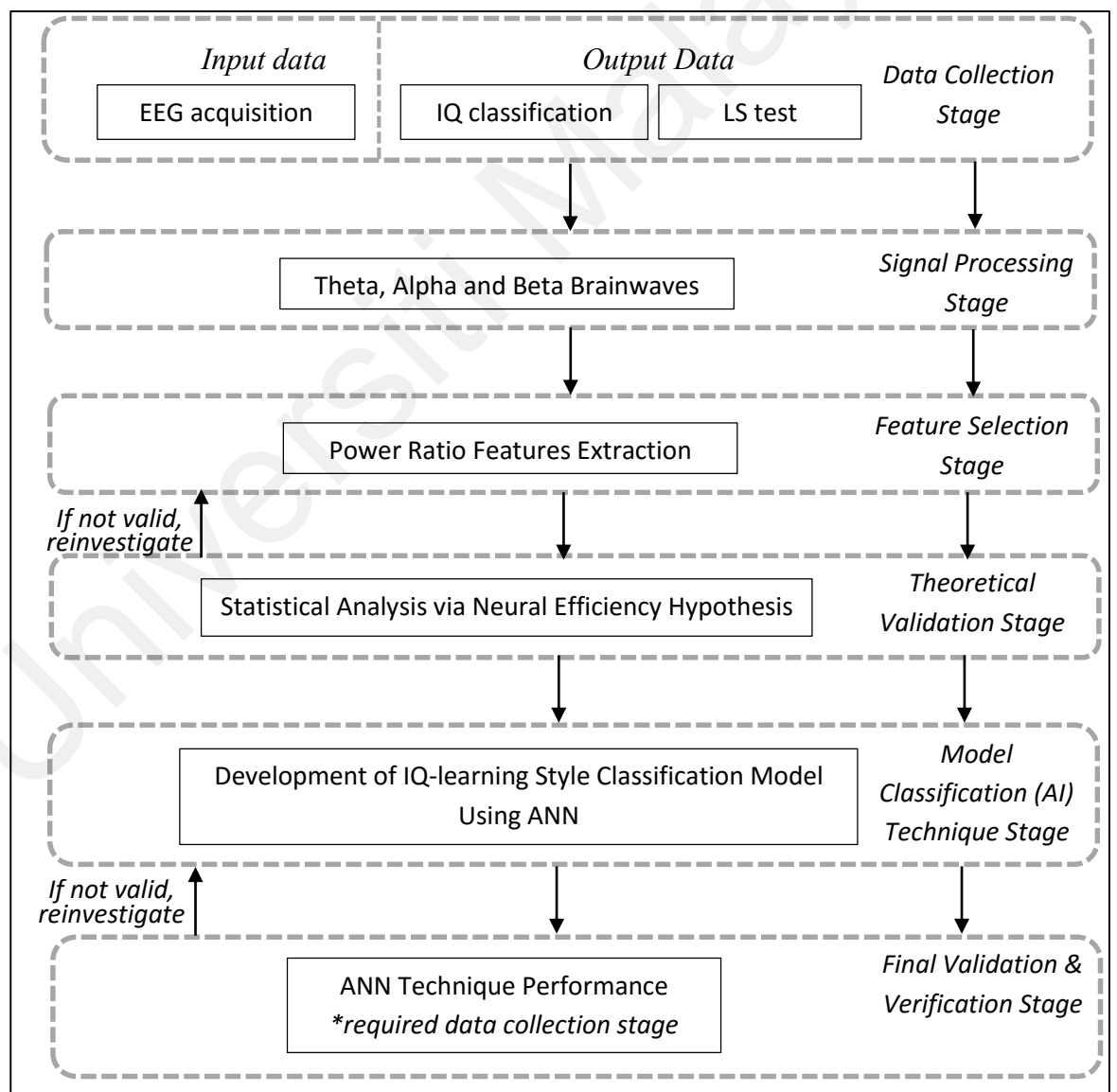


Figure 3.1: General concept of research methods



Data acquisition are involved the brainwaves collection, IQ classification via established model, and learning style test. Signal pre-processing involved filtering and feature extraction, while synthetic data was utilized after valid statistical analysis. Classification Model was involved from Model development via ANN until the end. The elaboration will be discussed through sub-section in methodology part.

Generally, theta, alpha and beta brainwaves are used for signal processing stage. The reason of using these three sub-band brainwaves is because previously, numerous researchers have been using these three sub-band brainwaves for cognitive study. Once obtaining the brainwaves, power ratio (PR) features extraction will be used for feature selection stage which gives large impact on accomplishment of classification system.

To ensure the that input data is validate, the statistical analysis was utilized using Neural Efficiency Hypothesis. Studies have also established through the Neural Efficiency Hypothesis that the brain of intelligent individual exhibits efficient use of cortical areas compared to the less gifted ones (Neubauer & Fink, 2009a). In addition, this stage also provided significant pattern between LS and IQ through box plot. Clean data can be obtained after removing or minimizing the outliers, which are unrelated to the real data.

Multiple input multiple output (MIMO) model structure is required to develop classification model. MIMO ANN comprises of three inputs which are theta, alpha, beta ratio features and two outputs which are IQ levels and LS groups. By using this structure, it can classify both output (IQ levels and LS groups), simultaneously. Once the model has been developed, the model validation and verification will use auto correlation function and cross correlation function test technique.

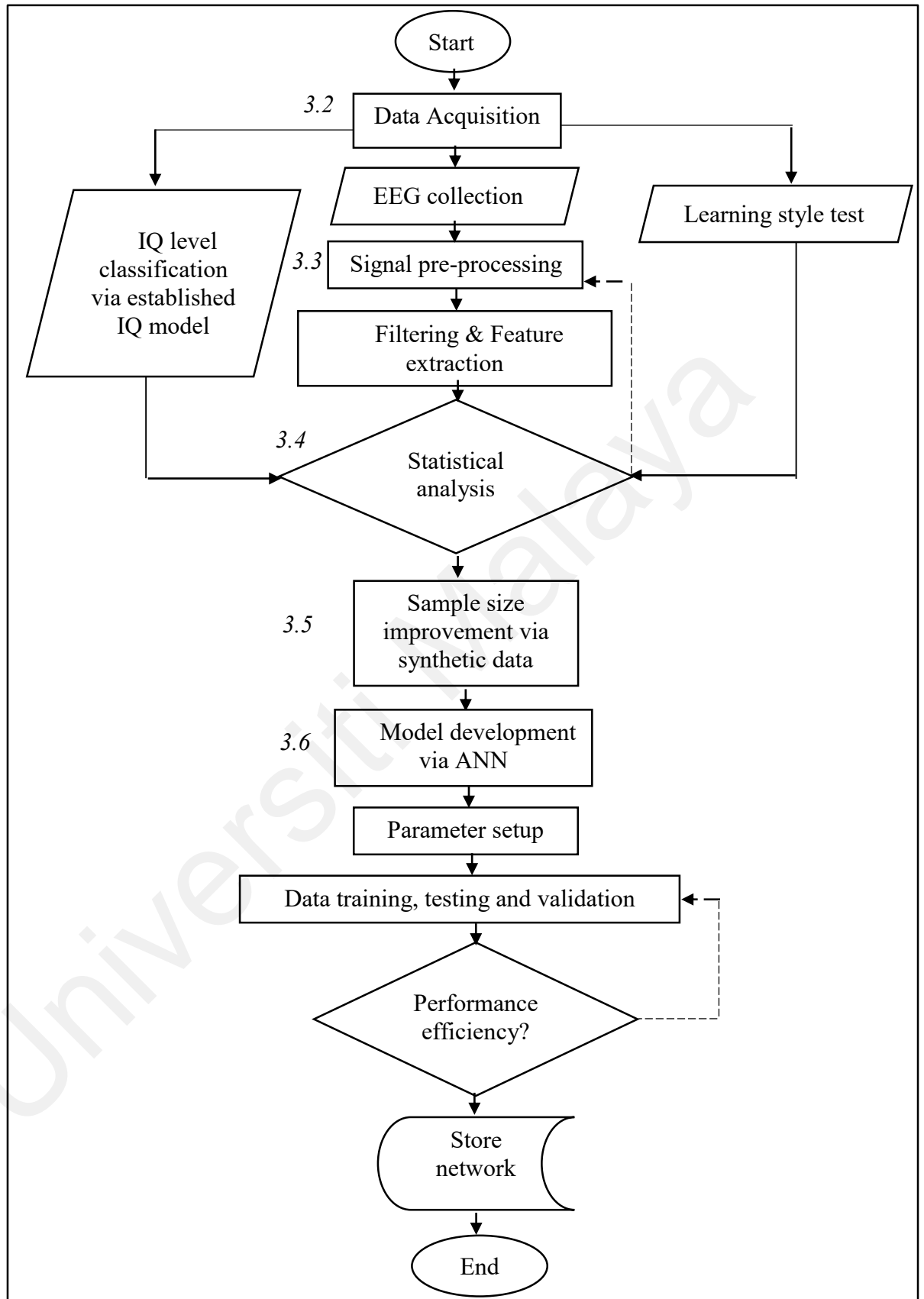


**Figure 3.2: Summarization of the development EEG-Based IQ-LS Classification using MIMO ANN model.**

Based on Figure 3.2, the experiment started with data acquisition which involved EEG collection, IQ classification using established IQ model and learning style test using Kolb's Learning Style Inventory. Throughout EEG data collection, the brainwaves signals need to be processed further for feature extraction purpose. Statistical analysis was required to check the sample size and pattern of the feature extraction. Based on flowchart in Figure 3.2, the implementation of this statistical analysis needs to ensure whether validate or not. If not, the signal pre-processing needs to recheck again or any other problems, while if yes, the process will proceed to sample size improvement via synthetic data.

This methodology procedure has been implemented in research practices through previous work. However, the implementation of conventional EEG machine via dry electrodes, utilizing different signal pre-processing technique, increase in sample size, ANN architecture, and parameter setup are still novelty, in order to achieve IQ-LS model classification performance.

### **3.2 Sample Selection, Data Acquisition and Cognitive Measures**

A total of 85 healthy people (mean age / standard deviation = 20.99/ 3.56), which involved 50 males and 35 females from various highest educational backgrounds which consists of 58 subjects with highest education of SPM level, 14 subjects with highest education of Foundation/STPM level, 4 subjects with highest education of Degree level and 9 subjects with highest education of Master level as in Figure 3.3. All subjects were selected for the study, aged between 17 to 40 years old. The subjects that participated in this study were given consent form and requirements under the ethical scrutiny and approval of the University Ethics Committee. With regards to this research activity,

healthy persons were selected to build the border classification that comprises non-diagnosed or medically treated person. This is important to set an establish baseline context in comparison with correspondence.

The experiment was carried out two stages. The first stage is to record the EEG signal with IQ classification using established IQ classification model (Jahidin et al., 2014) and the second stage is to implement the Kolb's Learning style inventory for the learning style test. With respect to stage 1, real-time EEG signal was recorded using Neurosky MobileWave Headset, which captured electrical activity from a specific brain location. In accordance to analyse the EEG signal, the connection between the device, software and computer were required wirelessly by using bluetooth connection. Subsequently, skin preparation was required before applying electrode placement. A dry electrode of the device was placed on Fp1 (left hemisphere of the brain), while ground and reference electrodes were placed on left earlobe conformed with line 10-20 international system of electrode placement as shown in Figure 3.4. This EEG device used the baud rate of 9600 bps and sampled frequency of 512Hz. The experiment was conducted in a quiet room to maintain the relaxing state of the mind and to avoid noise which could have interfered during recording. Attention meter and meditation meter using Neurosky Headset application had been monitored during the experiment. This attention meter was used to ensure the subject not in focusing mode during recording, meanwhile meditation meter was used to ensure the subject in relax condition. Hypothetically, through the resting state and eye-closed condition, the stability of the brainwaves for each individual existed as well as human trait-like to analysis (Erickson et al., 2018). During recording, the rejection raw data was not considered if the disturbance data are affected and damaged due to unethical scrutiny and the recording data was repeated. The reason is to avoid erroneous measurement and to achieve a valid signal by following the methodology

protocol. In order to obtain IQ classification, established IQ Classification Model (Jahidin et al., 2014) was implemented to classify IQ level.

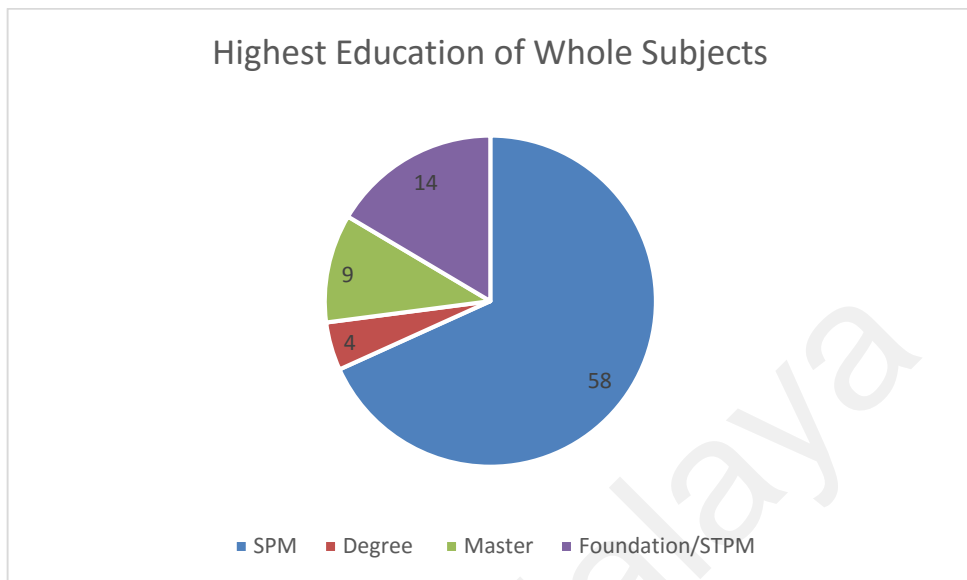


Figure 3.3: Distribution of highest education of all subjects participated in this study.

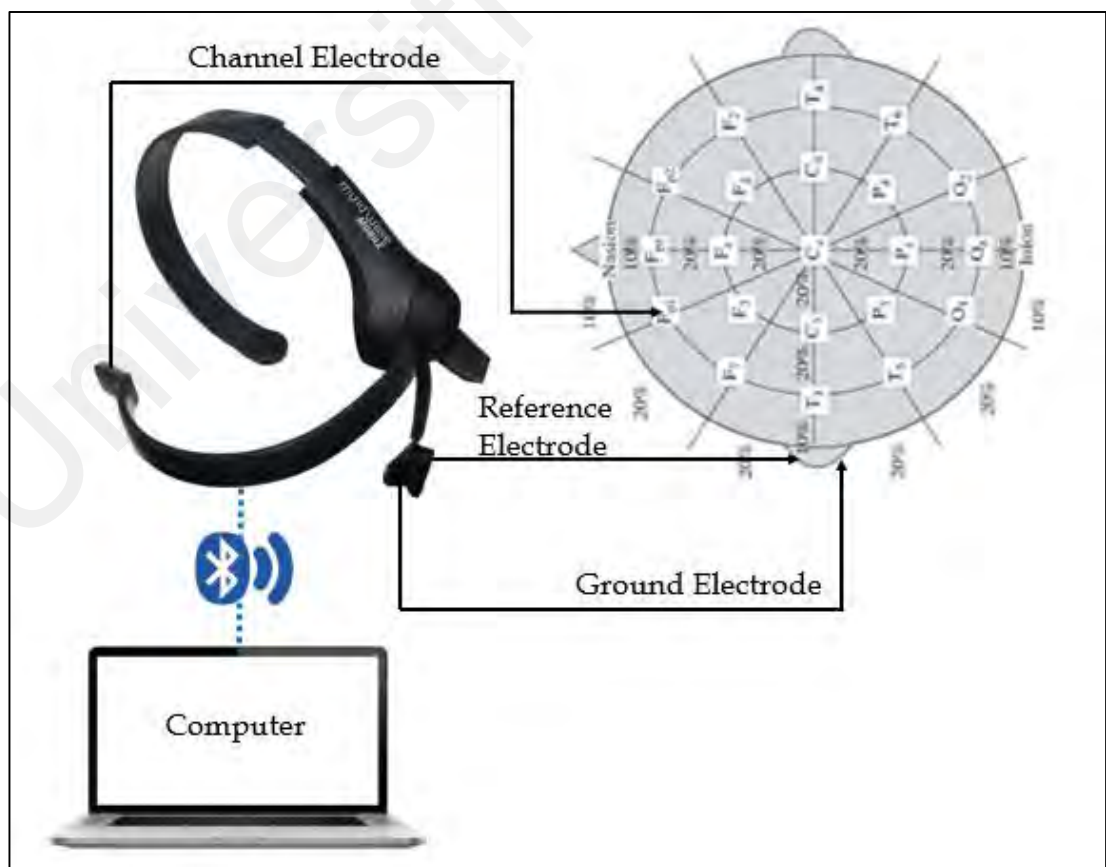


Figure 3.4: Methodology EEG tool experimental setup



**Figure 3.5: Subject with experimental setup**

With respect to the second stage, the subject will answer all questions provided in the learning style sheet questionnaire (as in Appendix K) with the guidance of the researcher to avoid any misunderstanding during answering the questions. The learning style classification is mapped using Kolb's Learning Style Inventory. All the learning style data will be recorded and mapped by using Microsoft Excel. The learning style data recorded into SPSS along with IQ and EEG sub-band data to investigate the relationship between IQ, LS, and EEG sub-bands.

### **3.3 Pre-processing, Filtering and Feature Extraction**

Raw data EEG signal was pre-processed using MATLAB 2017a. To reject electrooculogram (EOG) artifact rejection, the characteristic for voltages exceeding the range of  $\pm 100 \mu\text{V}$  rejection has been performed. Experimentally, EOG automatic rejection approach (Jahidin, Megat Ali, et al., 2015) has been employed due to the subject rest and static as protocol. Further analysis in this study limits the signal to the duration

of 2 minutes 30 seconds (Megat Ali, Taib, Md Tahir, Jahidin, & Yassin, 2014; Megat Ali, Jahidin, Taib, & Md Tahir, 2016). As recording total recording signal is 3 minutes, the initial of 20 seconds and the end of 10 seconds of the whole recorded signal was removed. This removal is to prevent signal analysis contains of any spike overshoot and uncontaminated EEG signal.

In order to extract the feature, EEG data was filtered using equiripple filters to minimize error function, robustness, stability and efficient performance (Megat Ali et al., 2014) into theta, alpha and beta sub-bands. Generally, Parks-McClellan algorithm (McClellan & Parks, 2005) is a variation of the Remez (Kuyu & Vatansever, 2016) exchange algorithm, and developed in equiripple filter to optimizes Chebyshev finite impulse response (FIR) (Karam & McClellan, 1999) filter or optimizes minimax criterion. In equiripple filters, an optimized filter order of 1264 was acquired through the Parks-McClellan algorithm. It would cause the frequency outcome to effect ideal filter characterization into the optimum fit with steep transition band and constant ripples in the passband and stopband regions (Megat Ali et al., 2014).

After taking off baseline and extracting common artifacts, the data was transformed into the non-parametric power spectral density (PSD) distribution for each wave sub-band by performing Fast Fourier Transform (FFT) via Welch's method. Throughout Welch's method, the power spectrum of a time series by collecting the frequency component of a stochastic waves (Hosseinifard, Moradi, & Rostami, 2013; Welch, 1967). In addition, Welch's method generates averaging squared-magnitude discrete Fourier transforms (DFTs) and improve on the standard periodogram spectrum computed on each signal block, thus beneficial on noise reduction. In order to gain DFT, Fast Fourier Transform (FFT) algorithm approach is utilized for features extraction (Abásolo, Hornero, Gómez, García, & López, 2006; Acharya, Vinitha Sree, Swapna, Martis, & Suri, 2013; Bettus et

al., 2008; Cannon, Krokmal, Lenth, & Murphey, 2010; Goodman, Rietschel, Lo, Costanzo, & Hatfield, 2013; Gotlib, Ranganath, & Rosenfeld, 1998; Howells et al., 2012; Kaminski, Brzezicka, & Wróbel, 2011; Piryatinska et al., 2009; Polat & Güneş, 2007; Poulos, Rangoussi, & Alezandris, 1999; Tomarken, Davidson, Wheeler, & Kinney, 1992; Übeyli & Güler, 2005). Throughout conversion frequency domain, PSD is computed through the equation below:

$$S(e^{j\omega}) = \frac{1}{N} \left| \sum_{i=1}^N x e^{-j\omega i} \right|^2 \quad (3.1)$$

Where N defines as data sequence number,  $\omega = 2\pi f$  and  $f$  refers to sampling frequency.

To estimate the power of a signal at various frequencies, Welch's method was used in approach to energy spectral density (ESD) estimation. The energy distribution is acquired by evaluating the area of PSD curve for each frequency sub-band. This energy distribution is known as energy spectral density (ESD). Then, the ESD which contains the whole energy distribution for each range of the frequency band is evaluated for each group.

To normalize ESD values, power ratio (PR) features of theta, alpha and beta are extracted from sub-band ESD features values. This feature method derived by splitting the respective frequency power band by the other frequency power band to gain a feature that is characterized to represent signal behavior. Finally, power ratio features allowed the relationship among various brain waves of distinct individual. Power ratio features of each respective frequency band are expressed mathematically as below:

$$\text{Theta power ratio} = \frac{ESD_{\theta}}{ESD_{\alpha} + ESD_{\theta}} \quad (3.2)$$

$$\text{Alpha power ratio} = \frac{ESD_{\alpha}}{ESD_{\alpha} + ESD_{\beta}} \quad (3.3)$$



$$\text{Beta power ratio} = \frac{ESD_{\beta}}{ESD_{\alpha} + ESD_{\beta}} \quad (3.4)$$

where  $ESD_{\theta}$  refers to  $\theta$ ,  $ESD_{\beta}$  refers to  $\beta$ , and  $ESD_{\alpha}$  refers to  $\alpha$ .

Normalization of power spectrum through theta, alpha and beta power ratio features, give benefit in experimenting the particular analysis. Power ratio features are then grouped into the respective IQ and learning style groups and the pattern is observed in IBM SPSS.

### 3.4 Statistical Analysis and Validation

In statistical analysis and validation, there are two parts involved; one in respect to IQ-LS clustering sample size and the other in respect to boxplot analysis. Based on IQ-LS clustering sample size, IQ classification set was divided into three, which are low, medium and high IQ level, meanwhile, LS classification set was divided into four sets, which are assimilator, converger, diverger and accommodator. This analysis will be visualized through bar graph chart.

Based on boxplot analysis, this analysis has been done via SPSS. The boxplot analysis indicates the pattern distribution of IQ and LS data. The box plots represent analysis on each group contributed by every single sub-band power ratio median values. There are two section represented using boxplot specification on IQ approach and LS approach. This analysis is studied through real data sample without any synthetic data improvement and with synthetic data improvement.

Ahead of developing the model, the outlier needs to be handled carefully. The normal outlier must be considered in analysis; however, the extreme outlier needs to be removed if the sample data consist less than 10% of the extreme outlier. This removal before

proceeding to synthetic improvement is to avoid misclassification and to increase neural network accuracy performance.

The pattern of features in boxplot analysis can be gained through power ratio pattern distribution in each classes. The result will be correlated to previous findings using several established theories in cognitive psychology in order to validate it. Apart from the Neural Efficiency Hypothesis, the results will also be benchmarked against the neural transmission error, cerebral arousability and alpha suppression theories.

### 3.5 Synthetic EEG Signals

To achieve certain ANN requirements or conditions, the synthetic data are used through generation of real data. Since the sample size is unbalanced, results may be biased toward the detection of the majority class in classifier performances (A. Bhattacharyya & Pachori, 2017). Adequate sample size data allows bias adjustment in data without resulting in any over-fitting due to stochastic EEG characteristics (Kaleem, Guergachi, & Krishnan, 2018). In order to unfold this issue, synthetic data generation was performed to increase the sample size among group classification (Jahidin, Taib, et al., 2015). Synthetic data was generated by including white Gaussian noise with sufficient controlled signal-to-noise ratio (SNR) to preserve as original data characteristics. Adequate SNR is needed in order to avoid ANN misclassification and 30db was implemented as similar to stochastic EEG characteristics (Jahidin et al., 2014).

Based on the formula given in equation 3.5 and 3.6, the synthetic EEG ( $V_{synt}$ ) was obtained by multiplying the generated noise ( $V_{noise}$ ) to original data ( $V_{EEG}$ ). In the meantime, the Noise array ( $V_{noise}$ ) was generated by multiplying the random white

Gaussian noise ( $W_{noise}$ ) and the noise voltage ( $V_{attn}$ ). Meanwhile, noise voltage ( $V_{attn}$ ) is the attenuated voltage from SNR (dB) relationship.

$$V_{synt} = V_{EEG} \times V_{noise} \quad (3.5)$$

$$V_{noise} = W_{noise} \times V_{attn} \quad (3.6)$$

Generation of synthetic data is useful for producing data which is like original data. However, ANN sample size condition requires minimum sample sizes to develop ANN model and will be discussed in section 3.6.2.

### **3.6 Intelligent IQ-LS Classification Model**

In order to develop model classification, a basic or general concept needs to be understood well as shown in Figure 3.5. This begins with data collection, signal processing, feature selection, theoretical validation, model classification (AI) technique and finally the validation and verification stage.

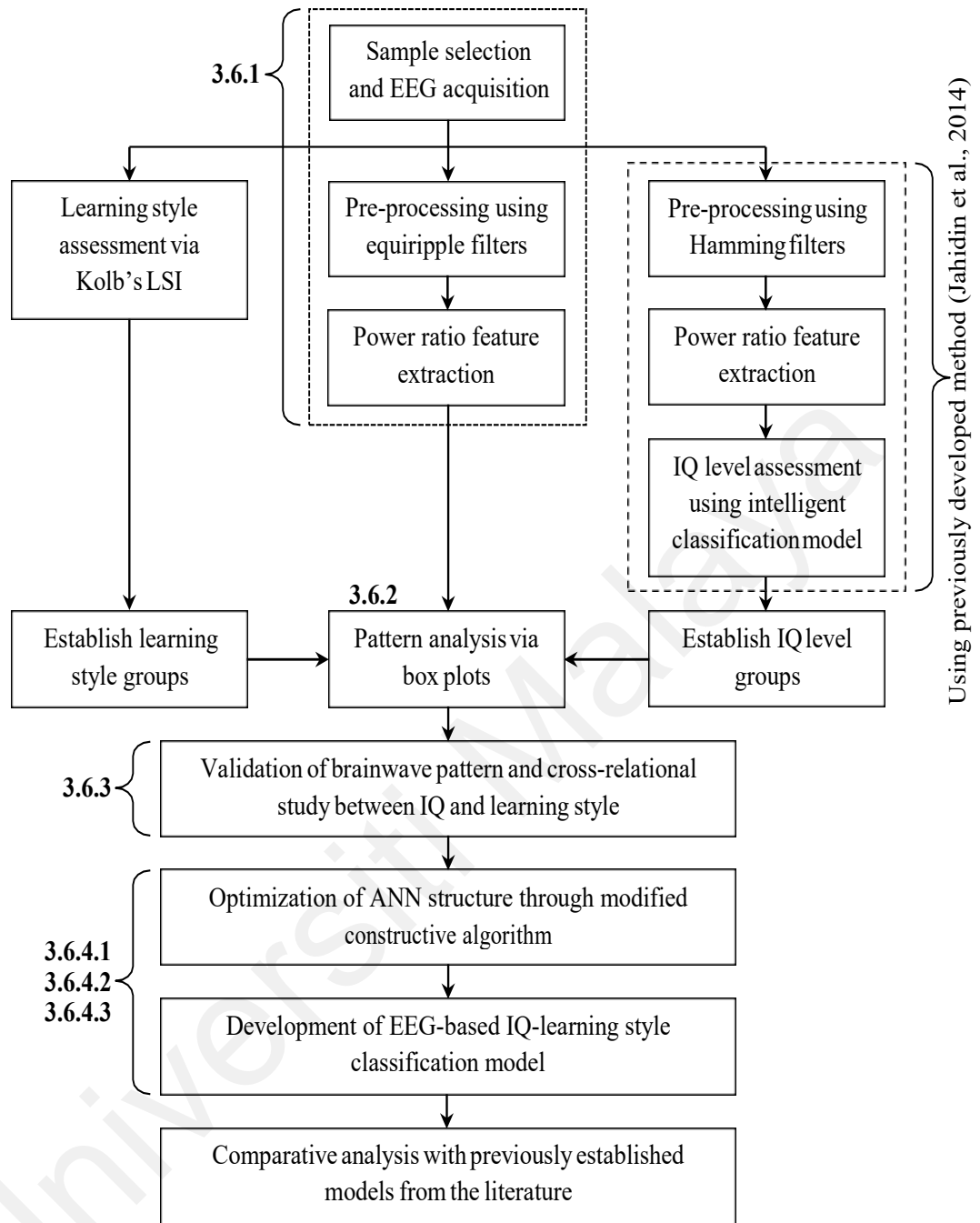


**Figure 3.6: Intelligent IQ-LS classification model network development**

### 3.6.1 IQ-LS Dataset

In order to classify the model via supervised machine learning, the input and output data are required. The input data are referred to the theta, alpha and beta ratios of IQ and LS dataset, respectively. Meanwhile, the outputs are referred to the index levels or groups of IQ and LS as a control groups. Throughout supervised technique, ANN will

ensure and learn to ensemble classifier to achieve best performance. As the data collection lead to valid classification, the ANN was used function optimization methods to synchronize neural network between input and output data. Finally, data validation and verification stage were crucial due to validation of model performance itself before establishing the model. In case the model produces high performance, this means the valid initial classification will be the same correlation with final classification via supervised technique.

### 3.6.2 Sample Size Requirement Analysis

Sample size improvement through synthetic data also benefitted in overcoming inadequate or imbalance sample size distribution condition. Commonly, the number of synthetic data improvement was decided by minimum sample size analysis or by common research practice by extending factor of 10 in minimum sample size (Alwosheel et al., 2018; Haykin, 2009). The minimum sample size analysis was analyzed through minimum sample size formula in confidence interval that also shows the precise requirement of sample size as Equation 3.7. Hence, this issue can be solved through common research practice through synthetic data to improve model or system performance.

$$n = \left( \frac{Z_{\alpha/2} \cdot \sigma}{E} \right)^2 \quad (3.7)$$

Where, n is minimum sample size required,  $Z_{\alpha/2}$  is confidence interval constant,  $\sigma$  is standard deviation of population, E is margin of error in same measurement in standard deviation. Commonly, the size sample was constructed in 95% confidence interval. The standard deviation and margin of error were evaluated through power ratio features.

### 3.6.3 Synthetic EEG Signals and Power Ratio Features Distribution Effects

To achieve certain ANN requirements, the synthetic data were used through generation of real data. Inadequate sample size data results biased toward the detection of the majority class in classifier performances (A. Bhattacharyya & Pachori, 2017). Based on this research, the synthetic data concerns on EEG signal, where the brainwaves signal is stochastic nature and fluctuate randomly over time (Lahiri, Rakshit, & Konar, 2017). Therefore, a random white Gaussian noise is integrated via simulation on real data, and converted into approximation of original data (Ur Rehman & Mandic, 2011). Based on Figure 3.6, the figure presents probability density function (PDF) of white Gaussian noise, which is a normally distributed.

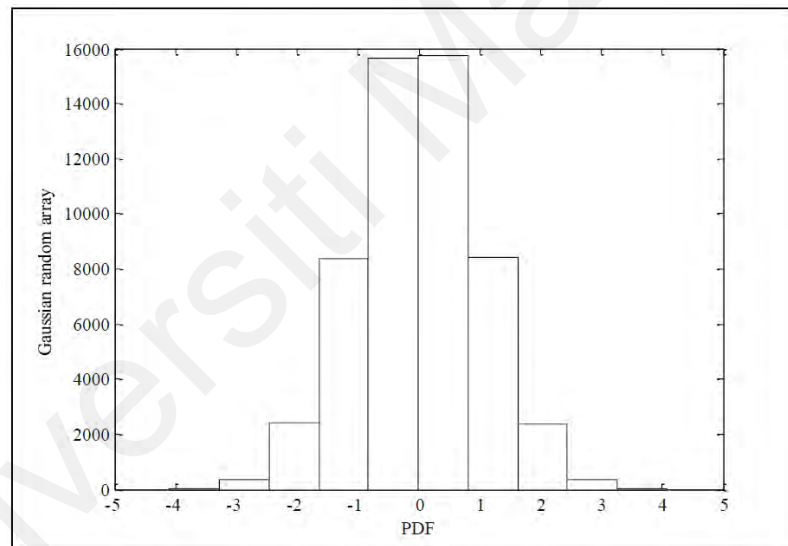


**Figure 3.7: Probability density function (PDF) of white Gaussian noise.**

### 3.6.4 Development of IQ-LS Classification Model using MIMO ANN

MIMO structure was implemented in Multilayer feed-forward network (MFFN) architecture. MFFN consist of 3 layers which are input, hidden and output layer (Svozil, Kvasnička, & Pospíchal, 1997). Based on the input layer, the network was trained to learn through unique pattern of Theta, Alpha and Beta sub-bands power ratio. Meanwhile,

based on output, there is multi-output algorithm to classify IQ levels and LS groups. Based on the hidden layer, the sigmoid activation function was implemented to the hidden layer meanwhile, linear activation function was implemented to the output layers, respectively. Based on model development, the data were segregated randomly into three datasets, which are the dataset for training (70%), testing (15%) and validating (15%) (Pulini, Kerr, Loo, & Lenartowicz, 2018). Training dataset was used to train the network, meanwhile testing dataset was used to analyze the generalization performance in the trained network. To validate, the validation dataset was used to periodically monitor the generalization ability through back-propagation algorithm. To prevent overfitting, the training is stopped as soon as the validation error raises for a certain iteration's number. These are standard scientific practice as many researchers have been used in previous researches (Jahidin et al., 2015; Pulini et al., 2018; Rao K, Premalatha, & Naveen, 2018).

#### **3.6.4.1 Parameter optimisation**

In order to evaluate the optimum number of hidden neurons, modification of a constructive algorithm has been developed (M.S.A. Megat Ali, Jahidin, Taib, Tahir, et al., 2016). This constructive algorithm was merged to constructive and pruning techniques. The optimization procedure utilizes the selection boundary between 3 hidden nodes to 15 hidden nodes. The process techniques were repeated to 40 times continuously for each cumulative single hidden node (begin by 3 hidden nodes and end by 15 hidden nodes). This approach leads the network into best average performance through varying the weight and biases. Commonly, in biomedical classification technique practice, the number of hidden nodes was decided between 2 until 30 (Belciug & Gorunescu, 2018). However, the procedure was repeated from the minimum limit of 3 until the maximum limit of 15 due to overfitting phenomenon of high hidden nodes number (Lolli et al.,

2017). Finally, the optimum hidden nodes were chosen with the highest accuracy of the performance to ensure the good classification model and were chosen with lowest MSE for both IQ and LS.

#### **3.6.4.2 Performance Measure and Test Fitting**

In this section, the methodology will setup to evaluate the performance and test fitting for both cognitive abilities (IQ and LS). This benefitted the network evaluation during the network as it was trained repeatedly to achieve best possible performance. Network evaluation was required to ensure the validity of classification model. The evaluation of the network performance can be achieved by constructing target threshold and confusion matrix. The detail elaboration related to this section will be divided into IQ evaluation performance setup and LS evaluation performance setup in the same model development.

##### **3.6.4.2.1 IQ Evaluation Performance Setup**

In order to target IQ threshold, threshold limits were determined to categorize the predicted (network) outputs. Threshold limits were setup in between minimum threshold ( $\hat{y}_{lim1}$ ) and maximum threshold ( $\hat{y}_{lim2}$ ), to classify IQ levels into low (1), medium (2) and high (3). Both IQ levels number and indicator will be utilized alternately onwards based on suitability. The indicator was determined by visual investigation of the predicted outputs distribution with the opportunity attained greatest accuracy. This visual investigation be used to assess the scattered data in between the threshold limit ranges before and after applying threshold limit.



**Table 3.1: IQ Level and IQ Indicator through Threshold Limit for the Prediction**

IQ Level	Low	Medium	High
IQ Indicator	1	2	3
Threshold Limit	$0.5 \leq \hat{y}_1 \leq 1.5$	$1.5 \leq \hat{y}_2 \leq 2.5$	$2.5 \leq \hat{y}_3 \leq 3.5$

IQ level prediction distribution begins with minimum threshold ( $\hat{y}_{lim1}$ ) and finishes at maximum threshold ( $\hat{y}_{lim2}$ ). In the middle of minimum and maximum threshold, the threshold has been segregated into  $\hat{y}_1$ ,  $\hat{y}_2$  and  $\hat{y}_3$  within threshold boundary by  $\pm 0.5$  for low, medium and high IQ level, respectively. In other words, the boundary of IQ levels limits the threshold into  $\hat{y}_{lim1} < \hat{y}_{IQ\ level} < \hat{y}_{lim2}$ , which is denoted as  $\hat{y}_1$ ,  $\hat{y}_2$  and  $\hat{y}_3$  as Table 3.1.

The different IQ levels can be classified when the predicted output drops into threshold limit ranges ( $\hat{y}_1$ ,  $\hat{y}_2$  and  $\hat{y}_3$ ). Despite that, the unclassified data can be obtained when the predicted output drops outward from threshold limit, where  $\hat{y}_1$  less than 0.5 and  $\hat{y}_3$  higher than 3.5 due to unfamiliar data set.

Based on IQ confusion matrix, the performance revealed the data information through the actual classification and predict classification which was being tested by classification model. Based on contingency table categorical of confusion matrix, there are True Positive (TP), True Negative (TN), False Positive (FP), and False Positive (FP). True and False refers to outcome correctness, meanwhile Positive and Negative refers to model outcome of classifier itself.

Throughout TP, TN, FP and FN performance which resulted by classification network, the value can be evaluated through actual output. Thus, the evaluation also can provide the assessments investigation via accuracy (Acc), sensitivity (Se) and precision

(Pp). Accuracy refers to rate of correct classification via sensitivity and precision of the classification model.

### 3.6.4.2.2 LS Evaluation Performance Setup

In order to target LS threshold, threshold limits were determined to categorize the predicted (network) outputs. Threshold limits were setup in between of minimum threshold ( $\hat{z}_{lim1}$ ) and maximum threshold ( $\hat{z}_{lim2}$ ), to classify LS group into accommodator, diverger, assimilator, and converger. Both LS group number and indicator will be utilized alternately onwards based on suitability. The indicator was determined by visual investigation of the predicted outputs distribution with the opportunity attaining greatest accuracy.

**Table 3.2: LS and LS Indicator through Threshold Limit for the Prediction**

LS Group	Accommodator	Diverger	Assimilator	Converger
LS Indicator	1	2	3	4
Threshold Limit	$0.5 \leq \hat{z}_1 \leq 1.5$	$1.5 \leq \hat{z}_2 \leq 2.5$	$2.5 \leq \hat{z}_3 \leq 3.5$	$3.5 \leq \hat{z}_4 \leq 4.5$

LS level prediction distribution begins with minimum threshold ( $\hat{z}_{lim1}$ ) and finishes at maximum threshold ( $\hat{z}_{lim2}$ ). In the middle of minimum and maximum threshold, the threshold been segregated into  $\hat{z}_1$ ,  $\hat{z}_2$ ,  $\hat{z}_3$  and  $\hat{z}_4$  within threshold boundary by  $\pm 0.5$  for accommodator, diverger, assimilator, and converger, respectively. In other words, the boundary of LS groups limits the threshold into  $\hat{z}_{lim1} < \hat{z}_{LS\ group} < \hat{z}_{lim2}$ , which denote as  $\hat{z}_1$ ,  $\hat{z}_2$ ,  $\hat{z}_3$  and  $\hat{z}_4$  as Table 3.2.

The different LS group can be classified when the predicted output drops into threshold limit ranges ( $\hat{z}_1$ ,  $\hat{z}_2$ ,  $\hat{z}_3$  and  $\hat{z}_4$ ). Despite that, the unclassified data can be

obtained when the predicted output drop outward from threshold limit, where  $\hat{z}_1$  less than 0.5 and  $\hat{z}_4$  higher than 4.5 due to unfamiliar data set.

Based on LS confusion matrix, the performance revealed the data information through the actual classification and predicted classification which was being tested by classification model. Based on contingency table categorical of confusion matrix, there are True Positive (TP), True Negative (TN), False Positive (FP), and False Positive (FP). True and False refers to outcome correctness, meanwhile Positive and Negative refers to model outcome of classifier itself.

#### **3.6.4.3 Correlation Function Test**

As IQ-LS classification architecture and parameter setup which has been developed before, the network was trained repeatedly to achieve best possible performance via the selected parameter. Then, correlation tests have been used to evaluate ANN model unbiasedness via residual correlation of all inputs and outputs within activation function layers. In this research, Auto Correlation Function (ACF) and Cross Correlation Function were involved, where ACF analyze the correlation between residual and input, while CCF analyze the correlation between residual and output. In optimized model, it was assumed the correlation at lag within 95% confidence limit except at the 0 lag (L. F. Zhang et al., 2009). As the ideal performance achieved, network pruning has been stopped and that neural network has been saved.

## RESULTS

### 4.1 Introduction

This section elaborates the result affirmed based on the methodology emphasis. The result of this research consists of:

1. Sample distribution of IQ and LS datasets,
2. EEG signal processing distribution of FFT spectrum,
3. ESD and PR features result,
4. Analysis of power ratio features via box plot,
5. Analysis on sample size requirement,
6. Synthetic EEG signals and PR features distribution; and
7. EEG-Based IQ-LS classification model using MIMO ANN.

These whole results reflect the methodology process in achieving the objective of this research.

### 4.2 Samples Distribution of IQ and LS Dataset

Eighty-five healthy volunteers in the age ranging from 17 to 40 years old (mean age / standard deviation = 20.99/ 3.56) were involved in this study. The subjects comprised of 50 males and 35 females from various educational and professional backgrounds. Throughout various background of subject volunteers, there are no biased issue on selection of specific background in this classification model development. Furthermore, the distribution of IQ and LS samples are shown in Figure 4.1 and Figure 4.2 respectively.

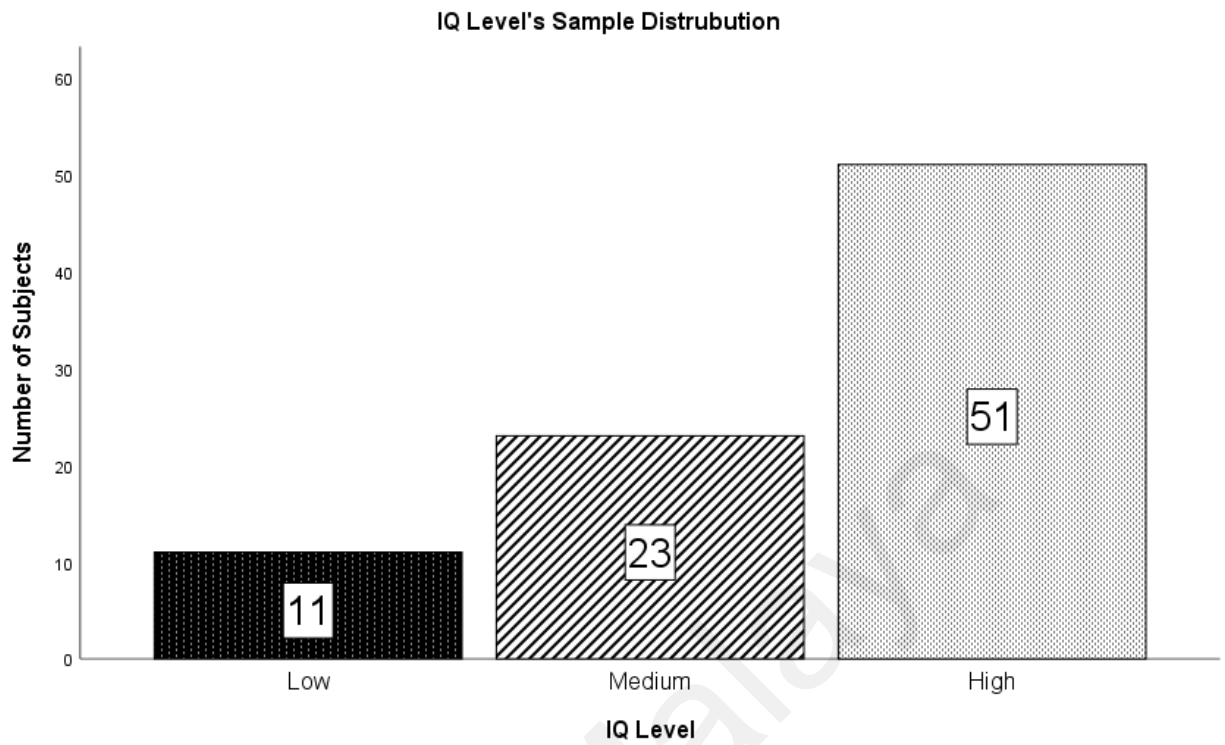


**Figure 4.1: Distribution of samples into three distinct IQ levels (85 samples)**

**Table 4.1: Learning style score assessment through learning style grid**

<b>Learning Style</b>	<b>AC-CE Score</b>	<b>AE-RO Score</b>
Accommodating	$\leq 7.0$	$\geq 6.5$
Diverging	$\leq 7.0$	$\leq 6.5$
Assimilating	$\geq 7.0$	$\leq 6.5$
Converging	$\geq 7.0$	$\geq 6.5$

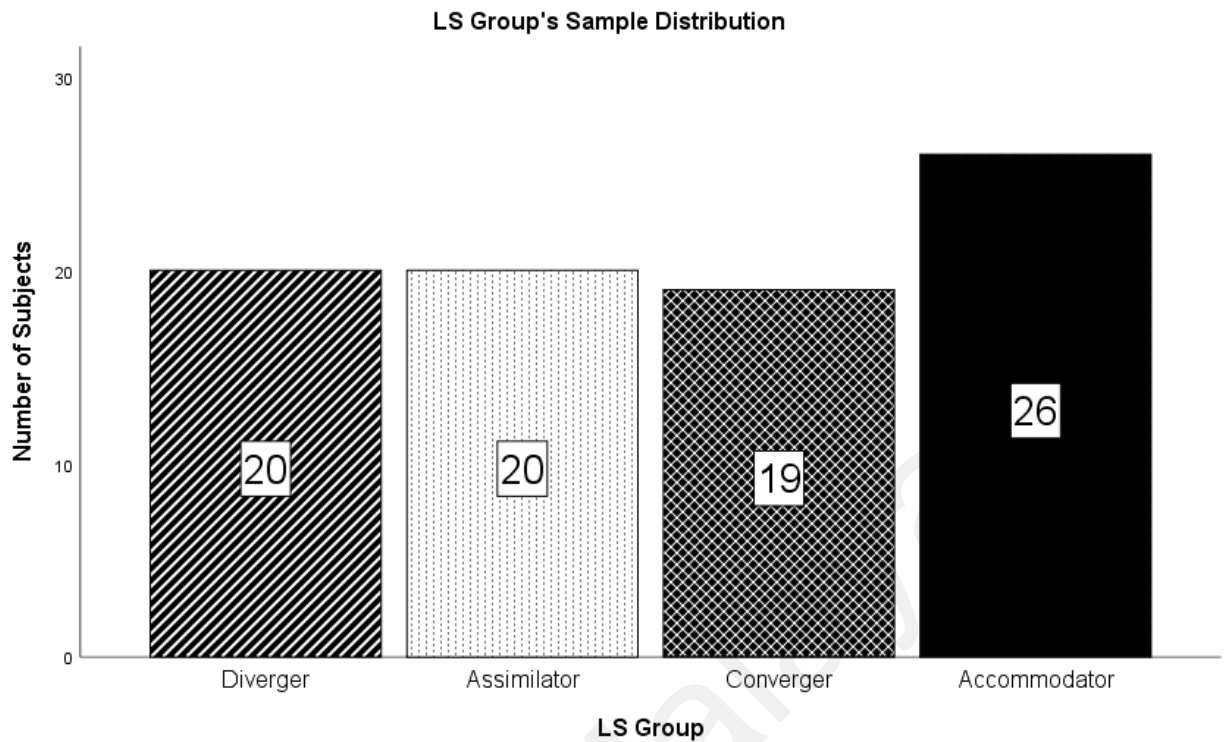


**Figure 4.2: Distribution of samples in four distinct LS groups (85 samples)**

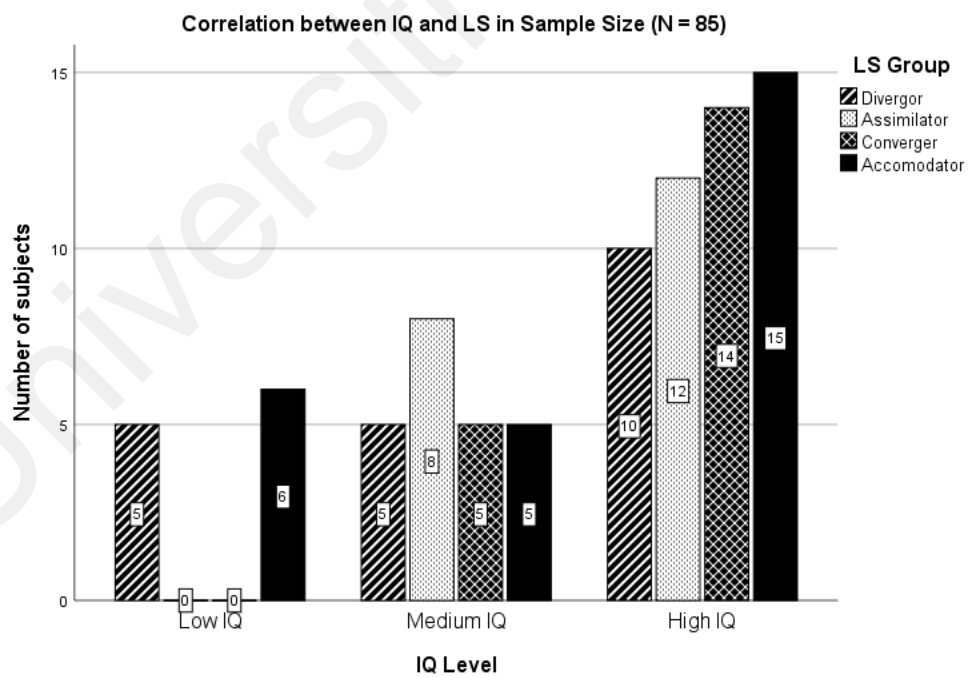


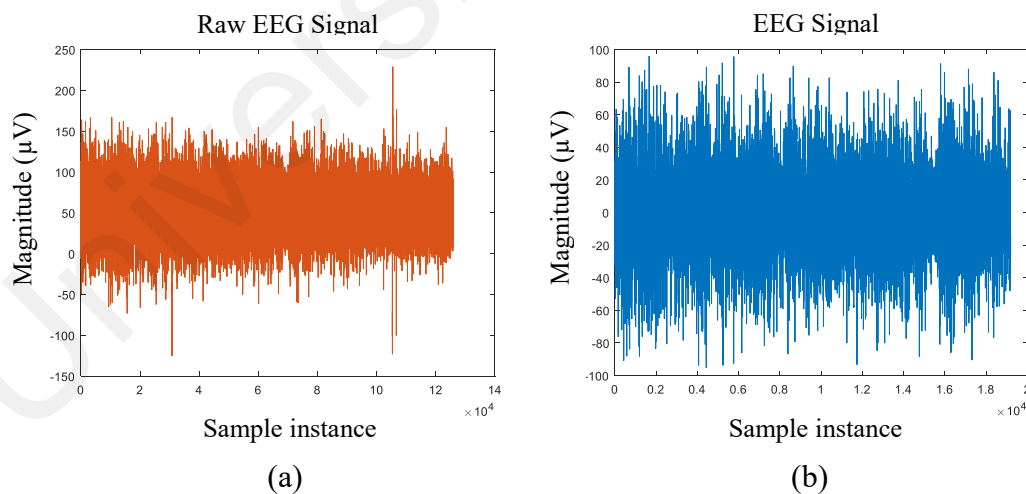
**Figure 4.3: Correlation between IQ level and LS group sample distribution.**

Individual learning style has been classified through learning style grid as Figure 2.10. Dominant learning style score has been determined through AC-CE score and AE-

RO score as shown in Table 4.1. Based on LS population (Figure 4.2), there are 20 divergers, 20 assimilators, 19 convergers and 26 accommodators from the total of 85 samples. In Figure 4.3, we depicted the correlation between IQ and LS group in the sample distribution. In the high IQ level, the LS group showed an increasing number of subjects which are dominant compared to other IQ levels. In the low IQ level, two classes of LS groups are absent (assimilator and converger) whereas in the medium IQ level, all the LS groups exist here with the assimilator shown to be more prominent.

### 4.3 EEG Signal Processing

This section will elaborate the EEG signal processing results from analysing brainwaves signal until the features is obtained. It consists of raw EEG data, filtered EEG data conversion, frequency domain conversion, ESD conversion, and PR extraction.



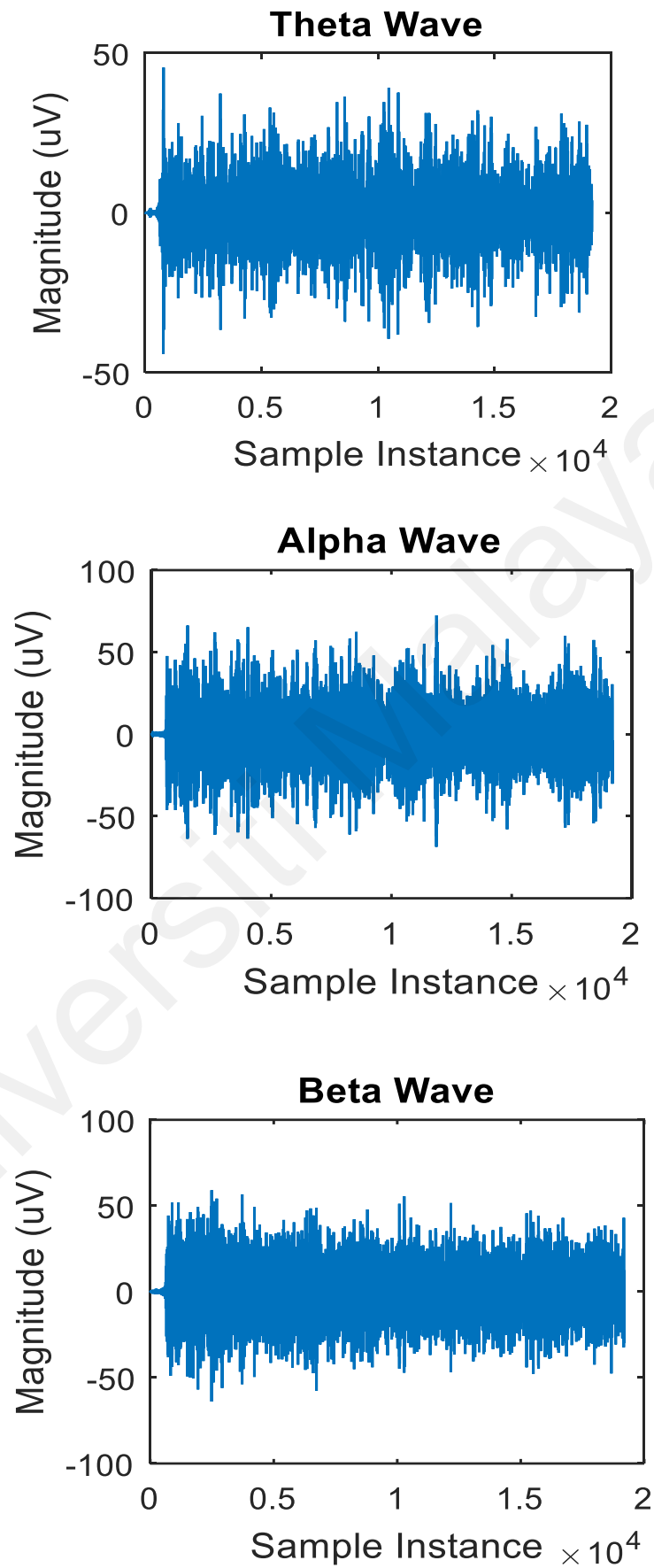
**Figure 4.4: EEG signal recorded; (a) Raw EEG signal approximately in three minutes duration, and (b) EEG signal after cut into 2 minutes 30 seconds.**

Figure 4.4(a) depicted the raw EEG signal for 3 minutes similar to EEG recording duration methodology. In this graph, we shown the magnitude (uV) over 512 Hz of

sample instances. In the Figure 4.4(b), we removed the first 20 seconds and the end of 10 seconds from the whole recorded signal (Megat Ali et al., 2014; Megat Ali et al., 2016). The intention was to prevent the signal analysis from containing any spike overshoot and uncontaminated EEG signal. To reject EOG artifact rejection, the characteristic for voltages exceeding the range of  $\pm 100 \mu\text{V}$  rejection has been performed. Experimentally, EOG automatic rejection approach (Jahidin, Megat Ali, et al., 2015) has been employed due to the subject rest and static as protocol.

Universiti Malaya





**Figure 4.5: Filtered EEG signal for theta, alpha and beta sub-band.**

Subsequently, Figure 4.5 shows the signal data splitted into three sub-band. These sub-band separation used equiripple filters to minimize error function, robust, stable and efficient performance (M. S A Megat Ali et al., 2014) into theta, alpha and beta sub-bands. The figure also shown the EEG signal has been filtered with  $\pm 100 \mu\text{V}$  rejection and adjusted powerline to zero with respect to each sub-band.

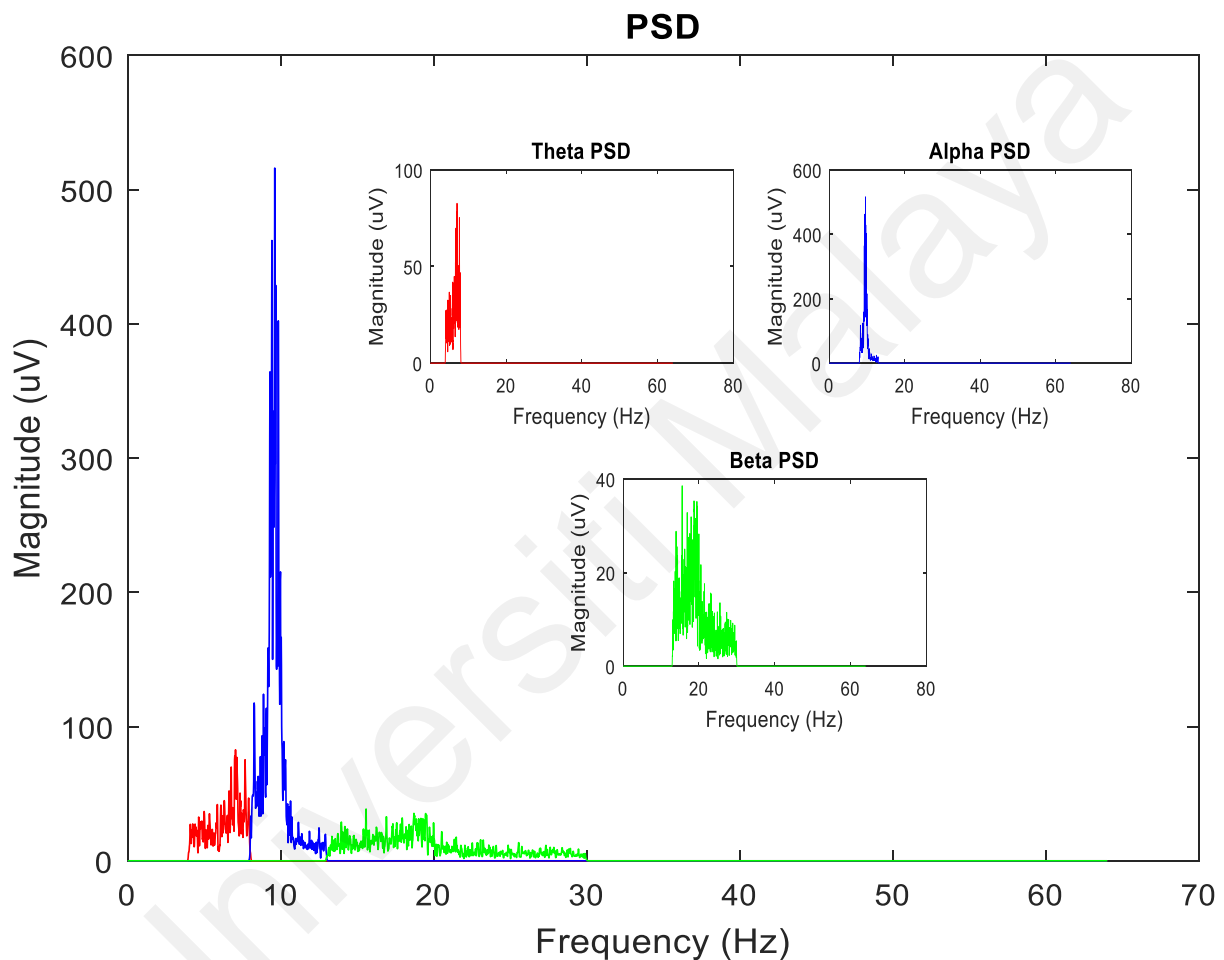


**Figure 4.6: Power spectrum density (PSD) transformation of each sub-band frequency via EEG signal processes. The red colour indicates theta sub-band, blue colour indicate alpha sub-band and green colour indicates beta sub-band.**

In Figure 4.6, the data was transformed into the non-parametric power spectral density (PSD) distribution for each wave sub-band by performing Fast Fourier Transform (FFT) via Welch's method. Welch's method computes the power spectrum of a time series by

collecting the frequency component of a stochastic waves (Hosseinifard et al., 2013; Welch, 1967). Prior to the sub-band ESD extraction, each frequency sub-band needs to be splitted separately into theta, alpha and beta sub-band as shown in Figure 4.6. Based on PSD conversion result, the alpha sub-band showed dominant features in magnitude compared to other sub-bands in this research protocol.

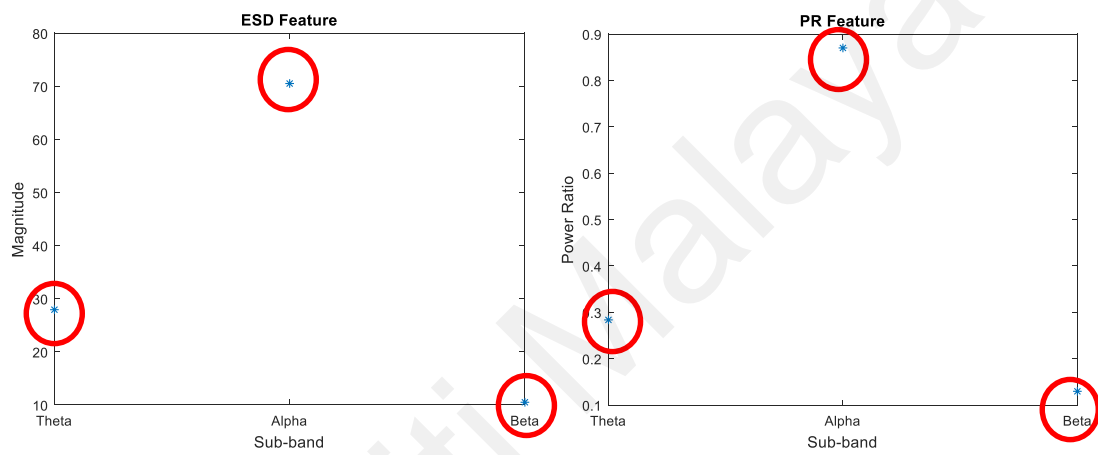


**Figure 4.7: (a) Energy spectrum density (ESD) transformation via power spectrum density (PSD) of each sub-band frequency and (b) power ratio (PR) feature transformation via energy spectrum density (ESD) of each sub-band frequency.**

Figure 4.7(a) shown the ESD transformation through power of a signal at various frequencies (PSD). Basically, the energy distribution is acquired by evaluating the area of PSD curve for each frequency sub-band. This energy distribution is known as energy spectral density (ESD). Then, the ESD which comprise of the overall energy distribution for each range of the frequency band is calculated for each group. Thus, the result of ESD value was shown as Figure 4.7(a) after calculation or evaluation.

To normalize the values, power ratio (PR) features of theta, alpha and beta are extracted from sub-band ESD features values. This feature method is derived by dividing the respective frequency power band with the other frequency power band to gain a

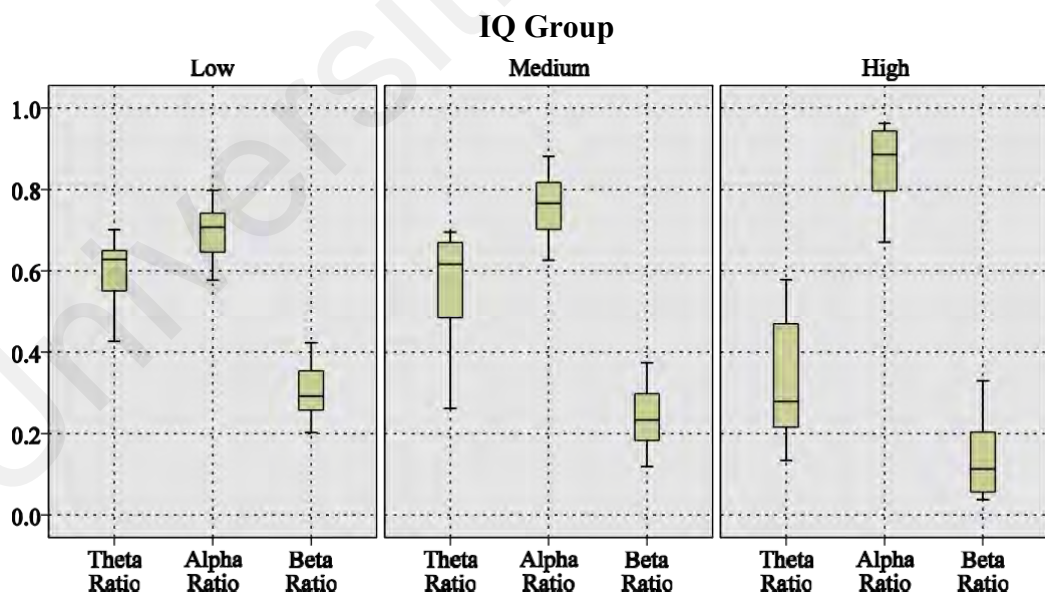
feature that is a character to represent signal behavior. Thus, the result of PR value is shown Figure 4.7(b) after calculation or evaluation.

#### 4.4 Observation of PR Features on IQ and LS using Box Plot

The PR features were analyzed using box plot that using SPSS software. The box plots represent the PR pattern of IQ and LS datasets, respectively.

##### 4.4.1 IQ Analysis

IQ analysis has been done through power ratio features of 85 number of real sample size using box plot technique.



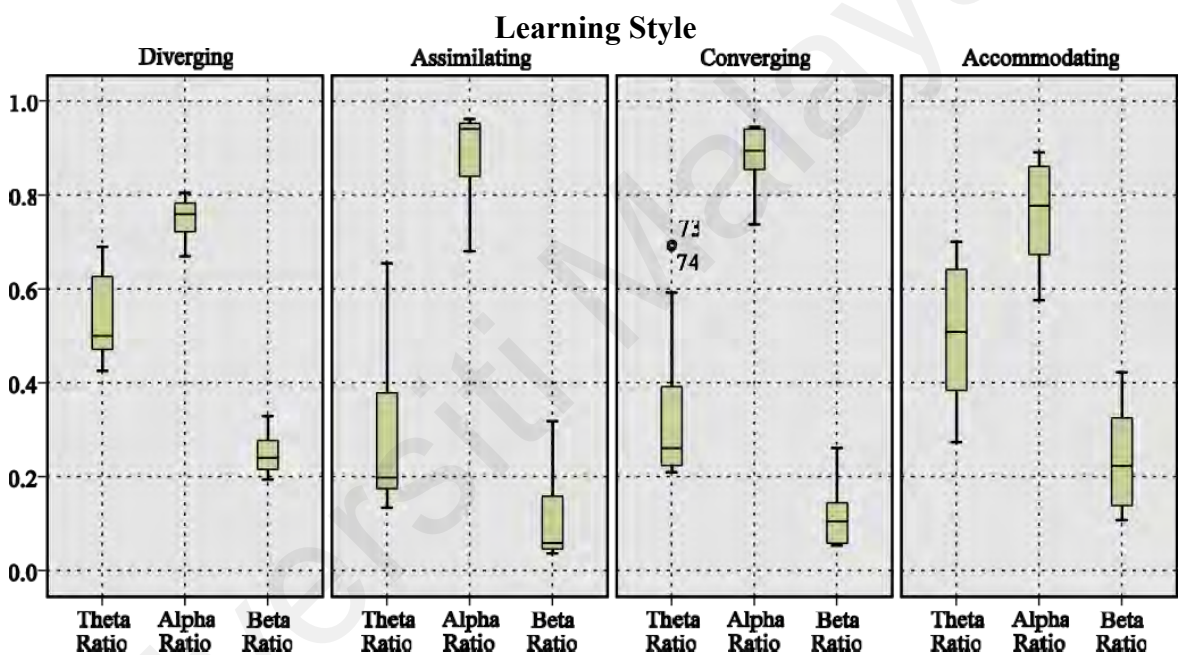
**Figure 4.8: Pattern and distribution of power ratio features for varying IQ levels (N=85).**

Figure 4.8 shows the theta, alpha and beta power ratio values against IQ levels. Finding shows the median theta PR pattern decreasing through increasing IQ level, meanwhile

the median alpha PR pattern increasing through decreasing IQ level. Subsequently, the pattern of median beta PR pattern decreasing through increasing IQ level. This beta pattern is similar as theta pattern.

#### 4.4.2 LS Analysis

LS analysis has been done through power ratio features of 85 number of real sample size using box plot technique.



**Figure 4.9: Pattern and distribution of power ratio features for different learning styles (N=85).**

Based on Figure 4.9, the pattern of median theta power ratio begins with assimilator, converger, diverger and accommodator. Meanwhile, the median alpha power ratio pattern starts with diverger, accommodator, converger and assimilator. The inverse pattern was found in the median beta power ratio pattern, which increased from assimilator, converger, accommodator and diverger. However, the median pattern values between

assimilator and converger are little different, and same pattern between diverger and accommodator also little different.

#### 4.4.3 IQ-LS Analysis

To analyze correlation between IQ and LS, the boxplot of power ratio features is required. In accordance with this analysis, LS group of each power ratio was segregated into each level of IQ. Thus, the result analysis exhibits the smooth visual through box plot individually respect to IQ level.

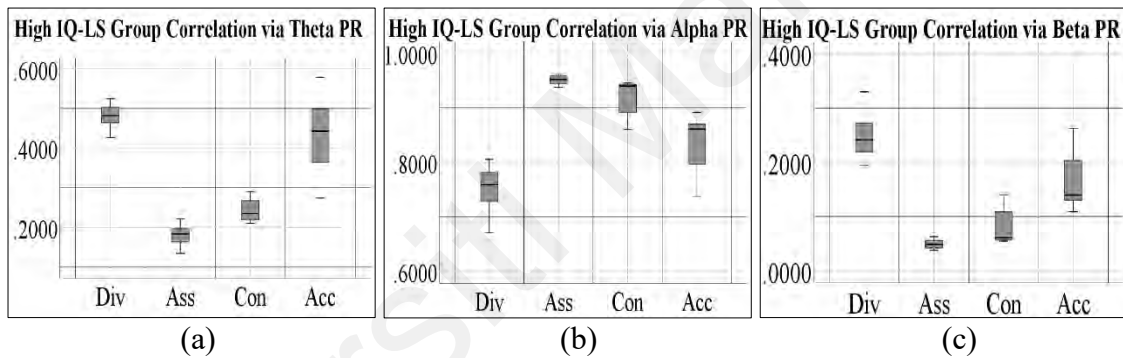


**Figure 4.10: Correlation among distinct LS groups and high IQ level referred (a) theta, (b) alpha and (c) beta sub-band PR. Div, Ass, Con and Acc are refer to Diverger, Assimilator, Converger and Accommodator, respectively.**

The pattern of LS in high IQ level is as shown in Figure 4.10, based on theta, alpha and beta power ratio, respectively. The result for correlation between high IQ and LS type in theta power ratio shows the median theta power ratio pattern begins with assimilator, converger, accommodator and diverger. Meanwhile, the result for correlation between high IQ and LS group in alpha power ratio shows the median alpha power ratio pattern begins with diverger, accommodator, converger and assimilator. Finally, the result for correlation between high IQ and LS group in beta power ratio shows the median beta

power ratio pattern same as theta power ratio which begins with assimilator, converger, accommodator and diverger.

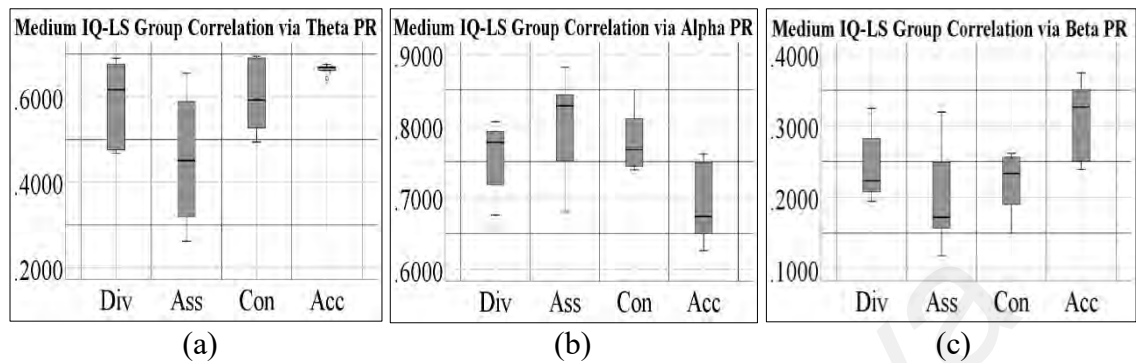


**Figure 4.11: Correlation among distinct LS groups and medium IQ level referred (a) theta, (b) alpha and (c) beta sub-band PR. Div, Ass, Con and Acc are refer to Diverger, Assimilator, Converger and Accommodator, respectively.**

Then, the pattern of LS in medium IQ level can be showed as Figure 4.11, based on theta, alpha and beta power ratio respectively. The result for correlation between medium IQ and LS group in theta power ratio shows the median theta power ratio pattern begins with assimilator, converger, diverger and accommodator. Meanwhile, the result for correlation between medium IQ and LS group in alpha power ratio shows the median alpha power ratio pattern begins with accommodator, converger, diverger and assimilator. Finally, the result for correlation between medium IQ and LS group in beta power ratio shows the median beta power ratio pattern begins with assimilator, diverger, converger and accommodator.

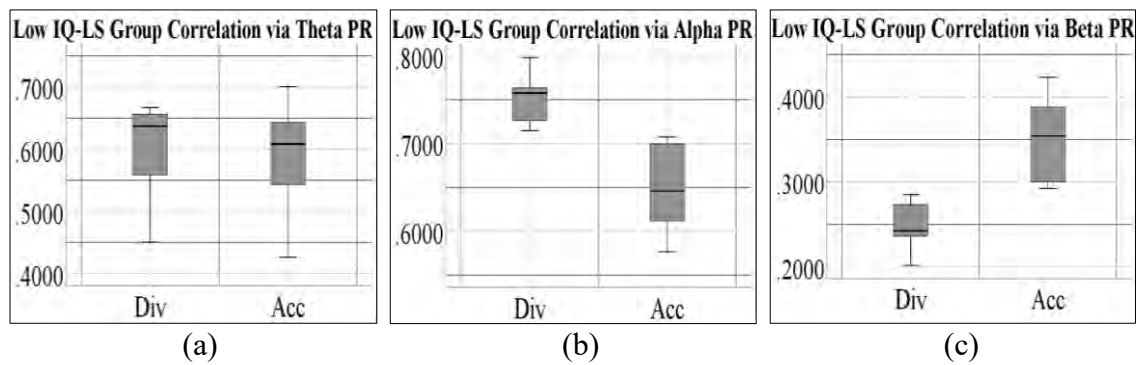


**Figure 4.12: Correlation among distinct LS groups and low IQ level referred (a) theta, (b) alpha and (c) beta sub-band PR. Div and Acc are refer to Diverger and Accommodator, respectively.**

Subsequently, the pattern of LS in low IQ level can be showed as Figure 4.12, based on theta, alpha and beta power ratio, respectively. However, the result is absent for assimilator and converger due to non population leading to low IQ level. The result for correlation between low IQ and LS group in theta power ratio shows the median theta power ratio pattern begins with accommodator and then diverger. However, the result for correlation between low IQ and LS group in alpha power ratio shows the median alpha power ratio pattern begins with accommodator and then diverger. Finally, the result for correlation between low IQ and LS group in beta power ratio shows the median beta power ratio pattern begins with diverger and then accommodator.

#### 4.5 Sample Size Requirement Analysis

Sample is a crucial part that assists to view inferences of the population. Research sample collection of entire data of the population is imposible and it is costly and time consuming. Generally, high sample size leads to time, cost and resource consuming, while, low sample size leads to data inaccuracy. Throughout sample size requirement, sample data create inferences of population by having proper sample size. There are some techniques has been utilized to evaluate sample size. Practically, sample size analysis through confidence interval has been utilized to achieve proper sample to be provided.



**Table 4.2: Minimum sample size evaluation via theta, alpha and beta power ratios.**

Formula	Theta	Alpha	Beta
$Z_{\alpha/2}$	1.960000	1.960000	1.960000
$\sigma$	0.174826	0.101127	0.101128
$E$	0.100725	0.432525	0.028200
n	11.56966 $\approx 12$	0.210000 $\approx 0$	49.403000 $\approx 49$

Analysis among three parameter of PR features are required and needed to investigate the minimum sample size of each features. Based on Table 4.2, the result show the number of sample size for theta, alpha and beta power ratio. The result shows the minimum sample size for theta power ratio is 12, the minimum sample size for alpha power ratio is 0, and the minimum sample size for beta power ratio is 49. This means inadequate data of theta PR feature required around 12 samples data, while beta PR feature required around 49 samples data. However, alpha power ratio has adequate data through zero value of analysis. Entirely, beta PR feature has highest value compared to theta and alpha PR features. Thus, 49 are selected due to highest value to complete the minimum sample size requirement. However, through common research practice by extending factor of 10 in minimum sample due to prune neural network (Alwosheel et al., 2018; Haykin, 2009). Hence, IQ dataset and LS dataset were rounded into 50 samples sizes from 49 samples sizes for each group via a factor of 10 improvements (by the minimum number of 5 samples).

#### 4.6 Synthetic EEG Signals and PR Features Distribution Effects.

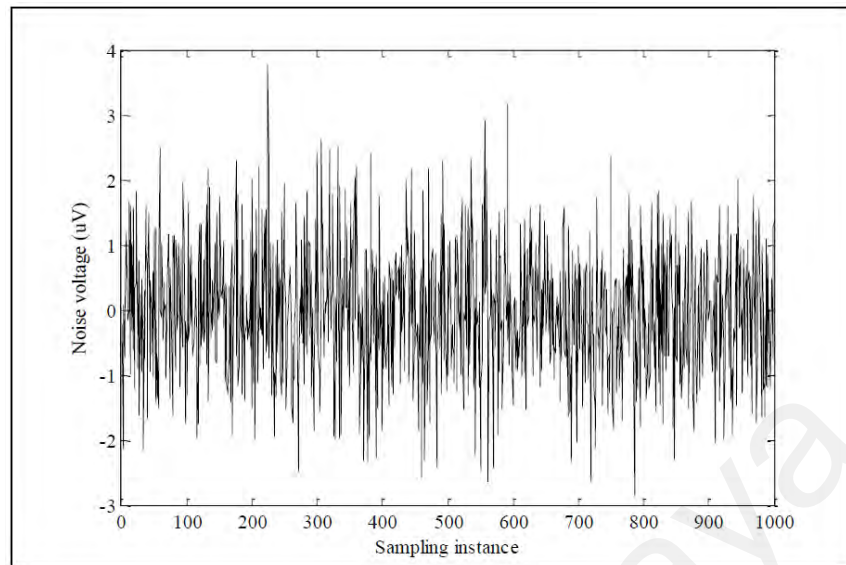


**Figure 4.13: Generated Random Array**

Based on Figure 4.13, the figure displays the generated random array of white Gaussian noise. The white noise is normally distributed with highest peak at zero value and decreases away from zero value.

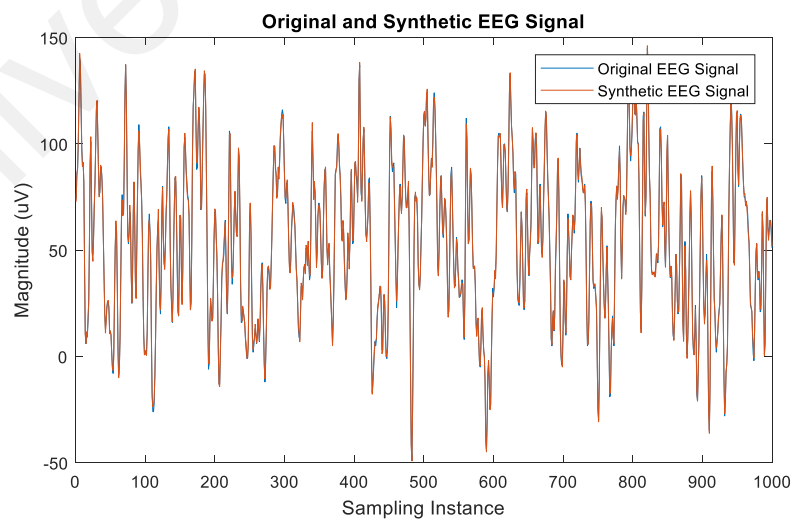
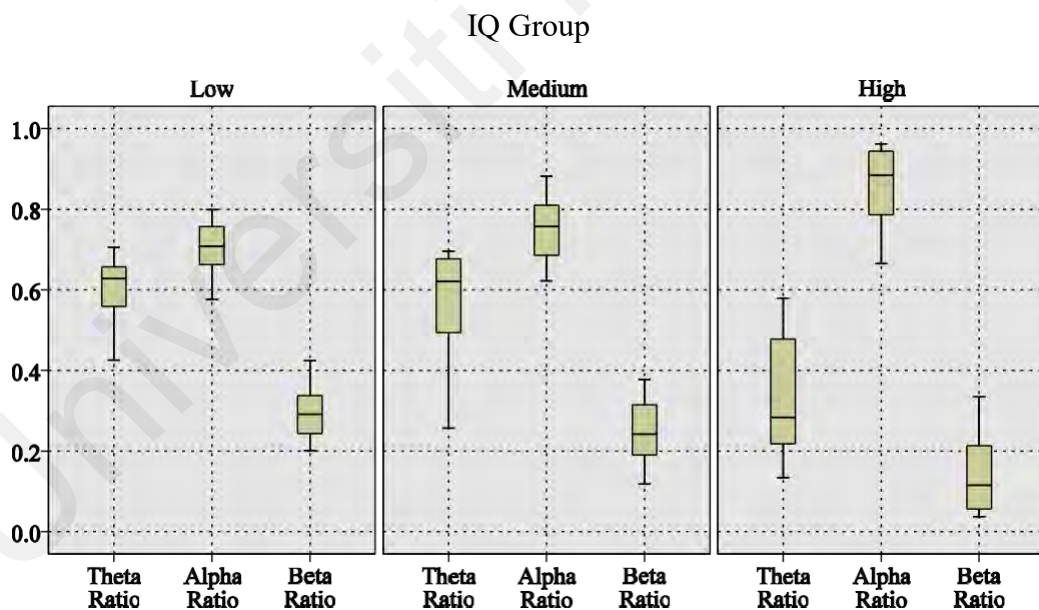


**Figure 4.14: Original data EEG signal and its Synthetic data EEG Signal with 30 dB SNR White Gaussian Noise, for 1000 Sampling Instances.**

Finally, the generation of EEG signal was created. The original data signal and synthetic data signal was illustrated as Figure 4.14. In order to show detail visualisation, the data signals were plotted into 1000 sampling instances. Despite that, these analysis will be using full signal range.

#### 4.6.1 Data Enhancement on IQ Analysis

As a result of data enhancement using synthetic data, the power ratio features were evaluated again to investigate the distribution via box plot analysis. These data enhancements were free from the outliers compared than before. Expansion of entire data via synthetic data was around 500 sample size from 85 real sample size.



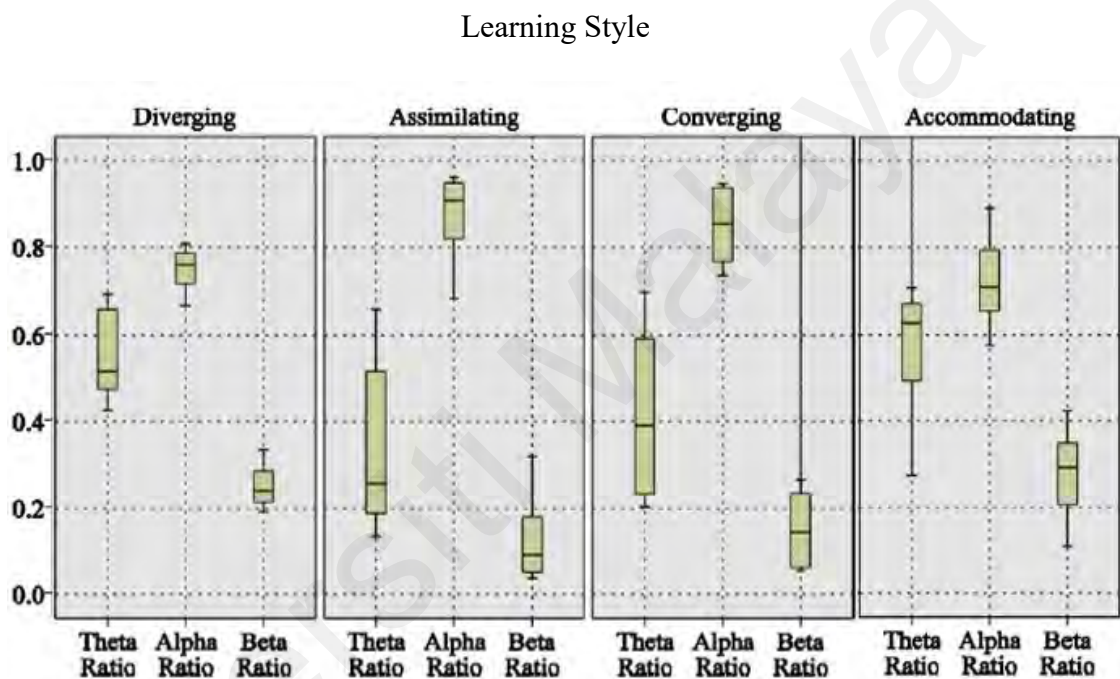
**Figure 4.15: Pattern and distribution of power ratio features for varying IQ levels (N=500).**

Figure 4.15 shows the result for IQ pattern that has been done through power ratio features of 500 number of sample size. Finding show the median theta PR pattern decreasing through increasing IQ level, meanwhile the median alpha PR pattern

increasing through decreasing IQ level. In addition, the median beta PR pattern decreasing through increasing IQ level. This beta pattern same as theta pattern.

#### 4.6.2 Data Enhancement on LS Analysis

LS analysis has been done through power ratio features of 500 numbers of sample size enhancing box plot analysis.



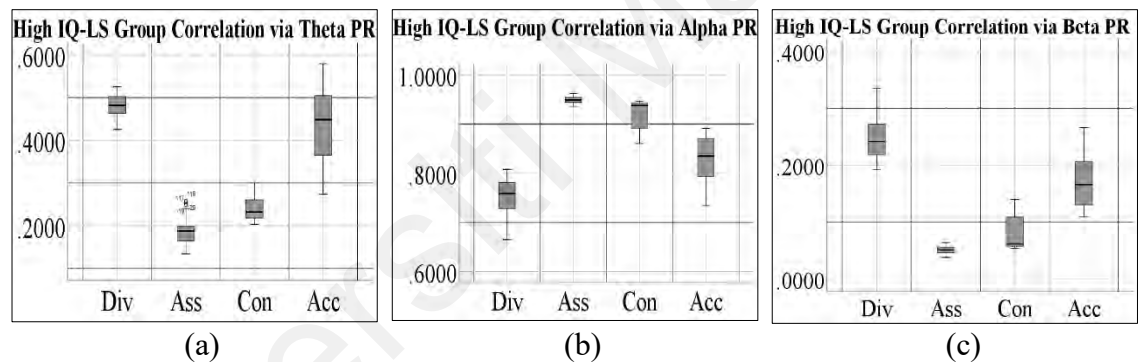
**Figure 4.16: Pattern and distribution of power ratio features for different learning styles (N=500).**

Figure 4.16 shows LS classification in theta, alpha and beta PR features. Finding shows the median theta power ratio pattern begins with assimilator, converger, diverger and accommodator. Meanwhile, the median alpha power ratio pattern starts with accommodator, diverger, converger and assimilator. The inverse pattern was found in the median beta power ratio pattern, which increased from assimilator, converger, diverger and accommodator. However, the median pattern values between assimilator and

converger are slightly similar and have also same pattern between diverger and accommodator also slightly similar.

#### 4.6.3 Data Enhancement on IQ-LS Analysis

To analyze correlation between IQ and LS, the boxplot of power ratio features is required. In accordance with this analysis, LS group of each power ratio was segregated into each level of IQ. Thus, the result analysis exhibits the smooth visual through box plot individually. As the result of data enhancement using synthetic data, the power ratio features were evaluated again to investigate the distribution via box plot analysis.



**Figure 4.17: Correlation among distinct LS groups and high IQ level referred (a) theta, (b) alpha and (c) beta sub-band PR through synthetic data enhancement. Div, Ass, Con and Acc are refer to Diverger, Assimilator, Converger and Accommodator, respectively.**

The pattern of LS in high IQ level can be showed as Figure 4.17, based on theta, alpha and beta power ratio, respectively. The result for correlation between high IQ and LS group in theta power ratio shows the median theta power ratio pattern begins with assimilator, converger, accommodator and diverger. Then, the result for correlation between high IQ and LS group in alpha power ratio shows the median alpha power ratio pattern begins with diverger, accommodator, converger and assimilator. Lastly, the result

for correlation between high IQ and LS group in beta power ratio shows the median beta power ratio pattern begins with assimilator, converger, accommodator and diverger.

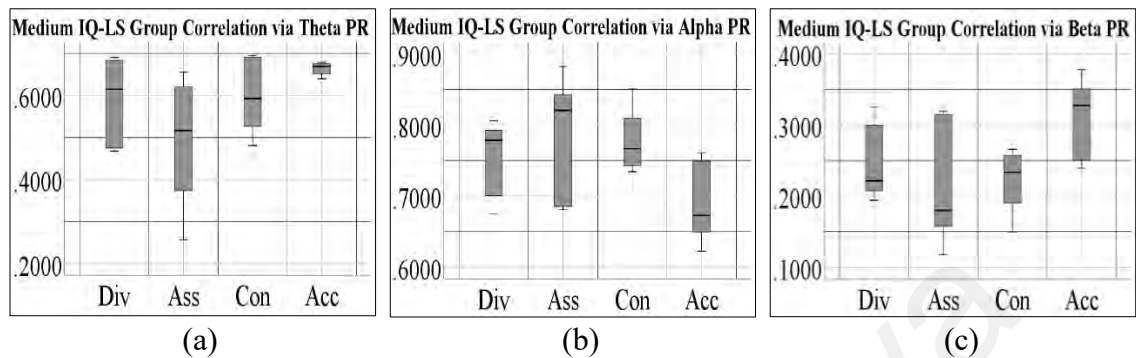


**Figure 4.18: Correlation among distinct LS groups and medium IQ level referred (a) theta, (b) alpha and (c) beta sub-band PR through synthetic data enhancement. Div, Ass, Con and Acc are refer to Diverger, Assimilator, Converger and Accommodator, respectively.**

Then, the pattern of LS in medium IQ level can be showed as Figure 4.18, based on theta, alpha and beta power ratio, respectively. The result for correlation between medium IQ and LS group in theta power ratio, the median theta power ratio pattern begins with assimilator, converger, diverger and accommodator. Besides, the result for correlation pattern of LS in medium IQ level in alpha power ratio shows the median alpha power ratio pattern begins with accommodator, converger, diverger and assimilator. Finally, the result for correlation between medium IQ and LS group in beta power ratio, the median beta power ratio pattern begins with assimilator, diverger, converger and accommodator.

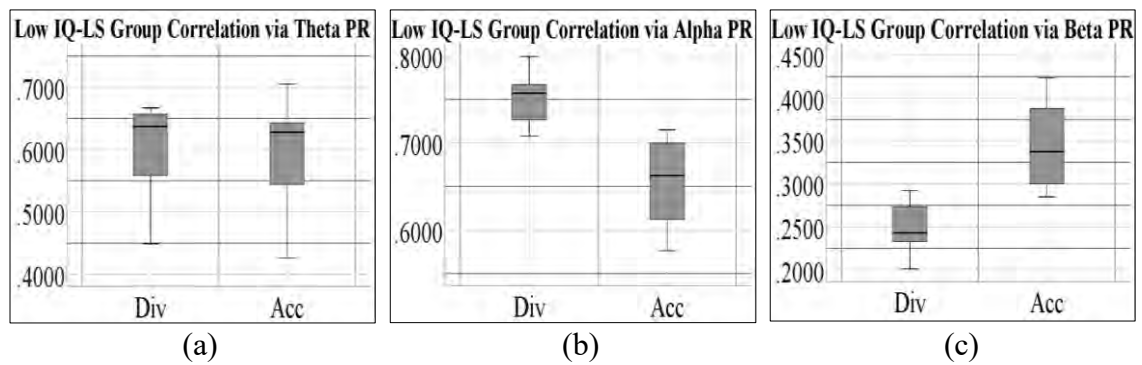


**Figure 4.19: Correlation among distinct LS groups and low IQ level referred (a) theta, (b) alpha and (c) beta sub-band PR through synthetic data enhancement. Div and Acc are refer to Diverger and Accommodator, respectively.**

Subsequently, the pattern of LS in low IQ level can be showed as Figure 4.19, based on theta, alpha and beta power ratio, respectively. The result is absent for assimilator and converger due to no population lead to low IQ level. As for the result correlation between low IQ and LS group in theta power ratio, the median theta power ratio pattern begins with accommodator and then diverger. Meanwhile, the result for correlation between low IQ and LS group in alpha power ratio shows the median alpha power ratio pattern begins with accommodator and then diverger. Lastly, the result for correlation between low IQ and LS group in beta power ratio shows the median beta power ratio pattern begins with diverger and then accommodator.

#### 4.7 EEG-Based IQ-LS Classification Model using MIMO MFNN (ANN)

In this section, the result related to EEG-based IQ-LS model classification using MIMO MFNN (ANN) will be elaborated. The resulting subsections will display on parameter of the network, performance measurement and test fitting. The detail elaboration related to this section will be focused at the discussion chapter.

#### 4.7.1 Parameter of the Network

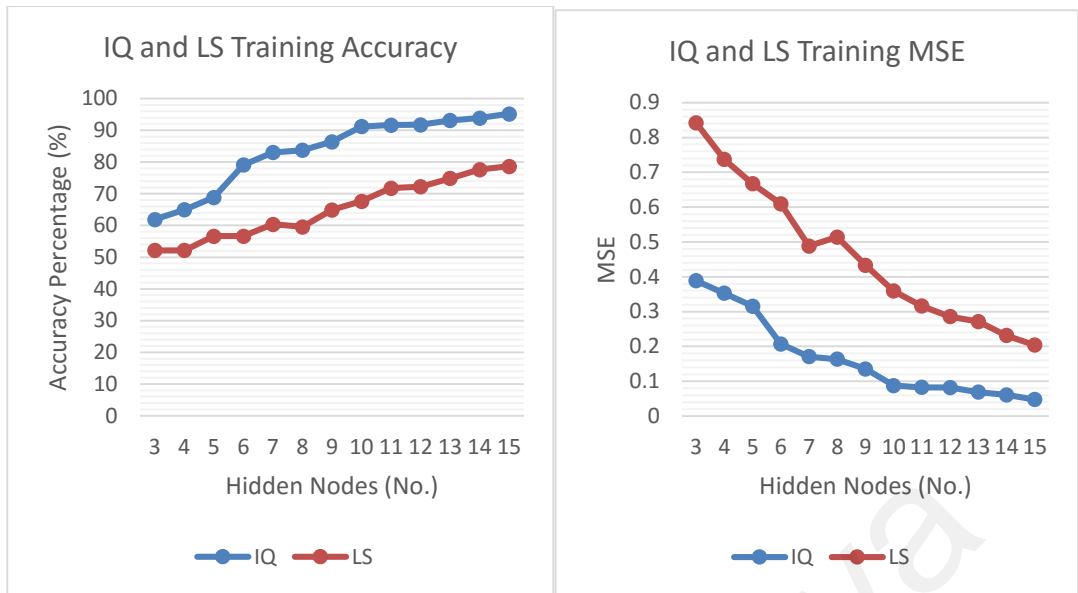
Final parameter was selected for development of EEG-based IQ-LS model via ANN. This model required power ratio (PR) features as the input vectors and the result psychometric test of IQ and LS as the output vectors. The power ratio (PR) features involved alpha, beta and gamma power ratio, thus there are three input nodes. Meanwhile, result for psychometric test consists of two test which are IQ classification result via established IQ classification model and LS test via KLSI test, thus there are two output nodes.

In addition, the number of hidden nodes was selected through modification of a constructive algorithm. Based on Figure 4.20, the 15 hidden nodes were selected due to maximum accuracy and minimum error of both classifications. The epoch was limited to 1000 for iteration training.

**Table 4.3: Final parameters of neural network.**

Network Structure	Finalized Parameters
Input nodes number	3
Hidden nodes number	15
Output nodes number	2
Activation function on hidden layer	Hyperbolic tangent sigmoid
Activation function on output layer	Pure linear
Learning Algorithm	Levenberg-Marquardt
Overfitting Control Method	Early-stopping criterion





(a)

(b)

**Figure 4.20: (a) IQ and LS training accuracy and (b) IQ and LS training MSE through the developed constructive algorithm using 40 repetition times for each cumulative hidden node.**

#### 4.7.2 Performance Measurement & Test Fitting

As for the IQ-LS classification architecture and parameter setup which has been developed before, the network was trained repeatedly to achieve best possible performance via the selected parameter. In this section, the result of IQ evaluation performance and LS evaluation performance are elaborated. Concisely, the evaluation performance based on targeting threshold and confusion matrix. The detail elaboration related to this section will be focused in the discussion chapter.

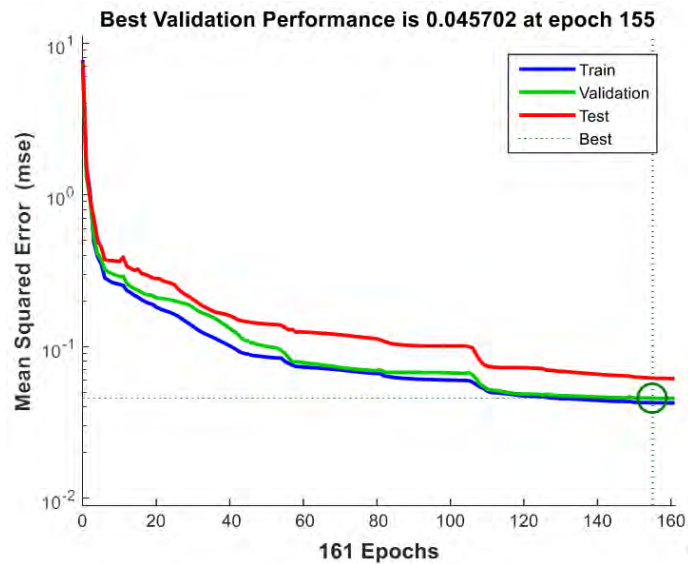


**Figure 4.21: Progression of network convergence.**

Based on Figure 4.21, figure shows the convergence of ANN model for both classification (IQ and LS). Testing and validation error decreases with training. However, beyond epoch 155, validation error started to increase, and this indicates that the network has started to overfit. Therefore, the early-stopping criterion takes effect which halts the network training and reverts to the preceding weights and biases. The best validation MSE is attained at 0.0457.

### 4.7.2.1 IQ Evaluation Performance

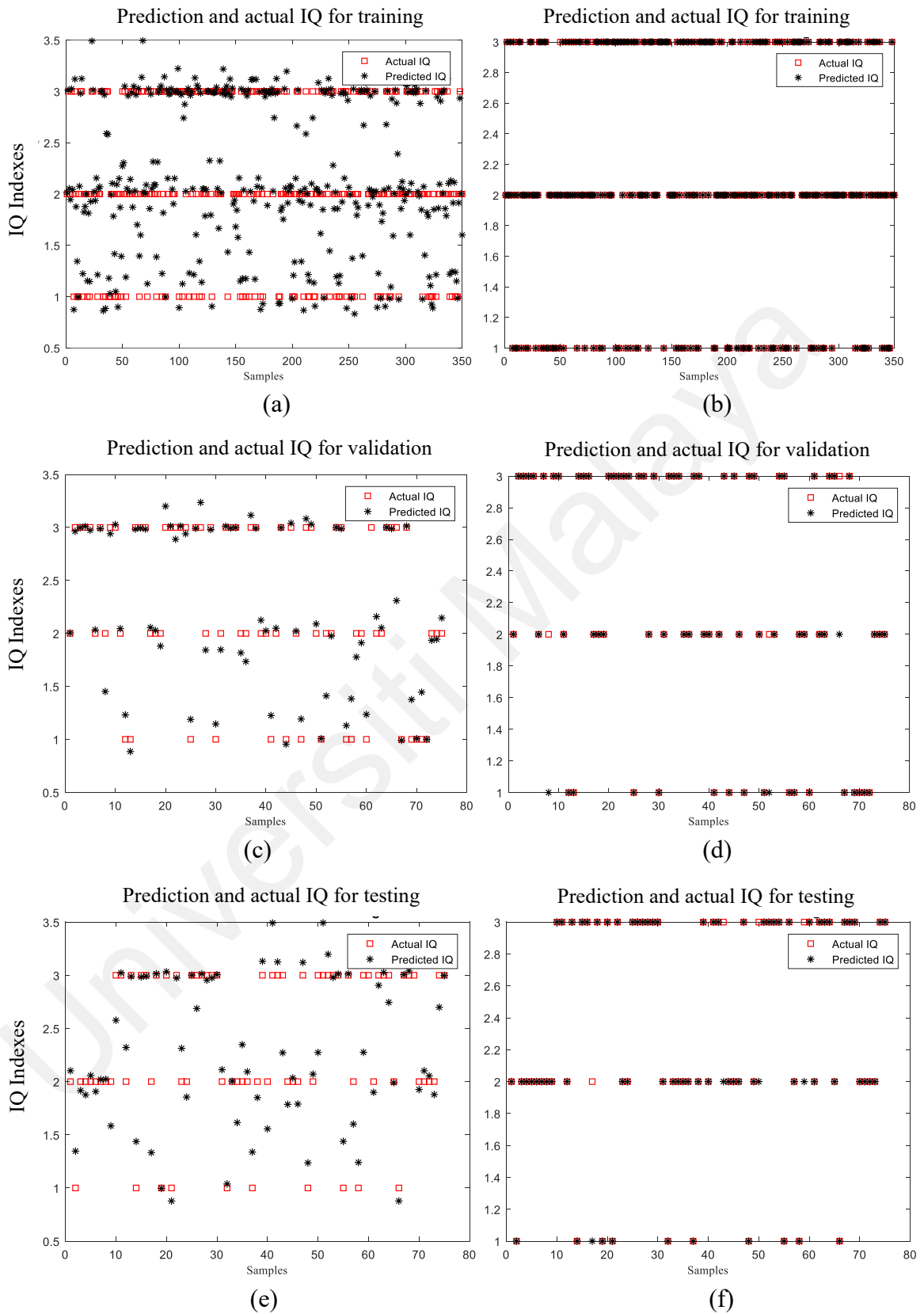


**Figure 4.22: Predicted and actual IQ (a) before Threshold (b) after Threshold in training dataset; (c) before threshold (d) after threshold in validation dataset; (e) before threshold (f) after threshold in testing dataset.**

Based on Figure 4.22(a) and 4.22(b), the figure shows the mapping IQ levels before and after applying threshold limit of both predicted and actual IQ in training dataset, meanwhile in Figure 4.22(c) and 4.22(d) was respect to validation dataset and in Figure 4.22(e) and 4.22(f) was respect to testing dataset. Figure 4.22(a), 4.22 (c) and 4.22 (e) shown the scattered data set in between the threshold limit ranges before applying threshold limit, meanwhile Figure 4.22(b), 4.22 (d) and 4.22 (f) shown the scattered data set results the whole predicted IQ datasets to be synchronized as the actual IQ levels after applying threshold limit. Misclassification during prediction after applying threshold limit can be occurred and effected the accuracy and error of the system. The red box without scattered data inside the box after applying threshold limit known as misclassification.

**Table 4.4: Accuracy and MSE of selected final network in training, validation, and testing datasets.**

Data Set	Training	Validation	Testing
Accuracy	98.3%	96.0%	94.7%
MSE	0.0171	0.0400	0.0533

**Table 4.5: Precision and sensitivity of overall accuracy for each IQ group samples.**

Title	IQ		
	1	2	3
Precision (%)	95.2	96.1	100.0
Sensitivity (%)	100.0	97.5	96.0
Overall Accuracy (%)	97.4		

To investigating network performance measurement, the conversion to the confusion matrix is benefited through threshold limit IQ level mapping. Based on Table 4.4, the table shows the accuracy and minimum square error (MSE) of confusion matrix for training, validation, and testing datasets. Meanwhile, based on Table 4.5, the

confusion matrix table shows overall arrangement observing the true and false predicted output of different IQ levels and to investigating precision and sensitivity of the network. This confusion matrix was reflected visually as Figure 4.22. Based on observation there are some misclassifications obtained in indicator 1 (low IQ), indicator 2 (medium IQ) and indicator 3 (high IQ). This involved false negative (FN) and false positive (FP) evaluation. FN was obtained when there was absence of predicted output in actual output, while FP was obtained when there exists predicted output in incorrect actual output. Therefore, FN and FP affected sensitivity and precision of final network which gain below than 100% in indicator 2 and indicator 3.

Based on the precision percentage values, the prediction of IQ levels output classified correctly into positive classification (TP) by overall positive classification (TP and FP) regardless of true or false prediction on respected to each IQ level class. For instance, precision of low IQ (threshold limit is 1) obtained by prediction of low IQ classify correctly at the output stage, while the data not classified into low IQ will plot correctly on medium and high IQ at the output stage. It shows how precise of low, medium, or high IQ classify correctly after going through the model classification. The precision percentage value also shown the exactness measurement of each IQ level, where the classification and evaluation are categorized correctly.

Based on sensitivity percentage values, the prediction of IQ levels output classified correctly into positive classification (TP) by summation with false prediction classify incorrectly (FN). The sensitivity values of each level show the low, medium and high IQ obtained by prediction of each level classify correctly, while the false prediction classify incorrectly. This sensitivity percentage values shown the completeness measurement of each IQ level, where the classification and evaluation are categorized correctly.

Finally, based on accuracy percentage values, the prediction of IQ level output classified correctly regardless of true or false output by overall dataset. The accuracy percentage values are crucial to evaluate of model performance classification since it involved overall dataset to consider. Accuracy also refers to rate of correct classification via sensitivity and precision of the classification model. Thus, all these parameters are important in this study to evaluate the model performance.

Universiti Malaya

### 4.7.2.2 LS Evaluation Performance

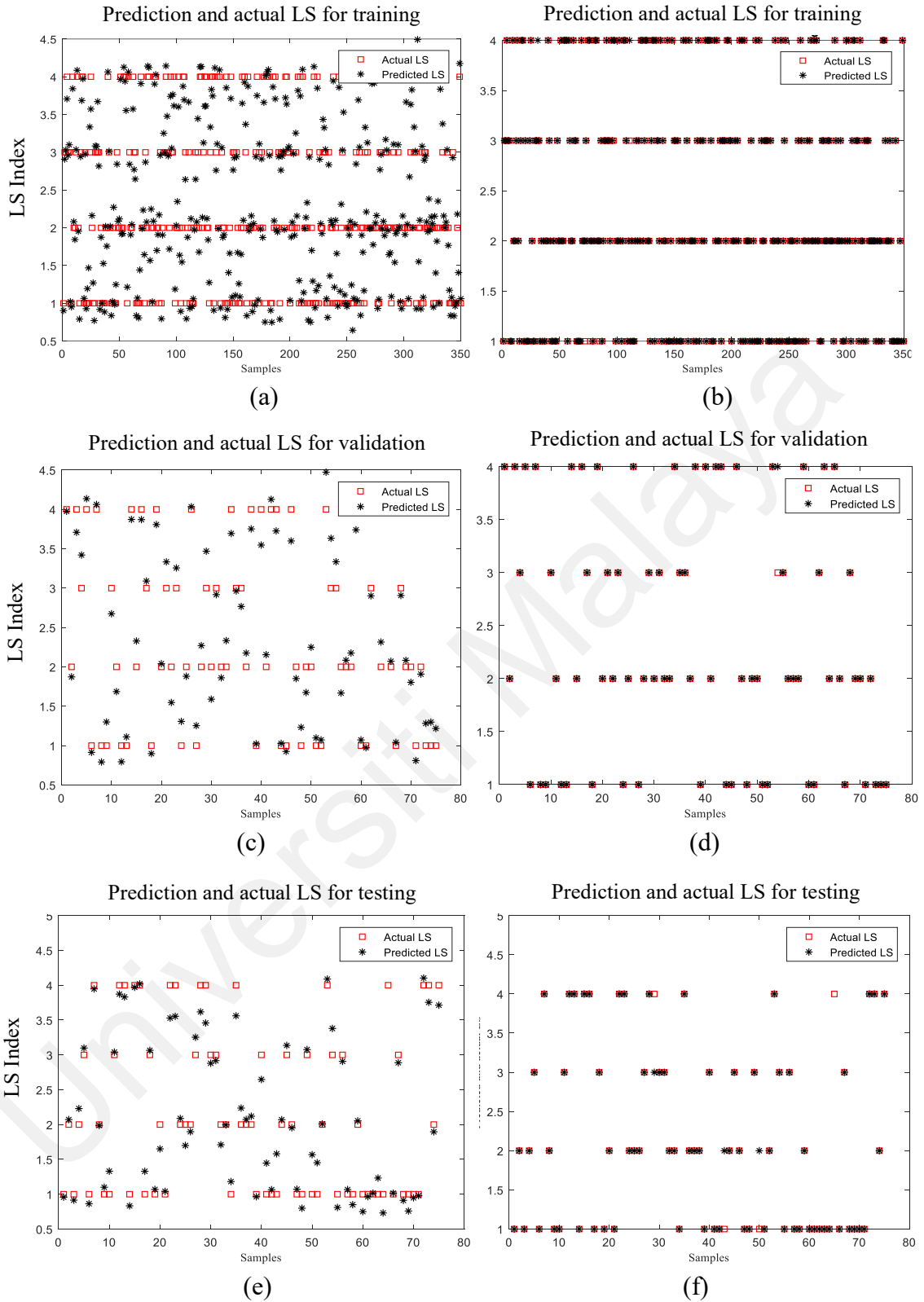


**Figure 4.23: Predicted and Actual LS (a) Before Threshold (b) After Threshold in training Dataset; (c) Before Threshold (d) After Threshold in Validation Dataset; (e) Before Threshold (f) After Threshold in Testing Dataset.**

Based on Figure 4.23(a) and 4.23(b), the figure shows the mapping LS group before and after applying threshold limit of both predicted and actual LS in training dataset, while Figure 4.23(c) and 4.23(d) shown the results for validation dataset, and Figure 4.23(e) and 4.23(f) shown the results for testing dataset. Scattered data set is in between the threshold limit ranges before applying threshold limit as shown in Figure 4.23(a), 4.23(c) and 4.23(e). Thereafter, the scattered data set results the whole predicted LS datasets to be synchronized as the actual LS group after applying threshold limit. However, there are misclassifications obtained via empty predicted output (\*) in actual output (red box) after applying threshold limit. Misclassification during prediction after applying threshold limit can be occurred and effected the accuracy and error of the system.

**Table 4.6: Accuracy and MSE of selected final network in training, validation, and testing datasets.**

Data Set	Training	Validation	Testing
Accuracy	96.9%	98.7%	80.0%
MSE	0.0314	0.0133	0.0438

**Table 4.7: Precision and sensitivity of overall accuracy for each LS group.**

Title	LS			
	1	2	3	4
Precision (%)	99.3	95.5	96.9	95.1
Sensitivity (%)	95.3	99.3	95.0	97.0
Overall Accuracy (%)	96.8			

To investigate network performance measurement, the conversion to the confusion matrix is benefited through threshold limit LS group mapping. Based on Table 4.6, the table shows the accuracy and minimum square error (MSE) of confusion matrix for training, validation, and testing datasets. Meanwhile, based on Table 4.7, the



confusion matrix table shows the overall arrangement by observing the true and false predicted output of different LS group and to investigate precision and sensitivity of the network. There is some slight misclassification obtained in every indicator. This involved false negative (FN) and false positive (FP) evaluation. FN obtained when there is absence of predicted output in actual output, while FP is obtained when there is existence of predicted output in incorrect actual output. Therefore, FN and FP affected sensitivity and precision of final network which gain below than 100% in each indicator.

Based on the precision percentage values, the prediction of LS group output classified correctly into positive classification (TP) by overall positive classification (TP and FP) regardless of true or false prediction on respected to each LS group class. For instance, precision of accommodator LS (threshold limit is 1) obtained by prediction of accommodator LS classify correctly at the output stage, while the data not classified into accommodator LS will plot correctly on diverger, assimilator and converger LS at the output stage. It shows how precise of accommodator, diverger, assimilator and converger LS classify correctly after going through the model classification. The precision percentage value also shown the exactness measurement of each LS group, where the classification and evaluation are categorized correctly.

Based on sensitivity percentage values, the prediction of LS group output classified correctly into positive classification (TP) by summation with false prediction classify incorrectly (FN). The sensitivity values of each group show accommodator, diverger, assimilator and converger LS obtained by prediction of each group classify correctly, while the false prediction classify incorrectly. This sensitivity percentage values shown the completeness measurement of each LS group, where the classification and evaluation are categorized correctly.

Finally, based on accuracy percentage values, the prediction of LS group output classified correctly regardless of true or false output by overall dataset. The accuracy percentage values are crucial to evaluate of model performance classification since it involved overall dataset to consider. Accuracy also refers to rate of correct classification via sensitivity and precision of the classification model. Thus, all these parameters are important in this study to evaluate the model performance.

### **4.7.3 Correlation Function Test**

The ideal model performance was achieved by investigating correlation tests in order to evaluate ANN model unbiasedness via residual correlation of all inputs and outputs within activation function layers. In this research, Auto Correlation Function (ACF) and Cross Correlation Function (CCF) were involved, where ACF analyze the correlation between residual and input, while CCF analyze the correlation between residual and output. In optimized model, it was assumed the correlation at lag within 95% confidence limit except at the 0 lag (L. F. Zhang et al., 2009). As the ideal performance achieved, network pruning has been stopped and that neural network has been saved.

#### **4.7.3.1 IQ Evaluation on Correlation Function Test**

In this section, it shows correlation test results on IQ evaluation. Based on Figure 4.24, the auto correlation function test (ACF) and cross correlation function est (CCF) results were revealed. As ACF has been observed, the maximum coefficient of ACF test is 1 at zero lag in all dataset. At the same time, all other lag within 95% confidence limit in training and testing. However, in validation, the others lag within 95% confidence limit except at lag 14.

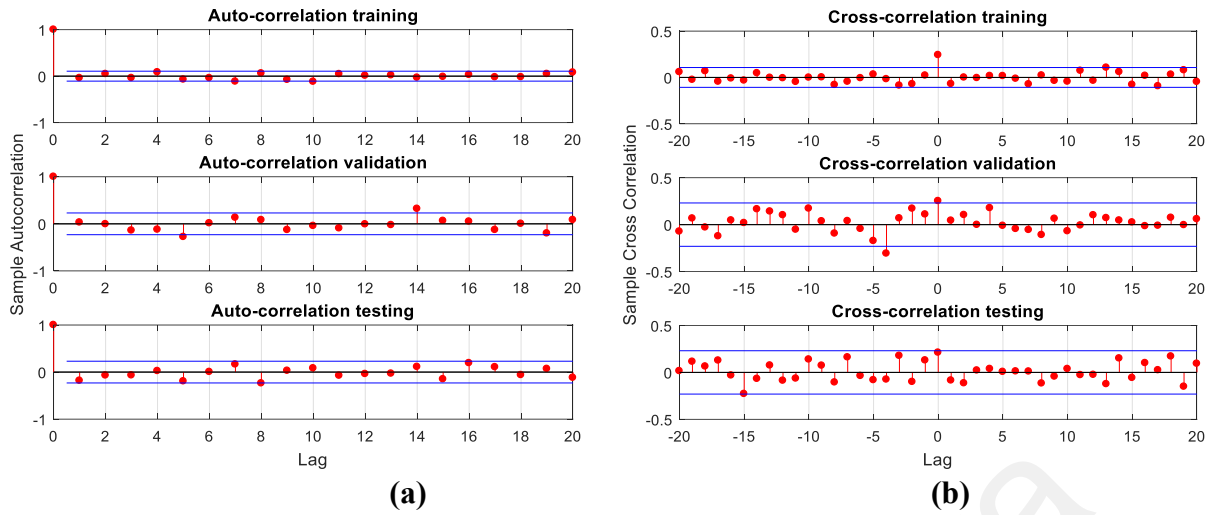


**Figure 4.24: Correlation function test results for IQ (a) ACF test result of final network model in training, validation, and testing datasets (b) CCF test result of final network model in training, validation, and testing datasets.**

As CCF has been observed, the correlation within 95% confidence limit except  $\tau = 0$  in training, validation and testing. However, in validation, the other lags within 95% confidence limit except at lag -4.

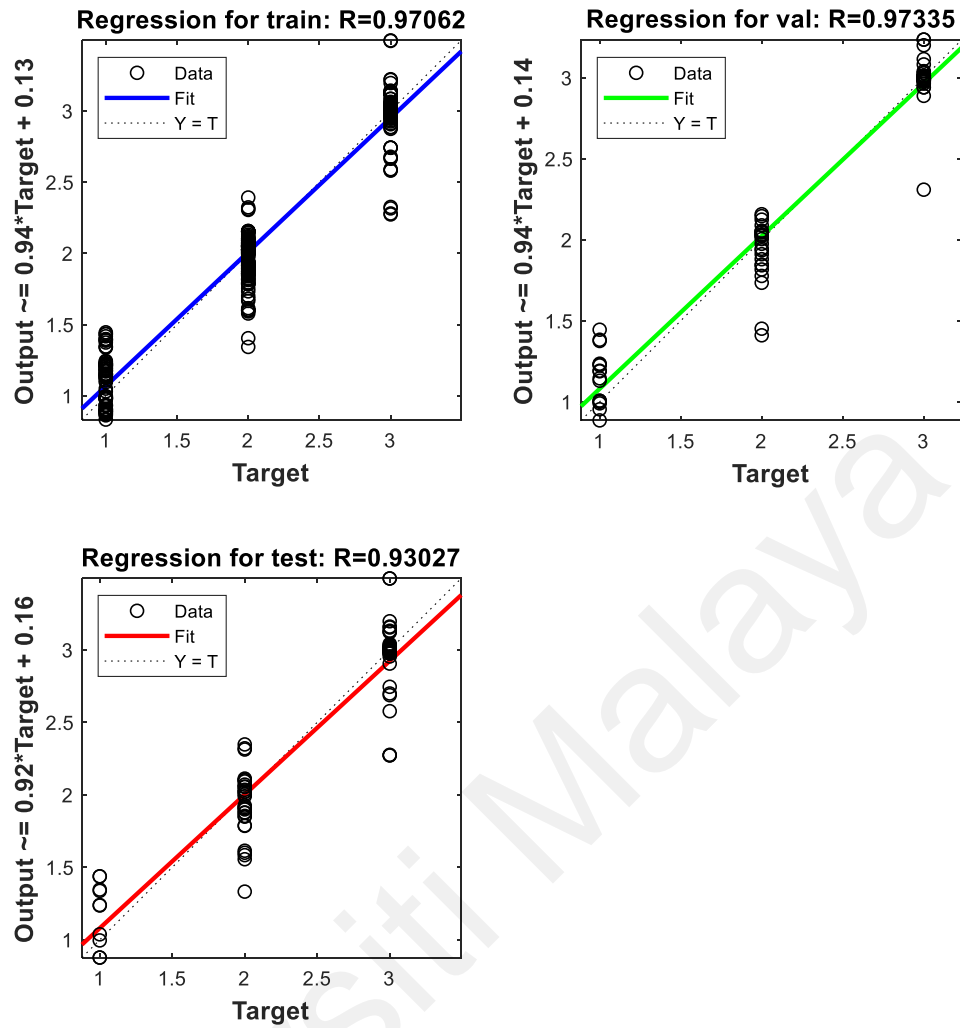


**Figure 4.25: IQ Regression Plot for Training, Validation and Testing Datasets.**

Statistically, regression analysis refers to relationship between dependent and independent variables. In this research, regression was used to predict the modeling problems that concern on predict input as numeric value. This regression analysis was required to ensure the good performance classification. Based on Figure 4.25, the actual output as dependent variable and the target output as independent variable were plotted. The residual will be obtained when the data which avoid from fit line. Based on observation, the data were closed to regression line, thus the result shown the acceptable model prediction respect to actual and target output.

### 4.7.3.2 LS Evaluation on Correlation Function Test

In this section, it show correlation test results on LS evaluation. Based on Figure 4.27, the auto correlation function test (ACF) and cross correlation function est (CCF) results were revealed. As ACF has been observed, the maximum coefficient of ACF test is 1 at zero lag in all dataset. At the same time, all other lags are within 95% confidence limit in training, validation and testing.

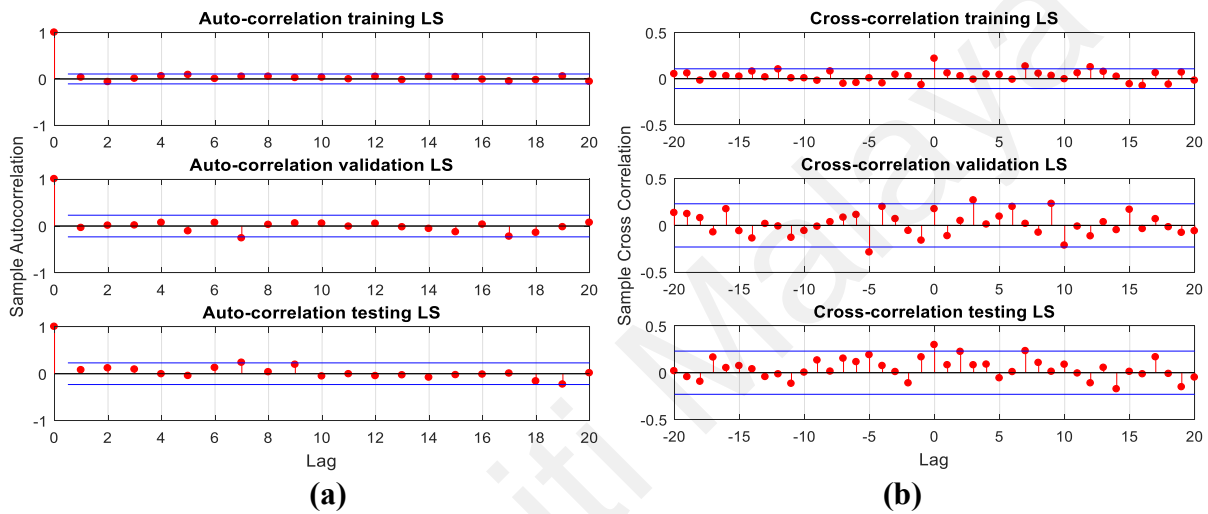


**Figure 4.26: Correlation function test results for LS (a) ACF test result of final network model in training, validation, and testing datasets (b) CCF test result of final network model in training, validation, and testing datasets.**

As CCF has been observed, the correlation within 95% confidence limit except  $\tau = 0$  in training and testing. However, in training, the other lags within 95% confidence limit except at lag 7 and 12, meanwhile in validation, the other lags within 95% confidence limit except at lag -5 and 3. In testing, entire lags within 95% confidence limit.

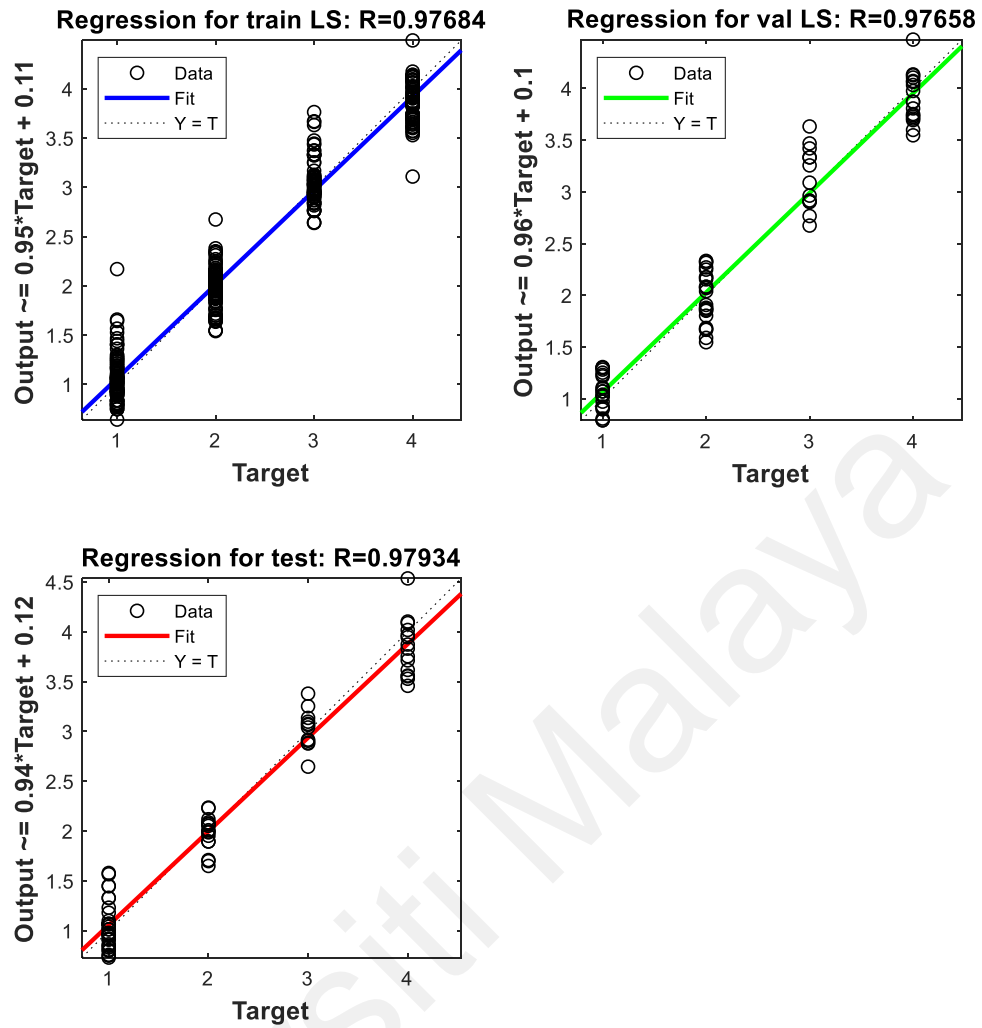


**Figure 4.27: LS Regression Plot for Training, Validation and Testing Datasets.**

Statistically, regression analysis refers to relationship between dependent and independent variables. In this research, regression was used to predict the modeling problems that concern on predict input as numeric value. This regression analysis was required to ensure the good performance classification. Based on Figure 4.27, the actual output as dependent variable and the target output as independent variable were plotted. The residual will be obtained when the data which avoid from fit line. Based on observation, the data were closed to regression line, thus the result shown the acceptable model prediction respect to actual and target output.

#### 4.7.4 Weights and Biases of the Network

Generally, the ANN model has 3 x 15 connecting weights from input nodes to the hidden nodes, and 15 x 2 connecting weights from hidden nodes to the output nodes. Table 4.8 and Table 4.9 each show the values of weights and biases in the network structure.

**Table 4.8: Neural network weights connecting from input nodes to hidden nodes, and from hidden nodes to output nodes**

Hidden Nodes, $h_j$	Weights, $w_{ik}$ , from Input Nodes, $x_i$			Weights, $w_{jk}$ , to Output Nodes, $y_k$	
	$x_1$	$x_2$	$x_3$	$y_1$	$y_2$
$h_1$	-19.4980	-13.4765	16.5316	-9.3142	-20.8170
$h_2$	-77.7513	-30.6185	28.0822	0.0399	-1.1049
$h_3$	-7.7243	-3.5344	2.7278	-0.0550	2.3480
$h_4$	-23.3949	7.3491	-9.5470	0.1009	-2.4987
$h_5$	2.2996	-2.5505	-12.8069	-0.1448	25.8110
$h_6$	5.0378	-0.2020	4.9546	2.6026	-1.4624
$h_7$	25.7393	-90.5453	86.4512	-0.0770	-1.1178
$h_8$	0.8982	-3.4121	-1.6605	-13.1407	23.9807
$h_9$	0.8610	0.0444	2.4061	8.3589	-21.7590
$h_{10}$	-13.2923	2.1518	-4.7241	-1.3612	1.8604
$h_{11}$	-1.0394	-7.3017	-1.4694	0.0303	9.5266
$h_{12}$	-17.3860	-11.2644	13.9646	9.5958	22.4772
$h_{13}$	-2.7843	-10.7738	2.2718	-0.1227	17.6044
$h_{14}$	-8.4805	6.2736	-4.3054	-0.1770	1.6644
$h_{15}$	-9.7075	19.0814	-19.9759	0.4521	-0.4731

**Table 4.9: Biases at hidden nodes and output nodes**

Nodes	Biases	
	$\theta_j$	$\theta_k$
1	-8.6361	0.1099
2	38.5389	0.0760
3	4.3085	
4	23.1972	
5	-6.0112	
6	-0.4316	
7	29.2413	
8	-0.8347	
9	-1.1285	
10	12.1489	
11	3.6785	
12	-6.5289	
13	7.6350	
14	-10.1367	
15	-19.0265	

Universiti Malaysia



## DISCUSSION

### 5.1 Introduction

In this chapter, the essential discovery with respect to the research investigation and elaboration are epitomized based on the findings found in this thesis. The sections in this chapter are quite straightforward via general concept strategy to the develop EEG-Based IQ-LS Classification Model via ANN. Despite that, converting strategies into argument is significantly complicated and the verification are needed in this chapter. Besides, the research results obtained need to clarify as well as presented model implementation performances. In accordance with findings from literature review, the correspondence and comparison of previous work will be evaluated. Therefore, the research findings will elaborate the implementation of valid model performance. This chapter presents a discussion of the crucial findings from the research to achieve the objective.

### 5.2 IQ-LS Data Distribution

Sample distribution indicated the probability distribution of a given statistics based on a random sample set population. Based on IQ population obtained from research results, the high IQ is dominant in sample distribution, the medium IQ is in second place and the low IQ is minor in sample distribution. Beyond that, the dominant population of the high IQ effected by numerous subject samples comprised of high educational and have professional backgrounds. With regards to LS population, various LS group having balance proportion depend on their own unique LS group type.

Based on the result of correlation between IQ and LS, as the dominant samples distribution of high IQ sample, thus, various LS group in high IQ is numerous rather than low and medium IQ levels. There are distinct groups of LS in each IQ levels except low

IQ, which consists two groups of LS (diverger and accommodator group). Behind the incident, the established IQ classification model was developed via fluid intelligence, which concerns on logical thinking and visual problem solving. This leads the high IQ of assimilators and convergers group into dominant position. However, these group are absent in low IQ by cause of their analytical thinking dominant in medium and high IQ (Cattell, 1963; Gyeong & Myung, 2008). The result on Figure 4.3, support and augment these findings by showing no mapping for low IQ level has been observed in assimilators and convergers.

### 5.3 EEG Signal Processing Analysis

First of all, the crucial features strategy with respect to sequence EEG signal processing begin by raw EEG data, filtered EEG data conversion, frequency domain conversion, ESD conversion, and PR conversion. Fp1 raw EEG data is obtained by using Mindwave Headset Neurosky as mention before.

The sampling instances as Figure 4.4 to 4.5, refer to recording instances bin. The EEG signal is of stochastic nature and fluctuates randomly over time in several instances and contained artefacts. Rejection of artefacts which exceeding  $\pm 100 \mu\text{V}$  is rejected and can be seen in Figure 4.4(b) before proceeding to filtering and feature extraction processes. Furthermore, Figure 4.4(b) also shows the filtering EEG signal with baseline correction using 1264th-order equiripple bandpass filter. Based on Figure 4.5, the EEG signal was filtered into three main sub-bands. EEG filtering processing refers to preliminary processing data by rejecting noise due to obtain actual neural signal.

The conversion of PSD via FFT with respect to theta sub-band, alpha sub-band and beta sub-band and separation of PSD can be observed in Figure 4.6. Based on these figures, it is noticed that using equiripple filter caused the sharp frequency separation on

4–8 Hz for theta, 8–13 Hz for alpha and 13–30 Hz for beta. This EEG signal pre-processing results supports the finding by showing the equiripple filters is benefit to minimize error function, robust, stable and efficient performance (M. S A Megat Ali et al., 2014). In addition, the higher amplitude of spectrums obtains slow wave in comparison to fast wave with respect to frequency theory. The spectrum magnitude of the signal in SI unit (International System of Units) is microvolt ( $\mu\text{V}$ ) for time domain and Hertz (Hz) for frequency domain.

Conceptually, the energy distribution is acquired by evaluating the area of PSD curve for each frequency sub-band and known as energy spectral density (ESD). This ESD which contains the whole energy distribution for each range of the frequency band is evaluated for each sub-band group. The pattern of the ESD can be shown in Figure 4.7(a) consistent with fundamental sub-band characteristics protocol. Besides that, the result shows high ESD alpha sub-band is produced high values compared theta and beta sub-band in each subjects' pattern. In accordance with EEG closed-eyes and relaxed state recording protocol, thus the alpha sub-band has been activated causing high amplitude, while the beta sub-band inactivated causing low amplitude. Inactivation of theta sub-band is in respect to unconscious state, however there are impacts on mental and attention processes (A. P. Anokhin et al., 1999; van Son et al., 2018).

To normalize ESD values, power ratio (PR) features of theta, alpha and beta are extracted from sub-band ESD features values. The correlation values pattern between ESD and PR features is similar pattern as PR just to normalize ESD values, where this feature method derived by splitting the respective frequency power band by the other frequency power band to gain a feature that is characterized to represent signal behavior. These correlations can be conformed in Figure 4.7.

The pattern of the PR can be shown in Figure 4.7(b) consistent with fundamental sub-band characteristics protocol. As the values normalized from ESD, the result shows high PR alpha sub-band is producing high values compared to theta and beta sub-band in each subjects' pattern. Respect to the result, the alpha-band has been activated caused high amplitude, while the beta sub-band and theta sub-band inactivated caused low amplitude based on methodology recording protocol impact.

#### **5.4 Evaluation on IQ Level and LS Group Analysis (N=85)**

Evaluations on PR features extraction via IQ level and LS group have been discussed forward in the following subsections. This evaluation focused on box plot analysis, where these analyses are required in order to interpret EEG data and in order to handling abnormal data. In this section, the discussion shows investigation through box plots analysis, which indicates the pattern distribution of IQ and LS data. The observation for consequence impact through the pattern were concerned on significant methodology protocol.

##### **5.4.1 Intelligence Quotient Analysis**

Generally, intelligence is defined as the ability to comprehend complex ideas, to efficiently adapted to the surroundings, to be engaged in different forms of reasoning, taking thought to resolve obstacles and learning from experience (Haler et al., 1992; Jeng & Huang, 2018; Sobkow, Traczyk, Kaufman, & Nosal, 2018). Individual differences in intelligence are quantified as intelligence quotient (IQ). In this section, the discussion shows investigation individual differences in intelligence through box plots analysis, which indicates the pattern distribution of EEG sample data. The box plots represent

analysis on each group contributed by single sub-band power ratio median values. This analysis is analyzed through real data sample without any synthetic data improvement.

The significant results can be observed among 3 IQ levels for theta, alpha and beta PR features. The box plots demonstrate the median sub-band PR feature values through various IQ levels involved low, medium, and high IQ levels. Based on Figure 4.8, the theta power ratio decreases through increasing IQ level, whereas low IQ presents highest median values, and high IQ presents lowest median values. Contrariwise, the alpha power ratio increases through increasing IQ level, whereas low IQ presents lowest median values, and high IQ presents highest median values. The highest alpha sub-band values on high IQ level compared to low and medium IQ refers to increased Alpha suppression due to increase attention (Craddock, Poliakoff, El-dereby, Klepousniotou, & Lloyd, 2017; Hanslmayr et al., 2005; MacLean, Arnell, & Cote, 2012; Scally, Burke, Bunce, & Delvenne, 2018). In addition, the alpha distribution is also constant with previous findings that specify samples in the high-ability level presented increase in alpha power on the frontal brain region (Gevins, 2000; Jahidin, Taib, Tahir, Megat Ali, & Lias, 2013). However, the beta power ratio pattern follows the theta power ratio as it is decreased through increasing IQ level. The beta power ratio pattern result supported with previous finding, where the beta power ratio represents the energy expenditure (Colom, Karama, Jung, & Haier, 2010; Haier et al., 1988; Haler et al., 1992). As we can see, the low IQ has higher beta power ratio value, which use more energy expenditure, while high IQ has lower beta power ratio, which use minimum energy expenditure (Colom, Karama, Jung, & Haier, 2010; Haier et al., 1988; Haler et al., 1992). Thus, to conclude the IQ level pattern, the theta and beta sub-band pattern are opposite to relationship with alpha sub-band.

Besides that, throughout Figure 4.8, the observation on intelligence pattern starts increasing from beta, theta, and alpha power ratio in each IQ level pattern. These were proven as previous study analysis as it reflects the varying levels of alpha dominance for each IQ levels (M.M. Anoor et al., 2018). In addition, the pattern also approved through Neural Efficiency Hypothesis of intelligence which outlines brighter individuals produced high alpha pattern (Neubauer & Fink, 2009b).

In accordance with the outcome, the results are constant with previous studies (M. Doppelmayr et al., 2002; Fink et al., 2009; Klimesch, 1999; Neubauer & Fink, 2009a), that were discussed in literature review. Other than that, previous studies also validated the acceptable correlation between EEG and intelligence (Michael Doppelmayr et al., 2005; Jaušovec, 2000), which can be conformed through resting state without any cognitive demanding tasks (L. Wang et al., 2011). Therefore, this thesis provides acceptable findings by implementing PR features as input to distinguish IQ levels in relaxed with eyes closed state.

Based on ANN system generation, PR features is the input vector to model classifier. Furthermore, PR method can overcome extreme outliers' existence from ESD features. This original dataset will be improved through synthetic data and the elaboration will discuss in further sub-section. To improve high classification accuracy, the sample data end up with 500 data (N=50 per group). So, Section 5.5 will be interpreted on the synthetic signals' generation ahead of the ANN model that can be optimized with PR features input.

#### **5.4.2 Learning Style Analysis**

In this section, learning style analysis refers to Kolb's Learning Style. Kolb's ELT has defined learning to be the process whereby knowledge is created through the transformation of experience. The ELT portrays two dialectically related modes of Absorption and Comprehension dimensions also known as grasping and transforming

experience, respectively. Absorption dimension refers to the process of taking in information, while Comprehension dimension is how individuals interpret and act on that information (Magfirah, 2017). The Absorption dimension comprises of Concrete Experience (CE) and Abstract Conceptualization (AC) learning modes, while the comprehension dimension is comprised of Reflective Observation (RO) and Active Experimentation (AE) learning modes (A. Kolb & Kolb, 2005). Combination of dominant modes in both dimensions results in preferred learning style; Converging, Diverging, Accommodating and Assimilating styles. Each of styles influences how individuals learn (Kolb, 2007).

Kolb's learning style was constructed through four orthogonal axes quarterly refer to associate of preferences or styles that define a certain manner to handle with problem solving (D. A. Kolb, 1974). Each one of learning style has its own basic strength and unique characteristics. Particularly a dominant learning style might perform well in certain learning situation, but still the other minor learning style should be considered as the dominant style cannot be put superior to another (Larkin-Hein & Budny, 2003). Nevertheless, a learner is effectual to obtain great understanding and gain the excellent learning outcomes by attaching through whole four components of learning cycle (Chan, 2012). The individual that has balanced ability interpreted that the individual is using differ learning styles (Kolb & Kolb, 2005)

In this section, the discussion focuses on the individual differences in LS through box plots analysis, which indicates the pattern distribution of EEG sample data. The box plots represent analysis on each group contributed of every single sub-band power ratio median values. This analysis is analyzed through real data sample without any synthetic data improvement. Referring to Figure 4.9, throughout LS classification in power ratio features, the median theta power ratio pattern begins with assimilator, converger, diverger

and accommodator. Meanwhile, the median alpha power ratio pattern starts with diverger, accommodator, converger and assimilator. The inverse pattern was found in the median beta power ratio pattern, which increased from assimilator, converger, accommodator and diverger. However, the median pattern values between assimilator and converger are approximately similar, and same pattern between diverger and accommodator also approximately similar.

This evaluation can be done through comparison with previous work using power features extraction as mentioned in literature review. Based on theta sub-band, the results on theta PR features agreed with previous finding where the lowest theta median belongs to assimilator, followed by converger, diverger and accommodator (Megat Ali, Jahidin, Md Tahir, et al., 2014). However, based on alpha sub-band, the PR values on accommodator and diverger are the lowest, while converger and assimilator are highest agreed with previous work although the position of LS group slightly difference (Megat Ali, Jahidin, Md Tahir, et al., 2014; Rashid et al., 2011). Based on beta sub-band, the patterns of LS group are difference from previous work, which using PSD features (Rashid et al., 2013) and there are no approach related to PR features yet.



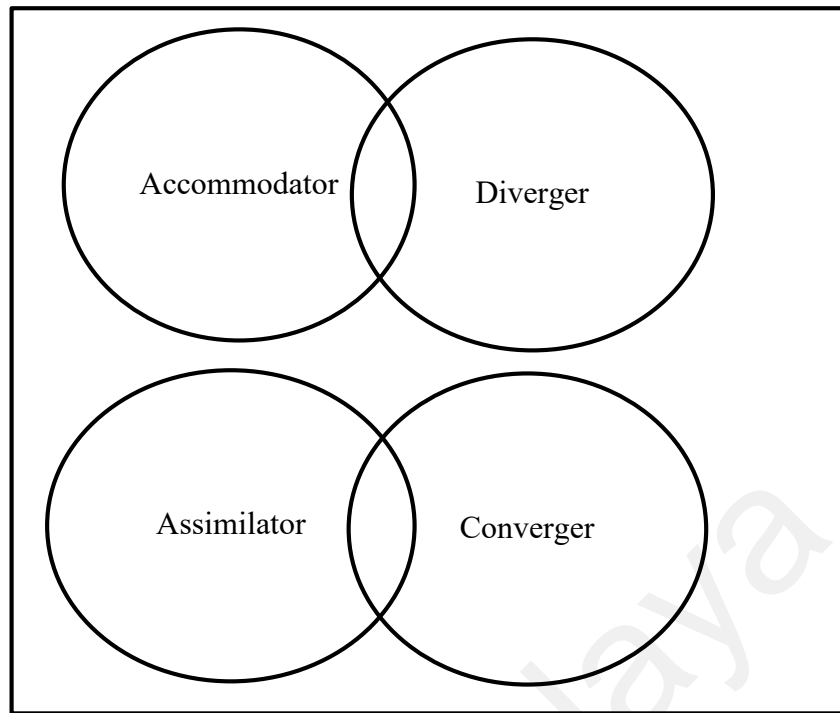


**Figure 5.1: Dataset for LS groups, where accommodator union with diverger, while assimilator union with converger in universal set.**

The research's main finding on PR features values suggest assimilator and converger are intersected with each other, while accommodator and diverger are both intersected as shown in Figure 5.1. Figure 5.1 was proven by result analysis on Figure 4.9 and Figure 4.16, before and after dataset enhancement with synthetic EEG. The theta, alpha and beta sub-band PR median values quite similar through assimilator-converger union and accommodator-diverger union. The theta power ratio increases beginning with assimilator-converger union, and then accommodator-diverger union for both before and after enhancement with synthetic data. Based on median alpha power ratio, the pattern increases from diverger, accommodator, converger, and assimilator before synthetic data enhancement, while after enhancement, the pattern begins with accommodator, diverger, converger, and assimilator. Based on median beta power ratio, the pattern increases from assimilator, converger, accommodator and diverger before synthetic data enhancement, while after enhancement, the pattern begins with assimilator, converger, diverger and

accommodator. Hence, these suggested the union of assimilator-converger union and accommodator-diverger, which also supported the correlation LS pattern through each IQ level.

Overall, the results support and augment these findings by showing accommodator and diverger preferred in informative manner and imaginative ability in assigning task by resisting problem solving (Cagiltay, 2008; Richmond & Cummings, 2005), meanwhile assimilator and converger preferred reasoning and problem solving in assign task (Cagiltay, 2008; Healey & Jenkins, 2000; Richmond & Cummings, 2005). Based on Figure 5.1, the figure shows the union of LS group collaboration based on overlapping PR values. The result patterns are also constant with Kolb's experiential learning cycle description and intelligence definition. In next sub-section, the discussion related learning style with intelligence and brainwaves signal will deeply elaborate.

#### **5.4.3 Intelligence Quotient and Learning Style Analysis**

In IQ-LS pattern discussion, the basic principle between IQ and LS must be understood. The primitive difference between intelligence theories and learning style theories is intelligences roles as a core on the learning contents and products process, meanwhile learning style roles as a side core and focused on differences in learning process (Snyder, 1999). Although there are absences of researcher's approach exploring learning style and intelligence utilizing Kolb's ELT and IQ, there are several previous research are related with the finding to justify and analyse the results.

Generally, Cattell (1963) asserts that the fluid intelligence refers to intentional mental operations to solve novel problems and abstract thinking (Cattell, 1963), which is related to abstract conceptualization based on Kolb's ELT (David A. Kolb, 2007). Abstract

conceptualization was concerned with most of the critical thinking dispositions: analyticity, self-confidence, truth-seeking, systematicity and maturity (S. M. Wechsler et al., 2018). Accordingly, Patterson's (1994) work, supported the view that accommodators scored lowest in critical thinking (Patterson, 1995), meanwhile Gyeong and Myung's (2008) found the divergers correlated with the lowest and converges with the highest critical thinking (Gyeong & Myung, 2008). Despite that, others finding also present that assimilator and converger encompass thinking in their learning process related to the critical thinking dispositions (Andreou et al., 2014). The cognitive processing of intelligence involved with the performance of problem solving, which reflects to neurocognitive mechanism based on problem-solved processing happen in the brain (Hernán, Córdova, Cifuentes, Cañete, & Palominos, 2015).

Based on high IQ and LS correlation as Figure 4.10, the assimilator and converger have higher alpha PR median values compared to theta PR and beta PR values. In accordance with assimilator and converger group, these groups are associated with greatest critical thinking dispositions (Andreou et al., 2014), thus high alpha PR median values is created. This is supported by intelligence principle which are correlated to novel problems solution and abstract thinking (Cattell, 1963). In addition, Hernán et al., 2015, argued that critical learning approach was in correspondence with particular complex mental processing (Hernán et al., 2015). Therefore, these statements supported that theta, alpha and beta PR median values in high IQ-LS correlation has highest median value compared to medium IQ-LS correlation and low IQ-LS correlation.

Based on medium IQ and LS correlation as Figure 4.11, the same pattern can be found, where assimilator and converger have higher alpha median PR values compared to theta PR and beta PR values. However, the beta PR median value does not follow the pattern, but the interquartile length of PR values follows the pattern and considered reasonable.

In accordance with accommodator and diverger group, these group are associated with lowest critical thinking dispositions (Gyeong & Myung, 2008; Patterson, 1995), thus low alpha PR median values is created. As critical thinking dispositions decrease, they caused reduce intelligence ability where correlated to novel problems solution and abstract thinking (Cattell, 1963). In addition, Hernán et al., 2015, argued that critical learning approach was corresponding with particular complex mental processing (Hernán et al., 2015). Thus, these statements were supported that theta, alpha and beta PR median values in medium IQ-LS correlation has higher median value compared to low IQ-LS correlation but lower compared to high IQ-LS correlation.

Based on low IQ and LS correlation as Figure 4.12, the result presents accommodator and diverger group only with the absent assimilator and converger group due to non population lead to low IQ level. However, all groups of learning style were supported on high IQ and medium IQ levels (Hernán et al., 2015). This nonexistent group is supported with the intelligence principle, where active intelligence has high critical thinking (Cattell, 1963; Gyeong & Myung, 2008). Based on the alpha sub-band result, diverger has high median value compared to accommodator, where beta sub-band shows inversed pattern where, accommodator has high median value compared to diverger. Meanwhile, theta sub-band median value between accommodator and diverger has approximately similar values. Based on alpha and beta sub-band PR median values, the results support the finding as the previous research (Hernán et al., 2015; Megat Ali, Jahidin, Md Tahir, et al., 2014), where diverger has high median value compared to accommodator in alpha sub-band and contrawise in beta sub-band. However, different theta sub-band pattern was observed, and this research suggests approximate median values between accommodator and diverger.

Despite that, based on McKenna theoretical demonstrations there are several differences between intelligence and learning style (Diseth, 2002; McKenna, 1984). First, intelligence ability is more related with achievement level, while learning style concerns on the way of achievement. Secondly, intelligence ability is unipolar which means ability dimension is valued and the other is not, whereas learning style is bipolar which mean ability dimension neither end nor been considered better overall. Finally, intelligence ability has a limited range of application compare to learning style, which has diverse range of application. This can be summarized that, even low IQ involved between accommodator and diverger group, by having suitable intelligence levels enable learners to obtain the most suitable learning styles, which enhance human performance such achievement level.

Integration of learning style and intelligence into learning systems can be matched with adaptive learning system that can adapt the content for the purpose of ensuring the better performance in the learning process (Hamada & Hassan, 2017). That means suitable intelligence levels enable learners to obtain the most suitable learning preferences that might be matched with their learning styles. In addition, previous investigation between intelligence ability and learning style, found that learning style has significant positive influence via intelligence ability (Busato et al., 2000). Thus, this new finding enhances the education authorities to improve education arrangement, methodological strategies option, effective assist resources and others in education field.

## **5.5 Evaluation on Synthetic Data Analysis (N=500)**

To achieve certain ANN requirements or conditions, the synthetic data were used through generation of real data. Inadequate sample size data results biased toward the detection of the majority class in classifier performances (A. Bhattacharyya & Pachori,

2017). Thus, this sensible and popular approach to experimental design through synthetic data generation caused the structures of research and modeling performance to improve in the modelling process.

Before generating synthetic data, two outliers have been found in real dataset (N=85) based on Figure 4.9. This outlier must be considered in sample data, as this data is not the extreme outlier. If the sample data consist of less than 10% of the extreme outlier, it must be removed before proceeding to synthetic improvement to increase neural network accuracy performance. Then, the original IQ and LS data are enhanced through synthetic data. Synthetic data signal is shown as the white Gaussian noise,  $W_{noise}$ , which was added to the original brainwaves signal. Results show that identical pattern as before and after enhanced the data through synthetic data. Furthermore, the summation of synthetic data has enhanced and is free from outliers.

Based on IQ level evaluation after adding synthetic data, the pattern prior to before and after through theta, alpha and beta sub-band PR median values position precisely similar. Based on Figure 4.15, the theta power ratio decreases through increasing of IQ level, whereas low IQ presents highest median values, and high IQ presents lowest median values. Contrariwise, the alpha power ratio increases through increasing IQ level, whereas low IQ presents lowest median values, and high IQ presents highest median values. However, the beta ratio pattern follows the theta power ratio as it is decreased through increasing IQ level. Thus, theta and beta sub-band opposite relationship with alpha sub-band.

Based on LS group evaluation after adding synthetic data, the pattern prior to before and after through theta, alpha and beta sub-band PR median values quite similar through assimilator-converger union and accommodator-diverger union. Based on Figure 4.16, the theta power ratio increases beginning with assimilator-converger union, and then

accommodator-diverger union. Contrariwise, the median alpha power ratio increases from accommodator-diverger union, and then assimilator-converger. However, the beta ratio pattern follows the theta power ratio as increase begins with assimilator-converger union, and then accommodator-diverger union. Thus, theta and beta sub-band show opposite relationship with alpha sub-band.

Based on IQ-LS evaluation after adding synthetic data, the patterns are observed prior to before and after through theta, alpha and beta sub-band PR median values. Based on high IQ and LS correlation via Figure 4.17, the assimilator and converger have higher alpha PR median values compared to theta PR and beta PR values. In accordance with assimilator and converger group, these group associated with greatest critical thinking dispositions (Andreou et al., 2014), thus high alpha PR median value is created. This is supported by intelligence principle where its correlated to novel problems solution and abstract thinking (Cattell, 1963). Furthermore, the pattern between after and before adding synthetic data, shows the results with the same position LS group. Therefore, the theta, alpha and beta PR median values in high IQ-LS correlation has highest median value compared to medium IQ-LS correlation and low IQ-LS correlation.

Based on medium IQ and LS correlation via Figure 4.18, the same pattern can be found, where assimilator and converger have higher alpha median PR values compared to theta PR and beta PR values. However, the beta and alpha PR median value do not follow the pattern, but the interquartile length of PR values follow the pattern and considered reasonable. In accordance with accommodator and diverger group, these group associated with lowest critical thinking dispositions (Gyeong & Myung, 2008; Patterson, 1995), thus low alpha PR median values is created. As critical thinking dispositions decreases, it caused reduce intelligence ability where correlated to novel problems solution and abstract thinking (Cattell, 1963). Thus, the theta, alpha and beta

PR median values in medium IQ-LS correlation has higher median value compared to low IQ-LS correlation but lower compared to high IQ-LS correlation.

Based on low IQ and LS correlation via Figure 4.19, the result presents accommodator and diverger group only with the absent assimilator and converger group due to no population lead to low IQ level. This nonexistent group is supported with the intelligence principle, where active intelligence has high critical thinking (Cattell, 1963; Gyeong & Myung, 2008). Based on the alpha sub-band result, diverger has high median value compared to accommodator, where beta sub-band shows inversed pattern where, accommodator has high median value compared to diverger. Meanwhile, theta sub-band median value between accommodator and diverger has approximately similar values. Based on alpha and beta sub-band PR median values, the results support the finding as the previous research (Megat Ali, Jahidin, Md Tahir, et al., 2014), where diverger has high median value compared to accommodator in alpha sub-band and contrawise in beta sub-band. However, different theta sub-band pattern was observed, and this research suggests approximate median values between accommodator and diverger. Overall, the pattern on the real data (N=85) is quite same after synthetic data enhancement (N=500).

## **5.6 IQ-LS Network Model Optimization Analysis**

This section, and the subsequent subsections will describe the findings on EEG-Based IQ-LS Classification Model using ANN, or specifically MIMO ANN. The subsections will elaborate the parameters setup, performance measures and test fitting, and correlation function tests of final model selection. Based on this research, this model was developed through supervised machine learning method, which required input and output data at the first place. To solve the model system, ANN model created the neural network model between input and output, through non-linear and linear structure ANN architectures.



Once finishing the model, the evaluation and validation are required through this section. A detail elaboration related to this section will be highlighted at each of subsection as mention before.

### 5.6.1 Parameter

Practically, ANN model composed of non-linear and linear structure between input and output to solve the model pattern via ANN learning process. In simple words, during ANN learning process, knowledge of the system is obtained by neural network to achieve the performance (Alarabi & Mishra, 2010). To gain positive performance, the parameters setup is required via input nodes setup, output nodes setup, hidden nodes setup, and epochs setup.

Based on parameters setup, the model was constructed using three sub-band PR features as the inputs to MFFN single hidden layer. These three sub-band PR features composed of theta, alpha and beta PR sub-band. Meanwhile for the outputs, the model was constructed using two output of psychometric test results, which are IQ and LS. IQ classification results gain through established IQ classification model directly using brainwaves (Jahidin, Taib, et al., 2015) and LS test results gain through Kolb's Learning Style Inventory (KLSI) (David A. Kolb, 2007). The selection of hyperbolic tangent sigmoid as activation function on hidden layer is because we wish to maximize the feature differences before proceeding to the output layer. Meanwhile, predict the selection of pure linear as activation function on output layer is because we wish to map the output to integer numbers (Zhangyang Wang, Liu, & Huang, 2019) that represent IQ and LS indexes. In addition, the epoch was limited to 1000 for training iteration to allow for best possible network model with the best performance.

In order to evaluate the optimum number of hidden neurons, modification of a constructive algorithm has been developed (M.S.A. Megat Ali, Jahidin, Taib, Tahir, et al., 2016). This constructive algorithm was merged with the constructive and pruning techniques. The optimization procedure utilizes the selection boundary between 3 hidden nodes to 15 hidden nodes. The process techniques were repeated to 40 times continuously for each cumulative single hidden node (begin by 3 hidden nodes and end by 15 hidden nodes). This approach leads the network into best average performance through varying the weight and biases (Muhammad Marwan Anoor, Jahidin, Arof, & Megat Ali, 2020).

Based on finding the best hidden neurons number through accuracy as in Figure 4.20(a), the lowest accuracy for both IQ and LS training is on 3 hidden neurons, where 61.9% for IQ and 52.2% for LS. Meanwhile the highest accuracy for both IQ and LS training on 15 hidden neurons, where 95.2% for IQ and 78.7% for LS. Based on finding the best hidden neurons number through MSE as Figure 4.20(b), the lowest error for both IQ and LS training on 15 hidden neurons, where 0.04771 for IQ and 0.20395 for LS. Meanwhile the highest accuracy for both IQ and LS training on 15 hidden neurons, where 0.38850 for IQ and 0.84186 for LS. To select the best hidden neurons number, the parameter was setup through high accuracy, where high state of being correct or precise, and low MSE, where minimum errors of average squared difference between real and estimated values. Thus, 15 hidden nodes were selected due to maximum accuracy and minimum error of both classifications. These 15 hidden neurons number avoid overfitting if hidden neurons are more than 15. In addition, this was supported that too higher hidden neurons in network can easily fit the training but not forming a good generalization (Burns & Whitesides, 1993).

In parameters setup summarization, Table 4.3 shows the MIMO MFFN architecture and the training parameters that were finalized of this model development. The table

tabulates input, output and hidden neurons that utilized for training the network through PR features. Input layer consists of 3 neurons composed of theta, alpha and beta PR sub-band obtain from Fp1 brain frontal position, while the output layer composed of two neurons, which classify IQ and LS. The single hidden layer composed of 15 neurons through constructive algorithm optimization of hidden neurons. Once, the training process completed, the neural network was saved and then, can be used to classify IQ and LS.

### **5.6.2 Performance Measures and Test Fitting**

As IQ-LS classification architecture and parameter setup which has been developed before, the network was trained repeatedly to achieve best possible performance via the selected parameter. In this section, topic will be elaborating the result of IQ evaluation performance and LS evaluation performance. Concisely, the evaluation performance based on targeting threshold and confusion matrix. The detail elaboration related to this section will be discuss in subsection below.

#### **5.6.2.1 IQ Evaluation Performance**

Based on IQ evaluation performance, the evaluation was gain via threshold mapping, accuracy, and mean square error of actual and predicted IQ levels shown in training dataset, validation dataset and testing dataset. In IQ training dataset, Figure 4.22(a) shows the mapping of actual IQ levels and predicted IQ levels before implementing threshold limit, meanwhile Figure 4.22(b) shows the mapping of actual IQ levels and predicted IQ levels after implementing threshold limit. In the first moment, the predicted IQ (\*) scattered in between threshold limits ranges is obviously shows in Figure 4.22(a). Once

the threshold limits were employed, the predicted output fits with actual output and the result clearly shows in Figure 4.22(b). This misclassification decreases accuracy and increases MSE value in training dataset.

In IQ validation dataset, Figure 4.22(c) shows the mapping of actual IQ levels and predicted IQ levels before implementing threshold limit, meanwhile Figure 4.22(d) shows the mapping of actual IQ levels and predicted IQ levels after implementing threshold limit. In the first moment, the predicted IQ (\*) scattered in between threshold limits ranges is obviously shows in Figure 4.22(c). Once the threshold limits were employed, the predicted output fit with actual output and the result clearly shows in Figure 4.22(d). However, there are misclassification obtain as indicator 2 (medium IQ) was predicted to indicator 1 (low IQ) after threshold. This misclassification decreases accuracy and increases MSE value in validation dataset.

In IQ classification dataset, Figure 4.22(e) shows the mapping of actual IQ levels and predicted IQ levels before implementing threshold limit / threshold limit was implemented, meanwhile Figure 4.22(f) shows the mapping of actual IQ levels and predicted IQ levels after implementing threshold limit. In the first moment, the predicted IQ (\*) scattered in between threshold limits ranges is obviously shows in Figure 4.22(e). Once the threshold limits were employed, the predicted output fit with actual output and the result clearly shows in Figure 4.22(f). However, there are some misclassifications obtain as indicator 2 (medium IQ) was predicted to indicator 1 (low IQ) and indicator 3 (high IQ) was predicted to indicator 2 (medium IQ) after threshold. This misclassification decreases accuracy and increases MSE value in testing dataset.

Comprehensively, to gain best generalization, training, validation and testing datasets by investigating the accuracy and minimum square error (MSE). These three datasets, the training network involved training set and validation set, meanwhile testing set used after

EEG-based IQ-LS Classification model network trained to validate network accuracy. First, training set was used to compute the gradient and adjust the weights on the neural network during training iterations. Then, validation set was used to assist training network by minimize overfitting issues and not used in adjusting the weights via minimum validation error through ES approach (Prechelt, 1998). Last but not least, testing data set was used to verify actual prediction network performance and determine the generalization error of the completed trained network using unbiased or unknown data set (C.M. Bishop, 1996; Gardner & Dorling, 1998; Polat & Güneş, 2007; Prechelt, 1998).

Subsequently, to investigate network performance measurement, the conversion to the confusion matrix is benefited through actual and predicted IQ levels mapping. In summarization, Table 4.4 shows the accuracy and minimum square error (MSE) of confusion matrix for training, validation, and testing datasets for IQ level. Based on finalized model, the accuracy in IQ level datasets presents 98.3% for training dataset, 96.0% for validation dataset and 94.7% for testing dataset. Accuracy refers to state of being correct or precise, and the values closer to 100% means good predictive model. In addition, the previous work's performance was obtained by 100% accuracy in training, 100% accuracy in validation, and 88.9% accuracy in testing (A. H. Jahidin et al., 2014). Due to non-complex algorithm, the previous work obtained high accuracy via single output classification training compared to this research, which required pruning algorithm to classify multiple output classification.

MSE can indicate dissimilarity error between the predicted observation values and the actual observation values of the model. Commonly, MSE used to estimate the prediction capability of intended models and the values of MSE closer to zero means good model classification. Meanwhile, MSE in IQ level datasets presents 0.0171 for training dataset, 0.0400 for validation dataset and 0.0533 for testing dataset. However, in previous model,

MSE error had been obtained 0.01 in training, 0.02 in validation and 0.05 in testing (A. H. Jahidin et al., 2014). There is higher MSE error in this research work compared to previous work, but the MSE error for this research work is still acceptable. Based on finalized model result, the output MSE for training considered sufficiently trained with minimum error and generalized well in testing dataset as minimum error nearest to zero (Pardo & Sberveglieri, 2002; Prechelt, 1998). Last but not least, these results were supported by previous research which states ES as an effective work to avoid overfitting and enhance accuracy and MSE performance (Gençay & Qi, 2001).

Entirely, the overall accuracy in confusion matrix is summarized in Table 4.5. Based on this table, it also shows the sensitivity and precision in each IQ group samples. The sensitivity result shows 100.0% for low IQ, 97.5% for medium IQ and 96.0% for high IQ. Sensitivity refers to evaluation of true positive predictions number by the proportion of overall positives number. In other words, it reflects the completeness of evaluation. In addition, the precision result shows 95.2% for low IQ, 96.1% for medium IQ and 100.0% for high IQ. Precision refers to evaluation of true positive predictions number by the proportion the overall positives predictions number. In other words, it reflects the exactness of evaluation. Based on overall accuracy, the accuracy was utilized to evaluate model classifier performance. Therefore, the finalized model gains 97.4% for overall accuracy and the best accuracy nearly to 100.0%. This shows a better model fit and well-trained network, with minimal error to predict distinct IQ levels.

### **5.6.2.2 LS Evaluation Performance**

Based on LS evaluation performance, the evaluation was gained via threshold mapping, accuracy, and mean square error of actual and predicted LS groups shown in training dataset, validation dataset and testing dataset. In LS training dataset, Figure

4.23(a) shows the mapping of actual LS groups and predicted LS groups before implementing threshold limit, meanwhile Figure 4.23(b) shows the mapping of actual LS groups and predicted LS groups after implementing threshold limit. In the first moment, the predicted LS (\*) scattered in between threshold limits ranges is obviously shows in Figure 4.23(a). Once the threshold limits were employed, the predicted output fit with actual output and the result clearly shows in Figure 4.23(b). However, there are misclassification obtain via empty predicted output (\*) in actual output (red box) after applying threshold limit. This misclassification decreases accuracy and increases MSE value in training dataset.

In LS validation dataset, Figure 4.23(c) shows the mapping of actual LS groups and predicted LS groups before implementing threshold limit, meanwhile Figure 4.23(d) shows the mapping of actual LS groups and predicted LS groups after implementing threshold limit. In the first moment, the predicted LS (\*) scattered in between threshold limits ranges is obviously shows in Figure 4.23(c). Once the threshold limits were employed, the predicted output fit with actual output and the result clearly shows in Figure 4.23(d). However, there are misclassification obtain via empty predicted output (\*) in actual output (red box) after applying threshold limit. This misclassification decreases accuracy and increases MSE value in validation dataset.

In LS testing dataset, Figure 4.23(e) shows the mapping of actual LS groups and predicted LS groups before implementing threshold limit, meanwhile Figure 4.23(f) shows the mapping of actual LS groups and predicted LS groups after implementing threshold limit. In the first moment, the predicted LS (\*) scattered in between threshold limited ranges is obviously shown in Figure 4.23(e). Once the threshold limits were employed, the predicted output fit with actual output and the result clearly shows in Figure 4.23(f). However, there are misclassification obtain via empty predicted output (\*) in

actual output (red box) after applying threshold limit. This misclassification decreases accuracy and increases MSE value in testing dataset.

Comprehensively, to gain best generalization, training, validation and testing datasets by investigating the accuracy and minimum square error (MSE). These three datasets, the training network involved training set and validation set, meanwhile testing set was used after EEG-based IQ-LS Classification model network trained to validate network accuracy. First, training set was used to compute the gradient and adjust the weights on the neural network during training iterations. Then, validation set was used to assist training network by minimize overfitting issues and not used in adjusting the weights via minimum validation error through ES approach (Prechelt, 1998). Last but not least, testing data set was used to verify actual prediction network performance and determine the generalization error of the completed trained network using unbiased or unknown data set (Bishop, 1996; Gardner & Dorling, 1998; Polat & Güneş, 2007; Prechelt, 1998).

Subsequently, to investigate network performance measurement, the conversion to the confusion matrix is benefited through actual and predicted LS groups mapping. In summarization, Table 4.6 shows the accuracy and minimum square error (MSE) of confusion matrix for training, validation, and testing datasets for LS groups. Based on finalized model, the accuracy in LS group datasets presents 96.9% for training dataset, 98.7% for validation dataset and 80.0% for testing dataset. Accuracy refers to state of being correct or precise, and the values closer to 100% means good predictive model. Compared to previous work, this model performance discovered 85.1% accuracy in training dataset, 91.3% accuracy in testing dataset and regardless of validation dataset result (Megat Ali, Jahidin, Taib, Tahir, et al., 2016).

MSE can indicate dissimilarity error between the predicted observation values and the actual observation values of the model. Commonly, MSE is used to estimate the



prediction capability of intended models and the values of MSE closer to zero means good model classification. MSE in LS group datasets presents 0.0314 for training dataset, 0.0133 for validation dataset and 0.0438 for testing dataset. Compared to MSE error of previous work, MSE error was 0.0995 in training dataset, 0.0901 in testing dataset and neglected validation dataset result (M.S.A. Megat Ali, Jahidin, Taib, Tahir, et al., 2016). Thus, this research performance obtained higher performance with consideration of validation dataset compared to previous work performance. Based on finalized model result, the output MSE for training considered sufficiently trained with minimum error and generalized well in testing dataset as minimum error nearest to zero (Pardo & Sberveglieri, 2002; Prechelt, 1998). Last but not least, these results was supported by previous research which states ES as an effective work to avoid overfitting and enhance accuracy and MSE performance (Gençay & Qi, 2001).

Entirely, the overall accuracy in confusion matrix is summarized in Table 4.7. Based on this table, it also shows the sensitivity and precision in each LS group samples. The sensitivity result shows 95.3% for accommodator, 99.3% for diverger, 95.0% for assimilator and 97.0% for converger. Sensitivity refers to evaluation of true positive predictions number by the proportion the overall positives number. In other words, it reflects to completeness evaluation. In addition, the precision result shows 99.3% for accommodator, 95.5% for diverger, 96.9% for assimilator and 95.1% for converger. Precision refers to evaluation of true positive predictions number by the proportion of the overall positive predictions number. In other words, it reflects to exactness of evaluation. Based on overall accuracy, the accuracy was utilized to evaluate model classifier performance. Therefore, the finalized model gains 96.8% for overall accuracy and the best accuracy nearly to 100.0%. This shows a better model fit and well-trained network, with minimal error to predict distinct LS groups.

### 5.6.3 Correlation Function Tests

In accordance to IQ correlation test evaluation, the auto correlation function test (ACF) and cross correlation function test (CCF) results were revealed based on Figure 4.24. As ACF has been observed, the maximum coefficient of ACF test is 1 at zero lag in all dataset. At the same time, all other lags are within 95% confidence limit in training and testing. However, in validation, the other lags are within 95% confidence limit except at lag 14. The ACF result support and augment these white noise auto-correlation definition, where the lags within 95% confidence limit except at zero lag (Awadz et al., 2010; Rahiman et al., 2009). Based on CCF observation, the correlation within 95% confidence limit except  $\tau = 0$  in training, validation and testing. However, in validation, the other lags are within 95% confidence limit except at lag -4. Findings indicated that the residuals were uncorrelated for all lags of actual output (Awadz et al., 2010; Rahiman et al., 2009). Entirely, the correlation tests on this model which implemented PR features as inputs showed acceptable model for practical implementation.

In accordance to LS correlation test evaluation, the auto correlation function test (ACF) and cross correlation function test (CCF) results were revealed based on Figure 4.27. As ACF has been observed, the maximum coefficient of ACF test is 1 at zero lag in all dataset. At the same time, all other lags within 95% confidence limit in training, validation and testing. The ACF result support and augment these white noise auto-correlation definition, where the lags within 95% confidence limit except at zero lag (Awadz et al., 2010; Rahiman et al., 2009). Based on CCF observation, the correlation within 95% confidence limit except  $\tau = 0$  in training and testing. However, in training, the other lags were within 95% confidence limit except at lag 7 and 12, meanwhile in validation, the other lags were within 95% confidence limit except at lag -5 and 3. In testing, entire lags within 95% confidence limit. Findings indicated that the residuals were uncorrelated for all lags of actual output (Awadz et al., 2010; Rahiman et al., 2009). Entirely, the

correlation tests on this model which implemented PR features as inputs showed acceptable model for practical implementation.

## 5.7 Summary

Final neural network performance and validation was summarized in Table 5.1 and Table 5.2 for both IQ and LS. Based on model development, the dataset size was segregated randomly into three datasets, where 350 samples (70%) was used for training, 75 samples (15%) used for validation, and the remaining 75 samples (15%) for testing (Pulini et al., 2018). Statistical data analysis using this data was supported as the cognitive ability characteristic is equivalent to previous theory. In addition, this experimental model revealed that power ratio from left frontal hemisphere can be classified into two output by using MIMO neural network where it can classify into high accuracy and low MSE. As the model was developed through high performance, this research gives positive effect on social development as matching intelligent and learning style of the individual with social environment.

**Table 5.1: Accuracy and MSE of IQ and LS through training, validation, and testing.**

IQ-LS Model		Training	Validation	Testing
Accuracy (%)	IQ	98.3	96.0	94.7
	LS	96.9	98.7	80.0
MSE	IQ	0.0171	0.0400	0.0533
	LS	0.0314	0.0133	0.0438

**Table 5.2: Precision and sensitivity of overall accuracy for each group samples.**

Title	IQ			LS			
	1	2	3	1	2	3	4
Precision (%)	95.2	96.1	100.0	99.3	95.5	96.9	95.1
Sensitivity (%)	100.0	97.5	96.0	95.3	99.3	95.0	97.0
Overall Accuracy (%)	97.4			96.8			

Universiti Malaya

## CONCLUSION

### 6.1 Conclusion

In conclusion, this thesis offers a new approach in classifying IQ-LS simultaneously based on brainwave features integrated with ANN using multiple input and output model approach for relatively more complex in cognitive abilities assessment. The study shown the succesful model classification by having the correct feature algorithm for classification model, evaluation on characterizing IQ and LS of an individual and most optimum computational model for assessing both IQ and LS.

For the first objective, the use of power ratio feature has been proposed for this research. Implementation of equiripple filters ensures that the extracted sub-band power ratio features are robust. This is important for an efficient classification model that are capable of quickly to classifying both traits. Results have shown that IQ levels and LS groups through power ratio feature analyzed in this study demonstrated the promising result as the previous studies and consistent with fundamental sub-band characteristics protocol. The research proves that specific pattern of resting theta, alpha and beta power ratio feature extraction can be observed from learning style with varying IQ levels. The results have demonstrated that the higher IQ levels lead to assimilator and converger learning style, meanwhile the lowest IQ levels lead to diverger and accommodator learning style.

Subsequently, the second objective has identified the MIMO structure of ANN as suitable for development of the model. Theta, alpha and beta ratio obtained from resting brainwave from the left prefrontal cortex as input to the ANN. Meanwhile the output from the network comprises of two nodes, each addressing the respective IQ and LS indexes. Single hidden layer has been used and the constructive algorithm was implemented to determine the optimum number of hidden nodes. Based on the analysis, a 15-hidden node

structure has shown to produce the best average training accuracy with the lowest average MSE.

For the third objective, the proposed MIMO ANN model has been proven capable of producing reliable result for classifying IQ and LS from the power ratio features. The classification model has achieved 97.4 percent for IQ and 96.8 percent for LS. In addition, the MSE in all datasets is less than 0.1 with regression coefficient of more than 0.9 for both traits of cognition. Both ACF and CCF tests have fulfilling the essential requirement, which indicates the model is adequate for practical implementation.

This potential application of classification model using the brainwave signal can solve the conventional psychometric tests which is time-consuming and exposed to bias issues and language barrier. The use of brainwaves for assessing these traits of cognition will potentially solve the limitations of the conventional assessment methods. As the classification model was developed through optimum performance, this research gives positive impact on social development as the outcome can match individual intelligence and learning style with social environment. Assessment of IQ can be analysed to understand individual education conflict, which is often associated with learning difficulties. Therefore, these can potentially be followed by appropriate remedial approaches by psychologists and educators. That means suitable level of intelligence levels enable learners to obtain the best learning environment that matches with their learning styles. Thus, these enable individuals to understand their preferences and increase awareness on the most optimum learning experience.

## 6.2 Limitations and Future Work

This proposed work has limitation capability. EEG-based IQ-LS classification model able to produce the outcome specifically for IQ and LS. However, the other aspects of various cognitive abilities and in term of medical treatment can be utilized for other models that are recommended further. In addition, this model was specifically focused on one dominant learning style, such accommodator, assimilator, converger and diverger along with fluid intelligence. Thus, integration with the combination of dominant learning style can be utilized in further model such as combination accommodator and diverger. The approach of the technique and methodology will be similar as this research, however there are increasing number of output LS classification and require numerous sample size to develop the model classification. Besides that, this essential relationship of specific EEG features with cognitive abilities provides the human brain potential by itself. Future work can be improved by extending this model with applications in teaching pedagogies, along with intelligent and learning capability advancements.

Furthermore, the present model research is restricted with approved limited sample size. However, the work repetition with huge sample population is advised to improve statistical analysis persistent of various stochastic human brainwaves. In addition, the sample selection and preparation are required via normal and healthy sample population due to control of the variable. This model research did not involve prescribed medications and abnormal subjects such ADHD, autism, epilepsy, learning and reading disabilities, brain lateralization lesions, and mental retardation. Throughout traditional method (psychometric assessment test), cognitive abilities can be achieved for clinical subjects. However, these clinical subjects have their own EEG signal pattern than normal person. The future work can be done, by collecting numerous samples of clinical subjects as the controlled variable. It is crucial for disable persons knowing their true cognitive abilities to enhance their life and improve community prevalence.

## REFERENCES

- Abásolo, D., Hornero, R., Gómez, C., García, M., & López, M. (2006). Analysis of EEG background activity in Alzheimer's disease patients with Lempel-Ziv complexity and central tendency measure. *Medical Engineering and Physics*, 28(4), 315–322. <https://doi.org/10.1016/j.medengphy.2005.07.004>
- Abdul Rashid, N., Taib, M. N., Lias, S., & Sulaiman, N. (2010). Classification of learning style based on Kolb's Learning Style Inventory and EEG using cluster analysis approach. *2010 2nd International Congress on Engineering Education: Transforming Engineering Education to Produce Quality Engineers, ICEED2010*. <https://doi.org/10.1109/ICEED.2010.5940765>
- Abdulkader, S. N., Atia, A., & Mostafa, M. S. M. (2015). Brain computer interfacing: Applications and challenges. *Egyptian Informatics Journal*. <https://doi.org/10.1016/j.eij.2015.06.002>
- Acharya, U. R., Vinitha Sree, S., Swapna, G., Martis, R. J., & Suri, J. S. (2013). Automated EEG analysis of epilepsy: A review. *Knowledge-Based Systems*. <https://doi.org/10.1016/j.knosys.2013.02.014>
- Acı, Ç. İ., Kaya, M., & Mishchenko, Y. (2019). Distinguishing mental attention states of humans via an EEG-based passive BCI using machine learning methods. *Expert Systems with Applications*, 134, 153–166. <https://doi.org/https://doi.org/10.1016/j.eswa.2019.05.057>
- Adrian, E. D., & Matthews, B. H. C. (1934). The berger rhythm: Potential changes from the occipital lobes in man. *Brain*. <https://doi.org/10.1093/brain/57.4.355>
- Adrian, E. D., & Yamagiwa, K. (1935). The origin of the berger rhythm. *Brain*. <https://doi.org/10.1093/brain/58.3.323>
- Agwu, O. E., Akpabio, J. U., Alabi, S. B., & Dosunmu, A. (2018). Artificial intelligence techniques and their applications in drilling fluid engineering: A review. *Journal of Petroleum Science and Engineering*, 167, 300–315. <https://doi.org/https://doi.org/10.1016/j.petrol.2018.04.019>
- Ahmad, A. S., Hassan, M. Y., Abdullah, M. P., Rahman, H. A., Hussin, F., Abdullah, H., & Saidur, R. (2014). A review on applications of ANN and SVM for building electrical energy consumption forecasting. *Renewable and Sustainable Energy Reviews*, 33, 102–109. <https://doi.org/10.1016/J.RSER.2014.01.069>
- Ahmadi, H., Gholamzadeh, M., Shahmoradi, L., Nilashi, M., & Rashvand, P. (2018). Diseases diagnosis using fuzzy logic methods: A systematic and meta-analysis review. *Computer Methods and Programs in Biomedicine*, 161, 145–172. <https://doi.org/https://doi.org/10.1016/j.cmpb.2018.04.013>
- Ajil, K. S., Thapliyal, P. K., Shukla, M. V., Pal, P. K., Joshi, P. C., & Navalgund, R. R. (2010). A New Technique for Temperature and Humidity Profile Retrieval From Infrared-Sounder Observations Using the Adaptive Neuro-Fuzzy Inference System. *IEEE Transactions on Geoscience and Remote Sensing*.



<https://doi.org/10.1109/TGRS.2009.2037314>

- Akobeng, A. K. (2007). Understanding diagnostic tests 1: Sensitivity, specificity and predictive values. *Acta Paediatrica, International Journal of Paediatrics*. <https://doi.org/10.1111/j.1651-2227.2006.00180.x>
- Alarabi, A., & Mishra, K. N. (2010). *Artificial Neural Network Based Technique Compare with "GA."* [https://doi.org/10.1007/978-3-642-14306-9\\_69](https://doi.org/10.1007/978-3-642-14306-9_69)
- Alazrai, R., Alwanni, H., & Daoud, M. I. (2019). EEG-based BCI system for decoding finger movements within the same hand. *Neuroscience Letters*, 698, 113–120. <https://doi.org/https://doi.org/10.1016/j.neulet.2018.12.045>
- Alharbi, N. (2018). A novel approach for noise removal and distinction of EEG recordings. *Biomedical Signal Processing and Control*, 39, 23–33. <https://doi.org/10.1016/J.BSPC.2017.07.011>
- Alizadehsani, R., Habibi, J., Hosseini, M. J., Mashayekhi, H., Boghrati, R., Ghandeharioun, A., ... Sani, Z. A. (2013). A data mining approach for diagnosis of coronary artery disease. *Computer Methods and Programs in Biomedicine*. <https://doi.org/10.1016/j.cmpb.2013.03.004>
- Almansour, N. A., Syed, H. F., Khayat, N. R., Altheeb, R. K., Juri, R. E., Alhiyafi, J., ... Olatunji, S. O. (2019). Neural network and support vector machine for the prediction of chronic kidney disease: A comparative study. *Computers in Biology and Medicine*, 109, 101–111. <https://doi.org/https://doi.org/10.1016/j.combiomed.2019.04.017>
- Alwosheel, A., van Cranenburgh, S., & Chorus, C. G. (2018). Is your dataset big enough? Sample size requirements when using artificial neural networks for discrete choice analysis. *Journal of Choice Modelling*, 28, 167–182. <https://doi.org/10.1016/J.JOCM.2018.07.002>
- Amaral, J. L. M., Lopes, A. J., Faria, A. C. D., & Melo, P. L. (2015). Machine learning algorithms and forced oscillation measurements to categorise the airway obstruction severity in chronic obstructive pulmonary disease. *Computer Methods and Programs in Biomedicine*. <https://doi.org/10.1016/j.cmpb.2014.11.002>
- Amaral, J. L. M., Lopes, A. J., Jansen, J. M., Faria, A. C. D., & Melo, P. L. (2015). An improved method of early diagnosis of smoking-induced respiratory changes using machine learning algorithms. *Computer Methods and Programs in Biomedicine*, 112(3), 441–454. <https://doi.org/10.1016/j.cmpb.2013.08.004>
- Amato, F., López, A., Peña-Méndez, E. M., Vañhara, P., Hampl, A., & Havel, J. (2013). Artificial neural networks in medical diagnosis. *Journal of Applied Biomedicine*, Vol. 11, pp. 47–58. <https://doi.org/10.2478/v10136-012-0031-x>
- Ambrose, J. (1973). Computerized transverse axial scanning (tomography): II. Clinical application. *British Journal of Radiology*. <https://doi.org/10.1259/0007-1285-46-552-1023>
- An, N., Zhao, W., Wang, J., Shang, D., & Zhao, E. (2013). Using multi-output

feedforward neural network with empirical mode decomposition based signal filtering for electricity demand forecasting. *Energy*. <https://doi.org/10.1016/j.energy.2012.10.035>

- Anderer, P., Roberts, S., Schlögl, A., Gruber, G., Klösch, G., Herrmann, W., ... Saletu, B. (1999). Artifact processing in computerized analysis of sleep EEG - A review. *Neuropsychobiology*. <https://doi.org/10.1159/000026613>
- Andreou, C., Papastavrou, E., & Merkouris, A. (2014). Learning styles and critical thinking relationship in baccalaureate nursing education: A systematic review. *Nurse Education Today*, Vol. 34, pp. 362–3371. <https://doi.org/10.1016/j.nedt.2013.06.004>
- Anokhin, A. P., Lutzenberger, W., & Birbaumer, N. (1999). Spatiotemporal organization of brain dynamics and intelligence: An EEG study in adolescents. *International Journal of Psychophysiology*. [https://doi.org/10.1016/S0167-8760\(99\)00064-1](https://doi.org/10.1016/S0167-8760(99)00064-1)
- Anokhin, A., & Vogel, F. (1996). EEG alpha rhythm frequency and intelligence in normal adults. *Intelligence*, 23(1), 1–14. [https://doi.org/10.1016/S0160-2896\(96\)80002-X](https://doi.org/10.1016/S0160-2896(96)80002-X)
- Anoor, M.M., Anwar, K. H. K., Ali, M. S. A. M., & Jahidin, A. H. (2018). Classification of students' IQ level using EEG-based intelligence classifier model. *Journal of Fundamental and Applied Sciences*, 9(5S), 684. <https://doi.org/10.4314/jfas.v9i5s.48>
- Anoor, Muhammad Marwan, Jahidin, A. H., Arof, H., & Megat Ali, M. S. A. (2020). EEG-based intelligent system for cognitive behavior classification. *Journal of Intelligent & Fuzzy Systems, Preprint*, 1–18. <https://doi.org/10.3233/JIFS-190955>
- Antanasijević, D., Pocajt, V., Perić-Grujić, A., & Ristić, M. (2018). Multiple-input–multiple-output general regression neural networks model for the simultaneous estimation of traffic-related air pollutant emissions. *Atmospheric Pollution Research*. <https://doi.org/10.1016/j.apr.2017.10.011>
- Arabasadi, Z., Khorasani, M., Akhlaghi, S., Fazilat, H., Gedde, U. W., Hedenqvist, M. S., & Shiri, M. E. (2013). Prediction and optimization of fireproofing properties of intumescent flame retardant coatings using artificial intelligence techniques. *Fire Safety Journal*, 61, 193–199. <https://doi.org/https://doi.org/10.1016/j.firesaf.2013.09.006>
- Awadz, F., Yassin, I. M., Rahiman, M. H. F., Taib, M. N., Zabidi, A., & Hassan, H. A. (2010). System identification of essential oil extraction system using Non-Linear Autoregressive Model with Exogenous Inputs (NARX). *2010 IEEE Control and System Graduate Research Colloquium (ICSGRC 2010)*, 20–25. <https://doi.org/10.1109/ICSGRC.2010.5562527>
- Azami, H., Mohammadi, K., & Bozorgtabar, B. (2012). An Improved Signal Segmentation Using Moving Average and Savitzky-Golay Filter. *Journal of Signal and Information Processing*. <https://doi.org/10.4236/jsip.2012.31006>
- Azar, A. T. (2013). Fast neural network learning algorithms for medical applications. *Neural Computing and Applications*, 23(3–4), 1019–1034. <https://doi.org/10.1007/s00521-012-1026-y>

- Ba, L. J., & Caruana, R. (2014). Do deep nets really need to be deep? *Proceedings of the 27th International Conference on Neural Information Processing Systems - Volume 2*, pp. 2654–2662. Retrieved from <https://dl.acm.org/citation.cfm?id=2969123>
- Babusiak, B., Borik, S., & Balogova, L. (2018). Textile electrodes in capacitive signal sensing applications. *Measurement*, *114*, 69–77. <https://doi.org/10.1016/J.MEASUREMENT.2017.09.024>
- Barnichon, R., & Matthes, C. (2018). Functional Approximation of Impulse Responses. *Journal of Monetary Economics*, *99*, 41–55. <https://doi.org/https://doi.org/10.1016/j.jmoneco.2018.04.013>
- Bartholow, B. D. (2018). The aggressive brain: insights from neuroscience. *Current Opinion in Psychology*, *19*, 60–64. <https://doi.org/10.1016/j.copsyc.2017.04.002>
- Barwick, D. D. (1971). Hans Berger on the electroencephalogram of man. The fourteen original reports on the human electroencephalogram. *Journal of the Neurological Sciences*. [https://doi.org/10.1016/0013-4694\(69\)91207-3](https://doi.org/10.1016/0013-4694(69)91207-3)
- Bastiaansen, M., Straatman, S., Driessen, E., Mitas, O., Stekelenburg, J., & Wang, L. (2018). My destination in your brain: A novel neuromarketing approach for evaluating the effectiveness of destination marketing. *Journal of Destination Marketing & Management*, *7*, 76–88. <https://doi.org/https://doi.org/10.1016/j.jdmm.2016.09.003>
- Bautu, A., & Breaban, M. E. (2015). On meta-heuristics in optimization and data analysis. Application to geosciences. In *Artificial Intelligent Approaches in Petroleum Geosciences*. [https://doi.org/10.1007/978-3-319-16531-8\\_2](https://doi.org/10.1007/978-3-319-16531-8_2)
- Belciug, S., & Gorunescu, F. (2018). Learning a single-hidden layer feedforward neural network using a rank correlation-based strategy with application to high dimensional gene expression and proteomic spectra datasets in cancer detection. *Journal of Biomedical Informatics*. <https://doi.org/10.1016/j.jbi.2018.06.003>
- Benedek, M., & Fink, A. (2019). Neuroscience: EEG. In *Reference Module in Neuroscience and Biobehavioral Psychology*. <https://doi.org/https://doi.org/10.1016/B978-0-12-809324-5.23685-7>
- Bettus, G., Wendling, F., Guye, M., Valton, L., Régis, J., Chauvel, P., & Bartolomei, F. (2008). Enhanced EEG functional connectivity in mesial temporal lobe epilepsy. *Epilepsy Research*. <https://doi.org/10.1016/j.eplesyres.2008.04.020>
- Bhattacharyya, A., & Pachori, R. B. (2017). A Multivariate Approach for Patient-Specific EEG Seizure Detection Using Empirical Wavelet Transform. *IEEE Transactions on Biomedical Engineering*. <https://doi.org/10.1109/TBME.2017.2650259>
- Billings, S. A., Jamaluddin, H. B., & Chen, S. (1992). Properties of neural networks with applications to modelling non-linear dynamical systems. *International Journal of Control*, *55*(1), 193–224. <https://doi.org/10.1080/00207179208934232>
- Birney, D. P., Beckmann, J. F., Beckmann, N., & Double, K. S. (2017). Beyond the intellect: Complexity and learning trajectories in Raven's Progressive Matrices

depend on self-regulatory processes and conative dispositions. *Intelligence*, 61, 63–77. <https://doi.org/10.1016/J.INTELL.2017.01.005>

Bishop, C.M. (1996). Neural networks: a pattern recognition perspective. *Neural Networks*. <https://doi.org/10.1.1.46.8742>

Bishop, Chris M. (1994). Neural networks and their applications. *Review of Scientific Instruments*. <https://doi.org/10.1063/1.1144830>

Blair, C., Gamson, D., Thorne, S., & Baker, D. (2005). Rising mean IQ: Cognitive demand of mathematics education for young children, population exposure to formal schooling, and the neurobiology of the prefrontal cortex. *Intelligence*, 33(1), 93–106. <https://doi.org/10.1016/j.intell.2004.07.008>

Blume, C., Lechinger, J., del Giudice, R., Wislowska, M., Heib, D. P. J., & Schabus, M. (2015). EEG oscillations reflect the complexity of social interactions in a non-verbal social cognition task using animated triangles. *Neuropsychologia*, 75, 330–340. <https://doi.org/https://doi.org/10.1016/j.neuropsychologia.2015.06.009>

Boonyakitanont, P., Lek-uthai, A., Chomtho, K., & Songsiri, J. (2020). A review of feature extraction and performance evaluation in epileptic seizure detection using EEG. *Biomedical Signal Processing and Control*, 57, 101702. <https://doi.org/https://doi.org/10.1016/j.bspc.2019.101702>

Brouwers, S. A., Van de Vijver, F. J. R., & Van Hemert, D. A. (2009). Variation in Raven's Progressive Matrices scores across time and place. *Learning and Individual Differences*, 19(3), 330–338. <https://doi.org/10.1016/j.lindif.2008.10.006>

Bunge, S. A., & Kahn, I. (2010). Cognition: An Overview of Neuroimaging Techniques. In *Encyclopedia of Neuroscience* (pp. 1063–1067). <https://doi.org/10.1016/B978-008045046-9.00298-9>

Burns, J. A., & Whitesides, G. M. (1993). Feed-Forward Neural Networks in Chemistry: Mathematical Systems for Classification and Pattern Recognition. *Chemical Reviews*. <https://doi.org/10.1021/cr00024a001>

Busato, V. V., Prins, F. J., Elshout, J. J., & Hamaker, C. (2000). Intellectual ability, learning style, personality, achievement motivation and academic success of psychology students in higher education. *Personality and Individual Differences*, 29(6), 1057–1068. [https://doi.org/10.1016/S0191-8869\(99\)00253-6](https://doi.org/10.1016/S0191-8869(99)00253-6)

Buscema, P. M., Massini, G., Breda, M., Lodwick, W. A., Newman, F., & Asadi-Zeydabadi, M. (2018). Artificial neural networks. In *Studies in Systems, Decision and Control* (Vol. 131, pp. 11–35). [https://doi.org/10.1007/978-3-319-75049-1\\_2](https://doi.org/10.1007/978-3-319-75049-1_2)

Buxton, R. B. (2002). Introduction to Functional Magnetic Resonance Imaging: Principles and Techniques. *Energy*. <https://doi.org/10.1017/CBO9780511605505>

Cabeza, R., Nyberg, L., & Park, D. (2016). *Cognitive neuroscience of aging: Linking cognitive and cerebral aging*. Retrieved from <https://books.google.com/books?hl=en&lr=&id=31PjDQAAQBAJ&oi=fnd&pg=PP1&dq=cognitive+abilities+neuroscience&ots=weQbuay3JX&sig=F->

- Cagiltay, N. E. (2008). Using learning styles theory in engineering education. *European Journal of Engineering Education*, 33(4), 415–424. <https://doi.org/10.1080/03043790802253541>
- Caldwell, J. H. (2010). Action Potential Initiation and Conduction in Axons. In *Encyclopedia of Neuroscience* (pp. 23–29). <https://doi.org/10.1016/B978-008045046-9.01642-9>
- Callegari, S., & Bizzarri, F. (2015). Optimal design of the noise transfer function of  $\Delta\Sigma$  modulators: IIR strategies, FIR strategies, FIR strategies with preassigned poles. *Signal Processing*, 114, 117–130. <https://doi.org/https://doi.org/10.1016/j.sigpro.2015.02.001>
- Campisi, P., La Rocca, D., & Scarano, G. (2012). EEG for automatic person recognition. *Computer*. <https://doi.org/10.1109/MC.2012.233>
- Cannon, J. A., Krokhmal, P. A., Lenth, R. V., & Murphey, R. (2010). An algorithm for online detection of temporal changes in operator cognitive state using real-time psychophysiological data. *Biomedical Signal Processing and Control*. <https://doi.org/10.1016/j.bspc.2010.03.005>
- Cassidy, S. (2004). Learning styles: An overview of theories, models, and measures. *Educational Psychology*, Vol. 24, pp. 419–444. <https://doi.org/10.1080/0144341042000228834>
- Casson, A. J., Yates, D. C., Smith, S. J. M., Duncan, J. S., & Rodriguez-Villegas, E. (2010). Wearable electroencephalography. *IEEE Engineering in Medicine and Biology Magazine*, 29(3), 44–56. <https://doi.org/10.1109/MEMB.2010.936545>
- Cattell, R. B. (1963). Theory of fluid and crystallized intelligence: A critical experiment. *Journal of Educational Psychology*. <https://doi.org/10.1037/h0046743>
- Cestari, D. M., & Rosa, J. L. G. (2017). Stochastic and deterministic stationarity analysis of EEG data. *2017 International Joint Conference on Neural Networks (IJCNN)*, 63–70. <https://doi.org/10.1109/IJCNN.2017.7965837>
- Cha, K.-M., & Lee, H.-C. (2019). A novel qEEG measure of teamwork for human error analysis: An EEG hyperscanning study. *Nuclear Engineering and Technology*, 51(3), 683–691. <https://doi.org/https://doi.org/10.1016/j.net.2018.11.009>
- Chan, C. K. Y. (2012). Exploring an experiential learning project through Kolb's Learning Theory using a qualitative research method. *European Journal of Engineering Education*. <https://doi.org/10.1080/03043797.2012.706596>
- Chang, F. J., Chiang, Y. M., & Chang, L. C. (2007). Multi-step-ahead neural networks for flood forecasting. *Hydrological Sciences Journal*. <https://doi.org/10.1623/hysj.52.1.114>
- Chaparro, L. F., & Akan, A. (2019). Chapter 1 - Continuous-Time Signals. In L. F. Chaparro & A. Akan (Eds.), *Signals and Systems Using MATLAB (Third Edition)*

(Third Edit, pp. 59–114). <https://doi.org/https://doi.org/10.1016/B978-0-12-814204-2.00011-9>

- Chaudhari, D., & Patil, P. (2015). Emerging Neurosky Mind-Wave Bci System To Perceive Detection. *International Journal of Advances in Electronics and Computer Science*.
- Chen, D. S., & Jain, R. C. (1994). A Robust Back Propagation Learning Algorithm for Function Approximation. *IEEE Transactions on Neural Networks*. <https://doi.org/10.1109/72.286917>
- Chen, S., & Billings, S. A. (1992). Neural networks for nonlinear dynamic system modelling and identification. *International Journal of Control*. <https://doi.org/10.1080/00207179208934317>
- Chen, S. H., Jakeman, A. J., & Norton, J. P. (2008). Artificial Intelligence techniques: An introduction to their use for modelling environmental systems. *Mathematics and Computers in Simulation*. <https://doi.org/10.1016/j.matcom.2008.01.028>
- Chi, Y. M., Jung, T. P., & Cauwenberghs, G. (2010). Dry-contact and noncontact biopotential electrodes: Methodological review. *IEEE Reviews in Biomedical Engineering*. <https://doi.org/10.1109/RBME.2010.2084078>
- Chuang, C. C., Su, S. F., & Hsiao, C. C. (2000). The Annealing Robust Backpropagation (ARBP) learning algorithm. *IEEE Transactions on Neural Networks*. <https://doi.org/10.1109/72.870040>
- Çiçek, M., & Nalçac, E. (2001). Interhemispheric asymmetry of EEG alpha activity at rest and during the Wisconsin Card Sorting Test: relations with performance. *Biological Psychology*. [https://doi.org/10.1016/S0301-0511\(01\)00103-X](https://doi.org/10.1016/S0301-0511(01)00103-X)
- Clark, D. L., Boutros, N. N., & Mendez, M. F. (2010). *The Brain and Behavior*. <https://doi.org/10.1017/CBO9780511776915>
- Coffield, F., Moseley, D., Hall, E., & Ecclestone, K. (2004). Learning styles and pedagogy in post-16 learning A systematic and critical review. *Learning and Skills Research Centre*. [https://doi.org/10.1016/S0022-5371\(81\)90483-7](https://doi.org/10.1016/S0022-5371(81)90483-7)
- Cohen, M. X. (2017a). Where Does EEG Come From and What Does It Mean? *Trends in Neurosciences*, 40(4), 208–218. <https://doi.org/10.1016/J.TINS.2017.02.004>
- Cohen, M. X. (2017b). Where Does EEG Come From and What Does It Mean? *Trends in Neurosciences*, 40(4), 208–218. <https://doi.org/10.1016/J.TINS.2017.02.004>
- Cohen, M. X. (2017c, April 1). Where Does EEG Come From and What Does It Mean? *Trends in Neurosciences*, Vol. 40, pp. 208–218. <https://doi.org/10.1016/j.tins.2017.02.004>
- Colom, R., Karama, S., Jung, R. E., & Haier, R. J. (2010). Human intelligence and brain networks. *Dialogues in Clinical Neuroscience*, 12(4), 489–501. Retrieved from <http://www.ncbi.nlm.nih.gov/pubmed/21319494><http://www.pubmedcentral.nih.gov/articlerender.fcgi?artid=PMC3181994>

- Colucciello, M. L. (1999). Relationships between critical thinking dispositions and learning styles. *Journal of Professional Nursing*, 15(5), 294–301. [https://doi.org/10.1016/S8755-7223\(99\)80055-6](https://doi.org/10.1016/S8755-7223(99)80055-6)
- Corballis, P. M. (2003). Visuospatial processing and the right-hemisphere interpreter. *Brain and Cognition*, Vol. 53, pp. 171–176. [https://doi.org/10.1016/S0278-2626\(03\)00103-9](https://doi.org/10.1016/S0278-2626(03)00103-9)
- Craddock, M., Poliakoff, E., El-dereby, W., Klepousniotou, E., & Lloyd, D. M. (2017). Pre-stimulus alpha oscillations over somatosensory cortex predict tactile misperceptions. *Neuropsychologia*. <https://doi.org/10.1016/j.neuropsychologia.2016.12.030>
- Crawford, J. R., Allan, K. M., Stephen, D. W., Parker, D. M., & Besson, J. A. O. (1989). The Wechsler adult intelligence scale-Revised (WAIS-R): factor structure in a U.K. sample. *Personality and Individual Differences*, 10(11), 1209–1212. [https://doi.org/10.1016/0191-8869\(89\)90091-3](https://doi.org/10.1016/0191-8869(89)90091-3)
- Croft, R. J., & Barry, R. J. (2000). Removal of ocular artifact from the EEG: A review. *Neurophysiologie Clinique*. [https://doi.org/10.1016/S0987-7053\(00\)00055-1](https://doi.org/10.1016/S0987-7053(00)00055-1)
- Cybenko, G. (1989). Approximation by Superpositions of Sigmoidal Function. *Mathematics of Control, Signals and Systems*. <https://doi.org/10.1007/BF02836480>
- Dande, P., & Samant, P. (2018). Acquaintance to Artificial Neural Networks and use of artificial intelligence as a diagnostic tool for tuberculosis: A review. *Tuberculosis*, 108, 1–9. <https://doi.org/10.1016/j.tube.2017.09.006>
- Davidson, R. J., Chapman, J. P., Chapman, L. J., & Henriques, J. B. (1990). Asymmetrical Brain Electrical Activity Discriminates Between Psychometrically-Matched Verbal and Spatial Cognitive Tasks. *Psychophysiology*, 27(5), 528–543. <https://doi.org/10.1111/j.1469-8986.1990.tb01970.x>
- Deary, I. J. (2001). Human intelligence differences: Towards a combined experimental-differential approach. *Trends in Cognitive Sciences*, Vol. 5, pp. 164–170. [https://doi.org/10.1016/S1364-6613\(00\)01623-5](https://doi.org/10.1016/S1364-6613(00)01623-5)
- Deary, I. J., Penke, L., & Johnson, W. (2010). The neuroscience of human intelligence differences. *Nature Reviews Neuroscience*, Vol. 11, pp. 201–211. <https://doi.org/10.1038/nrn2793>
- Debener, S., Beauducel, A., Nessler, D., Brocke, B., Heilemann, H., & Kayser, J. (2000). Is resting anterior EEG alpha asymmetry a trait marker for depression? Findings for healthy adults and clinically depressed patients. *Neuropsychobiology*. <https://doi.org/10.1159/000026630>
- Dehn, M. J. (2017). How working memory enables fluid reasoning. *Applied Neuropsychology: Child*, 6(3), 245–247. <https://doi.org/10.1080/21622965.2017.1317490>
- DellaBadia, J., Bell, W. L., Keyes, J. W., Mathews, V. P., & Glazier, S. S. (2002). Assessment and cost comparison of sleep-deprived EEG, MRI and PET in the

prediction of surgical treatment for epilepsy. *Seizure*, 11(5), 303–309.  
<https://doi.org/10.1053/seiz.2001.0648>

Demuth, H., Beale, M., & MathWorks, I. (1998). *Neural Network Toolbox for Use with MATLAB: User's Guide*. Retrieved from <https://books.google.com.my/books?id=WzwynQEACAAJ>

Demuth, H., & Raele, M. H. (2009). Neural Network Toolbox User's Guide For Use with MATLAB. *The MathWorks*. <https://doi.org/10.1016/j.neunet.2005.10.002>

Deng, X., Liu, Q., Deng, Y., & Mahadevan, S. (2016). An improved method to construct basic probability assignment based on the confusion matrix for classification problem. *Information Sciences*, 340–341, 250–261.  
<https://doi.org/https://doi.org/10.1016/j.ins.2016.01.033>

Dias, G. P., Palmer, S., O'Riordan, S., de Freitas, S. B., Habib, L. R., Bevilaqua, M. C. do N., & Nardi, A. E. (2015). Perspectives and challenges for the study of brain responses to coaching: Enhancing the dialogue between the fields of neuroscience and coaching psychology. *The Coaching Psychologist*, 11(1), 11–19.

Diseth, Å. (2002). The Relationship between Intelligence, Approaches to Learning and Academic Achievement. *Scandinavian Journal of Educational Research*, 46(2), 219–230. <https://doi.org/10.1080/00313830220142218>

Dockree, P. M., Kelly, S. P., Foxe, J. J., Reilly, R. B., & Robertson, I. H. (2007). Optimal sustained attention is linked to the spectral content of background EEG activity: Greater ongoing tonic alpha (~10 Hz) power supports successful phasic goal activation. *European Journal of Neuroscience*, 25(3), 900–907.  
<https://doi.org/10.1111/j.1460-9568.2007.05324.x>

Doppelmayr, M., Klimesch, W., Stadler, W., Pöllhuber, D., & Heine, C. (2002). EEG alpha power and intelligence. *Intelligence*, 30(3), 289–302.  
[https://doi.org/10.1016/S0160-2896\(01\)00101-5](https://doi.org/10.1016/S0160-2896(01)00101-5)

Doppelmayr, Michael, Klimesch, W., Sauseng, P., Hödlmoser, K., Stadler, W., & Hanslmayr, S. (2005). Intelligence related differences in EEG-bandpower. *Neuroscience Letters*, 381(3), 309–313.  
<https://doi.org/10.1016/j.neulet.2005.02.037>

Duckworth, A. L., & Yeager, D. S. (2015). Measurement Matters. *Educational Researcher*, 44(4), 237–251. <https://doi.org/10.3102/0013189X15584327>

Duff, A. (2004). A note on the problem solving style questionnaire: An alternative to Kolb's learning style inventory? *Educational Psychology*, 24(5), 699–709.  
<https://doi.org/10.1080/0144341042000262999>

Duncan, J., Chylinski, D., Mitchell, D. J., & Bhandari, A. (2017). Complexity and compositionality in fluid intelligence. *Proceedings of the National Academy of Sciences*, 114(20), 5295–5299. <https://doi.org/10.1073/pnas.1621147114>

Duncan, J., Emslie, H., Williams, P., Johnson, R., & Freer, C. (1996). Intelligence and the Frontal Lobe: The Organization of Goal-Directed Behavior. *Cognitive*



- Duncan, J., Seitz, R. J., Kolodny, J., Bor, D., Herzog, H., Ahmed, A., ... Emslie, H. (2000). A Neural Basis for General Intelligence. *Science*, 289(5478), 457–460. <https://doi.org/10.1126/science.289.5478.457>
- Duta, M., Alford, C., Wilson, S., & Tarassenko, L. (2004). Neural network analysis of the mastoid EEG for the assessment of vigilance. *International Journal of Human-Computer Interaction*. [https://doi.org/10.1207/s15327590ijhc1702\\_4](https://doi.org/10.1207/s15327590ijhc1702_4)
- Ebrahimzadeh, A., & Khazaei, A. (2010). Detection of premature ventricular contractions using MLP neural networks: A comparative study. *Measurement: Journal of the International Measurement Confederation*, 43(1), 103–112. <https://doi.org/10.1016/j.measurement.2009.07.002>
- Eddy, J. K., & Glass, A. L. (1981). Reading and listening to high and low imagery sentences. *Journal of Verbal Learning and Verbal Behavior*, 20(3), 333–345. [https://doi.org/10.1016/S0022-5371\(81\)90483-7](https://doi.org/10.1016/S0022-5371(81)90483-7)
- Entekhabi, E., Nazarpak, M. H., Sedighi, M., & Kazemzadeh, A. (2020). Predicting degradation rate of genipin cross-linked gelatin scaffolds with machine learning. *Materials Science and Engineering: C*, 107, 110362. <https://doi.org/https://doi.org/10.1016/j.msec.2019.110362>
- Erickson, B., Truelove-Hill, M., Oh, Y., Anderson, J., Zhang, F. (Zoe), & Kounios, J. (2018). Resting-state brain oscillations predict trait-like cognitive styles. *Neuropsychologia*, 120, 1–8. <https://doi.org/https://doi.org/10.1016/j.neuropsychologia.2018.09.014>
- Faisal, T., Ibrahim, F., & Taib, M. N. (2010). A noninvasive intelligent approach for predicting the risk in dengue patients. *Expert Systems with Applications*, 37(3), 2175–2181. <https://doi.org/10.1016/j.eswa.2009.07.060>
- Fatoorechi, M., Parkinson, J., Prance, R. J., Prance, H., Seth, A. K., & Schwartzman, D. J. (2015). A comparative study of electrical potential sensors and Ag/AgCl electrodes for characterising spontaneous and event related electroencephalogram signals. *Journal of Neuroscience Methods*, 251, 7–16. <https://doi.org/https://doi.org/10.1016/j.jneumeth.2015.04.013>
- Fatourech, M., Bashashati, A., Ward, R. K., & Birch, G. E. (2007). EMG and EOG artifacts in brain computer interface systems: A survey. *Clinical Neurophysiology*. <https://doi.org/10.1016/j.clinph.2006.10.019>
- Felder, R. M. (1988). Learning and Teaching Styles In Engineering Education (updated 2002). *Engineering Education*, 78(June), 674–681. <https://doi.org/10.1109/FIE.2008.4720326>
- Ferda, J., Ferdová, E., Hes, O., Mraček, J., Kreuzberg, B., & Baxa, J. (2017). PET/MRI: Multiparametric imaging of brain tumors. *European Journal of Radiology*, 94, A14–A25. <https://doi.org/10.1016/J.EJRAD.2017.02.034>
- Fernandez de Canete, J., Gonzalez-Perez, S., & Ramos-Diaz, J. C. (2012). Artificial

neural networks for closed loop control of in silico and ad hoc type 1 diabetes. *Computer Methods and Programs in Biomedicine*.  
<https://doi.org/10.1016/j.cmpb.2011.11.006>

Ferree, T. C., Luu, P., Russell, G. S., & Tucker, D. M. (2001). Scalp electrode impedance, infection risk, and EEG data quality. *Clinical Neurophysiology*, 112(3), 536–544.  
[https://doi.org/10.1016/S1388-2457\(00\)00533-2](https://doi.org/10.1016/S1388-2457(00)00533-2)

Fidelman, U. (1999). Neural transmission-errors, cerebral arousability and hemisphericity. *Kybernetes*, 28(6/7), 695–725.  
<https://doi.org/10.1108/03684929910282962>

Fink, A., Grabner, R. H., Benedek, M., Reishofer, G., Hauswirth, V., Fally, M., ... Neubauer, A. C. (2009). The creative brain: Investigation of brain activity during creative problem solving by means of EEG and fMRI. *Human Brain Mapping*, 30(3), 734–748. <https://doi.org/10.1002/hbm.20538>

Fogel, D. B. (1995). Review of Computational Intelligence: Imitating Life [Book Reviews]. *Proceedings of the IEEE*, 83(11), 1588–1592.  
<https://doi.org/10.1109/JPROC.1995.481636>

Fonseca, C., Silva Cunha, J. P., Martins, R. E., Ferreira, V. M., Marques De Sá, J. P., Barbosa, M. A., & Martins Da Silva, A. (2007). A novel dry active electrode for EEG recording. *IEEE Transactions on Biomedical Engineering*.  
<https://doi.org/10.1109/TBME.2006.884649>

Gajic, D., Djurovic, Z., Di Gennaro, S., & Gustafsson, F. (2014). Classification of EEG Signals for Detection of Epileptic Seizures Based on Wavelets and Statistical Pattern Recognition. *Biomedical Engineering: Applications, Basis and Communications*, 26(02), 1450021. <https://doi.org/10.4015/S1016237214500215>

Gardner, M. W., & Dorling, S. R. (1998). Artificial neural networks (the multilayer perceptron) - a review of applications in the atmospheric sciences. *Atmospheric Environment*. [https://doi.org/10.1016/S1352-2310\(97\)00447-0](https://doi.org/10.1016/S1352-2310(97)00447-0)

Gareta, R., Romeo, L. M., & Gil, A. (2006). Forecasting of electricity prices with neural networks. *Energy Conversion and Management*.  
<https://doi.org/10.1016/j.enconman.2005.10.010>

Gass, S. I. (1983). Decision-Aiding Models: Validation, Assessment, and Related Issues for Policy Analysis. *Operations Research*. <https://doi.org/10.1287/opre.31.4.603>

Gass, W. S., Tarrant, R. T., Pawate, B. I., Gammel, M., Rajasekaran, P. K., Wiggins, R. H., & Covington, C. D. (1987). Multiple digital signal processor environment for intelligent signal processing. *Proceedings of the IEEE*, 75(9), 1246–1259.  
<https://doi.org/10.1109/PROC.1987.13877>

Gençay, R., & Qi, M. (2001). Pricing and hedging derivative securities with neural networks: Bayesian regularization, early stopping, and bagging. *IEEE Transactions on Neural Networks*, 12(4), 726–734. <https://doi.org/10.1109/72.935086>

Genovese, C. R., Lazar, N. A., & Nichols, T. (2002). Thresholding of statistical maps in

functional neuroimaging using the false discovery rate. *NeuroImage*.  
<https://doi.org/10.1006/nimg.2001.1037>

Gevins, A. (2000). Neurophysiological Measures of Working Memory and Individual Differences in Cognitive Ability and Cognitive Style. *Cerebral Cortex*.  
<https://doi.org/10.1093/cercor/10.9.829>

Ghaedi, A. (2015). Simultaneous prediction of the thermodynamic properties of aqueous solution of ethylene glycol monoethyl ether using artificial neural network. *Journal of Molecular Liquids*. <https://doi.org/10.1016/j.molliq.2015.04.015>

Ghani, U., Wasim, M., Khan, U. S., Mubasher Saleem, M., Hassan, A., Rashid, N., ... Kashif, A. (2018). Efficient FIR Filter Implementations for Multichannel BCIs Using Xilinx System Generator. *BioMed Research International*, 2018.  
<https://doi.org/10.1155/2018/9861350>

Ghritlahre, H. K., & Prasad, R. K. (2018). Application of ANN technique to predict the performance of solar collector systems - A review. *Renewable and Sustainable Energy Reviews*, 84, 75–88.  
<https://doi.org/https://doi.org/10.1016/j.rser.2018.01.001>

Göksu, H. (2018). EEG based epileptiform pattern recognition inside and outside the seizure states. *Biomedical Signal Processing and Control*, 43, 204–215.  
<https://doi.org/https://doi.org/10.1016/j.bspc.2018.03.004>

Golnar-Nik, P., Farashi, S., & Safari, M.-S. (2019). The application of EEG power for the prediction and interpretation of consumer decision-making: A neuromarketing study. *Physiology & Behavior*, 207, 90–98.  
<https://doi.org/https://doi.org/10.1016/j.physbeh.2019.04.025>

Goodman, R. N., Rietschel, J. C., Lo, L. C., Costanzo, M. E., & Hatfield, B. D. (2013). Stress, emotion regulation and cognitive performance: The predictive contributions of trait and state relative frontal EEG alpha asymmetry. *International Journal of Psychophysiology*. <https://doi.org/10.1016/j.ijpsycho.2012.09.008>

Goodwin, G. M., Holmes, E. A., Andersson, E., Browning, M., Jones, A., Lass-Hennemann, J., ... Visser, R. M. (2018). From neuroscience to evidence based psychological treatments – The promise and the challenge, ECNP March 2016, Nice, France. *European Neuropsychopharmacology*, 28(2), 317–333.  
<https://doi.org/10.1016/j.euroneuro.2017.10.036>

Gordan, M., Razak, H. A., Ismail, Z., & Ghaedi, K. (2017). Recent developments in damage identification of structures using data mining. *Latin American Journal of Solids and Structures*. <https://doi.org/10.1590/1679-78254378>

Gotlib, I. H., Ranganath, C., & Rosenfeld, J. P. (1998). Frontal EEG Alpha Asymmetry, Depression, and Cognitive Functioning. *Cognition and Emotion*.  
<https://doi.org/10.1080/026999398379673>

Grasha, T., Claxton, C. S., & Murrell, P. H. (2006). Learning Styles: Implications for Improving Educational Practices. *Teaching Sociology*, 17(2), 254.  
<https://doi.org/10.2307/1317484>

- Gray, J. R., Chabris, C. F., & Braver, T. S. (2003). Neural mechanisms of general fluid intelligence. *Nature Neuroscience*, 6(3), 316–322. <https://doi.org/10.1038/nn1014>
- Gray, J. R., & Thompson, P. M. (2004). Neurobiology of intelligence: science and ethics. *Nature Reviews Neuroscience*, 5(6), 471–482. <https://doi.org/10.1038/nrn1405>
- Grey, S., Williams, J. N., & Rebuschat, P. (2015). Individual differences in incidental language learning: Phonological working memory, learning styles, and personality. *Learning and Individual Differences*, 38, 44–53. <https://doi.org/10.1016/j.lindif.2015.01.019>
- Grozea, C., Voinescu, C. D., & Fazli, S. (2011). Bristle-sensors - Low-cost flexible passive dry EEG electrodes for neurofeedback and BCI applications. *Journal of Neural Engineering*. <https://doi.org/10.1088/1741-2560/8/2/025008>
- Guger, C., Krausz, G., Allison, B. Z., & Edlinger, G. (2012). Comparison of dry and gel based electrodes for P300 brain-computer interfaces. *Frontiers in Neuroscience*. <https://doi.org/10.3389/fnins.2012.00060>
- Gundlich, B., Musmann, P., Weber, S., Nix, O., & Semmler, W. (2006). From 2D PET to 3D PET: Issues of Data Representation and Image Reconstruction. *Zeitschrift Für Medizinische Physik*, 16(1), 31–46. <https://doi.org/10.1078/0939-3889-00290>
- Güven, A., Günal, A. Y., & Günal, M. (2017). Multi-output neural networks for estimation of synthetic unit hydrograph parameters: A case study of a catchment in Turkey. *Acta Physica Polonica A*, 132(3), 591–594. <https://doi.org/10.12693/APhysPolA.132.591>
- Gyeong, J. A., & Myung, S. Y. (2008). Critical thinking and learning styles of nursing students at the Baccalaureate nursing program in Korea. *Contemporary Nurse*, 29(1), 100–109. Retrieved from <http://www.ncbi.nlm.nih.gov/pubmed/18844547>
- Hagan, M. T., Demuth, H. B., & Beale, M. H. (2014). Neural Network Design. *Boston Massachusetts PWS*. <https://doi.org/10.1007/1-84628-303-5>
- Hagan, M. T., & Menhaj, M. B. (1994). Training Feedforward Networks with the Marquardt Algorithm. *IEEE Transactions on Neural Networks*, 5(6), 989–993. <https://doi.org/10.1109/72.329697>
- Haier, R. J., Siegel, B. V., Nuechterlein, K. H., Hazlett, E., Wu, J. C., Paek, J., ... Buchsbaum, M. S. (1988). Cortical glucose metabolic rate correlates of abstract reasoning and attention studied with positron emission tomography. *Intelligence*, 12(2), 199–217. [https://doi.org/10.1016/0160-2896\(88\)90016-5](https://doi.org/10.1016/0160-2896(88)90016-5)
- Haler, R. J., Siegel, B., Tang, C., Abel, L., & Buchsbaum, M. S. (1992). Intelligence and Changes in Regional Cerebral Glucose Metabolic Rate Following Learning. *INTELLIGENCE*, 16, 415–426. [https://doi.org/10.1016/0160-2896\(92\)90018-M](https://doi.org/10.1016/0160-2896(92)90018-M)
- Hamada, M., & Hassan, M. (2017). An enhanced learning style index: Implementation and integration into an intelligent and adaptive e-Learning system. *Eurasia Journal of Mathematics, Science and Technology Education*, 13(8), 4449–4470. <https://doi.org/10.12973/eurasia.2017.00940a>

- Hanslmayr, S., Sauseng, P., Doppelmayr, M., Schabus, M., & Klimesch, W. (2005). Increasing individual upper alpha power by neurofeedback improves cognitive performance in human subjects. *Applied Psychophysiology Biofeedback*. <https://doi.org/10.1007/s10484-005-2169-8>
- Hara, J. H., Wu, A., Villanueva-Meyer, J. E., Valdes, G., Daggubati, V., Mueller, S., ... Raleigh, D. R. (2018). Clinical applications of quantitative three-dimensional MRI analysis for pediatric embryonal brain tumors. *International Journal of Radiation Oncology\*Biophysics\*Physics*. <https://doi.org/10.1016/J.IJROBP.2018.05.077>
- Harmony, T., Fernández, T., Silva, J., Bernal, J., Díaz-Comas, L., Reyes, A., ... Rodríguez, M. (1996). EEG delta activity: An indicator of attention to internal processing during performance of mental tasks. *International Journal of Psychophysiology*. [https://doi.org/10.1016/S0167-8760\(96\)00053-0](https://doi.org/10.1016/S0167-8760(96)00053-0)
- Haykin, S. (2005). Neural networks: a comprehensive foundation. In *The Knowledge Engineering Review*. <https://doi.org/10.1017/S0269888998214044>
- Haykin, S., & Kosko, B. (1998a). Special Issue on Intelligent Signal Processing. *Proceedings of the IEEE*, Vol. 86, pp. 2119–2120. <https://doi.org/10.1109/JPROC.1998.726783>
- Haykin, S., & Kosko, B. (1998b). Special Issue on Intelligent Signal Processing. *Proceedings of the IEEE*, Vol. 86, pp. 2119–2120. <https://doi.org/10.1109/JPROC.1998.726783>
- Haykin, S. S., & Kosko, B. (2001). *Intelligent signal processing*. Retrieved from <https://dl.acm.org/citation.cfm?id=558427>
- Healey, M., & Jenkins, A. (2000). Kolb's experiential learning theory and its application in geography in higher education. *Journal of Geography*. <https://doi.org/10.1080/00221340008978967>
- Hernán, D. M., Córdova, F. M., Cifuentes, F., Cañete, L., & Palominos, F. (2015). Identifying problem solving strategies for learning styles in engineering students subjected to intelligence test and EEG monitoring. *Procedia Computer Science*, 55(Itqm), 18–27. <https://doi.org/10.1016/j.procs.2015.07.003>
- Hikosaka, O. (1998). Neural systems for control of voluntary action — A hypothesis. *Advances in Biophysics*, 35, 81–102. [https://doi.org/10.1016/S0065-227X\(98\)80004-X](https://doi.org/10.1016/S0065-227X(98)80004-X)
- Hoadley, M. E., & Hopkins, S. J. (2013). Overcoming matrix matching problems in multiplex cytokine assays. *Journal of Immunological Methods*, 396(1), 157–162. <https://doi.org/https://doi.org/10.1016/j.jim.2013.07.005>
- Hogeveen, J., Salvi, C., & Grafman, J. (2016). 'Emotional Intelligence': Lessons from Lesions. *Trends in Neurosciences*, 39(10), 694–705. <https://doi.org/10.1016/J.TINS.2016.08.007>
- Holinka, C. (2015). Stress, Emotional Intelligence, and Life Satisfaction in College Students. *College Student Journal*, 49(2), 300–311. Retrieved from

<http://ezproxy.shu.edu/login?url=http://search.ebscohost.com/login.aspx?direct=true&db=a9h&AN=103235394&site=eds-live>

- Horn, J. L. (1982). The Theory of Fluid and Crystallized Intelligence in Relation to Concepts of Cognitive Psychology and Aging in Adulthood. In *Aging and Cognitive Processes* (pp. 237–278). [https://doi.org/10.1007/978-1-4684-4178-9\\_14](https://doi.org/10.1007/978-1-4684-4178-9_14)
- Hosseinfard, B., Moradi, M. H., & Rostami, R. (2013). Classifying depression patients and normal subjects using machine learning techniques and nonlinear features from EEG signal. *Computer Methods and Programs in Biomedicine*, *109*(3), 339–345. <https://doi.org/10.1016/j.cmpb.2012.10.008>
- Hounsfield, G. . (1973). Computerized transverse axial scanning(tomography):Part I description of system. *British Journal of Radiology*. <https://doi.org/10.1259/0007-1285-46-552-1016>
- Howells, F. M., Ives-Deliperi, V. L., Horn, N. R., & Stein, D. J. (2012). Mindfulness based cognitive therapy improves frontal control in bipolar disorder: A pilot EEG study. *BMC Psychiatry*. <https://doi.org/10.1186/1471-244X-12-15>
- Huang, S., Yang, J., Fong, S., & Zhao, Q. (2020). Artificial intelligence in cancer diagnosis and prognosis: Opportunities and challenges. *Cancer Letters*, *471*, 61–71. <https://doi.org/https://doi.org/10.1016/j.canlet.2019.12.007>
- Huber, L., Tse, D. H. Y., Wiggins, C. J., Uludağ, K., Kashyap, S., Jangraw, D. C., ... Ivanov, D. (2018). Ultra-high resolution blood volume fMRI and BOLD fMRI in humans at 9.4 T: Capabilities and challenges. *NeuroImage*, *178*, 769–779. <https://doi.org/https://doi.org/10.1016/j.neuroimage.2018.06.025>
- Ibarra, E., & Jimenez-Lizarraga, M. (2014). Robust High Order Sliding Mode Optimization for Linear Time Variant Systems. *IFAC Proceedings Volumes*, *47*(3), 6050–6055. <https://doi.org/https://doi.org/10.3182/20140824-6-ZA-1003.02600>
- Ibrahim, F, Faisal, T., Salim, M. I., & Taib, M. N. (2010). Non-invasive diagnosis of risk in dengue patients using bioelectrical impedance analysis and artificial neural network. *Med Biol Eng Comput*, *48*(11), 1141–1148. <https://doi.org/10.1007/s11517-010-0669-z>
- Ibrahim, Fatimah, Taib, M. N., Abas, W. A. B. W., Guan, C. C., & Sulaiman, S. (2005). A novel dengue fever (DF) and dengue haemorrhagic fever (DHF) analysis using artificial neural network (ANN). *Computer Methods and Programs in Biomedicine*. <https://doi.org/10.1016/j.cmpb.2005.04.002>
- İçer, S., Kara, S., & Güven, A. (2006). Comparison of multilayer perceptron training algorithms for portal venous doppler signals in the cirrhosis disease. *Expert Systems with Applications*. <https://doi.org/10.1016/j.eswa.2005.09.037>
- Illes, P., & Verkhatsky, A. (2016). Purinergic neurone-glia signalling in cognitive-related pathologies. *Neuropharmacology*, *104*, 62–75. <https://doi.org/10.1016/j.neuropharm.2015.08.005>
- Iplikci, S. (2010). A support vector machine based control application to the experimental

three-tank system. *ISA Transactions*, 49(3), 376–386.  
<https://doi.org/https://doi.org/10.1016/j.isatra.2010.03.013>

Irving, J. A., & Williams, D. I. (1995). Experience of group work in counsellor training and preferred learning styles. *Counselling Psychology Quarterly*, 8(2), 139–144.  
<https://doi.org/10.1080/09515079508256331>

Ives-Deliperi, V., & Butler, J. T. (2018). WITHDRAWN: The relationship between EEG electrode and functional cortex in the international 10-20 system. *Clinical Neurophysiology Practice*, 0(0). <https://doi.org/10.1016/j.cnp.2018.02.002>

Jahidin, A. H., Megat Ali, M. S. A., Taib, M. N., Tahir, N. M., Yassin, I. M., & Lias, S. (2014). Classification of intelligence quotient via brainwave sub-band power ratio features and artificial neural network. *Computer Methods and Programs in Biomedicine*, 114(1), 50–59. <https://doi.org/10.1016/j.cmpb.2014.01.016>

Jahidin, A. H., Taib, M. N., Md. Tahir, N., Megat Ali, M. S. A., Lias, S., Fuad, N., & Omar, W. R. W. (2012). Brainwave sub-band power ratio characteristics in intelligence assessment. *Proceedings - 2012 IEEE Control and System Graduate Research Colloquium, ICSGRC 2012*.  
<https://doi.org/10.1109/ICSGRC.2012.6287184>

Jahidin, A. H., Taib, M. N., Tahir, N. M., Ali, M. S. A. M., Yassin, I. M., Lias, S., ... Fuad, N. (2013). Classification of intelligence quotient using EEG sub-band power ratio and ANN during mental task. *Proceedings - 2013 IEEE Conference on Systems, Process and Control, ICSPC 2013*, 204–208.  
<https://doi.org/10.1109/SPC.2013.6735132>

Jahidin, A.H., Taib, M. N., Tahir, N. M., Megat Ali, M. S. A., & Lias, S. (2013). Asymmetry Pattern of Resting EEG for Different IQ Levels. *Procedia - Social and Behavioral Sciences*. <https://doi.org/10.1016/j.sbspro.2013.10.229>

Jahidin, Aisyah Hartini. (2015). *Artificial neural network modelling for IQ classification based on EEG signals*. Retrieved from <http://ir.uitm.edu.my/15601/>

Jahidin, Aisyah Hartini, Megat Ali, M. S. A., Taib, M. N., Md Tahir, N., & Yassin, A. I. M. (2015). Cross-relational study between intelligence and brain asymmetry abilities using EEG-based IQ classification model. *Journal of Theoretical and Applied Information Technology*, 81(1), 43–50.

Jahidin, Aisyah Hartini, Taib, M. N., Tahir, N. M., & Ali, M. S. A. M. (2015). IQ Classification via Brainwave Features: Review on Artificial Intelligence Techniques. *International Journal of Electrical and Computer Engineering (IJECE)*, 5(1), 84–91. <https://doi.org/10.11591/ijece.v5i1.6924>

Jaušovec, N. (1998). Are gifted individuals less chaotic thinkers? *Personality and Individual Differences*, 25(2), 253–267. [https://doi.org/10.1016/S0191-8869\(98\)00039-7](https://doi.org/10.1016/S0191-8869(98)00039-7)

Jaušovec, N. (2000). Differences in cognitive processes between gifted, intelligent, creative, and average individuals while solving complex problems: An EEG study. *Intelligence*, Vol. 28, pp. 213–237. [https://doi.org/10.1016/S0160-2896\(00\)00037-4](https://doi.org/10.1016/S0160-2896(00)00037-4)

- Javidi, S., Mandic, D., Cheong Took, C., & Cichocki, A. (2011). Kurtosis based blind source extraction of complex noncircular signals with application in EEG artifact removal in real-time. *Frontiers in Neuroscience*, Vol. 5, p. 105. Retrieved from <https://www.frontiersin.org/article/10.3389/fnins.2011.00105>
- Jebelli, H., Hwang, S., & Lee, S. (2018). EEG-based workers' stress recognition at construction sites. *Automation in Construction*, 93, 315–324. <https://doi.org/https://doi.org/10.1016/j.autcon.2018.05.027>
- Jeng, Y.-L., & Huang, Y.-M. (2018). Dynamic learning paths framework based on collective intelligence from learners. *Computers in Human Behavior*. <https://doi.org/https://doi.org/10.1016/j.chb.2018.09.012>
- Jensen, A. R. (1993). Why Is Reaction Time Correlated With Psychometric  $g$ ? *Current Directions in Psychological Science*, 2(2), 53–56. <https://doi.org/10.1111/1467-8721.ep10770697>
- Jeunet, C., Glize, B., McGonigal, A., Batail, J.-M., & Micoulaud-Franchi, J.-A. (2018). Using EEG-based brain computer interface and neurofeedback targeting sensorimotor rhythms to improve motor skills: Theoretical background, applications and prospects. *Neurophysiologie Clinique*. <https://doi.org/https://doi.org/10.1016/j.neucli.2018.10.068>
- Jisna, P., Varghese, E., Wilson, A., & Bineesh, M. (2017). A novel method for brain proficiency analysis based on audio tracking. *Ieeexplore.Ieee.Org*, 1–5. <https://doi.org/10.1109/ICCPCT.2017.8074319>
- Kaleem, M., Guergachi, A., & Krishnan, S. (2018). Patient-specific seizure detection in long-term EEG using wavelet decomposition. *Biomedical Signal Processing and Control*, 46, 157–165. <https://doi.org/10.1016/J.BSPC.2018.07.006>
- Kalogirou, S. A. (2000). Applications of artificial neural-networks for energy systems. *Applied Energy*. [https://doi.org/10.1016/S0306-2619\(00\)00005-2](https://doi.org/10.1016/S0306-2619(00)00005-2)
- Kamaruddin, S. A., & Shogar, I. (2011). *Artificial Neural Network and Its Islamic Relevance*. 01(03), 138–148.
- Kaminski, J., Brzezicka, A., & Wróbel, A. (2011). Short-term memory capacity ( $7\pm 2$ ) predicted by theta to gamma cycle length ratio. *Neurobiology of Learning and Memory*. <https://doi.org/10.1016/j.nlm.2010.10.001>
- Kane, M. J., & Engle, R. W. (2002). The role of prefrontal cortex in working-memory capacity, executive attention, and general fluid intelligence: An individual-differences perspective. *Psychonomic Bulletin and Review*, 9(4), 637–671. <https://doi.org/10.3758/BF03196323>
- Kappel, S. L., Rank, M. L., Toft, H. O., Andersen, M., & Kidmose, P. (2019). Dry-Contact Electrode Ear-EEG. *IEEE Transactions on Biomedical Engineering*. <https://doi.org/10.1109/TBME.2018.2835778>
- Kappenman, E. S., & Luck, S. J. (2010). The effects of electrode impedance on data quality and statistical significance in ERP recordings. *Psychophysiology*.



<https://doi.org/10.1111/j.1469-8986.2010.01009.x>

- Kara, S., Güven, A., & Öner, A. Ö. (2006). Utilization of artificial neural networks in the diagnosis of optic nerve diseases. *Computers in Biology and Medicine*. <https://doi.org/10.1016/j.combiomed.2005.01.003>
- Karakas, T., & Yildiz, D. (2020). Exploring the influence of the built environment on human experience through a neuroscience approach: A systematic review. *Frontiers of Architectural Research*. <https://doi.org/https://doi.org/10.1016/j.foar.2019.10.005>
- Karam, L. J., & McClellan, J. H. (1999). Chebyshev digital FIR filter design. *Signal Processing*, 76(1), 17–36. [https://doi.org/10.1016/S0165-1684\(98\)00244-8](https://doi.org/10.1016/S0165-1684(98)00244-8)
- Kerson, C., deBeus, R., Lightstone, H., Arnold, L. E., Barterian, J., Pan, X., & Monastra, V. J. (2019). EEG Theta/Beta Ratio Calculations Differ Between Various EEG Neurofeedback and Assessment Software Packages: Clinical Interpretation. *Clinical EEG and Neuroscience*, 51(2), 114–120. <https://doi.org/10.1177/1550059419888320>
- Khan, I. Y., Zope, P. H., & Suralkar, S. R. (2013). Importance of Artificial Neural Network in Medical Diagnosis Disease Like Acute Nephritis Disease and Heart Disease. *International Journal of Engineering Science and Innovative Technology (IJESIT)*, 2(2), 210–217.
- Khan, J., Wei, J. S., Ringnér, M., Saal, L. H., Ladanyi, M., Westermann, F., ... Meltzer, P. S. (2001). Classification and diagnostic prediction of cancers using gene expression profiling and artificial neural networks. *Nature Medicine*, 7(6), 673–679. <https://doi.org/10.1038/89044>
- Kim, K., Lee, S.-J., Kang, C. S., Hwang, S., Lee, Y.-H., & Yu, K.-K. (2014). Toward a brain functional connectivity mapping modality by simultaneous imaging of coherent brainwaves. *NeuroImage*, 91, 63–69. <https://doi.org/10.1016/J.NEUROIMAGE.2014.01.030>
- Kim, S.-K., & Kang, H.-B. (2018). An analysis of smartphone overuse recognition in terms of emotions using brainwaves and deep learning. *Neurocomputing*, 275, 1393–1406. <https://doi.org/10.1016/J.NEUCOM.2017.09.081>
- Kitoko, V., Nguyen, T. N., Nguyen, J. S., Tran, Y., & Nguyen, H. T. (2011). Performance of dry electrode with bristle in recording EEG rhythms across brain state changes. *Proceedings of the Annual International Conference of the IEEE Engineering in Medicine and Biology Society, EMBS*. <https://doi.org/10.1109/IEMBS.2011.6089896>
- Klimesch, W. (1999). EEG alpha and theta oscillations reflect cognitive and memory performance: A review and analysis. *Brain Research Reviews*, Vol. 29, pp. 169–195. [https://doi.org/10.1016/S0165-0173\(98\)00056-3](https://doi.org/10.1016/S0165-0173(98)00056-3)
- Knyazev, G., Merkulova, E., Savostyanov, A., Bocharov, A., & Saprigyn, A. (2019). Personality and EEG correlates of reactive social behavior. *Neuropsychologia*, 124, 98–107. <https://doi.org/https://doi.org/10.1016/j.neuropsychologia.2019.01.006>

- Koc, E., & Boz, H. (2018). Chapter 5 - How Can Consumer Science Be Used for Gaining Information About Consumers and the Market?: The role of psychophysiological and neuromarketing research. In A. Cavicchi & C. Santini (Eds.), *Case Studies in the Traditional Food Sector* (pp. 129–152). <https://doi.org/10.1016/B978-0-08-101007-5.00013-0>
- Kolb, A., & Kolb, D. (2005). The Kolb learning style inventory—version 3.1 2005 technical specifications. *Boston, MA: Hay Resource Direct*, 1–72. [https://doi.org/10.1016/S0260-6917\(95\)80103-0](https://doi.org/10.1016/S0260-6917(95)80103-0)
- Kolb, A. Y., & Kolb, D. A. (2009). Experiential learning theory: A dynamic, holistic approach to management learning, education and development. *The SAGE Handbook of Management Learning, Education and Development*, (May 2016), 42–68. <https://doi.org/http://dx.doi.org/10.4135/9780857021038.n3>
- Kolb, D. A. (1974). *On management and the learning process*. In D. A. Kolb, I. M. Rubin, & J. M. McIntyre (O. psychology: A. book of Readings, Ed.). Oxford, England: Prentice-Hall.
- Kolb, David A. (2006). Experiential learning: experience as the source of learning and development. *Prentice Hall, Inc.*, (1984), 20–38. <https://doi.org/10.1016/B978-0-7506-7223-8.50017-4>
- Kolb, David A. (2007). *The Kolb learning style inventory : LSI workbook* (Version 3.). Boston, Mass. : HayGroup.
- Kounios, J., Fleck, J. I., Green, D. L., Payne, L., Stevenson, J. L., Bowden, E. M., & Jung-Beeman, M. (2008). The origins of insight in resting-state brain activity. *Neuropsychologia*, 46(1), 281–291. <https://doi.org/10.1016/j.neuropsychologia.2007.07.013>
- Kumar, R., Aggarwal, R. K., & Sharma, J. D. (2013). Energy analysis of a building using artificial neural network: A review. *Energy and Buildings*. <https://doi.org/10.1016/j.enbuild.2013.06.007>
- Kumar, T. S., Kanhangad, V., & Pachori, R. B. (2015). Classification of seizure and seizure-free EEG signals using local binary patterns. *Biomedical Signal Processing and Control*, 15, 33–40. <https://doi.org/10.1016/j.bspc.2014.08.014>
- Kupusinac, A., Stokić, E., & Doroslovački, R. (2014). Predicting body fat percentage based on gender, age and BMI by using artificial neural networks. *Computer Methods and Programs in Biomedicine*. <https://doi.org/10.1016/j.cmpb.2013.10.013>
- Kuruvilla, J., & Gunavathi, K. (2014). Lung cancer classification using neural networks for CT images. *Computer Methods and Programs in Biomedicine*, 113(1), 202–209. <https://doi.org/10.1016/j.cmpb.2013.10.011>
- Kuyu, Y. C., & Vatansever, F. (2016). A new intelligent decision making system combining classical methods, evolutionary algorithms and statistical techniques for optimal digital FIR filter design and their performance evaluation. *AEU - International Journal of Electronics and Communications*, 70(12), 1651–1666. <https://doi.org/10.1016/J.AEUE.2016.10.004>

- La Vaque, T. J. (1999). The History of EEG Hans Berger. *Journal of Neurotherapy*. [https://doi.org/10.1300/J184v03n02\\_01](https://doi.org/10.1300/J184v03n02_01)
- Lahiri, R., Rakshit, P., & Konar, A. (2017). Evolutionary perspective for optimal selection of EEG electrodes and features. *Biomedical Signal Processing and Control*, *36*, 113–137. <https://doi.org/10.1016/J.BSPC.2017.03.022>
- Langer, N., Pedroni, A., Gianotti, L. R. R., Hänggi, J., Knoch, D., & Jäncke, L. (2012). Functional brain network efficiency predicts intelligence. *Human Brain Mapping*, *33*(6), 1393–1406. <https://doi.org/10.1002/hbm.21297>
- Larkin-Hein, T., & Budny, D. D. (2003). Why bother learning about learning styles and psychological types? *ASEE Annual Conference Proceedings*.
- Lazor, J. W., Schmitt, J. E., Loevner, L. A., & Nabavizadeh, S. A. (2018). Metabolic Changes of Brain Developmental Venous Anomalies on 18F-FDG-PET. *Academic Radiology*. <https://doi.org/10.1016/J.ACRA.2018.05.021>
- Le Van Quyen, M. (2011). The brainweb of cross-scale interactions. *New Ideas in Psychology*, *29*(2), 57–63. <https://doi.org/10.1016/j.newideapsych.2010.11.001>
- Lee, T. W., Wu, Y. Te, Yu, Y. W. Y., Wu, H. C., & Chen, T. J. (2012). A smarter brain is associated with stronger neural interaction in healthy young females: A resting EEG coherence study. *Intelligence*, *40*(1), 38–48. <https://doi.org/10.1016/j.intell.2011.11.001>
- Leiser, S. C., Dunlop, J., Bowlby, M. R., & Devilbiss, D. M. (2011). Aligning strategies for using EEG as a surrogate biomarker: A review of preclinical and clinical research. *Biochemical Pharmacology*. <https://doi.org/10.1016/j.bcp.2010.10.002>
- Lhermitte, F., Pillon, B., & Serdaru, M. (1986). Human autonomy and the frontal lobes. Part I: Imitation and utilization behavior: A neuropsychological study of 75 patients. *Annals of Neurology*, *19*(4), 326–334. <https://doi.org/10.1002/ana.410190404>
- Li, A., Yetkin, F. Z., Cox, R., & Haughton, V. M. (1996). Ipsilateral hemisphere activation during motor and sensory tasks. *AJNR. American Journal of Neuroradiology*, *17*(4), 651–655. Retrieved from <http://www.ncbi.nlm.nih.gov/pubmed/8730183>
- Li, G., Wang, S., & Duan, Y. Y. (2017). Towards gel-free electrodes: A systematic study of electrode-skin impedance. *Sensors and Actuators B: Chemical*, *241*, 1244–1255. <https://doi.org/10.1016/J.SNB.2016.10.005>
- Li, L. (2010). The differences among eyes-closed, eyes-open and attention states: An EEG study. *2010 6th International Conference on Wireless Communications, Networking and Mobile Computing, WiCOM 2010*. <https://doi.org/10.1109/WICOM.2010.5600726>
- Liano, K. (1996). Robust error measure for supervised neural network learning with outliers. *IEEE Transactions on Neural Networks*. <https://doi.org/10.1109/72.478411>
- Liao, L. De, Lin, C. T., McDowell, K., Wickenden, A. E., Gramann, K., Jung, T. P., ...

- Chang, J. Y. (2012). Biosensor technologies for augmented brain-computer interfaces in the next decades. *Proceedings of the IEEE*. <https://doi.org/10.1109/JPROC.2012.2184829>
- Lisboa, P. J. G. (2002). A review of evidence of health benefit from artificial neural networks in medical intervention. *Neural Networks*, *15*(1), 11–39. [https://doi.org/10.1016/S0893-6080\(01\)00111-3](https://doi.org/10.1016/S0893-6080(01)00111-3)
- Lisman, J. (2015). The Challenge of Understanding the Brain: Where We Stand in 2015. *Neuron*, *86*(4), 864–882. <https://doi.org/10.1016/J.NEURON.2015.03.032>
- Lolli, F., Gamberini, R., Regattieri, A., Balugani, E., Gatos, T., & Gucci, S. (2017). Single-hidden layer neural networks for forecasting intermittent demand. *International Journal of Production Economics*. <https://doi.org/10.1016/j.ijpe.2016.10.021>
- Lou, S., Feng, Y., Li, Z., Zheng, H., & Tan, J. (2020). An integrated decision-making method for product design scheme evaluation based on cloud model and EEG data. *Advanced Engineering Informatics*, *43*, 101028. <https://doi.org/https://doi.org/10.1016/j.aei.2019.101028>
- Lu, Y., Wang, M., Wu, W., Han, Y., Zhang, Q., & Chen, S. (2020). Dynamic entropy-based pattern learning to identify emotions from EEG signals across individuals. *Measurement*, *150*, 107003. <https://doi.org/https://doi.org/10.1016/j.measurement.2019.107003>
- Luger, G. F. (2005). Artificial Intelligence: Structures and Strategies for Complex Problem Solving. In *Zywienie Czlowieka I Metabolizm*. <https://doi.org/citeulike-article-id:1048507>
- Luo, S., & Johnston, P. (2010). A review of electrocardiogram filtering. *Journal of Electrocardiology*, *43*(6), 486–496. <https://doi.org/10.1016/j.jelectrocard.2010.07.007>
- Lutzenberger, W., Birbaumer, N., Flor, H., Rockstroh, B., & Elbert, T. (1992). Dimensional analysis of the human EEG and intelligence. *Neuroscience Letters*, *143*(1–2), 10–14. [https://doi.org/10.1016/0304-3940\(92\)90221-R](https://doi.org/10.1016/0304-3940(92)90221-R)
- MacLean, M. H., Arnell, K. M., & Cote, K. A. (2012). Resting EEG in alpha and beta bands predicts individual differences in attentional blink magnitude. *Brain and Cognition*. <https://doi.org/10.1016/j.bandc.2011.12.010>
- MacLennan, B. J. (2017). Chapter 3 - Field computation: A framework for quantum-inspired computing. In S. Bhattacharyya, U. Maulik, & P. Dutta (Eds.), *Quantum Inspired Computational Intelligence* (pp. 85–110). <https://doi.org/https://doi.org/10.1016/B978-0-12-804409-4.00003-6>
- Magfirah, T. (2017). *Students' reading and listening comprehension based on their learning styles*. Retrieved from <http://repository.wima.ac.id/12487/>
- Mahela, O. P., Shaik, A. G., & Gupta, N. (2015). A critical review of detection and classification of power quality events. *Renewable and Sustainable Energy Reviews*,

41, 495–505. <https://doi.org/https://doi.org/10.1016/j.rser.2014.08.070>

- Maier, H. R., Jain, A., Dandy, G. C., & Sudheer, K. P. (2010). Methods used for the development of neural networks for the prediction of water resource variables in river systems: Current status and future directions. *Environmental Modelling and Software*. <https://doi.org/10.1016/j.envsoft.2010.02.003>
- Mamlook, R., Badran, O., & Abdulhadi, E. (2009). A fuzzy inference model for short-term load forecasting. *Energy Policy*, 37(4), 1239–1248. <https://doi.org/https://doi.org/10.1016/j.enpol.2008.10.051>
- Mammadli, S. (2017). Financial time series prediction using artificial neural network based on Levenberg-Marquardt algorithm. *Procedia Computer Science*, 120, 602–607. <https://doi.org/https://doi.org/10.1016/j.procs.2017.11.285>
- Manolis, C., Burns, D. J., Assudani, R., & Chinta, R. (2013). Assessing experiential learning styles: A methodological reconstruction and validation of the Kolb Learning Style Inventory. *Learning and Individual Differences*, 23, 44–52. <https://doi.org/10.1016/J.LINDIF.2012.10.009>
- Marieb, E. N., & Hoehn, K. (2015). *Essentials of Human Anatomy & Physiology* (11th ed.). Retrieved from <http://books.google.com/books?id=tyLGINMexIwC&pgis=1>
- Martindale, C., Hines, D., Mitchell, L., & Covello, E. (1984). EEG alpha asymmetry and creativity. *Personality and Individual Differences*, 5(1), 77–86. [https://doi.org/10.1016/0191-8869\(84\)90140-5](https://doi.org/10.1016/0191-8869(84)90140-5)
- Martins, L., & Szrek, H. (2019). The impact of the decision environment on consumer choice of mobile service plans: An experimental examination. *Utilities Policy*, 56, 20–32. <https://doi.org/https://doi.org/10.1016/j.jup.2018.10.009>
- Masters, T. (1993). Practical neural network recipes in C. In *booksgooglecom*. <https://doi.org/10.1016/B978-0-08-051433-8.50001-X>
- Matei, O., Pop, P. C., & Vălean, H. (2013). Optical character recognition in real environments using neural networks and k-nearest neighbor. *Applied Intelligence*. <https://doi.org/10.1007/s10489-013-0456-2>
- Mathworks. (2017). *Statistics and Machine Learning Toolbox™ User's Guide R2017a. MatLab*.
- Matta, B., Menon, D., & Smith, M. (2011). *Core topics in neuroanaesthesia and neurointensive care*. Retrieved from [https://books.google.com/books?hl=en&lr=&id=272rEV9qj4AC&oi=fnd&pg=PR3&dq=Core+Topics+in+Neuroanaesthesia+and+Neurointensive+Care&ots=NTtkW-ksXz&sig=rPJ6KTTbEGm-Q\\_qbQ40k-ffOwxo](https://books.google.com/books?hl=en&lr=&id=272rEV9qj4AC&oi=fnd&pg=PR3&dq=Core+Topics+in+Neuroanaesthesia+and+Neurointensive+Care&ots=NTtkW-ksXz&sig=rPJ6KTTbEGm-Q_qbQ40k-ffOwxo)
- McClellan, J. H., & Parks, T. W. (2005). A personal history of the Parks-McClellan algorithm. *IEEE Signal Processing Magazine*, 22(2), 82–86. <https://doi.org/10.1109/MSP.2005.1406492>
- McFarland, D. J., McCane, L. M., David, S. V., & Wolpaw, J. R. (1997). Spatial filter

selection for EEG-based communication. *Electroencephalography and Clinical Neurophysiology*, 103(3), 386–394. [https://doi.org/10.1016/S0013-4694\(97\)00022-2](https://doi.org/10.1016/S0013-4694(97)00022-2)

McKenna, F. P. (1984). Measures of field dependence: Cognitive style or cognitive ability? *Journal of Personality and Social Psychology*, 47(3), 593–603. <https://doi.org/10.1037/0022-3514.47.3.593>

Medaglia, J. D., Lynall, M.-E., & Bassett, D. S. (2015). Cognitive Network Neuroscience. *Journal of Cognitive Neuroscience*, 27(8), 1471–1491. [https://doi.org/10.1162/jocn\\_a\\_00810](https://doi.org/10.1162/jocn_a_00810)

Megat Ali, M. S. A., Jahidin, A. H., Taib, M. N., Tahir, N. M., & Yassin, I. M. (2016). Classification of Kolb's learning styles using EEG sub-band spectral centroid frequencies and artificial neural network. *Asian Journal of Scientific Research*, 9(5), 234–241. <https://doi.org/10.3923/ajsr.2016.234.241>

Megat Ali, M. S A, Taib, M. N., Md Tahir, N., Jahidin, A. H., & Yassin, M. (2014). EEG sub-band spectral centroid frequencies extraction based on Hamming and equiripple filters: A comparative study. *Proceedings - 2014 IEEE 10th International Colloquium on Signal Processing and Its Applications, CSPA 2014*, 199–203. <https://doi.org/10.1109/CSPA.2014.6805747>

Megat Ali, M.S.A., Jahidin, A. H., Taib, M. N., & Md Tahir, N. (2016). Eeg SUB-BAND spectral centroid frequency and amplitude ratio Features: A comparative study in learning style classification. *Jurnal Teknologi*. <https://doi.org/10.11113/jt.v78.4100>

Megat Ali, M.S.A., Jahidin, A. H., Taib, M. N., Tahir, N. M., & Yassin, I. M. (2016). Classification of Kolb's Learning Styles Using EEG Sub-band Spectral Centroid Frequencies and Artificial Neural Network. *Asian Journal of Scientific Research*, 9(5), 234–241. <https://doi.org/10.3923/ajsr.2016.234.241>

Megat Ali, Megat Syahirul Amin, Jahidin, A. H., Md Tahir, N., & Taib, M. N. (2014). Learning Style Classification via EEG Sub-band Spectral Centroid Frequency Features. *International Journal of Electrical and Computer Engineering (IJECE)*, Vol. 4(Engineering and Science), 931–938. Retrieved from <http://iaesjournal.com/online/index.php/IJECE/article/viewFile/6833/3628>

Megat Ali, Megat Syahirul Amin, Jahidin, A. H., Tahir, N. M., & Taib, M. N. (2014). Learning style classification via EEG sub-band spectral centroid frequency features. *International Journal of Electrical and Computer Engineering*. <https://doi.org/10.11591/ijece.v4i6.6833>

Megat Ali, Megat Syahirul Amin, Jahidin, A. H., Taib, M. N., & Md Tahir, N. (2016). Eeg SUB-BAND spectral centroid frequency and amplitude ratio Features: A comparative study in learning style classification. *Jurnal Teknologi*, 78(2), 15–23. <https://doi.org/10.11113/jt.v78.4100>

Messarlis, G. A. T., Georgakopoulos, D. N., Zampakis, P., Kalogeropoulou, C. P., Petsas, T. G., & Panayiotakis, G. S. (2018, July 17). Patient dose in brain perfusion imaging using an 80-slice CT system. *Journal of Neuroradiology*. <https://doi.org/10.1016/j.neurad.2018.06.005>

- Messick, S. (1984). The nature of cognitive styles: Problems and promise in educational practice. *Educational Psychologist*, 19(2), 59–74. <https://doi.org/10.1080/00461528409529283>
- Mestre, L. S., & Mestre, L. S. (2012). Overview of learning style theories and learning style results from the Mestre study. *Designing Effective Library Tutorials*, 19–31. <https://doi.org/10.1016/B978-1-84334-688-3.50002-0>
- Meyer-Baese, A., & Schmid, V. (2014). Chapter 8 - Transformation and Signal-Separation Neural Networks. In A. Meyer-Baese & V. Schmid (Eds.), *Pattern Recognition and Signal Analysis in Medical Imaging (Second Edition)* (Second Edition, pp. 245–289). <https://doi.org/https://doi.org/10.1016/B978-0-12-409545-8.00008-X>
- Michel, C. M., Murray, M. M., Lantz, G., Gonzalez, S., Spinelli, L., & Grave De Peralta, R. (2004). EEG source imaging. *Clinical Neurophysiology*. <https://doi.org/10.1016/j.clinph.2004.06.001>
- Millett, D. (2001). Hans Berger: From Psychic Energy to the EEG. *Perspectives in Biology and Medicine*. <https://doi.org/10.1353/pbm.2001.0070>
- Minguillon, J., Lopez-Gordo, M. A., & Pelayo, F. (2017). Trends in EEG-BCI for daily-life: Requirements for artifact removal. *Biomedical Signal Processing and Control*, 31, 407–418. <https://doi.org/https://doi.org/10.1016/j.bspc.2016.09.005>
- Moran, A. (1991). What can Learning Styles Research Learn from Cognitive Psychology? *Educational Psychology*, 11(3–4), 239–245. <https://doi.org/10.1080/0144341910110303>
- Morton, S. M., & Bastian, A. J. (2004). Cerebellar Control of Balance and Locomotion. *The Neuroscientist*, 10(3), 247–259. <https://doi.org/10.1177/1073858404263517>
- Mota, A. R., Duarte, L., Rodrigues, D., Martins, A. C., Machado, A. V., Vaz, F., ... Fonseca, C. (2013). Development of a quasi-dry electrode for EEG recording. *Sensors and Actuators, A: Physical*. <https://doi.org/10.1016/j.sna.2013.06.013>
- Mouloodi, S., Rahmanpanah, H., Burvill, C., & Davies, H. M. S. (2020). Prediction of load in a long bone using an artificial neural network prediction algorithm. *Journal of the Mechanical Behavior of Biomedical Materials*, 102, 103527. <https://doi.org/https://doi.org/10.1016/j.jmbbm.2019.103527>
- Mullen, T. R., Kothe, C. A. E., Chi, Y. M., Ojeda, A., Kerth, T., Makeig, S., ... Cauwenberghs, G. (2015). Real-time neuroimaging and cognitive monitoring using wearable dry EEG. *IEEE Transactions on Biomedical Engineering*. <https://doi.org/10.1109/TBME.2015.2481482>
- Najafi, A., Nowruzi, H., & Ghassemi, H. (2018). Performance prediction of hydrofoil-supported catamarans using experiment and ANNs. *Applied Ocean Research*, 75, 66–84. <https://doi.org/https://doi.org/10.1016/j.apor.2018.02.017>
- Nazmi, N., Rahman, M. A. A., Yamamoto, S.-I., & Ahmad, S. A. (2019). Walking gait event detection based on electromyography signals using artificial neural network. *Biomedical Signal Processing and Control*, 47, 334–343.

<https://doi.org/https://doi.org/10.1016/j.bspc.2018.08.030>

- Negnevitsky, M. (2005). Artificial intelligence: a guide to intelligent systems. Pearson Education. In *Artificial intelligence: A guide to intelligent systems* (pp. 87–113). Retrieved from [https://books.google.ae/books/about/Artificial\\_Intelligence.html?id=1BxYQnrFv9MC&redir\\_esc=y](https://books.google.ae/books/about/Artificial_Intelligence.html?id=1BxYQnrFv9MC&redir_esc=y)
- Nelles, O. (2001). Nonlinear system identification: from classical approaches to neural networks and fuzzy models. In *Book*. <https://doi.org/10.1007/978-3-662-04323-3>
- Neubauer, A. C., & Fink, A. (2009a). Intelligence and neural efficiency: Measures of brain activation versus measures of functional connectivity in the brain. *Intelligence*, 37(2), 223–229. <https://doi.org/10.1016/j.intell.2008.10.008>
- Neubauer, A. C., & Fink, A. (2009b). Intelligence and neural efficiency. *Neuroscience and Biobehavioral Reviews*, Vol. 33, pp. 1004–1023. <https://doi.org/10.1016/j.neubiorev.2009.04.001>
- Neubauer, A. C., Fink, A., & Schrausser, D. G. (2002). Intelligence and neural efficiency: The influence of task content and sex on the brain - IQ relationship. *Intelligence*, 30(6), 515–536. [https://doi.org/10.1016/S0160-2896\(02\)00091-0](https://doi.org/10.1016/S0160-2896(02)00091-0)
- Neubauer, A. C., Grabner, R. H., Fink, A., & Neuper, C. (2005). Intelligence and neural efficiency: Further evidence of the influence of task content and sex on the brain-IQ relationship. *Cognitive Brain Research*, 25(1), 217–225. <https://doi.org/10.1016/j.cogbrainres.2005.05.011>
- Nicolardi, V. (2018). Self-related and moral contextual cues modulate pain perception during social interactions. Behavioural and EEG correlates. *International Journal of Psychophysiology*, 131, S11. <https://doi.org/https://doi.org/10.1016/j.ijpsycho.2018.07.034>
- Niedermeyer, E. (2003). The Clinical Relevance of EEG Interpretation. *Clinical EEG and Neuroscience*, 34(3), 93–98. <https://doi.org/10.1177/155005940303400303>
- Niedermeyer, Ernst, & Schomer, D. L. (2011). Historical Aspects of EEG. In *Niedermeyer's Electroencephalography: Basic Principles, Clinical Applications, and Related Fields*.
- Nilsson, N. J. (1998). *Artificial Intelligence: a new synthesis*. Morgan Kaufmann Publishers.
- Noreika, V., Georgieva, S., Wass, S., & Leong, V. (2020). 14 challenges and their solutions for conducting social neuroscience and longitudinal EEG research with infants. *Infant Behavior and Development*, 58, 101393. <https://doi.org/https://doi.org/10.1016/j.infbeh.2019.101393>
- Norgaard, M., Ravn, O., Poulsen, N., & Hansen, L. K. (2000). Neural networks for modelling and control of dynamic systems - A Practitioner's Handbook. In *Control Engineering Practice*. <https://doi.org/10.1186/1471-2148-7-1>



- Okoniewski, P., & Piskorowski, J. (2015). A concept of IIR filters with time-varying coefficients and equalised group delay response. *Measurement*, *60*, 13–24. <https://doi.org/10.1016/J.MEASUREMENT.2014.09.077>
- Ono, K., Mameya, G., Shimada, D., & Yamashita, M. (1982). Eeg correlation with intelligence test performance in senescence: A new pattern discriminative approach. *International Journal of Neuroscience*, *16*(1), 47–52. <https://doi.org/10.3109/00207458209147601>
- Pachori, R. B., & Patidar, S. (2014). Epileptic seizure classification in EEG signals using second-order difference plot of intrinsic mode functions. *Computer Methods and Programs in Biomedicine*, *113*(2), 494–502. <https://doi.org/10.1016/j.cmpb.2013.11.014>
- Pandey, D. S., Das, S., Pan, I., Leahy, J. J., & Kwapinski, W. (2016). *Artificial neural network based modelling approach for municipal solid waste gasification in a fluidized bed reactor*.
- Panteliadis, C. P., Vassilyadi, P., Fehlert, J., & Hagel, C. (2017). Historical documents on epilepsy: From antiquity through the 20th century. *Brain and Development*. <https://doi.org/10.1016/j.braindev.2017.02.002>
- Papousek, I., Wimmer, S., Lackner, H. K., Schulter, G., Perchtold, C. M., & Paechter, M. (2019). Trait positive affect and students' prefrontal EEG alpha asymmetry responses during a simulated exam situation. *Biological Psychology*, *148*, 107762. <https://doi.org/https://doi.org/10.1016/j.biopsycho.2019.107762>
- Papp, Z., Peceli, G., Bago, B., & Pataki, B. (1988). Intelligent medical instruments. *IEEE Engineering in Medicine and Biology Magazine*, *7*(2), 18–23. <https://doi.org/10.1109/51.1969>
- Pardo, M., & Sberveglieri, G. (2002). Learning from data: A tutorial with emphasis on modern pattern recognition methods. *IEEE Sensors Journal*, *2*(3), 203–217. <https://doi.org/10.1109/JSEN.2002.800686>
- Patterson, G. E. (1995). Establishing a relationship between learning styles and critical thinking skills in baccalaureate nursing students. *Dissertation Abstracts International: Section B: The Sciences and Engineering*, *55*(9-B), pp.
- Pedrycz, W. (1990). Fuzzy sets in pattern recognition: Methodology and methods. *Pattern Recognition*. [https://doi.org/10.1016/0031-3203\(90\)90054-O](https://doi.org/10.1016/0031-3203(90)90054-O)
- Pérez, D., Wohlberg, B., Lovell, T. A., Shoemaker, M., & Bevilacqua, R. (2014). Orbit-centered atmospheric density prediction using artificial neural networks. *Acta Astronautica*, *98*(1), 9–23. <https://doi.org/10.1016/j.actaastro.2014.01.007>
- Piccolino, M. (1997). Luigi Galvani and animal electricity: two centuries after the foundation of electrophysiology. *Trends Neurosci*. [https://doi.org/10.1016/S0166-2236\(97\)01101-6](https://doi.org/10.1016/S0166-2236(97)01101-6)
- Piri, S., Delen, D., & Liu, T. (2018). A synthetic informative minority over-sampling (SIMO) algorithm leveraging support vector machine to enhance learning from

- imbalanced datasets. *Decision Support Systems*, 106, 15–29. <https://doi.org/https://doi.org/10.1016/j.dss.2017.11.006>
- Piryatinska, A., Terdik, G., Woyczynski, W. A., Loparo, K. A., Scher, M. S., & Zlotnik, A. (2009). Automated detection of neonate EEG sleep stages. *Computer Methods and Programs in Biomedicine*. <https://doi.org/10.1016/j.cmpb.2009.01.006>
- Piskorowski, J. (2013). Time-efficient removal of power-line noise from EMG signals using IIR notch filters with non-zero initial conditions. *Biocybernetics and Biomedical Engineering*, 33(3), 171–178. <https://doi.org/https://doi.org/10.1016/j.bbe.2013.07.006>
- Pivik, R. T., Broughton, R. J., Coppola, R., Davidson, R. J., Fox, N., & Nuwer, M. R. (1993). Guidelines for the recording and quantitative analysis of electroencephalographic activity in research contexts. *Psychophysiology*. <https://doi.org/10.1111/j.1469-8986.1993.tb02081.x>
- Plomin, R., & Spinath, F. M. (2004). Intelligence: Genetics, Genes, and Genomics. *Journal of Personality and Social Psychology*, 86(1), 112–129. <https://doi.org/10.1037/0022-3514.86.1.112>
- Polat, K., & Güneş, S. (2007). Classification of epileptiform EEG using a hybrid system based on decision tree classifier and fast Fourier transform. *Applied Mathematics and Computation*. <https://doi.org/10.1016/j.amc.2006.09.022>
- Poletti, E., Grisan, E., & Ruggeri, A. (2012). A modular framework for the automatic classification of chromosomes in Q-band images. *Computer Methods and Programs in Biomedicine*. <https://doi.org/10.1016/j.cmpb.2011.07.013>
- Poore, J. A., Cullen, D. L., & Schaar, G. L. (2014). Simulation-Based Interprofessional Education Guided by Kolb's Experiential Learning Theory. *Clinical Simulation in Nursing*, 10(5), e241–e247. <https://doi.org/10.1016/J.ECNS.2014.01.004>
- Posthuma, D., Neale, M. C., Boomsma, D. I., & De Geus, E. J. C. (2001). Are smarter brains running faster? Heritability of alpha peak frequency, IQ, and their interrelation. *Behavior Genetics*. <https://doi.org/10.1023/A:1013345411774>
- Potter, Kristin and Hagen, Hans and Kerren, Andreas and Dannenmann, P. (2006). Methods for Presenting Statistical Information: The Box Plot. *Visualization of Large and Unstructured Data Sets*, 4, 97–106.
- Poulos, M., Rangoussi, M., & Alezandris, N. (1999). Neural Network Based Person Identification Using Eeg. *Proceedings of International Conferences on Acoustics, Speech and Signal Processing 1999*. <https://doi.org/10.1016/j.crv.2007.01.008>
- Pourtois, G., Schettino, A., & Vuilleumier, P. (2013). Brain mechanisms for emotional influences on perception and attention: What is magic and what is not. *Biological Psychology*, 92(3), 492–512. <https://doi.org/https://doi.org/10.1016/j.biopsycho.2012.02.007>
- Power, M. (1993). The predictive validation of ecological and environmental models. *Ecological Modelling*. [https://doi.org/10.1016/0304-3800\(93\)90106-3](https://doi.org/10.1016/0304-3800(93)90106-3)

- Pradeepkumar, D., & Ravi, V. (2018). Soft computing hybrids for FOREX rate prediction: A comprehensive review. *Computers & Operations Research*, *99*, 262–284. <https://doi.org/https://doi.org/10.1016/j.cor.2018.05.020>
- Prechelt, L. (1998). Automatic early stopping using cross validation: Quantifying the criteria. *Neural Networks*, *11*(4), 761–767. [https://doi.org/10.1016/S0893-6080\(98\)00010-0](https://doi.org/10.1016/S0893-6080(98)00010-0)
- Priya, T. H., Mahalakshmi, P., Naidu, V., & Srinivas, M. (2020). Stress detection from EEG using power ratio. *2020 International Conference on Emerging Trends in Information Technology and Engineering (Ic-ETITE)*, 1–6. <https://doi.org/10.1109/ic-ETITE47903.2020.401>
- Pulini, A. A., Kerr, W. T., Loo, S. K., & Lenartowicz, A. (2018). Classification Accuracy of Neuroimaging Biomarkers in Attention-Deficit/Hyperactivity Disorder: Effects of Sample Size and Circular Analysis. *Biological Psychiatry: Cognitive Neuroscience and Neuroimaging*. <https://doi.org/10.1016/J.BPSC.2018.06.003>
- Purves, D., Augustine, G. J., Fitzpatrick, D., Katz, L. C., LaMantia, A.-S., McNamara, J. O., & Williams, S. M. (2001). *Neuroglial Cells*. Retrieved from <https://www.ncbi.nlm.nih.gov/books/NBK10869/>
- Qin, Z., & Li, Q. (2018). High rate BCI with portable devices based on EEG. *Smart Health*, *9–10*, 115–128. <https://doi.org/https://doi.org/10.1016/j.smhl.2018.07.006>
- Rahiman, M. H. F., Taib, M. N., & Salleh, Y. M. (2009). System identification for essential oil extraction system: An overview. *Proceedings of 2009 5th International Colloquium on Signal Processing and Its Applications, CSPA 2009*. <https://doi.org/10.1109/CSPA.2009.5069252>
- Ranganathan, A. (2004). The Levenberg-Marquardt Algorithm. *Internet Httpexcelsior Cs Ucsb Educoursescs*. <https://doi.org/http://dx.doi.org/10.1.1.10.2258>
- Rao K, D. V. S. K., Premalatha, M., & Naveen, C. (2018). Analysis of different combinations of meteorological parameters in predicting the horizontal global solar radiation with ANN approach: A case study. *Renewable and Sustainable Energy Reviews*, *91*, 248–258. <https://doi.org/10.1016/J.RSER.2018.03.096>
- Rashid, N. A., Nasir, T. M., Lias, S., Sulaiman, N., Murat, Z. H., & Abdul Kadir, R. S. S. (2011). Learners' Learning Style classification related to IQ and Stress based on EEG. *Procedia - Social and Behavioral Sciences*, *29*, 1061–1070. <https://doi.org/10.1016/j.sbspro.2011.11.339>
- Rashid, N. A., Taib, M. N. bin, Lias, S. bin, Sulaiman, N. bin, Murat, Z. binti, Kadir, R. S. binti S. A., & Samsudin, K. (2013). Summative EEG-based Assessment of the Relations between Learning Styles and Personality Traits of Openness. *Procedia - Social and Behavioral Sciences*, *97*, 98–104. <https://doi.org/10.1016/j.sbspro.2013.10.209>
- Rausch, I., Quick, H. H., Cal-Gonzalez, J., Sattler, B., Boellaard, R., & Beyer, T. (2017). Technical and instrumentational foundations of PET/MRI. *European Journal of Radiology*, *94*, A3–A13. <https://doi.org/10.1016/J.EJRAD.2017.04.004>

- Raven, J., Raven, J. C., & Court, J. (1998). Manual for Raven's progressive matrices and vocabulary scales. In *Raven manual* (1998 ed). Retrieved from <http://books.google.es/books?id=YrvAAQAACAAJ>
- Rayner, S. G. (2015). Cognitive Styles and Learning Styles. In J. D. Wright (Ed.), *International Encyclopedia of the Social & Behavioral Sciences (Second Edition)* (Second Edi, pp. 110–117). <https://doi.org/https://doi.org/10.1016/B978-0-08-097086-8.92008-7>
- Raza, K., & Jothiprakash, V. (2014). Multi-output ANN Model for Prediction of Seven Meteorological Parameters in a Weather Station. *Journal of The Institution of Engineers (India): Series A*. <https://doi.org/10.1007/s40030-014-0092-9>
- Redick, T. S., Shipstead, Z., Meier, M. E., Montroy, J. J., Hicks, K. L., Unsworth, N., ... Engle, R. W. (2016). Cognitive predictors of a common multitasking ability: Contributions from working memory, attention control, and fluid intelligence. *Journal of Experimental Psychology: General*, *145*(11), 1473–1492. <https://doi.org/10.1037/xge0000219>
- Refoufi, S., & Benmahammed, K. (2018). Control of a manipulator robot by neuro-fuzzy subsets form approach control optimized by the genetic algorithms. *ISA Transactions*, *77*, 133–145. <https://doi.org/https://doi.org/10.1016/j.isatra.2018.03.023>
- Ribeiro, D. M. D., Fu, L. S., Carlós, L. A. D., & Cunha, J. P. S. (2011). A novel dry active biosignal electrode based on an hybrid organic-inorganic interface material. *IEEE Sensors Journal*. <https://doi.org/10.1109/JSEN.2011.2114649>
- Richmond, A. S., & Cummings, R. (2005). Implementing Kolb ' s Learning Styles into Online Distance Education. *International Journal of Technology in Teaching and Learning*, *1*(1), 45–54. Retrieved from <http://citeseerx.ist.psu.edu/viewdoc/download?doi=10.1.1.385.3226&rep=rep1&type=pdf>
- Roberts, M. J. (2004). *Signals and systems*. McGraw-Hill.
- Rong, G., Mendez, A., Assi, E. B., Zhao, B., & Sawan, M. (2020). Artificial Intelligence in Healthcare: Review and Prediction Case Studies. *Engineering*. <https://doi.org/https://doi.org/10.1016/j.eng.2019.08.015>
- Rosenberg, R. N. (2009). Consciousness, Coma, and Brain Death—2009. *JAMA*, *301*(11), 1172. <https://doi.org/10.1001/jama.2009.224>
- Roweis, S. (1996). Levenberg-Marquardt Optimization. *Notes, University Of Toronto*. <https://doi.org/10.1038/nn1790>
- Ruano, A. E., Sam Ge, S., Guerra, T. M., Lewis, F. L., Principe, J. C., & Colnarič, M. (2014). Computational intelligence in control. *Annual Reviews in Control*, *38*(2), 233–242. <https://doi.org/https://doi.org/10.1016/j.arcontrol.2014.09.006>
- Ruuska, S., Hämäläinen, W., Kajava, S., Mughal, M., Matilainen, P., & Mononen, J. (2018). Evaluation of the confusion matrix method in the validation of an automated

- system for measuring feeding behaviour of cattle. *Behavioural Processes*, 148, 56–62. <https://doi.org/https://doi.org/10.1016/j.beproc.2018.01.004>
- Salchenberger, L., Ventat, E. R., & Venta, L. A. (1997). USING NEURAL NETWORKS TO AID THE DIAGNOSIS OF BREAST IMPLANT RUPTURE. *Computers Ops Res*, 24(5), 435–444.
- Salehi, H., & Burgueño, R. (2018). Emerging artificial intelligence methods in structural engineering. *Engineering Structures*, 171, 170–189. <https://doi.org/https://doi.org/10.1016/j.engstruct.2018.05.084>
- Sanei, S., & Chambers, J. A. (2013). EEG Signal Processing. In *EEG Signal Processing*. <https://doi.org/10.1002/9780470511923>
- Scally, B., Burke, M. R., Bunce, D., & Delvenne, J.-F. (2018). Resting-state EEG power and connectivity are associated with alpha peak frequency slowing in healthy aging. *Neurobiology of Aging*, 71, 149–155. <https://doi.org/https://doi.org/10.1016/j.neurobiolaging.2018.07.004>
- Schittenkopf, C., Deco, G., & Brauer, W. (1997). Two strategies to avoid overfitting in feedforward networks. *Neural Networks*. [https://doi.org/10.1016/S0893-6080\(96\)00086-X](https://doi.org/10.1016/S0893-6080(96)00086-X)
- Schlögl, A., Keinrath, C., Zimmermann, D., Scherer, R., Leeb, R., & Pfurtscheller, G. (2007). A fully automated correction method of EOG artifacts in EEG recordings. *Clinical Neurophysiology*. <https://doi.org/10.1016/j.clinph.2006.09.003>
- Schmid, R. G., Tirsch, W. S., & Scherb, H. (2002). Correlation between spectral EEG parameters and intelligence test variables in school-age children. *Clinical Neurophysiology*. [https://doi.org/10.1016/S1388-2457\(02\)00212-2](https://doi.org/10.1016/S1388-2457(02)00212-2)
- Schroeders, U., Schipolowski, S., & Wilhelm, O. (2015). Age-related changes in the mean and covariance structure of fluid and crystallized intelligence in childhood and adolescence. *Intelligence*, 48, 15–29. <https://doi.org/10.1016/J.INTELL.2014.10.006>
- Schwab, K. (2017). The Global Competitiveness Report The Global Competitiveness Report 2017-2018. In *World Economic Forum* (Vol. 5). <https://doi.org/92-95044-35-5>
- Searle, A., & Kirkup, L. (2000). A direct comparison of wet, dry and insulating bioelectric recording electrodes. *Physiological Measurement*. <https://doi.org/10.1088/0967-3334/21/2/307>
- Sellers, E. W., Turner, P., Sarnacki, W. A., McManus, T., Vaughan, T. M., & Matthews, R. (2009). A novel dry electrode for brain-computer interface. *Lecture Notes in Computer Science (Including Subseries Lecture Notes in Artificial Intelligence and Lecture Notes in Bioinformatics)*. [https://doi.org/10.1007/978-3-642-02577-8\\_68](https://doi.org/10.1007/978-3-642-02577-8_68)
- Sevgi, L. (2007). Synthetic radar-signal environment: Computer generation of signal, noise, and clutter. *IEEE Antennas and Propagation Magazine*. <https://doi.org/10.1109/MAP.2007.4395342>

- Shachmurove, Y., & Witkowska, D. (2001). Dynamic Interrelations among Major World Stock Markets: A Neural Network Analysis. *International Journal of Business*.
- Shan, X., Yang, E.-H., Zhou, J., & Chang, V. W. C. (2019). Neural-signal electroencephalogram (EEG) methods to improve human-building interaction under different indoor air quality. *Energy and Buildings*, *197*, 188–195. <https://doi.org/https://doi.org/10.1016/j.enbuild.2019.05.055>
- Sharma, N., Kolekar, M. H., Jha, K., & Kumar, Y. (2019). EEG and Cognitive Biomarkers Based Mild Cognitive Impairment Diagnosis. *IRBM*, *40*(2), 113–121. <https://doi.org/https://doi.org/10.1016/j.irbm.2018.11.007>
- Shirwaikar, R. D., U, D. A., Makkithaya, K., M, S., Srivastava, S., & U, L. E. S. L. (2019). Optimizing neural networks for medical data sets: A case study on neonatal apnea prediction. *Artificial Intelligence in Medicine*, *98*, 59–76. <https://doi.org/https://doi.org/10.1016/j.artmed.2019.07.008>
- Silvia, P. J. (2015). Intelligence and Creativity Are Pretty Similar After All. *Educational Psychology Review*, *27*(4), 599–606. <https://doi.org/10.1007/s10648-015-9299-1>
- Simon O. Haykin. (2009). *Neural Networks and Learning Machines, 3rd Edition* | Pearson. NJ, USA: Pearson Upper Saddle River.
- Smailovic, U., Koenig, T., Kåreholt, I., Andersson, T., Kramerberger, M. G., Winblad, B., & Jelic, V. (2018). Quantitative EEG power and synchronization correlate with Alzheimer's disease CSF biomarkers. *Neurobiology of Aging*, *63*, 88–95. <https://doi.org/10.1016/J.NEUROBIOLAGING.2017.11.005>
- Smith-Bindman, R., Lipson, J., Marcus, R., Kim, K. P., Mahesh, M., Gould, R., ... Miglioretti, D. L. (2009). Radiation dose associated with common computed tomography examinations and the associated lifetime attributable risk of cancer. *Archives of Internal Medicine*. <https://doi.org/10.1001/archinternmed.2009.427>
- Smith, L. H., & DeMyer, W. E. (2003). Anatomy of the brainstem. *Seminars in Pediatric Neurology*, *10*(4), 235–240. [https://doi.org/10.1016/S1071-9091\(03\)00076-7](https://doi.org/10.1016/S1071-9091(03)00076-7)
- Snyder, R. F. (1999). The Relationship between Learning Styles/Multiple Intelligences and Academic Achievement of High School Students. *The High School Journal*, *83*(2), 11-20 CR-Copyright &#169; 1999 University of No. <https://doi.org/10.2307/40364506>
- Sobkow, A., Traczyk, J., Kaufman, S. B., & Nosal, C. (2018). The structure of intuitive abilities and their relationships with intelligence and Openness to Experience. *Intelligence*, *67*, 1–10. <https://doi.org/https://doi.org/10.1016/j.intell.2017.12.001>
- Srinivasan, R. (1999). Methods to improve spatial resolution of EEG. *International Journal of Bioelectromagnetism*, *1*(1), 102–111. <https://doi.org/10.1109/IEMBS.1988.95290>
- Staudt, B., & Neubauer, A. C. (2006). Achievement, underachievement and cortical activation: A comparative EEG study of adolescents of average and above-average intelligence. *High Ability Studies*, *17*(1), 3–16.

<https://doi.org/10.1080/13598130600946855>

- Subasi, A., & Erçelebi, E. (2005). Classification of EEG signals using neural network and logistic regression. *Computer Methods and Programs in Biomedicine*. <https://doi.org/10.1016/j.cmpb.2004.10.009>
- Svozil, D., Kvasnička, V., & Pospíchal, J. (1997). Introduction to multi-layer feed-forward neural networks. *Chemometrics and Intelligent Laboratory Systems*. [https://doi.org/10.1016/S0169-7439\(97\)00061-0](https://doi.org/10.1016/S0169-7439(97)00061-0)
- Swartz, B. E., & Goldensohn, E. (1998). Timeline of the History of EEG and associated fields. *Electroencephalo Clin Neurophysiol*. [https://doi.org/10.1016/S0013-4694\(97\)00121-1](https://doi.org/10.1016/S0013-4694(97)00121-1)
- Taib, M. N., Andres, R., & Narayanaswamy, R. (1996). Extending the response range of an optical fibre pH sensor using an artificial neural network. *Analytica Chimica Acta*, 330(1), 31–40. [https://doi.org/10.1016/0003-2670\(96\)00149-3](https://doi.org/10.1016/0003-2670(96)00149-3)
- Talu, M. F., Gül, M., Alpaslan, N., & Yiğitcan, B. (2013). Calculation of melatonin and resveratrol effects on steatosis hepatis using soft computing methods. *Computer Methods and Programs in Biomedicine*. <https://doi.org/10.1016/j.cmpb.2013.04.020>
- Tamerabet, Y., Adjadj, F., & Bentrchia, T. (2018). Evaluation of the genetic algorithm performance for the optimization of the grand potential in the cluster variation method. *Calphad*, 61, 157–164. <https://doi.org/https://doi.org/10.1016/j.calphad.2018.03.007>
- Tariq, M., Trivailo, P. M., & Simic, M. (2018). Motor imagery based EEG features visualization for BCI applications. *Procedia Computer Science*, 126, 1936–1944. <https://doi.org/https://doi.org/10.1016/j.procs.2018.08.057>
- Tautan, A.-M., Mihajlovic, V., Chen, Y.-H., Grundlehner, B., Penders, J., & Serdijn, W. (2014). Signal Quality in Dry Electrode EEG and the Relation to Skin-electrode Contact Impedance Magnitude. *Proceedings of the International Conference on Biomedical Electronics and Devices (BIOSTEC 2014)*. <https://doi.org/10.5220/0004738700120022>
- te Velde, R. (2000). The Age of Spiritual Machines: When Computers Exceed Human Intelligence,. *Telecommunications Policy*. [https://doi.org/10.1016/S0308-5961\(99\)00064-6](https://doi.org/10.1016/S0308-5961(99)00064-6)
- Tee, T. K., Widad, O., & Yee, M. H. (2009). *Relationship between Learning Styles and Multiple Intelligences among Bachelor of Technology and Education*. Retrieved from <http://library.oum.edu.my/repository/549/>
- Teplan, M. (2008). FUNDAMENTALS OF EEG MEASUREMENT. *MEASUREMENT SCIENCE REVIEW*. <https://doi.org/10.1021/pr0703501>
- Thatcher, R. W., North, D., & Biver, C. (2005). EEG and intelligence: Relations between EEG coherence, EEG phase delay and power. *Clinical Neurophysiology*, 116(9), 2129–2141. <https://doi.org/10.1016/j.clinph.2005.04.026>

- Thatcher, R. W., North, D. M., & Biver, C. J. (2008). Intelligence and EEG phase reset: A two compartmental model of phase shift and lock. *NeuroImage*. <https://doi.org/10.1016/j.neuroimage.2008.06.009>
- Tomarken, A. J., Davidson, R. J., Wheeler, R. E., & Kinney, L. (1992). Psychometric Properties of Resting Anterior EEG Asymmetry: Temporal Stability and Internal Consistency. *Psychophysiology*. <https://doi.org/10.1111/j.1469-8986.1992.tb02034.x>
- Tsai, P. Y., Hu, W., Kuo, T. B. J., & Shyu, L. Y. (2009). A portable device for real time drowsiness detection using novel active dry electrode system. *Proceedings of the 31st Annual International Conference of the IEEE Engineering in Medicine and Biology Society: Engineering the Future of Biomedicine, EMBC 2009*. <https://doi.org/10.1109/IEMBS.2009.5334491>
- Tsuchiyama, T., Katsuhara, M., & Nakajima, M. (2017). Compensation of matrix effects in gas chromatography–mass spectrometry analysis of pesticides using a combination of matrix matching and multiple isotopically labeled internal standards. *Journal of Chromatography A*, *1524*, 233–245. <https://doi.org/https://doi.org/10.1016/j.chroma.2017.09.072>
- Tu, J. V. (1996). Advantages and disadvantages of using artificial neural networks versus logistic regression for predicting medical outcomes. *Journal of Clinical Epidemiology*, *49*(11), 1225–1231. Retrieved from <https://www.ncbi.nlm.nih.gov/pubmed/8892489>
- Übeyli, E. D., & Güler, I. (2005). Feature extraction from Doppler ultrasound signals for automated diagnostic systems. *Computers in Biology and Medicine*. <https://doi.org/10.1016/j.complbiomed.2004.06.006>
- Ur Rehman, N., & Mandic, D. P. (2011). Filter bank property of multivariate empirical mode decomposition. *IEEE Transactions on Signal Processing*. <https://doi.org/10.1109/TSP.2011.2106779>
- Vakili, S., Tehranchian, N., Tajziehchi, M., Mohammad Rezazadeh, I., & Wang, X. (2012). An empirical study on the relations between EEG alpha-beta entropy & EQ-IQ test scores. *Proceedings - IEEE-EMBS International Conference on Biomedical and Health Informatics: Global Grand Challenge of Health Informatics, BHI 2012*. <https://doi.org/10.1109/BHI.2012.6211572>
- Van Der Knaap, L. J., & Van Der Ham, I. J. M. (2011). How does the corpus callosum mediate interhemispheric transfer? A review. *Behavioural Brain Research*, *223*(1), 211–221. <https://doi.org/10.1016/j.bbr.2011.04.018>
- van Son, D., Blasio, F. M. De, Fogarty, J. S., Angelidis, A., Barry, R. J., & Putman, P. (2018). Frontal EEG theta/beta ratio during mind wandering episodes. *Biological Psychology*. <https://doi.org/https://doi.org/10.1016/j.biopsycho.2018.11.003>
- Varela, F., Lachaux, J. P., Rodriguez, E., & Martinerie, J. (2001). The brainweb: Phase synchronization and large-scale integration. *Nature Reviews Neuroscience*, *2*(4), 229–239. <https://doi.org/10.1038/35067550>



- Vargas, J., Spiotta, A., & Chatterjee, A. R. (2019). Initial Experiences with Artificial Neural Networks in the Detection of Computed Tomography Perfusion Deficits. *World Neurosurgery*, *124*, e10–e16. <https://doi.org/10.1016/j.wneu.2018.10.084>
- Verkhatsky, A., Parpura, V., & Rodríguez, J. J. (2011). Where the thoughts dwell: The physiology of neuronal-glia “diffuse neural net.” *Brain Research Reviews*, *66*(1–2), 133–151. <https://doi.org/10.1016/j.brainresrev.2010.05.002>
- Vernon, P. E. (1984). INTELLIGENCE, COGNITIVE STYLES, AND BRAIN LATERALIZATION. *International Journal of Psychology*, *19*(1–4), 435–455. <https://doi.org/10.1080/00207598408247540>
- Verpoort, P. C., MacDonald, P., & Conduit, G. J. (2018). Materials data validation and imputation with an artificial neural network. *Computational Materials Science*, *147*, 176–185. <https://doi.org/10.1016/j.commatsci.2018.02.002>
- Vishwanath, M., Jafarlou, S., Shin, I., Lim, M. M., Dutt, N., Rahmani, A. M., & Cao, H. (2020). Investigation of Machine Learning Approaches for Traumatic Brain Injury Classification via EEG Assessment in Mice. *Sensors*, *20*(7). <https://doi.org/10.3390/s20072027>
- Waldman, D. A., Balthazard, P. A., & Peterson, S. J. (2011). Social cognitive neuroscience and leadership. *The Leadership Quarterly*, *22*(6), 1092–1106. <https://doi.org/10.1016/J.LEAQUA.2011.09.005>
- Wang, L., Song, M., Jiang, T., Zhang, Y., & Yu, C. (2011). Regional homogeneity of the resting-state brain activity correlates with individual intelligence. *Neuroscience Letters*, *488*(3), 275–278. <https://doi.org/10.1016/j.neulet.2010.11.046>
- Wang, Zeyu, & Srinivasan, R. S. (2017). A review of artificial intelligence based building energy use prediction: Contrasting the capabilities of single and ensemble prediction models. *Renewable and Sustainable Energy Reviews*, *75*, 796–808. <https://doi.org/10.1016/j.rser.2016.10.079>
- Wang, Zhangyang, Liu, D., & Huang, T. S. (2019). Chapter 6 - Signal Processing. In Zhangyang Wang, Y. Fu, & T. S. B. T.-D. L. T. S. and L.-R. M. Huang (Eds.), *Computer Vision and Pattern Recognition* (pp. 121–142). <https://doi.org/10.1016/B978-0-12-813659-1.00006-8>
- Webster, J. (2009). *Medical Instrumentation: Application and Design*. 4th ed. Retrieved from [https://scholar.google.com/scholar?hl=en&as\\_sdt=0%2C5&q=G.+Webster%2C+Medical+Instrumentation%3A+Application+and+Design%2C+4th+ed.&btnG=](https://scholar.google.com/scholar?hl=en&as_sdt=0%2C5&q=G.+Webster%2C+Medical+Instrumentation%3A+Application+and+Design%2C+4th+ed.&btnG=)
- Webster, J. G. (2009). *Medical Instrumentation: Application and Design* (4th ed.). New Jersey: Wiley.
- Wechsler, D. (2008). Wechsler adult intelligence scale—Fourth Edition (WAIS—IV). *San Antonio, TX*: NCS Pearson.. Retrieved from <http://scholar.google.com/scholar?hl=en&btnG=Search&q=intitle:Wechsler+Adult+Intelligence+Scale+->

+3rd+edition#3%0Ahttp://www.statisticssolutions.com/academic-solutions/resources/directory-of-survey-instruments/wechsler-adult-intelligence-scale-fourth-edit

- Wechsler, S. M., Saiz, C., Rivas, S. F., Vendramini, C. M. M., Almeida, L. S., Mundim, M. C., & Franco, A. (2018). Creative and critical thinking: Independent or overlapping components? *Thinking Skills and Creativity*, 27, 114–122. <https://doi.org/https://doi.org/10.1016/j.tsc.2017.12.003>
- Welch, P. D. (1967). The Use of Fast Fourier Transform for the Estimation of Power Spectra: A Method Based on Time Averaging Over Short, Modified Periodograms. *IEEE Transactions on Audio and Electroacoustics*, 15(2), 70–73. <https://doi.org/10.1109/TAU.1967.1161901>
- Williamson, D. F., Parker, R. A., & Kendrick, J. S. (1989). The box plot: A simple visual method to interpret data. *Annals of Internal Medicine*. <https://doi.org/10.7326/0003-4819-110-11-916>
- Willingham, D. T., Hughes, E. M., & Dobolyi, D. G. (2015). The Scientific Status of Learning Styles Theories. *Teaching of Psychology*. <https://doi.org/10.1177/0098628315589505>
- Wróbel, A. (2000). Beta activity: A carrier for visual attention. *Acta Neurobiologiae Experimentalis*. <https://doi.org/10.1016/j.medmal.2009.01.007>
- Yang, J., & Ma, J. (2018). Feed-forward neural network training using sparse representation. *Expert Systems with Applications*. <https://doi.org/https://doi.org/10.1016/j.eswa.2018.08.038>
- Yang, L., Ma, R., Zhang, H. M., Guan, W., & Jiang, S. (2018). Driving behavior recognition using EEG data from a simulated car-following experiment. *Accident Analysis & Prevention*, 116, 30–40. <https://doi.org/10.1016/J.AAP.2017.11.010>
- Yao, S., & Zhu, Y. (2016). Nanomaterial-Enabled Dry Electrodes for Electrophysiological Sensing: A Review. *JOM*. <https://doi.org/10.1007/s11837-016-1818-0>
- Yazıcıoğlu, R. F., Van Hoof, C., & Puers, R. (2009). *Introduction to Biopotential Acquisition*. [https://doi.org/10.1007/978-1-4020-9093-6\\_2](https://doi.org/10.1007/978-1-4020-9093-6_2)
- Zadeh, A. E., Khazae, A., & Ranaee, V. (2010). Classification of the electrocardiogram signals using supervised classifiers and efficient features. *Computer Methods and Programs in Biomedicine*, 99(2), 179–194. <https://doi.org/10.1016/j.cmpb.2010.04.013>
- Zecchin, C., Facchinetti, A., Sparacino, G., & Cobelli, C. (2014). Jump neural network for online short-time prediction of blood glucose from continuous monitoring sensors and meal information. *Computer Methods and Programs in Biomedicine*. <https://doi.org/10.1016/j.cmpb.2013.09.016>
- Zhang, D., Jiao, L., Bai, X., Wang, S., & Hou, B. (2018). A robust semi-supervised SVM via ensemble learning. *Applied Soft Computing*, 65, 632–643.

<https://doi.org/https://doi.org/10.1016/j.asoc.2018.01.038>

Zhang, G. P. (2000). Neural networks for classification: a survey. *IEEE Transactions on Systems, Man and Cybernetics, Part C (Applications and Reviews)*, 30(4), 451–462. <https://doi.org/10.1109/5326.897072>

Zhang, L. F., Zhu, Q. M., & Longden, A. (2009). A correlation-test-based validation procedure for identified neural networks. *IEEE Transactions on Neural Networks*. <https://doi.org/10.1109/TNN.2008.2003223>

Universiti Malaya